Exploring New Routes Towards Photoactive Assemblies

By

Cerys Thomas

A Thesis submitted to the University of Wales in accordance with the requirements for the degree of Doctor of Philosophy in the Faculty of Science, Department of Chemistry, University of Wales, Cardiff.

September 2006

ProQuest LLC
789 East Eisenhower Parkway
P.O. Box 1346
Ann Arbor, MI 48106-1346

Acknowledgements

I must first thank Dr. Ian Fallis and Dr. Angelo Amoroso for their ideas and guidance throughout the last three years of my research.

I would like to thank the Mass Spectrometry Service Centre at Swansea and the department at Cardiff. Thanks also to Dr. Li Ling Ooi who carried out the crystallography described in this thesis. I would also like to thank Dr. Simon Aldridge for use of his chemicals and equipment. Many thanks to Rob, Robin, Gaz, Jobo, Sham, Alan, Ricky, Mal, Dave, Steve and the rest of the technical staff.

Big thanks must go to everyone in Labs 1.124 and 1.125 past and present for providing much entertainment. I have thoroughly enjoyed working with these people including Neha, Ruth, Anne, Tom, Becky, Mini, Debs, Bres, Graham, Dave, Steve, Matt, Tim, Gigi, Dan, Jo and Andrea.

Special thanks to Mam, Dad and Mamo who have always supported and encouraged me to do the best I can. Without their love and guidance over the past twenty-five years, I wouldn't be where I am now. I hope I have made them very proud. I would also like to thank Sue, Mal and Phil for their encouragement and much appreciated humour.

Finally, I would like to thank my husband-to-be Mark, for all his love, patience, and motivation. It is a pleasure to have him in my life and I couldn't have made it through the past four years without him making me laugh every day!

Contents

Chapter 2 –Quinones

Chapter 4 – Synthesis and complexation of tetraaza macrocycles functionalised with phenol side arms

Notes

The following abbreviations were used in the text:

Å	Angstrom
Ar	Aromatic
B	Broad
cm^{-1}	Reciprocal centimetres
C_o	Surface concentration of oxidised species
C_R	Surface concentration of reduced species
CV	Cyclic Voltammogram
Cyclam	1,4,8,11-Tetraazacyclotetradecane
Cyclen	1,4,7,10-Tetraazacyclododecane
d	Doublet
dd	Double doublet
DCNQ	2,3-Dichloro-1,4-naphthoquinone
DMSO	Dimethyl sulfoxide
δ	NMR chemical shift
E0	Standard Electrode Potential
EI	Electron ionisation
ES	Electrospray
FAB	Fast Atom Bombardment
F	Faraday constant
ε	Absorption coefficient
g	Grams
IR	Infrared
J	Coupling constant

KBr	Potassium bromide
λ	Wavelength
m	Multiplet (NMR), medium (IR)
M	Molar concentration
MeCN	Acetonitrile
Me	CH_3
MS	Mass spectrometry
mV	Millivolts
m/z	Mass/charge ratio
n	Number of moles
nm	Nanometre (10^{-9}m)
ν	Stretching mode
NMR	Nuclear magnetic resonance
ppm	Parts per million
PeT	Photoinduced electron transfer
PSII	Photosystem II
Q	Quinone
QH_2	Hydroquinol
q	Quartet
R	Universal Gas Constant
R_f	Relative front
s	Singlet (NMR), strong(IR)
t	Triplet
T	Absolute temperature
Tacn	1,4,7-Triazacyclononane

TMS	Trimethyl silyl
UV	Ultraviolet
V	Volts
w	Weak

Abstract

With increased interest in charge separated states formed in Photosystem II, we set out to synthesise a series of novel photoactive assemblies whereby the components comprising the arrays are linked by a variety of methods. We also considered the capabilities of the electron donors and acceptors separately with focus on porphyrins and quinones respectively.

Along this theme, we prepared a number of novel amine derivatives of 2,3-dichloro-1,4-naphthoquinone and studied their electrochemistry. Thiol and mixed thiol/amine derivatives of 2,3-dichloro-1,4-naphthoquinone were also synthesised and studied electrochemically.

Synthesis of a bis porphyrin-terpyridine molecular array was attempted using three methods. The method showing greatest promise is direct coupling of the porphyrins with the terpyridine. Comparison of the luminescence of *Meso*-5,10,15,20-tetrakis(4-iodophenyl)porphyrin with its bromo, chloro and hydrogen analogues was carried out in addition to their zinc complexes. As expected, iodine is the strongest quencher, followed by bromine, chlorine and hydrogen. Altering the substituents of the porphyrin has less of an effect on the luminescence when the porphyrin is metallated with zinc(II) than in the free base. A new route to synthesise 4-iodobenzaldehyde is reported starting with 4-iodotoluene. Two novel A_4-substituted porphyrins were prepared utilising the Heck reaction.

Using the Mannich reaction, we synthesised two novel tetraza macrocycles functionalised with phenol pendant arms and their lanthanide and transition metal complexes. Synthesis of cyclen bearing specific phenol and naphthol groups at all four positions was found to be hindered, possibly by the stability of the cyclen intermediate in addition to the lack of reactivity of these phenol and naphthol groups. Preparation of a novel cyclen-tetraporphyrin array was found to be forbidden for the same reasons. Following the synthesis of 5-iodovanillin, the preparation of the corresponding symmetrical porphyrin was reported which is a candidate for further work in this area.

Chapter 1

Introduction

1.1 Background to Photosynthesis

Photosynthetic organisms use light energy from the sun to reduce CO_2 to carbohydrate. Chlorophyll is vital in this process as exemplified by the fact that the prevalent colour of the Earth is green. In 1932, Emerson and Arnold demonstrated that only a few of the chlorophyll molecules located in the photosynthetic reaction centre actually take part in the photosynthetic process.[1] The function of the majority of chlorophyll molecules is light harvesting followed by transfer of electronic excited state energy to the reaction centre. Chlorophyll molecules are efficient in carrying out light harvesting since they are highly conjugated which results in them having high extinction coefficients. Two main types of chlorophyll molecules are found in the photosynthetic apparatus, Chlorophyll a and b. Chlorophyll a absorbs photons at maxima of 430 and 680nm whilst Chlorophyll b has maxima at 460 and 640 nm, hence the two molecules complement each other for maximum absorption of light.

The concept that 250 chlorophyll molecules assisted by carotenoids absorb sunlight and channel electronic energy to the reaction centre prompted Förster[2] and Oppenheimer[3] to develop an equation for the rate of transfer from donor to acceptor based on induced dipole-induced dipole interactions. Twenty years after this mechanism was suggested, Dexter[4] showed that another mechanism is also in action in such systems. This is electron exchange between the donor and acceptor and is more effective over distances of a few angstroms whereas the Coulomb mechanism of Förster[2] and Oppenheimer[3] is effective over distances of 20-50 angstroms. Therefore, the Exchange mechanism realised by Dexter can be used to account for the transfer of singlet and triplet excitations whereas the Coulomb mechanism applies only to singlet electron transfer. Since the proposal of these mechanisms, it has been

the aim of scientists to unravel the exact architecture of the Photosynthetic Reaction Centre.

1.2 Light and Dark Reactions

Photosynthesis is divided into two stages: the light reactions and the dark reactions, although both occur during daylight. The light reactions involve the splitting of 2 water molecules into dioxygen using photons of energy from the light. The dark reactions (Calvin cycle) uses protons from the light reaction to convert CO_2 to carbohydrate.

1.2.1 The Light Reaction

Two different systems comprise the light reactions, that is Photosystem I (PS I) and Photosystem II (PS II) and the two systems are linked by an electron transport complex. Both systems require excitation, PS II followed by PS I. Excitation of PS II occurs at its reaction centre P680 (P represents the pigment while 680 nm is the wavelength at which it absorbs). P680 consists of a pair of chlorophyll molecules known as the 'special pair'. In addition, PS II also contains a light-harvesting centre (LHC-II) made up of chlorophyll and caroteniods. Light harvesting complexes in close proximity to P680 absorb photons of energy and pass on this excited energy to LHC-II. When the energy reaches the reaction centre P680, it results in the formation of the excited state P680* which is short-lived and passes on its electron to pheophytin (Mg depleted analogue of Chlorophyll a). The charge separated states $P680^+$ and $pheo^-$ do not recombine since the electron from $pheo^-$ is passed onto the first of two plastoquinones. Following transfer of two electron and two protons to the second plastoquinone, QH_2 is formed and this compound forms the link between PS II

and PS I. In effect following charge separation the quinone acceptor transports protons across the membrane which powers the synthesis of adenosine triphosphate (ATP) which is a biological fuel. ATP fills the energy requirements of the photosynthetic organism. Deisenhoffer, Huber and Michel have contributed vastly to furthering the structural knowledge of the Photosynthetic apparatus due to their crystallographic studies on bacterial photosynthetic reaction centres which earned them the Nobel prize in 1987.[5]

1.3 Photosynthetic Apparatus of Purple bacteria

The Photosynthetic unit of the purple bacteria species is shown in figure 1.1.[6] In most purple bacteria, there are two light harvesting complexes, LHC-I and LHC-II.[7] Light harvesting system I is in direct contact with the reaction centre[8,9] however LH-II transfers energy to the reaction centre through LH-I.[10,11] Excitation following absorption of photons is transferred from the light harvesting complexes to the reaction centre, which results in a charge separated state of electron and hole. The quinone is reduced to a hydroquinone, which then oxidises the bc_1 complex and uses this exothermic reaction to generate a proton gradient for the synthesis of ATP.

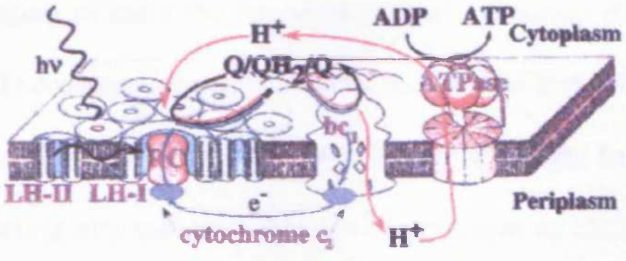

Figure 1.1:Photosynthetic apparatus of a purple bacteria

1.4 Current Research-model systems for photosynthetic reaction centre

Although the research of Deisenhoffer, Huber and Michel proved invaluable in advancing the structural knowledge of photosynthesis, much work has been carried out since in order to unravel the physical mechanisms of long-range electron transfer. The synthesis of systems to mimic the electron transfer leading to separation of photoseparated charges has become widely studied by many groups.[12-22] The aim of these investigations is to gain a more thorough understanding of how the systems achieve such astonishing efficiency and the organisation of molecules within the photosynthetic unit. Factors which dictate the mechanism, lifetime, kinetics and yields of the charge separated states include the type of electron exchanging centres themselves, the linking groups and distances between them, environment and orientation.

1.4.1 Model systems with Porphyrins as electron donors and Quinones as acceptors

The most thoroughly studied class of compounds used to mimic natural photosynthetic reaction centres are porphyrin macrocycles covalently linked to quinone acceptors.[12-18] Porphyrins absorb strongly in the blue and weakly in the green region of the solar spectrum hence mimicking the chlorophylls in the former case and accessory pigments such as carotenoids and bilins in the latter. The ease of synthesis of porphyrin in addition to its efficient light harvesting capabilities makes it an appealing alternative. The use of quinones as electron acceptors is preferential since they are the acceptors found in natural photosynthetic electron transport. Carotenoids, also found in natural photosynthetic systems are very often employed as secondary donors in these systems.

Momenteau and co-workers[12] have carried out studies in this area and the reaction centre model reported is shown in figure 1.2. This assembly consists of a carotenoid and a quinone (represented by **R**) along with a basket-handle porphyrin. The three components are linked via ester bonding. The quinone was unstable, rapidly converting to the hydroquinone. The molecular assemblies reported by the group were incorporated inside bilayer lipid membranes and with aqueous redox couples on either side of the membrane, the electrical photoconduction values were measured. The photocurrents observed were shown to be lower than those previously reported by Moore.[13] Possible explanations offered were the more hydrophobic environment of the basket-handle triad in addition to nature, length and linking groups between the three components.

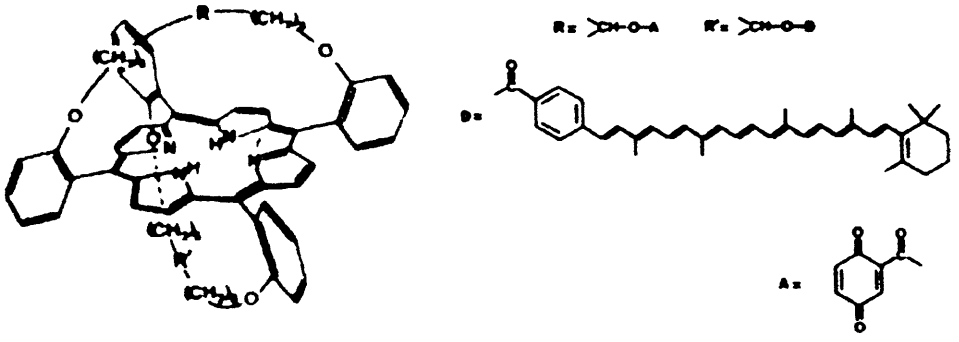

Figure 1.2:Carotenoporphyrin-Quinone Triad synthesised and investigated by Momenteau[13]

Further investigations of this kind have been undertaken by Beer and co-workers.[14] They have reported the synthesis, fluorescence and electrochemical studies of the novel porphyrin-ferrocene-quinone linked molecular array shown in figure 1.3. Both methods suggested rapid electron transfer from the porphyrin excited state to the quinone acceptor. Further studies by the group are being undertaken since there is the possibility that this compound could be utilised in redox reactions as an electron relay catalyst.

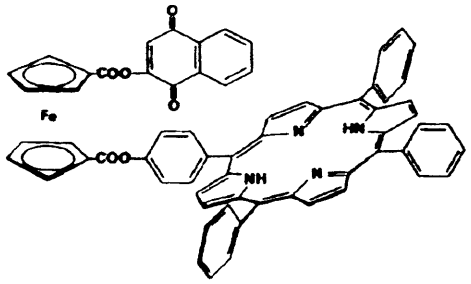

Figure 1.3: Porphyrin-Ferrocene Quinone array prepared by Beer[14]

Of significant interest to us is the work of Moore and co-workers. The group have conducted many studies based on artificial photosynthetic reaction centres and model systems for light-induced charge separation.[15-19] The preparation and investigation of the three triads shown in figure 1.4 was carried out.

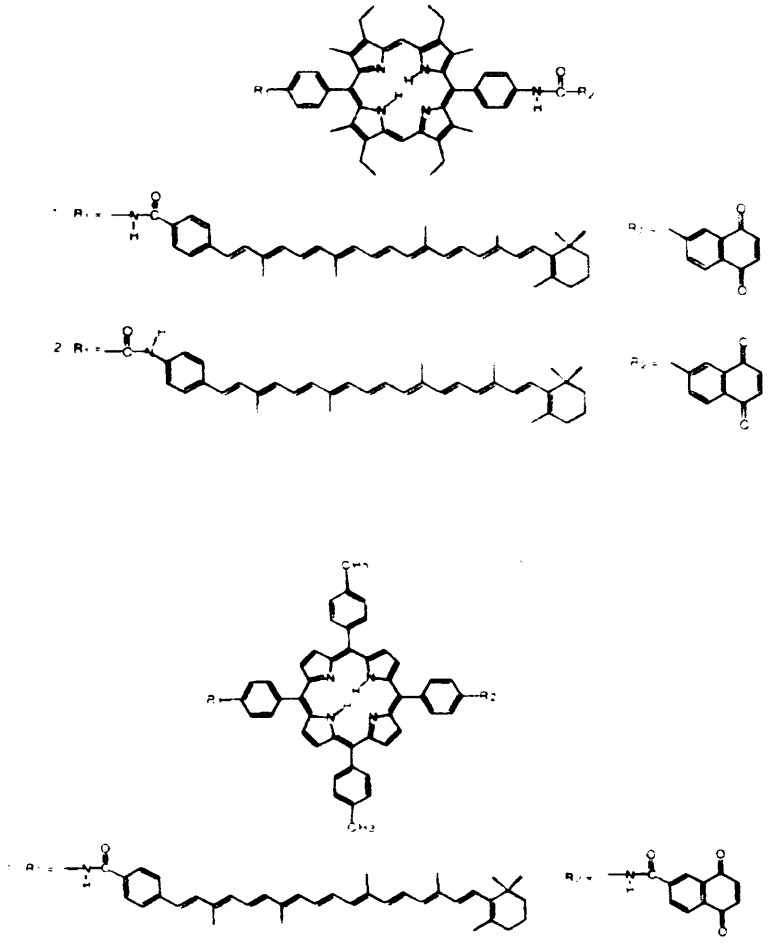

Figure 1.4: Triads **1** (top), **2** (middle) and **3** (lower) synthesised by Moore and Gust[15]

As illustrated in figure 1.5 (pathways leading to the charge separated states) when excited, the C-^{1}P-Q (carotenoid-singlet excited porphyrin-quinone triad) can decay via photophysical processes (intersystem crossing, fluorescence and quenching). However photoinduced electron transfer (PeT) to form C-P^{+}-Q^{-} is the competing process. Decay of this state may occur through charge recombination to the ground state C-P-Q or through further electron transfer to give C^{+}-P-Q^{-}. This final charge separated state will finally combine to form the ground state C-P-Q.

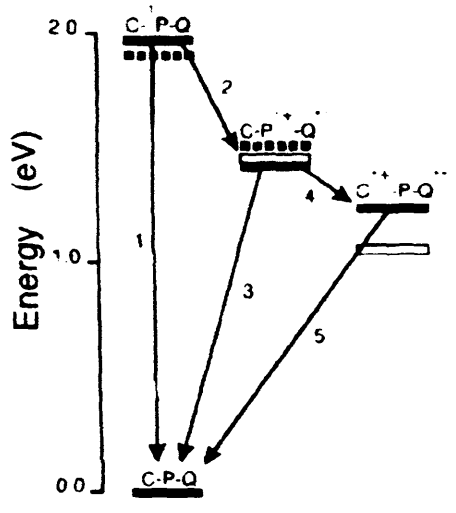

Figure 1.5: Energies of relevant states of the triads **1**, **2** and **3**
(Solid bar-Triad **1**, hollow bar-Triad **2**, dashed bar-Triad **3**)

Values for rate constants and quantum yields for triads **1-3** in benzonitrile are reported in table 1.1. In such systems, the electron transfer rate should depend upon the electronic coupling in addition to free energy change. Comparison of triad **1** and **3** was required in order to consider the effect of the steric factor of the methyl group on electron transfer rate. Although the electron transfer rate constants k_2 for triads **1** and **3** are almost identical, the free energy change (step 2) for triad **1** is -0.55eV and -0.39eV for triad **3**. After consideration of these results along with previous work on dyad models, it was concluded that the steric effect from the alkyl groups in the β-pyrrolic positions force the aryl ring to be orthogonal to the porphyrin reducing π-π

interactions between the macrocycle and aryl groups. This results in a decrease in the rate of PeT in triad **1** by a factor of one fifth. Even though k_4 for triad **3** is approximately 6 times larger than that for triad **1**, when free energy change is taken into consideration, it was concluded that the steric factors do not have an effect on electron transfer for k_4. The fact that the rate of charge recombination for $C\text{-}P^{\cdot+}\text{-}Q^{\cdot-}$ is approximately 8 times greater for triad **3** compared with **1** and the free energy difference was thought to have little effect on rate, suggests that the rate for this step is due to steric effects on electronic couplings. It was concluded that the presence of the methyl groups in the β-pyrrolic positions of the porphyrin decreases π-π overlap between the macrocycle and its meso substituents which decreases donor-acceptor coupling hence resulting in a slightly reduced rate of electron transfer. It is interesting to note that the recombination rate for $C^{\cdot+}\text{-}P\text{-}Q^{\cdot-}$ in triad **3** is 4 times greater than in triad **1** (and free energy changes are identical), owing to the steric effects of the β-methyl groups.

Compound	$k_1(s^{-1})$	$k_2(s^{-1})$	$k_3(s^{-1})$	$k_4(s^{-1})$	$k_5(s^{-1})$	$\Phi_{C\text{-}P^{\cdot-}\text{-}Q}$	$\Phi_{C^{\cdot-}\text{-}P\text{-}Q}$
1	1.6×10^8	9.5×10^9	5.3×10^{11}	3.3×10^{10}	3.2×10^6	0.98	0.057
2	1.4×10^8	1.1×10^{10}	5.3×10^{11}	3.7×10^{10}	3.8×10^6	0.96	0.063
3	4.6×10^8	8.6×10^9	4.2×10^{12}	2.0×10^{11}	1.5×10^7	0.95	0.044

Table 1.1: Rate constants and quantum yields for compounds 1-3

Comparison of triads **1** and **2** was necessary in order to assess the effect of the reversal of the amide link. As shown in table 1.1, the rate constant k_4 is 1.1 times greater in triad **2**, suggesting there is very little effect in reversing the direction of the link. Despite this, the free energy change for **2** is double that for **1** (0.40eV versus

0.19eV), therefore in effect, reversal of the amide link from **2** to **1** increases electron transfer by a factor of 30 therefore when the nitrogen atom of the amide group is attached to the porphyrin meso aryl group, the electronic coupling is greater.

In an attempt to obtain a system which is more similar to natural photosynthesis, Moore and his group studied dyads **1** and **2** shown in figure 1.6. In these systems, the apparatus are relatively insensitive to temperature and thermodynamic driving forces. The distance from the centre of the porphyrin ring to the centre of the quinone moiety in dyad **1** has been estimated as 6.7 angstroms whereas the corresponding distance in **2** is 8.8 angstroms. Results confirmed that both PeT and charge recombination in **2** slows as the solvent dielectric constant decreases. In addition, PeT was shown to cease in glass at low temperatures. However, even though charge recombination in dyad **1** slows slightly with decreasing dielectric constant of the solvent, PeT is not affected by solvent or temperature. This may be accounted for the small separation of the ions in the charge separated state for dyad **1**. At small ionic separations such that are observed in dyad **1**, electron transfer is not affected by temperature or solvent properties. It was concluded that PeT in dyad **1** is dictated by intramolecular vibrations. For both dyads studied, the rates of charge separation was substantially larger than rates for charge recombination, perhaps due to the rigid linkage and the small separations compared with other dyads previously reported.[18]

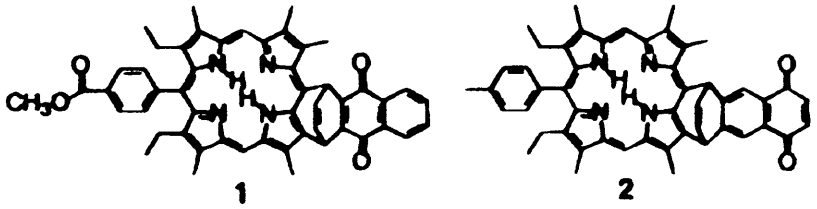

Figure 1.6:Dyads **1** and **2** synthesised by Moore and Gust[17]

More recently, Moore and co-workers have investigated a molecular tetrad consisting of a porphyrin and a triquinone.[19] The benefit of using multiple quinone moieties is that they appear to demonstrate two sequential electron transfer steps which give rise to an enhanced lifetime of the charge separated states. Long lifetime is due to weak electronic coupling between the radical anion and cation. Direct PeT was observed for a previously reported porphyrin-diquinone triad in which both quinones had similar reduction potentials.[20] In the latter case, sequential electron transfer did not occur and the singlet porphyrin excited state was quenched. However reports of porphyrins linked to two quinone moieties having sequentially increasing reduction potential have been shown to possess two sequential electron transfer steps which leads to a an enhanced lifetime of the photoseparated charges.[21] The tetrad synthesised and studied by Moore and co-workers is shown in figure 1.7.

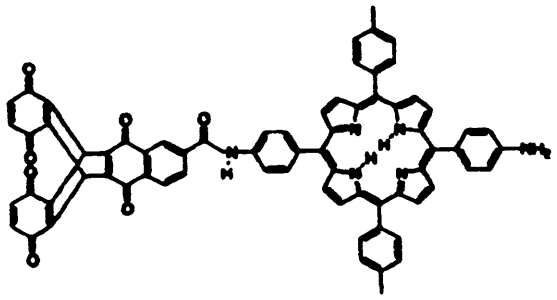

Figure 1.7: Tetrad prepared by Moore and Gust[19]
(P-NQ-BQ_2 Porphyrin-naphthoquinone-2xbenzoquinone)

Spectroscopic studies demonstrated that following excitation of the porphyrin chromophore, PeT occurs to afford the initial charge separated state $P^{\cdot+}$-$NQ^{\cdot-}$-BQ_2 with a quantum yield of unity. Following this, charge shift to produce $P^{\cdot+}$-NQ-($BQ^{\cdot-}$ BQ) occurs and the longer lifetime of this state compared with that of a porphyrin-quinone dyad proves that sequential multistep electron transfer can be used to enhance

the lifetimes of charge separated states. Parallel multistep electron transfer is also observed in this array since the photoexcited state $P^{\cdot+}$-$NQ^{\cdot-}$-BQ_2 is able to form $P^{\cdot+}$-NQ-($BQ^{\cdot-}$BQ) via two identical decay pathways. Compared with a porphyrin quinone dyad, the enhanced rate of PeT demonstrated for the tetrad is in line with the increase of the first reduction potential of the naphthoquinone arising from interactions with the attached benzoquinone moieties. There was no indication of direct singlet transfer from the initial excited state of the porphyrin to the benzoquinone.

1.4.2 Model systems with Porphyrins as electron donors and Fullerene as acceptors

In the past 5 years, research on mimicking photosynthetic apparatus has extended to fullerene which replaces quinone as the acceptor in such systems.[22, 23, 24, 25] The small total reorganisation energy of fullerene makes this an attractive alternative since according to the Marcus-Hush treatment,[26, 27] low reorganisation energy leads to greater rates of electron transfer at lower driving forces. Moore has synthesised and investigated the triad shown in figure 1.8.

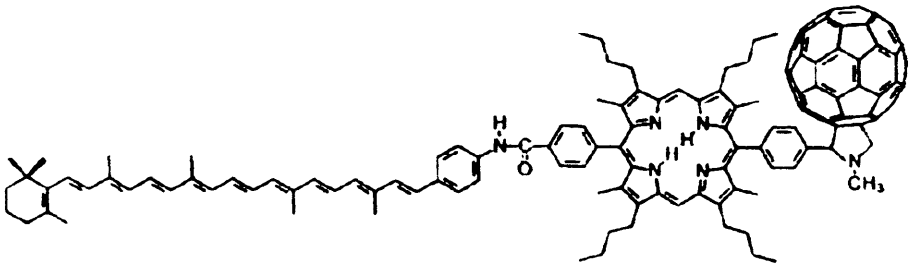

Figure 1.8: Carotenoporphyrin-fullerene triad (C-P-C_{60}) synthesised and investigated by Moore and Gust[22, 23]

The events following excitation of the triad are shown in figure 1.9.[23] With regards to formation of the triplet state, compared with its porphyrin-fullerene analogue, the two step electron transfer occurring for the triad, actually increases the

lifetime of charge separation by a factor of almost 1000. For the majority of model systems PeT ceases at low temperatures when the solvent becomes glassy, however this triad allows the formation of $C^{\cdot+}$-P-$C_{60}^{\cdot-}$ in glass at 8K. Transient dc photocurrent measurements by Moore and co-workers on the triad demonstrated that the $C^{\cdot+}$-P-$C_{60}^{\cdot-}$ charge separated state has a vast dipole moment close to 160 D.[22] It is interesting to note that the intermediate C-^{3}P-C_{60} converts to ^{3}C-P-C_{60} at a high rate, reflecting quenching of chlorophyll triplets by carotenoids in nature, in order to ensure that light-induced damage due to chlorophyll sensitised singlet oxygen formation does not occur.

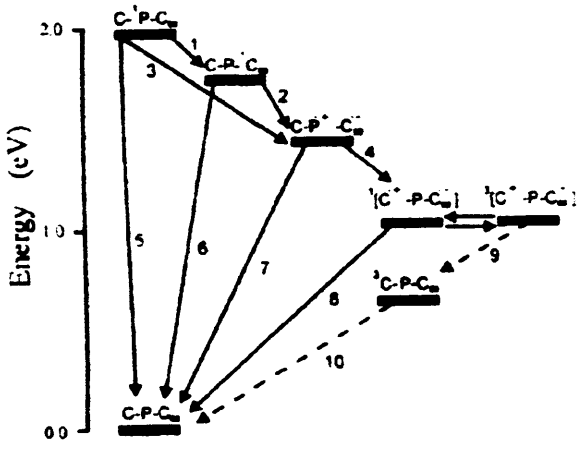

Figure 1.9: Energy states and interconversion pathways for carotenoporphyrin-fullerene triad[23]

Extension of these ideas to the development of artificial light harvesting antennas has attracted much attention. Moore and co-workers have studied the hexad shown in figure 1.10.[23] Time-resolved spectroscopic studies have demonstrated that excitation of one of the peripheral zinc porphyrins results in energy transfer to the central zinc porphyrin to give $(P_{Zn})_3$-$^1P_{Zn}$-P-C_{60}. Following this is migration of the singlet energy to the non-metallated porphyrin and ultimately decay to form the charge separated state $(P_{Zn})_3$-P_{Zn}-$P^{\cdot+}$-$C_{60}^{\cdot-}$ with a quantum yield and lifetime of 0.7 and 1.3 ns respectively. Arrays like the example shown here mimic the light-harvesting

antennas in addition to the reaction centre energy transfer, hence interest in synthesising larger arrays to afford complexes with longer lifetimes and higher quantum yields for charge separation is an area which has received much attention in recent years.[28-31] This shall be discussed in more detail later.

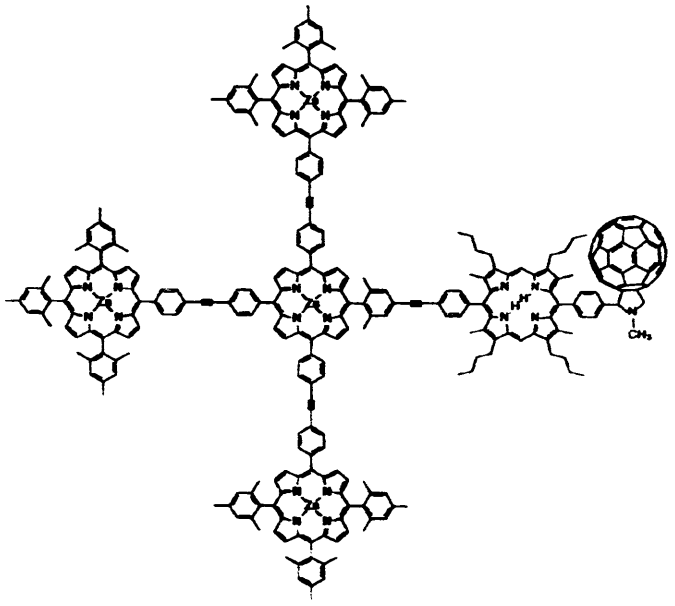

Figure 1.10: Hexad prepared by Gust and Moore[23]
$(P_{Zn})_3$-P_{Zn}-P-C_{60} (Peripheral zinc porphyrins-central zinc porphyrin-fullerene)

Resulting from the experience gained by Moore and co-workers on previous studies,[22,23] compound **1** shown in figure 1.11 was synthesised which incorporates mesityl groups at the 10 and 20 position of the porphyrin.[24] The major advantage in using the mesityl groups was their tendency to increase solubility. Spectroscopic investigation verified that formation of the $C^{\cdot+}$-P-$C_{60}^{\cdot-}$ state occurs with a yield close to unity (0.95). Again behaviour reminiscent to natural photosynthesis is observed with

charge recombination to the triplet state occurring.

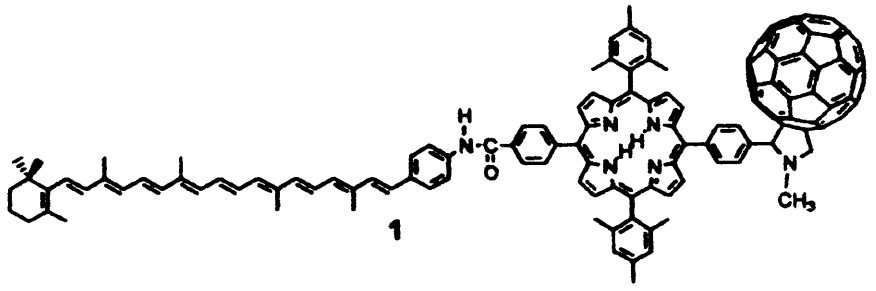

Figure 1.11: Triad **1** synthesised by Moore, Gust and co-workers[24]
C-P-C_{60} (Carotenoid-porphyrin-fullerene)

The idea that a second porphyrin attached to a porphyrin-fullerene dyad may enhance the light harvesting character prompted Moore and Gust to prepare the triads shown in figure 1.12.[25]

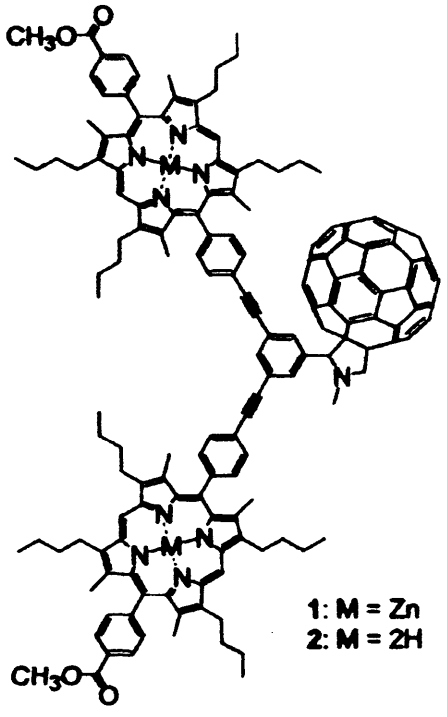

Figure 1.12: Diporphyrin-fullerene triads **1** and **2**[25]

The zinc triad showed PeT which was ten times faster than for the free base analogue. This may be explained in terms of the energy levels of the excited states shown in figure 1.13. The increased driving force of the zinc triad shown by scheme **a** (0.36V) compared to the free base shown by scheme **b** results in an increased rate of PeT for the zinc array. Additionally, for the zinc triad, the rate of charge recombination is greater. Even though the driving force for this is smaller than for the free base, it is evident that this reaction occurs in the inverted region of the Marcus-Hush[26,27] relationship where decreased driving force gives rise to an increased rate constant. Addition of the *meta*-phenyleneethynylene groups to the triad **2** was found to decrease the rate of PeT by a factor of 60 (which is relatively small) compared to an analogue minus these linking groups. Nevertheless, the phenyleneethylene orbitals assist electron transfer by a superexchange mechanism and these functional groups have been proven to be good electron transfer "wires" resulting from the highly conjugated π bonds of the phenyleneethylene linking groups.[32] Again the presence of two porphyrin molecules in the array enhanced the cross section for absorption of light energy.

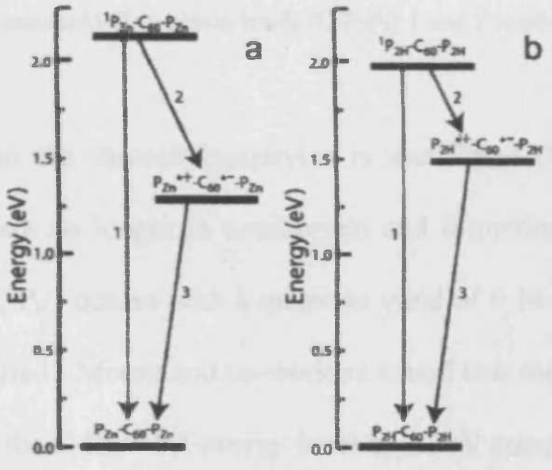

Figure 1.13: Energy states of triads 1 (a) and 2 (b) and interconversion pathways[25]

1.4.3 Porphyrins as donors and acceptors in model Reaction centres

A recent study by Moore and Gust[33] is dedicated to a triad consisting of two porphyrin macrocycles and a carotenoid. Porphyrins are used here as the electron donors and acceptors. The insolubility of fullerene derivatives in membranes forces a limitation on their use as electron acceptors. Also porphyrins are in fact the first electron acceptors found in natural photosynthetic apparatus. The triad shown in figure 1.14 undergoes PeT from the singlet state of dimesitylporphyrin (P) to the tris(heptafluoropropyl)porphyrin (P_F) to yield the charge separated state C-$P^{\cdot+}$-$P_F^{\cdot-}$. Electron transfer from the carotenoid results in the ultimate charge separaed state $C^{\cdot+}$-P-$P_F^{\cdot-}$ which decays to the triplet caroteniod state.

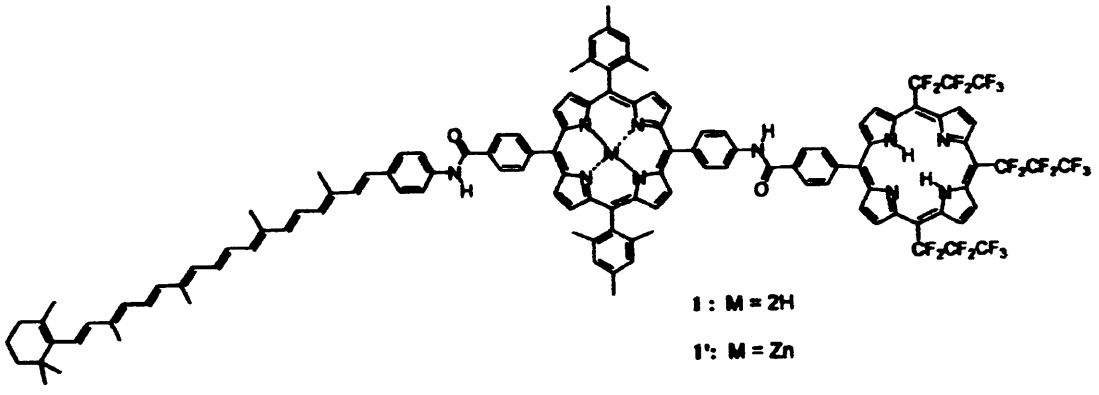

Figure 1.14: Carotenoid-diporphyrin triads (C-P-P_F) 1 and 2 synthesised by Moore and Gust[33]

When the dimesitylporphyrin is metallated (P_{Zn}), the excited states of the porphyrins are no longer in equilibrium and formation of the final charge separated state $C^{\cdot+}$-P_{Zn}-$P_F^{\cdot-}$ occurs with a quantum yield of 0.14 as opposed to 0.73 in the non-metallated triad. Moore and co-workers found that metallation in triad **1'** results in a lowering of the C-$P_{Zn}^{\cdot+}$-$P_F^{\cdot-}$ energy level by 0.2eV compared with triad **1** and therefore lowering the driving force explains why the quantum yield is reduced in the metallated case **1'**. It is thought that this difference of 0.2 eV also accounts for the

different mechanisms observed for the charge recombination processes. Recombination of the final charge separated state to the triplet carotenoid state echoes that observed in natural photosynthesis. Since PeT for both triads investigated was observed even at low temperatures, and charge recombination to the triplet carotenoids occurred, such systems incorporating porphyrins as donors and acceptors were shown to demonstrate properties very similar to those occurring in natural reaction centres. Despite the decreased quantum yield observed for the metallated triad **1'**, the increased driving force for this reaction (+0.2 eV) makes it appealing for use in artificial biological membranes which possess low dielectric environments.

1.5 Light-harvesting ability of Porphyrins

Returning to a purely light-harvesting perspective, much work has been carried out in recent years. Photosynthetic organisms are able to capture low intensity sunlight utilising light-harvesting complexes and funnel this energy to the reaction centres. The efficiency of light-harvesting complexes in transferring the harvested energy through a vast number of pigments whilst avoiding quenching is extraordinary. The design of synthetic molecular devices to mimic natural photosynthesis is a topic which has attracted a great amount of interest since more information regarding mechanisms occurring at the molecular level is required in order to fully comprehend photosynthesis.

The desired architecture for an efficient light-harvesting system requires a large number of accessory pigments that absorb light energy and transfer the resulting electronic excited energy to an acceptor with high efficiency. Selection of the appropriate pigments is not the only factor determining the efficiency of the structure. Planning of the three-dimensional architecture is a challenge to all that research this area of science.[34] Factors which influence the architecture include interpigment distances and orientations, chromophore substituents, linker types and pigment connection points. Without consideration of these aspects, there would be no control of essential properties such as mechanisms, efficiency and rates of energy transfer, direction of energy flow, spectral coverage, and efficiency of light-absorption in addition to solubility.

1.5.1 Mulitiporphyrin light-harvesting arrays

Many research groups are currently pursuing the design of porphyrin arrays for use in light-harvesting model systems. Lindsey and co-workers carry out significant research in this area. Their focus lies in the design of rigid, soluble arrays of covalently linked porphyrins in various metallation states.[28-31] Linking of the porphyrins has been achieved using homogeneous Pd-mediated coupling reactions under basic conditions. A number of impressive arrays have been prepared and are shown in figure 1.15. The main problems encountered in the preparation of these arrays were maintaining high yields, minimising butadiyne-linked dimer formation, maintaining solubility and ensuring metallation states were not affected. Rotation about the ethylene unit is allowed even though the centre-to-centre porphyrin distances are fixed. The use of a diphenylethyne spacer was found to provide rigid centre-to-centre distances which are an appropriate length for efficient light-harvesting.

In the case of the pentameric array shown overleaf,[28] the free base array and the zinc array displayed fluorescence emission yields characteristic of monomeric porphyrins indicating the absence of quenching processes.[31] The successful preparation of the pentameric porphyrin array prompted Lindsey and co-workers to attempt the synthesis of more elaborate arrays, the largest containing 21 porphyrin chromophores also illustrated in figure 1.15.[31]

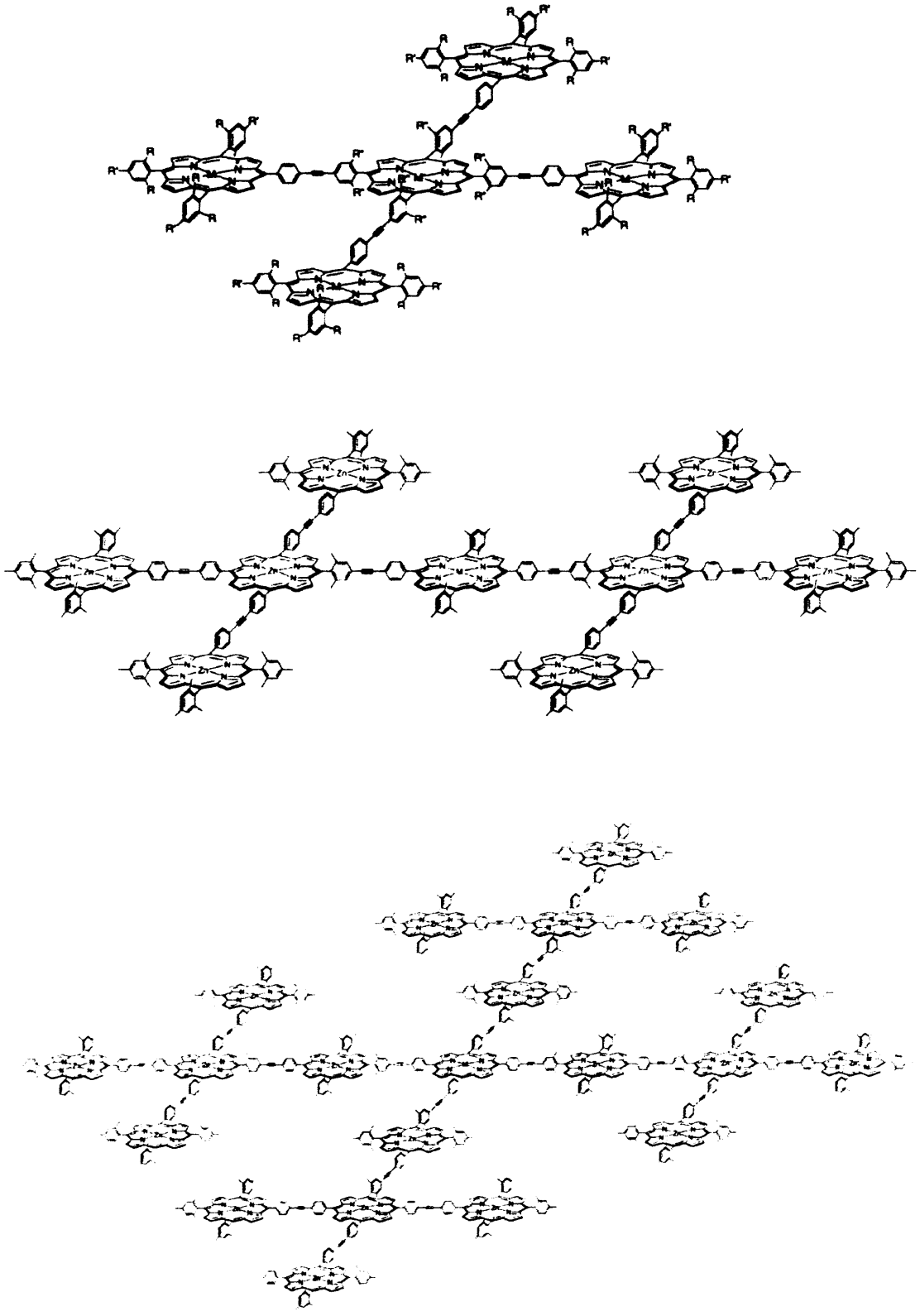

Figure 1.15: Porphyrin arrays prepared by Lindsey and co-workers

The synthesis of the larger porphyrin arrays by Lindsey and co-workers was achieved in a convergent manner (the periphery of the array is constructed first and synthesis proceeds inward towards the core) since this was found to yield fewer side products. Investigations by the group revealed that the most favourable coupling conditions employed tris(dibenzylidineacetone)dipalladium(0) in conjunction with triphenylarsine in toluene/triethylamine under anaerobic conditions at 35°C.[29]

In terms of UV/Vis absorption spectra, as the arrays increase in size, certain characteristics change whilst others remain the same. For instance, the Soret band which arises from excitation from the ground state to the second excited state (S_0-S_2) is found to red shift and split as the number of porhyrins in the array increases. This can be attributed to "pronounced exciton interactions between the large transition dipoles of the Soret transitions of adjacent porphyrins". The Q bands remain virtually unchanged however it is noteworthy that their extinction coefficients increase with increasing number of porphyrins in the array. This feature means that a larger optical cross section exists for the larger arrays thus enhancing the light-harvesting function. The vast increase in the extinction coefficients of the overlapping S_0-S_1 absorption bands of the light absorbing Zn porphyrins compared to the Fb (non-metallated or free base as it is commonly known) porphyrin acceptor is another factor reflecting the enhancement in light-harvesting ability of larger porphyrin arrays. Together the absorption and emission results for these multiporphyrin arrays established that relatively weak perturbations between the porphyrin excited states occurred and the excited state decay process appeared to be the same in the monomer as in the very large arrays. Energy transfer from the peripheral porphyrins to the core porphyrin was investigated using time-resolved absorption studies. The overall energy-transfer

efficiencies for all the arrays investigated were 92-98%. The major limitation of this work was the use of extensive and complex chromatography to isolate the large arrays in pure form.

1.5.2 Cyclic Porphyrin light-harvesting arrays

Further studies carried out by Lindsey and co-workers were based on the preparation of a shape-persistent cyclic hexameric array of covalently linked porphyrins possessing a cavity of approximately 35 Å.[30] Figure 1.16 illustrates how the cavity size was proved ideal for binding a tripyridyl template (**1**) or a trans-dipyridyl substituted porphyrin (**2**) with high affinity.

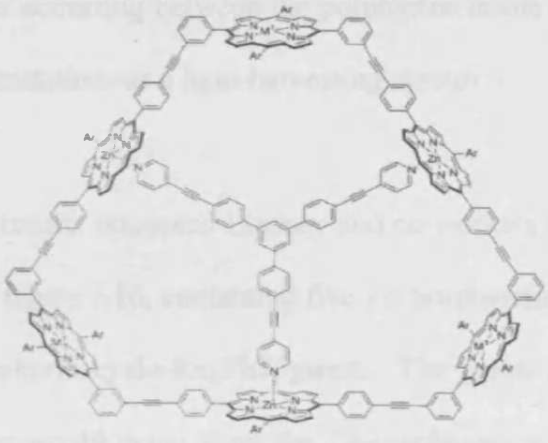

cyclo-Zn_3Fb_3U-1 Ar = mesityl; M^1 = H,H

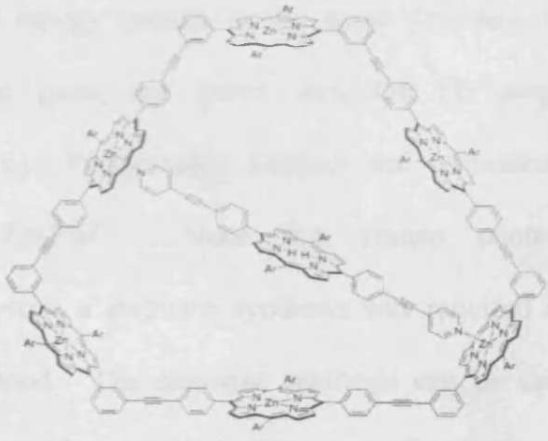

cyclo-Zn_6U-2 Ar = mesityl

Figure 1.16: Cyclic Hexameric Porphyrin Arrays synthesised by Lindsey

The light-harvesting array was prepared via a one-pot template directed synthesis. The linking of the porphyrin building blocks was achieved via the Sonogashira Pd-mediated coupling reaction. Clearly, various metallation patterns of the porphyrin cyclic array were prepared, allowing Lindsey and co-workers to study and attempt to control the flow of excited-state energy in these self-assembled light-harvesting arrays. Energy transfer within the cyclic array is via a through-bond process. The excited state energy of the Zn-porphyrin in **1** was found to lower upon co-ordination of the tripyridyl template guest and in **2** it was revealed that through-space energy transfer from any porphyrin in the cycle to the central free base porphyrin is possible. This transfer however is slow compared with the through-bond energy transfer occurring between the porphyrins in the wheel hence structure **2** will have certain limitations as a light-harvesting system.

These results prompted Lindsey and co-workers to construct arrays similar to structure **2** of figure 1.16, containing five Zn porphyrins and one non-metallated/free base (Fb) porphyrin-**cyclo-Zn_5FbU-guest.** The group envisaged that through-bond energy transfer would occur from the Zn porphyrins to the Fb porphyrins and then through-space energy transfer to the guest providing that the excited state energy levels of the guest are lower than the Fb porphyrin (eg. Phthalocyanine, bacteriochlorin). Furthermore, Lindsey and co-workers achieved the synthesis of **cyclo-$Zn_2Fb_2Zn_2$FbU**. Since this system contains a diverse pattern of metalloporphyrins, a stepwise synthesis was required instead of the formerly used one-flask method. The stepwise synthesis can be carried out in the presence or absence of a template while the presence of a template is essential for the one-pot

synthesis. Studies by the group regarding energy-transfer of the structures formed once the arrays are bound with the guests are ongoing.

1.6 Alternative linking group-Diphenylbutadiyne linked Porphyrins

In addition to the Sonogashira reaction,[35] Lindsey and co-workers have also used the Glaser coupling reaction[36] to yield a diphenylbutadiyne unit as the spacer group.[37] Figure 1.17 illustrates the dyads formed in the early stages of this work by the group. Copper insertion is avoided using magnesium porphyrin as the latent form of free base porphyrin which also aids in separation techniques. The Glaser reaction is relatively clean unlike the Sonogashira which yields a number of side products. It was therefore thought that the Glaser reaction would be preferable for the construction of multiporphyrin arrays. The individual properties of the monomers were retained as demonstrated and a through-bond energy transfer process was found to dominate. It was concluded that the diphenylbutadiyne linker allows fast and efficient energy transfer between the two porphyrins composing the dyad, comparable to that of the previously discussed diphenylethyne linker.

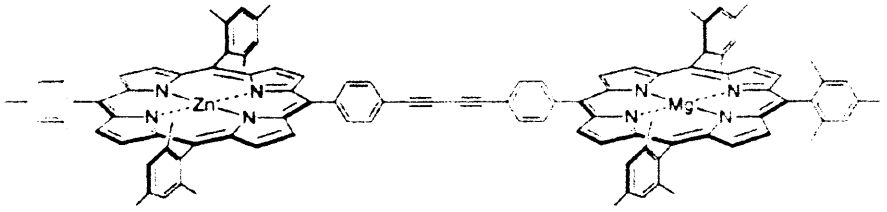

Figure 1.17: Porphyrin Dyad synthesised via the Glaser coupling reaction by Lindsey and co-workers

1.7 Polypyridine complexes in promoting energy transfer

In addition to porphyrins, transition metal polypyridine complexes are currently being used to develop our knowledge and understanding of the underlying mechanisms of photosynthesis. It is evident that the transition metal plays an important role in promoting fast energy transfer between states normally forbidden by spin multiplicity conservation rules. Attention to the design and synthesis of porphyrin-polypyridine arrays has become popular in the last decade and many groups have prepared molecular arrays in order to examine the energy transfer processes occurring between them.[38-40]

The group of Sauvage have determined the photoinduced processes occurring at low temperature in the molecular arrays shown in figure 1.18.[38] These compounds were found to favour energy-transfer processes with respect to the desired electron transfer resulting in these compounds failing to be of use in the study of charge separation. A lower reorganizational energy is required by energy-transfer processes than electron transfer. Nevertheless in terms of energy transfer, these compounds were found to display a variety of functions which allows them to be utilised as models for the photosynthetic system.

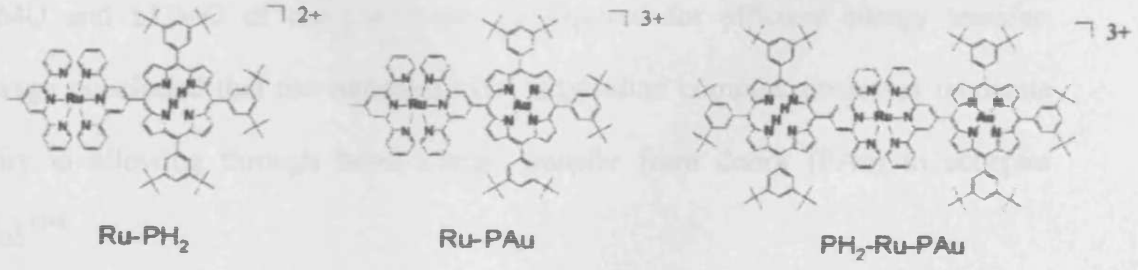

Figure 1.18: Multicomponent Arrays synthesised by Sauvage and co-workers

Long-range energy transfer from the triplet localized on the gold (III) porphyrin to the free-base porphyrin-localized triplet state was found to be non-existent at room temperature due to poor ability by the ruthenium complex to efficiently couple donor and acceptor in addition to the short lifetime of the donor. Repeating the investigation at low temperature, Sauvage and co-workers discovered that the phosphorescence of the gold (III) porphyrin could be quenched and that of the free-base porphyrin enhanced. Triplet energy transfer in these systems is exchange type in nature meaning that it involves concerted migration of an electron and a hole from donor to acceptor moieties. The migration from the ruthenium complex to either porphyrins in the triad is very fast and it was found to favour the gold (III) porphyrin. The energy transfer steps for this process are found to be through-space electron exchange. Triplet-triplet transfer from porphyrin to porphyrin in Sauvages' system was slower and since overlap of donor-acceptor orbitals is not an option, the transfer must utilise the ruthenium complex spacer. At such low temperatures, the intermediate PH_2-^{3}Ru-PAu is not possible. Closs and co-workers[41, 42] have studied the electron and hole transfers of bridging ligands. It is postulated that the electron transfer involves LUMO orbitals of the spacer which are higher than LUMO of donor and acceptor and hole transfer involves HOMO of the spacer lower than HOMO of donor and acceptor. Hence coupling of the HOMO and LUMO of the spacer with HOMO and LUMO of the porphyrins is required for efficient energy transfer. Sauvage concluded that the ruthenium (II) terpyridine complex possesses moderate ability in allowing through bond energy transfer from donor (PAu) to acceptor (PH_2).[38]

Similar studies have been undertaken by Ziessel and co-workers.[39] This involves energy transfer in molecular dyads consisting of metalloporphyrin and ruthenium (II) tris(2,2'-bipyridyl) where the spacer group is a trans Pt (II) bis-acetylide fragment bearing 2 tri-*n*-butylphosphine moieties. The structure of this supermolecule is shown in figure 1.19. The metal-to-ligand, charge-transfer absorption bands seemed well positioned for the Ru(II) complex to act as an acceptor for photons which are harvested by the porphyrin Soret band and it had been previously demonstrated that that the Pt(II) bis-acetylide may facilitate through-space instead of through-bond interactions.[43]

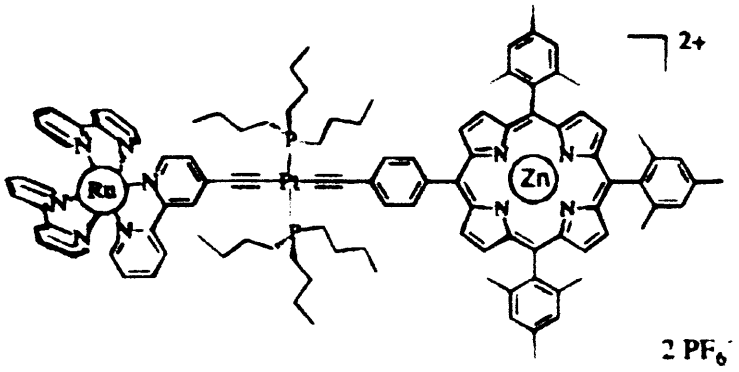

Figure 1.19: Supermolecule prepared by Ziessel and co-workers

Electrochemical studies concluded that the Pt(II) bis-acetylide spacer makes it more difficult for reduction of either fragments to occur. This has been attributed to charge donation from the Pt(II) centre to both terminals of the dyad. It was concluded by Ziessel and co-workers that the bipyridine-porphyrin dyad displays a variety of energy-transfer processes as follows: ultrafast singlet to singlet, fast triplet to triplet, fast singlet to triplet and possibly slow triplet to singlet. Virtually all the energy absorbed by the dyad results in the formation of the triplet excited state of Zn porphyrin and leading to this the singlet to singlet energy transfer from the S_2 (Soret)

porphyrin level to the Ru complex is far more rapid (1000-fold rate) than energy transfer from the S_1 (Soret) porphyrin level due to improved spectral overlap.

Ziessel and co-workers demonstrated the first example of a porphyrin based dyad by which reactions occur from the porphyrin S_2 level as opposed to the S_1 level. Further studies regarding this matter are underway since the only benefit of the system shown here in terms of the S_2 level was a faster rate. The Pt (II) bis-acetylide spacer showed promise in through-space electron transfer in contrast to polyacetylene spacers which promote through-bond transfer. The studies indicated the lack of excited states by the spacer to participate in the overall photoprocesses, hence demonstrating that the Pt (II) spacer could be vital in artificial light harvesting where it is important to eliminate extra electron transfer contributions.

Further work on this topic has been carried out by Branda and co-workers whose focus has been upon the assembly of a stable hydrogen-bonded porphyrin-iron(terpyridine) ion pair.[40] Since naturally occurring light harvesting systems depend on non-covalent interactions to correctly position chromophores, hydrogen bonding is considered an effective and simplistic way of designing such systems to mimic the abilities of those found in nature. The drawback of using hydrogen bonding in these systems is the limit in the choice of solvents available, however alternative methods which make use of ionic hydrogen bonding motifs composed of hydrogen bond partners of opposite charge make such bonding an appealing choice. The neutral complex displayed in figure 1.20, was designed and prepared by Branda and co-workers.[40] Mixing of equimolar quantities of porphyrin and iron terpyridine ions in methanol precipitated the desired compound shown.

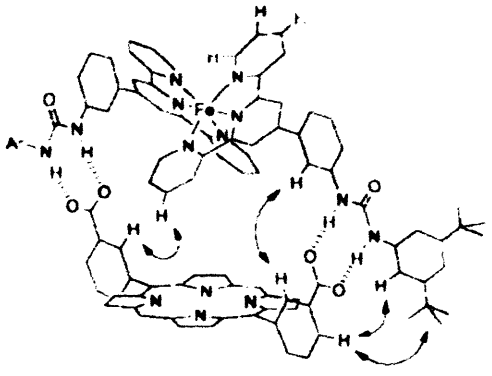

Figure 1.20: Complex prepared by Branda and co-workers

NMR spectra results indicate that the terpyridine complex is held directly over the porphyrin plane and is able to rotate slowly above the ring. An impressive value for the association constant was found which led to further studies which revealed that ion pairing is the major factor in the formation of this compound. However the hydrogen bonds present appear to maximise the efficiency of the ion pairing by close alignment of the two moieties. Fluorescence studies by the group indicated that rapid quenching of the porphyrin fluorescence took place when treated with a sample of the iron terpyridine unit due to the straddling nature of the terpyridine which allows close proximity of the two sub-units in order that the through-space communication is at its greatest efficiency. Such a system can be used as a starting point to develop further understanding of the electronic communication in photosynthesis. Altering the structure of the terpyridine fragment to the *N,N'*-dimethylated form forbids the above arrangement which has a significant impact upon its photophysical properties, in that quenching by the iron terpyridine is only slight. This is also true when rearranging the positioning of the hydrogen and carboxylate functions of the porphyrin. Additionally, the group have demonstrated similar photophysical properties of the successful supermolecule in a 10% H_2O/MeCN environment confirming the high association of the units.

1.8 Aims

Much interest and research has arisen towards the charge separated states formed in Photosystem II following light harvesting and energy transfer to the reaction centre. These charge separated states are composed of a series of linked electron donors and acceptors. We set out to synthesise and investigate a series of new photoactive compounds, which could be used as potential components in mimics of Photosystem II.

In addition to synthesis of the compounds (donors and acceptors), we also set out to investigate routes used to link the components. Since the electronic couplings between the individual donors and acceptors are a major factor in determining the rate of Photoinduced electron transfer (PeT), it is important that the linking groups are capable of efficient energy transfer, without the involvement of quenching.

Since our aim is to synthesise novel compounds to act as efficient electron donors and acceptors, we have focused on the donors and acceptors separately. Studies have been carried out on quinones, porphyrins and phenol containing ligands. Each of these will be discussed in the following three chapters.

1.9 References

1) A. Emerson, W. Arnold, *Gen. Physiol.*, 1932, **16,** 191-205.

2) T. Förster, *Ann. Phys.* (Leipzig) 1948, **2**, 55-75.

3) J. Oppenheimer, *Phys. Rev.* 1941, **60**, 158.

4) D. Dexter, *J. Chem. Phys.*, 1953, ***21****, 836.*

5) J. Deisenhofer, O. Epp, K. Miki, R. Huber, H. Michel, *J. Mol. Biol.*, 1984, **180**, 385.

6) K. Schulten, Simplicity and complexity in Proteins and Nucleic Acids, 1999 Dahlem University press, Chapter 14, 227-254.

7) H. Zuber, R. Brunisholz, Principles and variability in Chlorophylls, ed. H. Scheer, 1991, 627-692.

8) K. Miller, *Nature*, 1982, **300**, 53-55.

9) T. Walz, R. Ghosh, *J. Mol. Biol.*, 1997, **265**, 107-111.

10) T. Monger, W. Parson, *Biochim. Biophys. Acta*, 1977, **460**, 393-407.

11) R. van Grondelle, J. Dekker, T. Gillbro, V. Sundstrom, *Biochim. Biophys. Acta*, 1994, **1187,** 1-65.

12) M. Momenteau, B. Loock, P. Seta, E. Bienvenue, B. d'Epenoux, *Tetrahedron*, 1989, **Vol. 45**, No. 15, 4893.

13) P. Seta, E. Bienvenue, A. Moore, P. Liddell, P. Mathis, R. Benasson, P. Pessiki, A. Joy, T. Moore, D. Gust, *Nature*, 1985, **316**, 653.

14) P. Beer, S. Kurek, *J. Organometallic Chem.*, 1989, 366, C6-C8.

15) D. Kuciauskas, P. Liddell, S. Hung, S. Lin, S. Stone, G. Seely, A. Moore, T. Moore, D. Gust, *J. Phys. Chem. B.*, 1997, **101**, 429-440.

16) G. Steinberg-Yfrach, P. Liddell, S. Hung, A. Moore, T. Moore, D. Gust, *Nature*, 1997, **Vol. 385,** 239.

17) J. Sumida, P. Liddell, S.Lin, A. Macpherson, G. Seely, A. Moore, T. Moore, D. Gust, *J. Phys. Chem. A,* 1998, **102**, 5512-5519.

18) S. Hung, S. Lin, A. Macpherson, A. Degraziano, J. Kerrigan, P. Liddell, A. Moore, T. Moore, D. Gust, *J. Photochem. Photobiol. A: Chem,* 1994, **77,** 207-216.

19) J. Springer, G. Kodis, L. de la Garza, A. Moore, T. Moore, D. Gust, *J. Phys. Chem. A*, 2003, **107**, 3567-3575.

20) O. Korth, A. Wiele, H. Kurreck, B. Röder, *Chem. Phys.*, 1999, **246**, 363-372.

21) D. Gust, T. Moore, A, Moore, A. Macpherson, A. Lopez, J. DeGraziano, I. Gouni, E. Bittersmann, G. Seely, F. Gao, R. Nieman, X. Ma, L. Demanche, D. Luttrull, S. Lee, P. Kerrigan, *J. Am. Chem. Soc.*, 1993, **115,** 11141.

22) S. Smirnov, P. Liddell, I. Vlassiouk, A. Teslja, D. Kuciauskas, C. Braun, A. Moore, T. Moore, D. Gust, *J. Phys. Chem.A*, 2003, **107**, 7567-7573.

23) D. Gust, T. Moore, A. Moore, *Acc. Chem. Res.*, 2001, **34**, 40-48.

24) G. Kodis, P. Liddell, A. Moore, D. Gust, *J. Phys. Org. Chem.*, 2004, **17,** 724-734.

25) P. Liddell, G. Kodis, D. Kuciauskas, J. Andreasson, A. Moore, T. Moore, D. Gust, *Phys. Chem. Chem. Phys.*, 2004, **6**, 5509-5515.

26) R. Marcus, *J. Chem. Phys.*, 1956, **24**, 966-978.

27) N. Hush, *J. Chem. Phys.*, 1958, **28**, 962-972.

28) S. Prathapan, T.E Johnson, J.S Lindsey, *J. Am. Chem. Soc.*, 1993, **115**, 7519

29) R.W. Wagner, T.E. Johnson, F. Li, J.S. Lindsey, *J. Org. Chem.*, 1995, **60,** 5266.

30) L. Yu, J.S. Lindsey, *J. Org. Chem.*, **66, No. 22,** 2001, 7403.

31) M. del Rosario Benites, T.E. Johnson, S. Weghorn, L. Yu, P.D Rao, J.R. Diers, S.I. Yang, C. Kirmaier, D. F. Bocian, D. Holten, J.S. Lindsey, *J. Materials Chem.*, 2002, **12,** 65.

32) A. Harriman, R. Ziessel, *Chem. Commun.*, 1996, 1707.

33) S. Gould, G. Kodis, R. Palacios, L. de la Garza, A. Brune, D. Gust, T. Moore, A. Moore, *J. Phys. Chem. B.*, 2004, **108**, 10566-10580.

34) F. Li, S. Yang, Y. Ciringh, J. Seth, C. Martin, D. Singh, D. Kim, R. Birge, D. Bocian, D. Holten, J. Lindsey, *J. Am. Chem. Soc.*, 1998, **120,** 10001-10017.

35) K. Sonogashira, Y. Tohda, N. Hagihara, *Tet. Lett.* 1975, 4467.

36) C. Glaser, *Am. Chem. Pharm.*, 1870, **154**, 137.

37) W.J. Youngblood, D.T. Gryko, R.K. Lammi, D.F. Bocian, D. Holten, J.S. Lindsey, *J. Org. Chem.*, 2002, **67**, 2111.

38) L. Flamigni, F. Barigelletti, N. Armaroli, B. Ventura, J.P. Collin, J.P. Sauvage, J.A.G. Williams, *Inorg. Chem.*, 1999, **38**, 661.

39) A. Harriman, M. Hissler, O. Trompette, R. Ziessel, *J. Am. Chem. Soc.*, 1999, **121,** 2516.

40) T. B. Norsten, K. Chichak, N.R. Branda, *Chem. Comm.*, 2001, 1794.

41) G.L Closs, P. Piotrowiak, J.M. MacInnis, G.R. Fleming, *J. Am. Chem. Soc.*, 1988, **110**, 2652.

42) G.L. Closs, M.D Johnson, J.M. Miller, P. Piotrowiak, *J. Am. Chem. Soc.*, 1989, **111**, 3751.

43) 43) V. Grosshenny, A. Harriman, M. Hissler, R. Ziessler, *J. Chem. Soc., Faraday Trans.*, 1996, **92,** 2223.

Chapter 2

Quinones

2.1 Introduction to Quinones

Quinones are planar molecules, which are widespread in nature and produced synthetically by chemical industries. In nature, quinones are found in plants, fungi, bacteria and animals and are involved in photosynthesis (see chapter 1) as well as respiration and blood coagulation.[1] They range from pale yellow to black in colour, hence their primary use lies in the organic dye area, for example colour photography, electrophotography and lasers.[2] Their use also lies in many other areas such as biological activity.[3-12] The three main classes of quinones which exist are benzoquinones (figure 2.1-**1**), naphthoquinones(**2**) and anthraquinones(**3**).

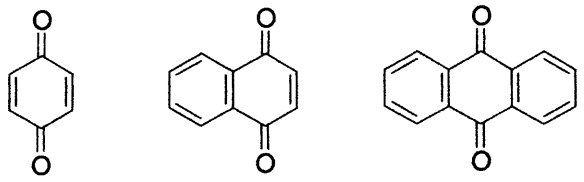

1 **2** **3**

Figure 2.1

Quinones are very efficient electron acceptors and many photosynthetic models exploit this factor using quinones as the electron acceptor species and porphyrins as the electron donors (refer to chapter 1). The electron accepting capabilities of quinones allows electrochemical analysis of them to be undertaken and this shall be discussed in more detail later.

2.2 Synthesis of Quinones

The main methods for preparing quinones in acceptable yields from non-quinonoidal precursors can be divided into four categories; Oxidative, Cyclization, Condensation and Annellation. Each of these is summarised as follows:

Oxidative methods

The substrate is usually phenolic and conversion into a quinone is carried out using Fremys' salt (potassium nitrosodisulphate). The Teuber reaction[13] for oxidation of phenols occurs under mild conditions from relatively cheap reagents and is a very efficient (> 70% yield) and rapid reaction. It is however inconvenient for large scale preparations. It is carried out in aqueous alcohol buffered with phosphate or acetate at room temperature. The mechanism proposed by Teuber[13] is shown in figure 2.2.

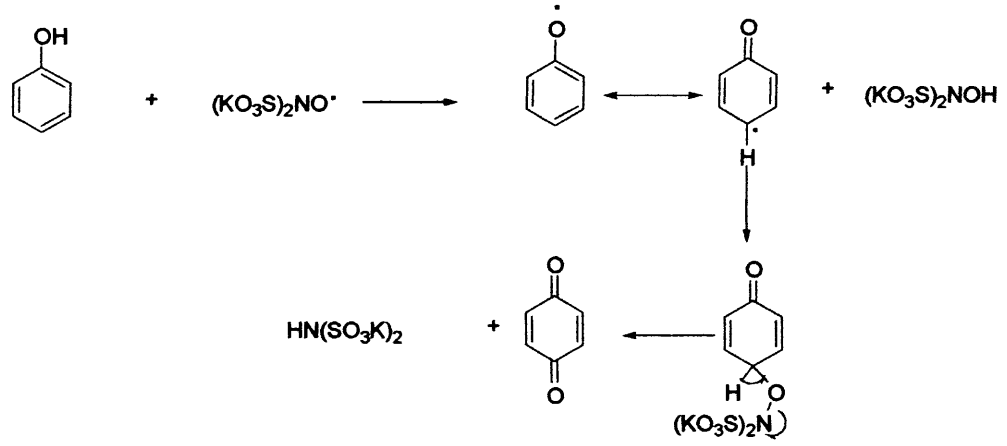

Figure 2.2: Mechanism for the Teuber reaction

Other oxidising agents are ferric chloride[14] and the hexachloroiridate anion.[15] These are 1-electron oxidants and unlike generating radicals, as does Fremys' salt, they generate cations in just 2 steps. Yields however are low. Figure 2.3 illustrates the reaction.

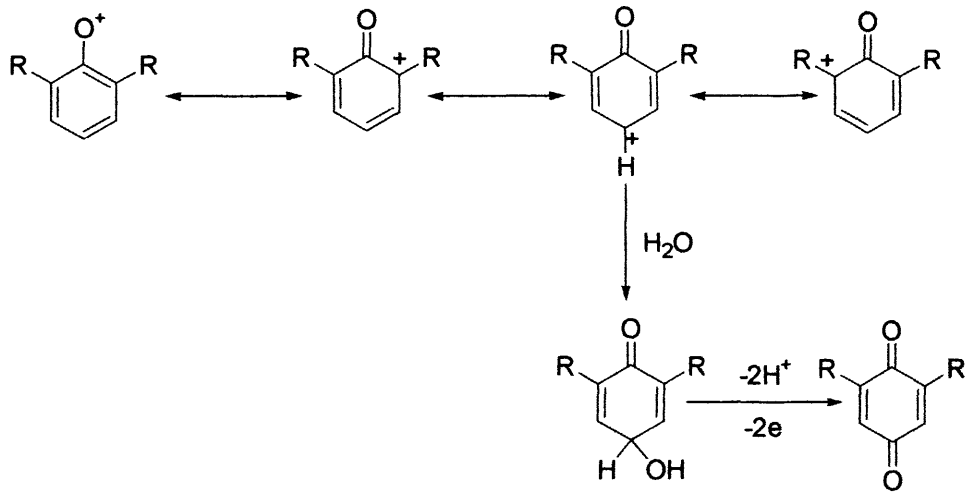

Figure 2.3: Scheme for oxidation of phenol by 1-electron oxidant

By far the easiest method for the synthesis of *p*-quinones is the oxidation of quinols. This involves the removal of 2 electrons and 2 protons using oxidants such as chromic acid, ferric ion or silver oxide.[16] It is noteworthy that quinones themselves are mild oxidants.

Cyclization methods

O-benzoylbenzoic acids are widely used in anthraquinone synthesis. Figure 2.4 shows the substrate **4** which is cyclized to **5** via an internal Friedel-Crafts reaction, normally by heating in sulphuric acid.[16]

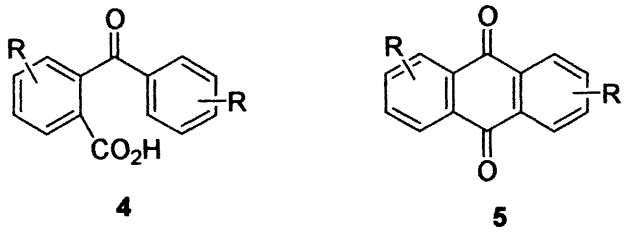

Figure 2.4: Friedel-Crafts cyclization

Another cyclization method available for the preparation of quinones is the Scholl reaction.[17] The reaction is considered to be an electrophilic substitution followed by oxidation and evidence for the presence of radical cations exists. Scholl reactions are primarily used for the synthesis of larger polycyclic quinones. Aluminium chloride is generally used as the reagent, along with a protic acid. Yields are improved vastly when mixtures are oxygenated.

Condensation methods

The condensation of quinols with cyclic anhydrides is used to synthesise higher polycyclic quinones.[16] The reaction is carried out in a melt of anhydrous aluminium chloride-sodium chloride and yields rarely exceed 50%. The reaction proceeds by formation of a keto-acid followed by cyclization under harsh conditions. A similar reaction (figure 2.5) is the condensation of 1,4-diketones with a 1,4-naphthoquinol in acetic acid-hydrochloric acid mixture to synthesise anthraquinones.[16]

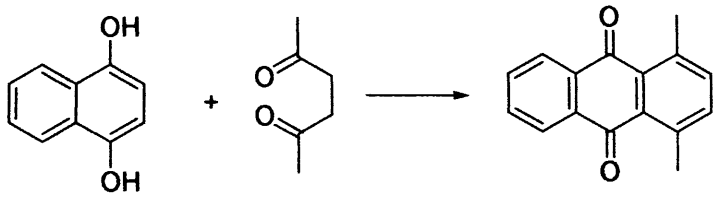

Figure 2.5: Condensation of 1,4-diketones with 1,4-naphthoquinol

Annelation method

The Diels-Alder reaction is widely used in quinone synthesis[16] since it is a very efficient way of fusing a benzene ring onto a quinone ring and generally yields are good. The steps are illustrated in figure 2.6 below.

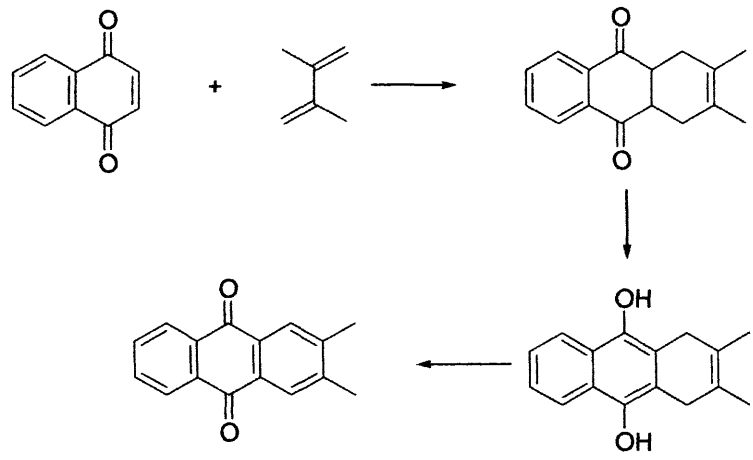

Figure 2.6: Scheme for Diels-Alder synthesis of quinones

Aromatization and oxidation may be accomplished in various ways, for example aeration in alkaline solution, warming in hydrochloric acid followed by addition of acid dichromate, nitrous acid followed by dehydrogenation using chromic acid or merely using hot nitrobenzene as the solvent, to name a few.[16]

2.3 Electrochemistry of quinones

Quinone/hydroquinone redox couples have been widely studied over the years and James Q. Chambers has written a detailed review on this.[18] The electron transfer rates and redox potentials of quinones have an influence on their biological action.[1] In aprotic solvents, quinones are reduced in two successive one electron steps. The second step is less reversible than the first and the product of the first step is the radical anion ($Q^{\cdot-}$), followed by the second step to give the quinone dianion(Q^{2-}).

$$Q + 2H^+ + 2e^- \leftrightarrow QH_2$$

OR

$$e^- + Q \leftrightarrow Q^{\cdot-}$$

AND

$$e^- + Q^{\cdot-} \leftrightarrow Q^{2-}$$

Early work on quinones was covered by Kolthoff and Lingane, Brezina and Zuman, Heyrovsky and Kuta, Mann and Barnes, Adams, Peover[19] and Patai.[18] The first report of a semiquinone radical anion was by Wawzonek and co-workers[20] and several years after this an ESR signal for the radical anion of anthraquinone by Austen and co-workers[21] confirmed this.

In order to clarify reversible (Nernstian) behaviour of a redox wave, a plot of peak height versus the square root of the scan rate should result in a straight line passing through the origin. The Nernst equation is as follows:

$$E = E^{0\prime} + RT/nF \ ln \ C_o/C_R$$

C_o and C_R correspond to the surface concentrations of oxidised and reduced species respectively and $E^{0'}$ refers to the formal reduction potential. Further information confirming reversibility includes the value of the peak potential separation being equal to 57/n mV and the peak current ratio being equal to one.

2.3.1 Cyclic Voltammetry of Benzoquinones

A cyclic voltammogram measured by Wigal and co-workers[1] for tetrachloro-1,4-benzoquinone in acetonitrile is shown in fig 2.7. Formal reduction potentials are determined for each step by taking an average value of the cathodic (causing reduction of quinone) and anodic (causing oxidation of hydroquinone) peak potentials.

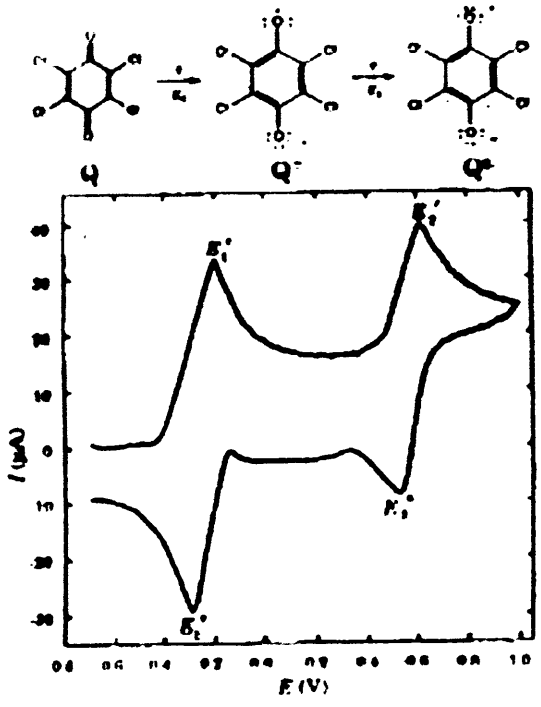

Figure 2.7: CV of tetrachloro-1,4-benzoquinone

2.3.2 The Hammett Parameter

The electronic properties of the substituents on the quinone determine the reduction potentials since groups, which are electron-withdrawing cause the reduction potentials to become more positive due to stabilisation of the quinone anion and dianion. Electron-donating groups have the opposite effect. The Hammett equation is used to determine the electronic properties of a substituent on an aromatic reaction centre:

$$\log K - \log K_0 = \log K/K_0 = \sigma\rho$$

K is the equilibrium constant for the substituted quinone

K_0 is the equilibrium constant for the parent quinone.

σ is the Hammett substituent

ρ is the reaction constant

If ρ has a positive value, this means that electron-withdrawing groups have the ability to enhance the reaction, whereas a negative value of ρ indicates the ability of electron-donating groups to do so. It is noteworthy that electron-withdrawing groups possess a positive σ value and electron-donating groups a negative value of the constant. K may also be expressed in the following way:

$$\log K = nFE^0/2.303RT$$

Upon combining and rearranging the previous two equations, the following evolves:

$$\log K/K_0 = (nF/2.303RT)\Delta E^0 = \sigma\rho$$

Table 2.1 illustrates Hammett and electrochemical data (1st reduction potentials) for a variety of substituted quinones measured by Wigal and co-workers.

Quinone	E^0	ΔE^0	$\Sigma\sigma$
1,4-Benzoquinone	-0.2586	0.0000	0.00
2,3-Dichloro-5,6-dicyano-1,4-benzoquinone	0.7121	0.9707	2.74
2,6-Dimethyl-1,4-benzoquinone	-0.4282	-0.1696	-0.34
2-Chloro-1,4-benzoquinone	-0.0885	0.1701	0.37
2-methyl-1,4-benzoquinone	-0.3430	-0.0844	-0.17
2-Phenyl-1,4-benzoquinone	-0.2545	0.0041	0.05
Tetrachloro-1,4-benzoquinone	0.2572	0.5158	1.48
Tetramethyl-1,4-benzoquinone	-0.5909	-0.3323	-0.68

Table 2.1: Electrochemical data for variety of substituted benzoquinones

2.3.3 Ease of reduction of quinones

Benzoquinones are more easily reduced than naphthoquinones and in turn naphthoquinones are more easily reduced than anthraquinones. The increasing numbers of aromatic moieties hinder formation of the radical anion and dianion species.

2.3.4 Effect of metal cations upon quinone reduction

Addition of metal cations has a large effect on the positions of the redox waves in cyclic voltammograms of quinones. Complexation and/or ion pairing of the semiquinone anion and the quinol dianion may occur, which has the effect of shifting

the first or second redox wave to more positive potentials. However, in some cases which are more complicated, various other waves can arise and in some instances the two one-electron waves are merged into one drawn-out two-electron process. Coupling of redox processes of quinones with cation binding equilibria leads to enhancement of cation binding. This principle has been utilised by Echegoyen and co-workers to enhance transport across model membranes.[22-29] The electrochemical cycle for such processes is illustrated in figure 2.8.

$$L + M^{+} \leftrightarrow LM^{+}$$

$$1\updownarrow \qquad \updownarrow 1'$$

$$L^{\cdot -} + M^{+} \leftrightarrow LM^{\cdot}$$

$$2\updownarrow \qquad \updownarrow 2'$$

$$L^{2-} + M^{+} \leftrightarrow LM^{-}$$

Figure 2.8: Electrochemical cycle for quinones/metal
Where L is the quinone ligand and M is the metal

2.4 Previous work

2.4.1 Quinone-substituted Lariat Ethers and Podands

Gokel, Echegoyen and co-workers have also spent years synthesising and testing various quinone compounds particularly anthraquinone containing compounds for use in the alteration of macrocyclic polyether cation binding properties by electrochemical switching.[22-30] They have reported the first example of cation binding enhancement by electrochemical switching in a lariat ether, which was achieved by a one or two-electron reduction of a quinone sidearm.[22] The comparison of the two species shown in figure 2.9 was undertaken. The first and second redox potentials for **15** were seen at –0.88V and –1.44V, whereas the values for **16** were –0.88V and –1.37V. These similar values demonstrate that in the absence of a guest cation, the presence of the lariat ether has little influence. Upon addition of various metal cations to a solution of **16,** the reduction-induced cation binding enhancement is less than that observed for **15** since the five extra oxygen atoms of the crown ether provide greater solvation of the cation and so reducing contact between the cation and quinone functions.

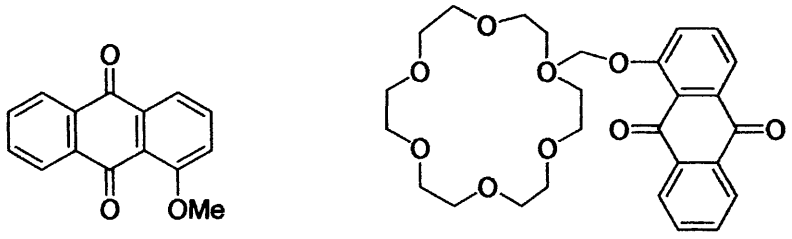

15 **16**

Figure 2.9: Anthraquinone ligands investigated by Gokel and co-workers.

Results from CPK molecular models of the two compounds clarified that the anthraquinone-substitued podand is more flexible than the lariat ether therefore upon reduction of the podand, its flexibility allows tighter ionic association than is allowed by the lariat ether. The polyether portion of the podand has the ability to form a better interaction with the cation hence giving a larger reduction-induced cation binding enhancement for the podand.

Torres and co-workers have investigated the nucleophilic aromatic substitution of fluoride by alkoxides of simple alcohols and lariat ethers.[31] Of interest to us are the novel ligands shown in figure 2.10 which were prepared by the group.

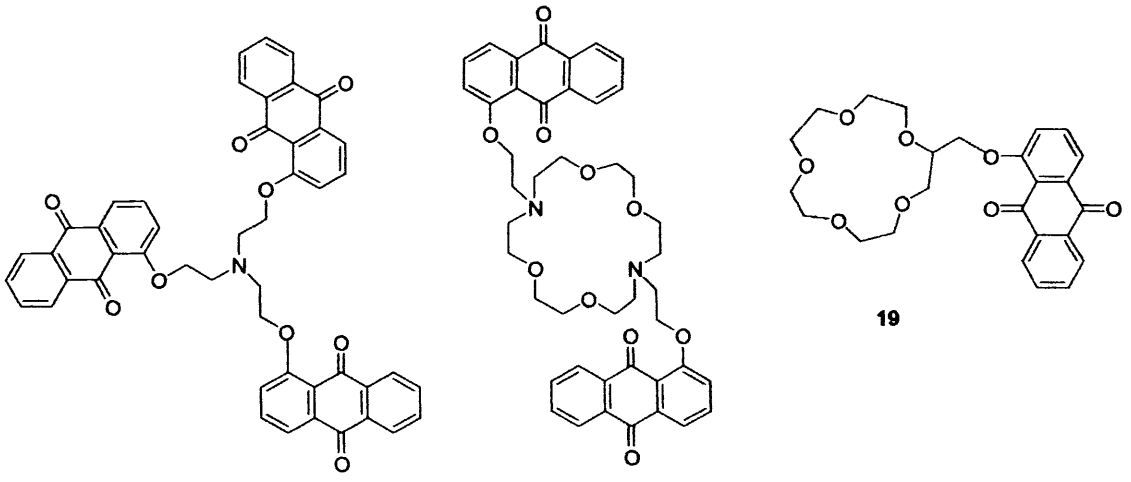

Figure 2.10: Anthraquinone ligands investigated by Torres and co-workers

For compounds **17** and **18**, two quasireversible redox pairs are observed. For **17**, each wave is representative of a three electron process whereas for **18**, each wave signifies a two electron process. Upon addition of Na^+, two additional peaks appeared in the cyclic voltammograms for both **17** and **18**. Gokel and co-workers had previously concluded that the occurrence of two CV waves per process arises when neutral ligand-guest binding is large, and weak binding gives rise to one anodically

shifted CV wave per process. This theory was confirmed by the significant values obtained for the binding enhancements of **17** and **18**. Identical testing carried out with **19** provided much smaller values for binding enhancement, indicating that both reduced quinone sidearms in compound **18** participate in cation binding.

Cooper and co-workers have an interest in coupled reactions of quinone crown ethers with cations.[32] One ligand under investigation is seen in figure 2.11. Other ligands synthesised are analogous to the one shown but with 6, 7 and 8 oxygen atoms comprising the crown. Diffraction studies have established the presence of a strong M-O(quinoid) bond. Additional studies demonstrated accommodation of various cations by pivoting of the quinoid group, a factor demanding the stiffening of the crown loop if selectivity is to be upgraded.

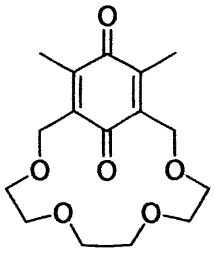

Figure 2.11: Benzoquinone Crown Ether investigated by Cooper

2.4.2 Calix(4)arenediquinones

A considerable amount of work surrounding calix(4)arenediquinones (figure 2.12) has been undertaken by Beer and co-workers.[33-35] His interest in advancing chemical sensor technology has led to some very elaborate electrochemical studies concerned with incorporating transition metal redox-active centres into macrocyclic receptor molecules.

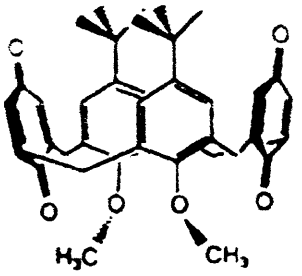

Figure 2.12: Example of a Calix(4)arenediquinone

Aside from their use for electrochemical recognition, these compounds have potential uses in charge transfer complexes, redox systems and are useful synthetic intermediates.[33] The studies carried out revealed that the electrochemical behaviour of this class of compounds is largely governed by conformational changes and the coulombic interaction of the two quinones is influenced by the mobility of the aromatic moieties linking them. Rotation of quinone groups was found to be slowed upon reduction[33] and it is noteworthy that calix(4)arenediquinones are more effective at distinguishing cation complexation from ion pairing than previously reported molecular receptors containing quinones.

For this class of compounds it appears there is a consistency in the third and fourth electron transfers for the free ligand merging into one irreversible wave in the cyclic voltammograms. Casnati and co-workers[33] have attributed this to the formation of CH_2-Cl_2-insoluble hydroquinone species. The repulsion between the reduced quinone groups upon protonation will be minimised resulting in a smaller potential separation between the third and fourth electron transfer hence the merging of the two waves into one. In addition, complexes of these ligands display an anodic shift (considerable in some cases) as expected, with the peaks/waves tending to merge into one upon addition of excess metal.

2.4.3 Di- and tri-aza Crown Ether Macrocycles containing quinone/ferrocene

Of greater interest to us is the work of Beer focusing on quinone based crown ether macrocycles.[35] The synthesis of novel redox-active di- and tri-aza crown ether macrocycles containing multiple quinone moieties in addition to the first example of a mixed ferrocene-quinone macrocyclic ligand has been reported. The two ligands of interest to us are illustrated in figure 2.13.

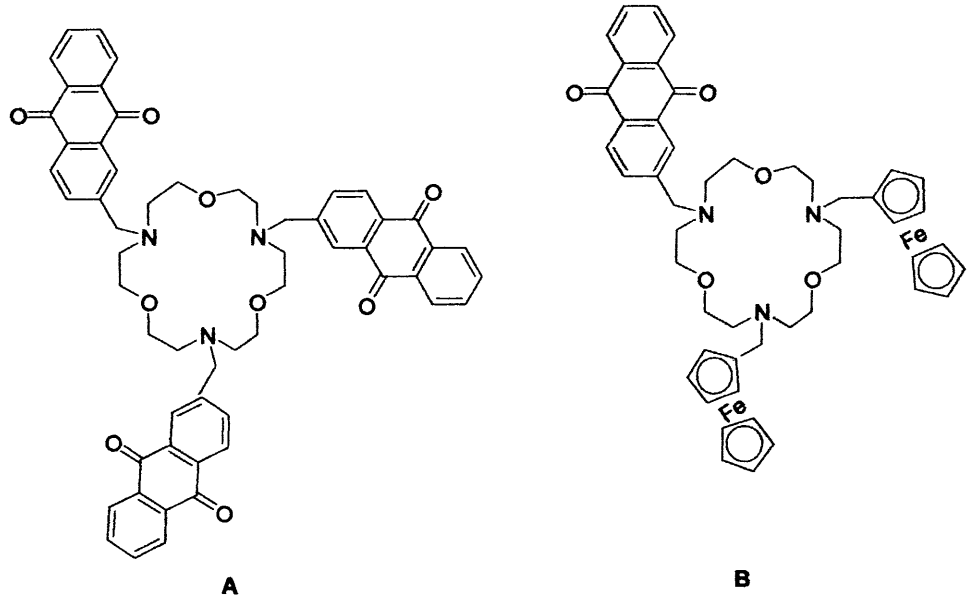

Figure 2.13: Anthraquinone Crown Ether macrocycles,investigated by Beer

It was found that the addition of NH_4^+ and K^+ to **A** and **B** gave rise to extremely small anodic shifts of less than 10mV. Previous work by Gokel and co-workers[24] have demonstrated that ion pairing between guest cation and reduced quinone anion radical and extra stabilisation due to the close proximity of the binding site of the macrocycle and the quinone functions determines the magnitude of anodic shifting. Results for both ligands shown here conclude that the cation is either not close enough to the quinone or communication is prevented.[35] Electrostatic or steric effects may account for this.

2.5 Aims and Objectives

Since quinones are used in photosynthetic models due to their efficient electron acceptor properties and are of course, among the acceptors found in nature (discussed in Chapter 1), an investigation into the preparation and electrochemical behaviour of quinone derivatives was undertaken.

To date little attention has been paid to amine substitution of quinones. Reports by Beer and co-workers on anthraquinones attached to aza crown ether macrocycles in addition to electrochemical analysis are available. No such investigations exist for various other amine macrocycles such as 1,4,7-triazacyclononane and 1,4,7,10-tetraazacyclododecane. The co-ordination abilities of such redox-active macrocyclic receptor molecules are also of interest. We therefore set out to investigate the synthesis and electrochemistry of various amine derivatives of 2,3-dichloro-1,4-naphthoquinone.

2.6 Experimental

All NMR spectra were recorded on a Bruker DPX400 or a Jeol Oxford 300 spectrometer. Infrared spectra (pressed KBr disc) were recorded on a Perkin-Elmer 1600 or a Jasco FT/IR-660 Plus. Ultraviolet absorption spectra were recorded on a Jasco V-570 UV/VIS/NIR Spectrophotometer. Emission and excitation spectra were recorded on a LS-50B instrument (Perkin-Elmer Instruments) equipped with a Hamamatsu R928 red-sensitive photomultiplier tube. Emission spectra were corrected from the wavelength dependence of the photomultiplier tube, according to the instrument guidebook. Mass spectra were performed by the EPSRC national mass spectromety service centre (Swansea) and the service at Cardiff. Electrochemistry was carried out using 0.1M tetrabutylammonium hexafluorophosphate as supporting electrolyte on an Autolab PGSTAT 12 Potentiometer with an Ag/Ag[NO_3] reference electrode (BAS Non-aqueous Reference Electrode Kit). X-Ray crystallography was performed by Dr. Li Ling Ooi at Cardiff University.

Experimental

2.6.1 Amine derivatives of 2,3-dichloro-1,4-naphthoquinone

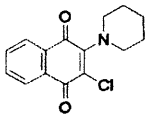

2-Chloro-(3-piperidine)-1,4-naphthoquinone (20).

To a solution of 2,3-dichloro-1,4-naphthoquinone (0.75g, 3.3mmol) and piperidine (0.28g, 3.3mmol) in acetonitrile (20mls) was added potassium carbonate (0.46g, 3.4mmol) and the mixture heated at reflux for 4hrs. After cooling, the red suspension was diluted with dichloromethane and filtered to remove the base. The red solution was evaporated under reduced pressure to yield the title compound as a red solid (0.83g, 91%). δ_H(400MHz, $CDCl_3$): 8.05 (1H, dd, J=1.32, 7.79, quinone C8-*H*), 7.95 (1H, dd, J= 1.21, 8.57, quinone C5-*H*), 7.65 (2H, m, quinone C6-*H* + C7-*H*), 3.5 (5H, m, piperidine *H*). δ_C: (100MHz, $CDCl_3$) 182.437; 178.440; 151.187; 134.350; 133.296; 132.089; 131.916; 127.199; 126.854; 122.532; 53.381; 27.280; 24.581. IR KBr/cm^{-1} : 2935 (m), 2835 (m), 1670 (s), 1638 (s), 1591 (m), 1559 (s), 1438 (m), 1403 (w), 1358 (w), 1283 (s), 1242 (s), 1210 (s), 1132 (w), 1111 (m), 1021 (m), 982 (s), 830 (w), 801 (s), 714 (s). UV(CH_2Cl_2)/nm: 507 (log ε 3.60), 286 (log ε 4.14), 248 (log ε 4.04), 229 (log ε 3.99). MS m/z ES+: 277.1 $[M+H]^+$ (100%), 242.1 $[M-Cl]^+$ (35%)

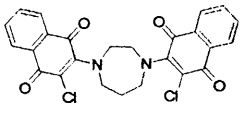

Bis(2-chloro-1,4-naphthoquinone)1,4-homopiperazine (21).

Potassium carbonate (2.28g, 16.47mmol) was added to a solution of homopiperazine (0.75g, 7.49mmol) and 2,3-dichloro-1,4-naphthoquinone (3.74g, 16.47mmol) in dry acetonitrile (50mls) under nitrogen and the resulting red suspension was refluxed for 24 hrs. After cooling, the red suspension was diluted with dichloromethane (300mls), filtered and the filtrate evaporated under reduced pressure. Column chromatography on silica gel ($CHCl_3$) afforded the title compound as a red solid (3.2g, 88%). δ_H

(400MHz, $CDCl_3$): 8.05 (2H, dd, J=1.47, 7.59, quinone C8-*H*), 7.95 (2H, dd, J=1.39, 7.39, quinone C5-*H*), 7.65 (2H, m, quinone C7-*H*, C6-*H*), 3.9 (4H, s, NCH_2CH_2N), 3.8 (4H, t, J=5.76, $NCH_2CH_2CH_2N$), 2.17 (2H, quin, J=2.24, CH_2). δc 181.34, 177.18, 150.42, 133.09, 132.23, 130.51, 130.46, 125.90, 125.59, 123.15, 54.22, 52.39, 28.87. IR KBr/cm^{-1}: 2909 (m), 2358 (s), 1668 (s), 1644 (m), 1590 (s), 1538 (s), 1487 (w), 1443 (m), 1399 (w), 1329 (w), 1261 (s), 1095 (s), 1018 (s), 802 (s). UV (dichloromethane)/nm: 502 (log ε 3.59), 342 (log ε 3.66), 282 (log ε 4.18), 242 (log ε 4.28). MS m/z ES+: 481.0 $[M+H]^+$ (100%), 445.0 $[M-Cl]^+$ (10%).

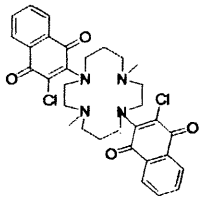

1,8-Dimethyl-4,11-(2-chloronaphthoquinone)-1,4,8,11-tetraazacyclotetradecane (22)

To a solution of dimethyl cyclam (0.228g, 0.998mmol), in acetonitrile (15mls), was added potassium carbonate (0.3g, 2.17mmol) and 2,3,dichloro-1,4-naphthoquinone (0.46g, 2.05mmol). The red suspension was heated for 12 hrs at 60°C. After cooling, a little more dried potassium carbonate was added and heated for a further 10 mins. After cooling, the suspension was diluted with dichloromethane (50mls) and filtered. The solution was evaporated under reduced pressure and the resulting solid recrystallised from ethanol(hot) and chloroform(hot) to give the title compound as a red solid (0.46g, 75%). NMR δ_H (400MHz, $CDCl_3$): 8.06 (2H, dd, J=1.52, 7.75, quinone C-8*H*); 7.97 (2H, dd, J=1.24, 7.33, quinone C-5*H*); 7.65 (4H, m, quinone C-7*H*, quinone C-6*H*); 3.78 (4H, t, J=8.44, quinone-N-CH_2CH_2-N-CH_3); 3.55 (4H, t, J=5.87, quinone-N- CH_2CH_2-N-CH_3); 2.73 (4H, t, J= 6.36, quinone-N-$CH_2CH_2CH_2$-N-CH_3); 2.43 (4H, t, J=4.93, quinone-N-$CH_2CH_2CH_2$-N-CH_3); 2.19 (6H, s, CH_3); 1.8 (4H, m, quinone-N-$CH_2CH_2CH_2$-N-CH_3). δ_C 182.46, 177.98, 134.03, 133.05, 131.71, 131.65, 126.87, 126.55, 55.59, 54.84, 51.93, 50.13, 43.74, 25.79, 1.04. IR KBr/cm^{-1}:

2875 (m), 1683 (s), 1635 (m), 1594 (m), 1542 (s), 1473 (w), 1447 (m), 1376 (w), 1278 (s), 1234 (w), 1197 (w), 1163 (m), 1115 (m), 1052 (m), 1035 (m), 1005 (m), 957(m), 786(w), 721(w). UV (dichloromethane)/nm: 508 (log ε 3.46), 285 (log ε 4.04), 247 (log ε 4.09), 228 (log ε 4.10). MS m/z ES+: 609.1 $[M+H]^+$ (100%), 574.1 $[M-Cl]^+$ (20%).

14,13-diaza(2-chloro-1,4-naphthoquinone)-18-crown-6;1,4,10,13 tetraoxa-7-16-diazacyclooctadecane (23).

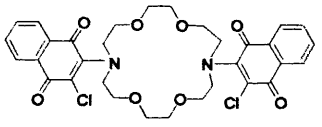

To a solution of 4,13-diaza-18-crown-6; 1,4,10,13 tetraoxa-7,16-diazacyclooctadecane (0.015g,0.051mmol) and 2,3-dichloro-1,4-naphthoquinone (0.0273g, 0.12mmol) in acetonitrile (6mls) was added potassium carbonate (0.0166g, 0.12mmol) and the solution refluxed for 12hrs. The resulting red suspension was diluted with dichloromethane, filtered and the red solution was evaporated under reduced pressure to give the title compound as a bright red solid, (88%). NMR δ_H (400MHz, $CDCl_3$): 8.06 (2H, dd, J=1.66, 7.75, quinone C-8 *H*), 7.9 (2H, dd, J=1.14, 7.02, quinone C-5 *H*), 7.65 (4H, m, quinone C-7 H + C-6 *H*), 3.81 (8H, t, J=5.11, quin-N-CH_2CH_2O), 3.72 (8H, t, J=5.10, OCH_2CH_2O), 3.55 (8H, s, quin-N-CH_2). δ_C: 181.22; 177.08; 150.38; 132.91; 132.14; 130.83; 130.47; 125.86; 125.52; 123.17; 70.10; 69.96; 52.06. IR KBr/cm^{-1}: 2955 (s), 1679 (s), 1654 (s), 1594 (m), 1558 (m), 1543 (m), 1458 (w), 1262 (s), 1091 (s,b), 1021 (s,b), 800 (s). UV (dichloromethane)/nm: 491 (log ε 3.66), 282 (log ε 4.29), 246 (log ε 4.31), 229 (log ε 4.32). MS m/z MALDI: 641.1 [M-3H] (100%), 453.2 $[M-C_{10}H_4O_2Cl]$ (40%).

Tris(2-chloro-1,4-naphthoquinone) 1,4,7-triazacyclononane (24).

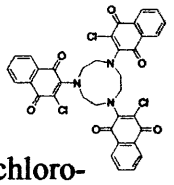

To a solution of 1,4,7-triazacyclononane (0.3g, 2.33mmol) and 2,3-dichloro-1,4-naphthoquinone (1.74g, 7.67mmol) in ethanol (170mls) was added triethylamine (2.36g, 23.26mmol). The reaction mixture was refluxed for 17hrs, then poured into ice water (400mls) and extracted with chloroform. The organic phase was concentrated in vacuo and the residue purified by column chromatography on silica gel ($CHCl_3$ 99%, MeOH 1%) and recrystallised from ethanol to give the title compound as a red solid (1.04g, 64%). NMR (400MHz, $CDCl_3$) δ_H 7.95 (3H, dd, J=1.87, 6.55, quinone C-8*H*); 7.81 (3H, dd, J=1.41, 5.59, quinone C-5*H*); 7.57 (6H, m, quinone C-7*H*, C-6*H*); 4.0 (12H, s, NCH_2). δ_C 182.81, 172.9, 150.21, 137.41, 134.01, 133.67, 127.64, 127.34, 120.38, 116.5, 55.74. IR KBr/cm^{-1}: 2960 (m), 1682 (s), 1652 (w), 1593 (m), 1559 (s), 1508 (s), 1458 (m), 1361 (w), 1330 (w), 1261 (s), 1224 (m), 1095 (s), 1019 (m), 799 (s), 719 (m) and 668 (s). UV (dichloromethane)/nm: 500 (log ε 3.35), 348 (log ε 3.99), 262 (log ε 4.05), 242 (log ε 4.11). MS m/z ES+: 703 $[M+H]^+$ (100%), 668.1 $[M-Cl]^+$ (25%).

1,4-(2,3(1,4-naphthoquinone)1,4,7-triazacyclononane (25).

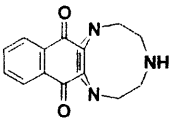

To a solution of 1,4,7-triazacyclononane (0.1g, 0.78mmol), in ethanol (15mls), was added triethylamine (0.15g, 1.55mmol) and 2,3,dichloro-1,4-napthoquinone (0.176g, 0.78mmol). The suspension was refluxed for 12 hrs then poured into ice water (100mls) and extracted with chloroform. The organic phase was concentrated in vacuo and the resulting solid purified by column chromatography on silica (98% $CHCl_3$ 2% MeOH) to yield the title compound as a blue solid. Yield 0.15g, 68%. NMR (400MHz, $CDCl_3$): δ_H 7.99 (2H, dd, J=2.41, 5.78, quinone C-5 + C-8*H*); 7.60 (

2H, dd, J=3.4, 5.75, quinone C-7 + C-6*H*); 3.9 (2H, m, CH_2exo tacn); 3.7 (2H, m, CH_2 endo tacn); 3.5 (2H, m, tacn); 3.15 (4H, m, tacn); 2.5 (2H, m, tacn). δ_C ($CDCl_3$): 179.56; 146.36; 132.18; 130.91; 125.20; 54.96; 52.72; 52.13. IR KBr/cm^{-1}: 3437 (m), 2955 (s), 2895 (m), 1654 (s), 1586 (s), 1559 (s), 1458 (m), 1378 (w), 1322 (m), 1261 (s), 1195 (s), 1099 (s), 1021 (s), 906 (w), 864 (w), 802 (s), 668 (m). UV (dichloromethane)/nm: 614 (log ε 2.91), 306 (log ε 3.88), 243 (log ε 4.04). MS m/z ES+ 284.14 $[M+H]^+$ (100%).

2.6.2 Thiol/ Mixed thiol-amine derivatives of 2,3-dichloro-1,4-naphthoquinone

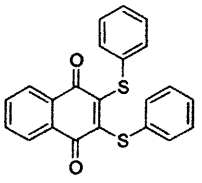

2,3-Bis-thiophenol-1,4-naphthoquinone (26).

To a solution of 2,3-dichloro-1,4-naphthoquinone (2g, 8.8mmol), and thiophenol (1.94g, 18mmol) in dimethylformamide (50mls) was added caesium carbonate (6.31g, 19mmol) and the yellow solution heated to reflux under nitrogen for 2 hours. After cooling, the orange solution was diluted with water (60mls) and extracted with dichloromethane (3 x 70mls). Combined organic extracts washed with brine (150mls), dried over magnesium sulphate, filtered and evaporated under reduced pressure to yield the title compound as an orange solid (2.6g, 79%). δ_H (400MHz, $CDCl_3$): 7.95 (2H, dd, J= 3.42, 5.69, quinone C5-*H* + C8-*H*), 7.6 (2H, dd, J=3.42, 5.86, quinone C7-*H* +C6-*H*), 7.3 (4H,dd, J=2.30, 6.04, Ar thiol C2-*H* + C6-*H*), 7.2 (6H, m, Ar thiol C3-*H*, C4-*H* + C5-*H*). δ_C: 178.75; 148.31; 133.83; 133.65; 132.76; 131.16; 129.09; 128.05; 127.45. UV (dichloromethane)/nm: 423 (log ε 3.44), 280 (log ε 4.02), 230 (log ε 4.31). IR KBr/cm^{-1}: 3017 (m), 1667 (s), 1592 (m), 1498 (s), 1474(m), 1441(w), 1291 (w), 1266 (s), 1158 (w), 1137 (s), 1079 (m), 1021 (m), 997 (w), 915 (w), 871 (w). MS m/z AP+: 375 $[M+H]^+$ (15%), 266 $[M-C_6H_5S]^+$ (40%).

2-Chloro-3-(thiophenol)-1,4-naphthoquinone (27)

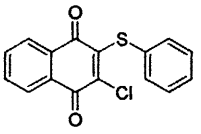

To a solution of 2,3-dichloro-1,4-naphthoquinone (2g, 8.8mmol), and thiophenol (0.97g, 8.8mmol) in dimethylformamide (50mls) was added caesium carbonate (4.29g, 13.2mmol) and the yellow solution heated to reflux under nitrogen for 2 hours. After cooling, the orange solution was diluted with water (60mls) and extracted with dichloromethane (3 x 70mls). Combined organic extracts washed with brine (150mls), dried over magnesium sulphate, filtered and evaporated under reduced pressure. Flash column chromatography on silica gel (dichloromethane) was carried out to yield the title compound as a purple solid (1.51g, 57%). δ_H (400MHz, $CDCl_3$): 8.06 (1H, dd, J=1.54, 7.6, quinone C8-*H*), 7.95 (1H, dd, J=1.33, 7.33, quinone C5-*H*), 7.65 (2H, m, quinone C7-*H* + C6-*H*),), 7.15 (2H, d, J=3.98, Ar thiol C2-*H*, C6-*H*), 7.05 (3H, m, Ar thiol C3-*H*, C4-*H*, C5-*H*). IR KBr/cm^{-1}: 2963 (s), 1679 (m), 1649 (m), 1553 (m), 1503 (m), 1408 (m), 1262 (s), 1091 (s), 1021 (s), 799 (s). UV (dichloromethane)/nm: 507 (log ε 3.09), 281 (log ε 3.34), 233 (log ε 4.15). MS m/z AP+: 266 $[M-Cl]^+$ (100%).

Bis(2-thiophenol-1,4-naphthoquinone)1,4-homopiperazine (28)

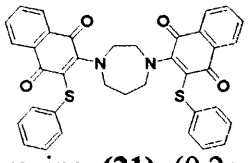

To a solution of bis(2-chloro-1,4-naphthoquinone)1,4-homopiperazine **(21)** (0.2g, 0.417mmol) and thiophenol (0.092g, 0.83mmol) in dimethylformamide (20mls) was added caesium carbonate (0.299g, 0.92mmol) and the red coloured solution heated to reflux for 3 hours under nitrogen. After cooling, the purple coloured solution was diluted with water (30mls) and extracted with dichloromethane (3 x 40ml). The combined organic extracts were washed with brine (100ml), dried over magnesium sulphate, filtered and evaporated under reduced pressure. The oily solid was purified

by recrystallisation from dichloromethane and ethanol to yield the title compound as a purple coloured solid (0.19g, 73%). δ_H (400MHz, $CDCl_3$): 8.02 (2H, dd, J=1.13, 7.59, quinone C8-*H*), 7.85 (2H, dd, J=1.02, 7.43, quinone C5-*H*), 7.60 (4H, m, quinone C6-*H* + C7-*H*), 7.15 (4H, d, J=1.87, Ar thiol C2-*H* + C6-*H*), 7.1 (6H, m, Ar thiol C3-*H*, C4-*H*+ C5-*H*), 3.35 (8H, m, NCH_2CH_2N + NCH_2CH2CH_2N), 1.75 (2H,quin, J=6.07, $NCH_2CH_2CH_2N$). δ_C: 181.70; 180.91; 152.04; 134.06; 132.83; 131.86; 131.37; 130.97; 127.88; 127.62; 125.75; 125.53; 125.38; 120.13; 52.92; 50.90; 28.02. IR KBr/cm^{-1}: 2955 (s), 2363 (s), 1654 (m), 1508 (m), 1261 (s), 1091 (s), 1016 (s). UV (dichloromethane)/nm: 527 (log ε 3.08), 422 (log ε 3.16), 288 (log ε 3.89), 250 (log ε 3.93), 228 (log ε 3.97). MS m/z ES+: 629.2 $[M+H]^+$ (98%), 365.1 $[M-C_{10}H_4O_2-C_6H_5S]^+$ (100%).

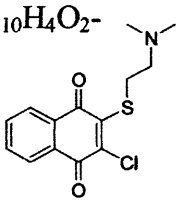

2-Chloro-3-(dimethylamino ethanethiol)-1,4-naphthoquinone (29)

To a solution of 2,3-dichloro-1,4-naphthoquinone (0.4g, 1.76mmol) and 2-(dimethylamino)ethane thiol hydrochloride 95% (0.25g, 1.76mmol) in dimethylformamide (20mls) was added caesium carbonate (1.14g, 3.52mmol) and the solution heated to reflux for 3 hours under nitrogen. After cooling, the purple coloured solution was diluted with water (30mls) and extracted with dichloromethane (3 x 40ml). The combined organic extracts were washed with brine (100ml), dried over magnesium sulphate, filtered and evaporated under reduced pressure. Flash column chromatography on silica gel (dichloromethane) was carried out to yield the title compound as a purple oily solid (0.28g, 54%). δ_H (400MHz, $CDCl_3$): 7.94 (1H, dd, J=2.14, 6.29, quinone C8-*H*), 7.89 (1H, dd, J=2.78, 5.48, quinone C5-*H*), 7.55 (2H, m, quinone C7-*H*, C6-*H*), 3.5 (2H, t, J=2.74, SCH_2), 2.9 (2H, t, J=2.85, NCH_2), 2.09 (6H, s, *CH3*). IR KBr/cm^{-1}: 2923 (s), 2853 (s), 2012 (s), 1996 (w), 1889 (s),

1838 (m), 1778 (s),1456 (s), 1415 (s), 1377 (m), 1340 (m), 1313 (m), 1265 (m), 1181 (m), 1107 (w), 1082 (s), 1059 (m), 1029 (s), 987 (s), 935 (s), 872 (s), 807 (m). UV (dichloromethane)/nm: 551 (log ε 3.18), 291 (log ε 3.88), 230 (log ε 4.04). MS m/z AP+: 246.1 $[M\text{-}Cl\text{-}CH_3]^+$ (100%).

Bis(2-dimethylamino ethanethiol-1,4-naphthoquinone)1,4-homopiperazine (30)

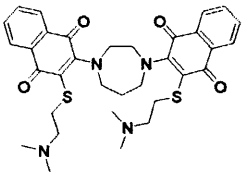

To a solution of bis(2-chloro-1,4-naphthoquinone)1,4-homopiperazine **(21).** (00.42g, 0.0875 mmol) and 2-(dimethylamino)ethane thiol hydrochloride 95% (0.025g, 0.175mmol) in dimethylformamide (10mls) was added caesium carbonate (0.125, 0.385mmol) and the solution heated to reflux for 3 hours under nitrogen. After cooling, the purple coloured solution was diluted with water (10mls) and extracted with dichloromethane (3 x 10ml). The combined organic extracts were washed with brine (20ml), dried over magnesium sulphate, filtered and evaporated under reduced pressure. Flash column chromatography with dichloromethane/MeOH, 95:5, followed by dimethylformamide gave the title compound as a purple oily solid (0.031g, 57%). δ_H (400MHz, $CDCl_3$): 7.96 (2H, dd, J=1.52, 8.89, quinone C-8*H*), 7,83 (2H, dd, J=1.35, 7.22, quinone C-5*H*), 7.55 (4H, m, quinone C-7*H* + C-6*H*), 3.85 (4H, s, NCH_2CH_2N), 3.76 (4H, t, J=5.66, $NCH_2CH_2CH_2N$), 2.9(2H, m, $NCH_2CH_2CH_2N$) 2.8 (4H, t, J=5.65, SCH_2), 2.45 (2H, t, J=7.36, NCH_2), 2.1 (12H, s, CH_3). IR KBr/cm^{-1}: 3090 (w), 2955 (m), 2845 (w), 2764 (w), 2353 (s), 1654 (s), 1592 (m), 1559 (s), 1522 (s), 1458 (m), 1393 (w), 1234 (w), 1261 (s), 1187 (w), 1122 (m), 1081 (m), 1035 (w), 1019 (w), 798.6(s), 720(m). UV (dichloromethane)/nm: 528 (log ε 2.84), 301 (log ε 3.28). MS m/z ES+: 619.1 $[M+H]^+$ (12%), 103.7 $[C_4H_{10}NS]^+$ (100%).

2.6.3 Cyclen Compounds synthesised for attempted reaction with 2,3-dichloro-1,4-naphthoquinone

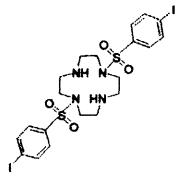

1,7-Dikis(iodobenzenesulphonyl)-1,4,7,10-tetraazacyclododecane (32).[36]

Iodobenzenesulphonyl chloride (2.2g, 7.26mmol) was added slowly to a solution of 1,4,7,10-tetraazacyclododecane (0.25g, 1.45mmol) in dry pyridine (5mls) under nitrogen and stirred for 12 hrs. The solution was diluted with dichloromethane (20mls) and washed with 10% aqueous hydrochloric acid followed by water and dried (magnesium sulphate). After filtration, the filtrate was evaporated under reduced pressure to give a yellow solid, which was dissolved in the minimum amount of hot methanol followed by addition of excess sodium hydroxide. The pH of the solution was adjusted to 10 via addition of water and after cooling, the white solid was collected by filtration. Yield: 0.811g, 80%. δ_H (400MHz, $CDCl_3$): 8.15 (4H, d, J=8.23, *H*2-aromatic, H6-aromatic), 7.70 (4H, d, J=8.23, *H*3-aromatic, H5-aromatic), 3.15 (8H, s, C*H*$_2$N), 2.95 (2H, s, N*H*), 2.75 (8H, s, C*H*$_2$N). δc 138.24, 136.86, 128.94, 101.19, 49.42, 48.59, 40.00, 38.75. IR KBr/cm^{-1}: 3265 (m), 3085 (w), 2973 (m), 2926 (m), 2806 (m), 1917 (w), 1644 (w), 1569 (s), 1467 (s), 1451 (s), 1382 (s), 1361 (s), 1340 (s), 1286 (m), 1271 (m), 1152 (s), 1086 (s), 1052 (s), 1002 (s), 978 (s), 936 (w), 914 (s), 816 (s), 725 (s), 701 (s), 678 (s), 592 (s), 575 (s), 528 (m), 480 (m). MS m/z APCI: 705 $[M+H]^+$ (100%).

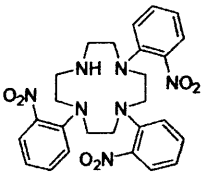

1,4,7-Tris(2-Nitrophenyl)-1,4,7,10-tetraazacyclododecane (34).[37]

Potassium carbonate (2.4g, 17.43 mmol) was added to a solution of cyclen (1g, 5.81mmol) and 1-fluoro-2-nitrobenzene (2.13g, 17.43mmol) in dry acetonitrile

(80mls) and the mixture refluxed for 12 hours. After cooling, water was added (50 mls) followed by chloroform (50mls). Separation of the organic layer afforded an orange solution which was washed with 2M NaOH solution (100mls). Extraction into 4M HCl solution (100mls) followed by washing with chloroform (2 x 50 mls) was carried out and the aqueous layer was basified (NaOH-pH 12) followed by further washing with chloroform (3 x 50 mls). The organic layers were dried (magnesium sulphate) and the solvent was removed. Recrystallisation from ethanol afforded compound **34** as an orange solid (65%). δ_H ($CDCl_3$, 400MHz): 7.55 (3H, m, aromatic H's), 7.35 (2H, m, aromatic H's), 7.19 (3H, m, aromatic H's), 6.95 (3H, m, aromatic H's), 6.83 (1H, m, aromatic H's), 2.9-3.5 (16H, m, cyclen). IR KBr/cm^{-1}: 3402 (m), 2835 (s), 1602 (s), 1577 (w), 1540 (s), 1501 (s), 1487 (s), 1400 (m), 1348 (w), 1235 (m), 1180 (m), 1030 (m), 989 (w), 836 (w).

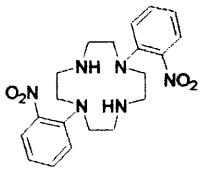

1,7-Bis(2-nitrophenyl)1,4,7,10-tetrazazcyclododecane (36).[37]

Same procedure as compound **34** using 1: 2 ratio of cyclen and 1-fluoro-2-nitrobenzene. Yield: 62%. δ_H ($CDCl_3$, 400MHz): 7.6 (6H, m, aromatic H's), 7.3 (2H, m, aromatic H's), 3.3 (8H, s, cyclen), 2.8 (8H, s, cyclen). IR KBr/cm^{-1}: 3390 (m), 2840 (s), 1605 (s), 1690 (w), 1580 (w), 1538 (s), 1511 (s), 1500 (s), 1412 (m), 1356 (w), 1367 (w), 1238 (m), 1176 (m), 1027 (m), 995 (w).

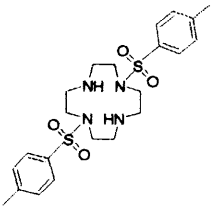

1,7-Bis(p-toluenesulfonyl)-1,4,7,10-tetraazacyclododecane (38).[36]

A solution of tosyl chloride (7.62g, 40mmol) in dry pyridine (100ml) under nitrogen, was cooled to 0°C and a solution of 1,4,7,10-tetraazacyclododecane (3.44g, 20mmol)

in dry pyridine (30ml) was added slowly under nitrogen over a period of 15 minutes. After allowing warming to room temperature, the mixture was stirred for a further 3hrs. The pyridine was removed by evaporation under reduced pressure and water (35ml) was added to the residue and stirred vigorously for 90 min. The bis-toluenesulfonamide was filtered, washed with water (2 x 25 ml), saturated potassium carbonate solution (2 x 25 ml), water (2 x 20 ml), and methanol (2 x 25 ml) and dried in an electric oven (120°C). The solid was dissolved in hot methanol and excess sodium hydroxide pellets were added, followed by addition of water until the pH of the solution reached 10. After cooling, the solid was filtered and dried to yield the title compound as a colourless solid (7.65g, 80%). δ_H (DMSO) 7.75 (4H, d, J=8.10, Ts H2, H6), 7.49 (4H, d, J=8.50, TsH3, H5), 3.0 (6H, s, CH_3), 2.8 (2H, s, NH), 2.5 (8H, s, cyclen), 2.4 (8H, s, cyclen). IR KBr/cm^{-1}: 3354 (m), 2975 (m), 2930 (m), 2806 (m), 1935 (w), 1644 (m), 1470 (s), 1446 (s), 1384 (s), 1377 (s), 1355 (s), 1290 (m), 1276 (m), 1162 (s), 1087 (s), 1052 (s), 945 (w), 920 (s), 845 (m), 767 (w).

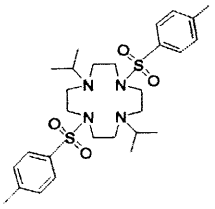

1,7-Bis(p-toluenesulfonyl)-4,10-bis(iso-propane)-1,4,7,10-tetraazacyclododecane (39).[36]

A mixture of 1,7-bis(p-toluenesulfonyl)-1,4,7,10-tetraazacyclododecane (4.058g, 8.5mmol), 2-bromopropane (10.38g, 85mmol), potassium carbonate (11.66g, 85mmol), tetrabutylammonium bromide (0.041g, 0.128mmol) and tetrabutylammonium iodide (0.002g, 0.0054mmol) in dry and degassed acetonitrile (20 ml) were heated at reflux for 100 hrs under nitrogen. After cooling, the mixture was filtered and the filter cake washed with chloroform (20 ml). The combined filtrates were evaporated under reduced pressure to yield a yellow oil. This residue was redissolved in chloroform (15 ml) and washed with 1M sodium hydroxide (15

ml). The organic layer was removed and the aqueous layer extracted with chloroform (3 x 5 ml). The combined chloroform layers were dried ($MgSO_4$) and the solvent removed under reduced pressure to yield the title compound (3.59g, 75%). δ_H (DMSO) 7.75 (4H, d, J=8.05, Ts *H*); 7.50 (4H, d, J=8.25, Ts *H*); 3.2 (6H, s, CH_3); 2.6 (8H, s, Cyclen *H*); 2.45 (8H, s, Cyclen *H*), 1.1 (12H, s, iso propane CH_3). IR KBr/cm^{-1}: 2970 (s), 2930 (s), 2810 (s), 1940 (w), 1643 (m), 1489 (s), 1498 (s), 1375 (s), 1365 (s), 1359 (s), 1298 (m), 1267 (m), 1178 (s), 1160 (s), 1087 (s), 1055 (s), 950 (w), 915 (s). MS m/z AP+: 565.6.

4,10-Bis(iso-propane)1,4,7,10-tetraazacyclododecane. HBr (40).[36]

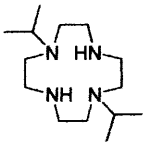

A solution of **39** (3.13g, 5.55mmol) in H_2SO_4 (20 mls) was heated at 100°C for 48 hrs under an atmosphere of nitrogen. After cooling, the solution was transferred to a dropping funnel and added drop wise with stirring to dry EtOH (50 mls) to give the polyhydrosulphate salt. After addition of dry ether (45mls), the solution was cooled to 0°C and the solid was filtered. The hydrosulphate salt was dissolved in the minimum amount of hot water (10mls) and HBr (5mls) was added to precipitate the hydrobromide salt of the product. After filtering and washing with small volumes of HBr and EtOH, the compound was dried to afford the salt as a cream coloured solid (62%). δ_H (D_2O, 400MHz) 2.7 (8H, t, J=3.03, cyclen H's), 2.5 (8H, t, J=3.11, cyclen H's), 0.9 (12H, s, CH_3). IR KBr/cm^{-1}: 3360 (w), 2930 (s), 2859 (s), 1953 (w), 1650 (m), 1604 (w), 1495 (m), 1508 (s), 1389 (s), 1359 (s), 1340 (s), 1318 (m), 1277 (w), 1178 (s), 1160 (s), 950 (w), 915 (s), 825 (w), 799 (w).

2.6.4 Metal complexes of Amine-quinone ligands

[Cu(II)1,8-Dimethyl-4,11-(2-chloronapthoquinone)-1,4,8,11-tetraazacyclotetradecane] $[NO_3]_2$

A solution of copper (II) nitrate (9.18mg, 0.0395mmol) in ethanol (4mls) was added to a heated solution of 1,8-dimethyl-4,11-(2-chloronapthoquinone)-1,4,8,11-tetraazacyclotetradecane **(22)** (24mg, 0.0395mmol) in ethanol (4mls). The resulting solution was heated under reflux for 1 hour. After cooling, the volume of ethanol was reduced to quarter the original volume and cooled for 12 hrs at -4°C. The suspension was filtered and the resulting brown/orange solution was evaporated under reduced pressure and dried under vacuum. IR KBr/cm^{-1}: 3427 (m), 2962 (m), 2614 (w), 1684 (m), 1604 (m), 1510 (s), 1447 (m), 1383 (w), 1261 (s), 1227 (m), 1095 (s), 1021 (s), 948 (w), 865 (w), 799 (s), 751 (w). UV (dichloromethane)/nm: 525 (log ε 2.1), 435 (log ε 3.07), 272 (log ε 4.23), 229 (log ε 4.14). MS m/z ES+: 634.3 $[M\text{-}Cl\text{-}2H]^+$ (100%).

[Ni(II)-1,8-Dimethyl-4,11-(2-chloronapthoquinone)-1,4,8,11-tetraazacyclotetradecane] $[NO_3]_2$

A solution of nickel (II) nitrate (11.95mg, 0.0411mmol) in ethanol (5mls) was added to a heated solution of 1,8-dimethyl-4,11-(2-chloronapthoquinone)-1,4,8,11-tetraazacyclotetradecane (**22**) (25mg, 0.0411mmol) in ethanol (5mls). The resulting solution was heated to reflux for 12 hrs. After cooling, the volume of ethanol was reduced to quarter its original volume and cooled for 12hrs at -4°C. The suspension was filtered and the resulting red solution was evaporated under reduced pressure. IR KBr/cm^{-1}: 3417 (m), 2945 (w), 1679 (m), 1654 (s), 1579 (s), 1508 (s), 1453 (w), 1384

(s), 1257 (s), 1223 (m), 1182 (w), 1090 (s), 1021 (s), 946 (w), 795 (s). UV(dichloromethane)/nm: 685 (log ε 2.33), 457 (log ε 4.01), 273 (log ε 4.9), 231 (log ε 4.92). MS m/z ES+: 629.4 $[M\text{-}Cl\text{-}2H]^+$ (100%)

2.6.5 Metal complexes of Amine-hydroquinol ligands

Nickel bis(2-chloro-1,4-hydronapthoquinol)1,4-homopiperazine

To a solution of **21** (0.05g, 0.104mmol) in ethanol (10ml), one drop of acetic acid was added followed by a catalytic amount of palladium on carbon. The suspension was stirred vigorously under an atmosphere of hydrogen for 30 minutes or until the solution appeared clear. The palladium on carbon was removed by filtration under nitrogen and nickel nitrate (0.03g, 0.104mmol) was added to the hydrogenated solution and stirred for 1 hr. The ethanol was removed to afford an orange coloured solid (0.041g, 73%). IR KBr/cm^{-1}: 3390 (s,b), 1629 (w), 1588 (w), 1384 (s), 1261 (m), 1079 (w), 1019 (w), 857 (m), 800 (m), 767 (m). UV (EtOH)/nm: 487 (log ε 2.8), 342 (log ε 3.7), 248 (log ε 4.25), 212 (log ε 4.53). MS m/z ES+: 485.1 $[M\text{-}Ni]^+$ (25%), 503.2 $[M\text{-}Cl\text{-}4H]^+$ (30%).

Nickel tris(2-chloro-1,4-hydronapthoquinol) 1,4,7-triazacyclononane

To a solution of **24** (0.01g, 0.0142mmol) in ethanol (10ml), one drop of acetic acid was added followed by a catalytic amount of palladium on carbon. The suspension was stirred vigorously under an atmosphere of hydrogen for 30 minutes or until the solution appeared clear. The palladium on carbon was removed by filtration under nitrogen and nickel nitrate (0.004g, 0.0142mmol) was added to the hydrogenated solution and heated at 50°C for 2 hr. The ethanol was removed to afford a pale yellow/green precipitate (0.007g, 64%). IR KBr/cm^{-1}: 3426 (s,b), 2962 (m), 2276

(m), 1636 (s), 1384 (s), 1261 (s), 1094 (s), 1020 (s), 801 (s). UV (dichloromethane)/nm: 521 (log ε 2.5), 347 (log ε 3.6), 221 (log ε 4.16). MS m/z ES+: 730.3 $[M\text{-}Cl\text{-}3H+H]^+$ (25%).

2.6.6 Metal complexes of Thiol/mixed thiol amine-quinone ligands

[Pd (II) 2,3-bis-thiophenol-1,4-napthoquinone] $[Cl]_2$

To a solution of 2,3-bis-thiophenol-1,4-napthoquinone(**26**) (0.3g, 0.81mmol) in acetonitrile (4mls) was added palladium (II) dichloride (0.14g, 0.81mmol) and the solution heated under reflux for 4 days. After cooling a bright yellow coloured precipitate was collected by filtration (0.38g, 86%). δ_H (400MHz, DMSO): 7.99 (2H, dd, J=2.40, 5.67, quinone C8-*H*, C5-*H*), 7.85 (2H, dd, J=3.72, 5.72, quinone C6-*H*, C7-*H*), 7.45 (4H, dd, J= 1.54, 8.47, Ar thiol C2-*H* + C6-*H*), 7.35 (6H, m, Ar thiol C3-*H*, C4-*H* + C5-*H*). IR KBr/cm^{-1}: 1677 (s), 1582 (s), 1566 (m), 1474 (m), 1441 (s), 1329 (w), 1264 (s), 1157 (w), 1137 (s), 1073 (m), 1019 (w), 998 (w), 917 (w), 835 (w), 802 (w), 789 (m), 742 (s), 710 (s), 681 (s). UV (dimethylformamide)/nm: 425 (log ε 3.76), 277 (log ε 4.46), 266 (log ε 4.56). MS m/z ES+: 514.9 $[M\text{-}Cl]^+$ (10%), 375.1 $[M\text{-}PdCl_2]^+$ (15%).

[Ni (II) bis(2-thiophenol-1,4-naphthoquinone)1,4-homopiperazine] $[NO_3]_2$

Nickel (II) nitrate (0.023g, 0.0796mmol) and **28** (0.05g, 0.0796mmol) were suspended in ethanol and refluxed together for 5 hrs. After allowing cooling to room temperature, a purple solid precipitated which, was filtered and the resulting solution evaporated under reduced pressure to yield the title compound as a red solid (0.031g, 56%). IR KBr/cm^{-1}: 3397 (s,b), 2956 (w), 2353 (m), 1636 (s), 1522 (m), 1384 (s), 1261 (m), 1095 (s), 1022 (s). UV (dichloromethane)/nm: 685 (log ε 2.93), 521 (log ε

3.22), 421 (log ε 3.64), 371 (log ε 3.81), 341 (log ε 3.95), 290 (log ε 4.67). MS m/z ES+: 673.1 $[M-O]^+$ (25%).

[Cu (I) bis(2-thiophenol-1,4-naphthoquinone)1,4-homopiperazine] [I]

Copper (I) iodide (0.0039g, 0.021mmol) and **28** (0.013g, 0.021mmol) were suspended in ethanol and refluxed together for 5 hrs. After allowing cooling to room temperature, a purple solid precipitated which was filtered and the resulting solution evaporated under reduced pressure to yield the title compound as a red solid (0.009g, 64%). δ_H (400MHz, $CDCl_3$): 8.02 (2H, dd, J=1.13, 7.59, quinone C8-*H*), 7.85 (2H, dd, J=1.02, 7.43, quinone C5-*H*), 7.60 (4H, m, quinone C6-*H* + C7-*H*), 7.15 (4H, d, J=1.74, Ar thiol C2-*H* + C6-*H*), 7.1 (6H, m, Ar thiol C3-*H*, C4-*H*+ C5-*H*), 3.35 (8H, m, NCH_2CH_2N + NCH_2CH2CH_2N), 1.75 (2H,quin, J=6.07, $NCH_2CH_2CH_2N$). IR KBr/cm^{-1}: 2963 (s), 1663 (s), 1630 (s), 1590 (m), 1534 (m), 1508 (s), 1438 (s), 1364 (m), 1271 (s), 1193 (w), 1156 (w), 1127 (m), 1064 (m), 1019 (w), 958 (m). UV (dichloromethane)/nm: 535 (log ε 3.49), 287 (log ε 4.08), 242 (log ε 4.71). MS m/z ES+: 691.1 $[M]^+$ (5%), 629.2 $[M-Cu]^+$ (30%), 220.9 $[C_6H_5S_2C_6H_5]^+$ (30%).

2.7 Results and discussion

2.7.1 Amine derivatives of 2,3-dichloro-1,4-naphthoquinone

A number of amine derivatives of 2,3-dichloro-1,4-naphthoquinone (DCNQ) have been prepared and are shown below in figure 2.14. All compounds have been fully characterised.

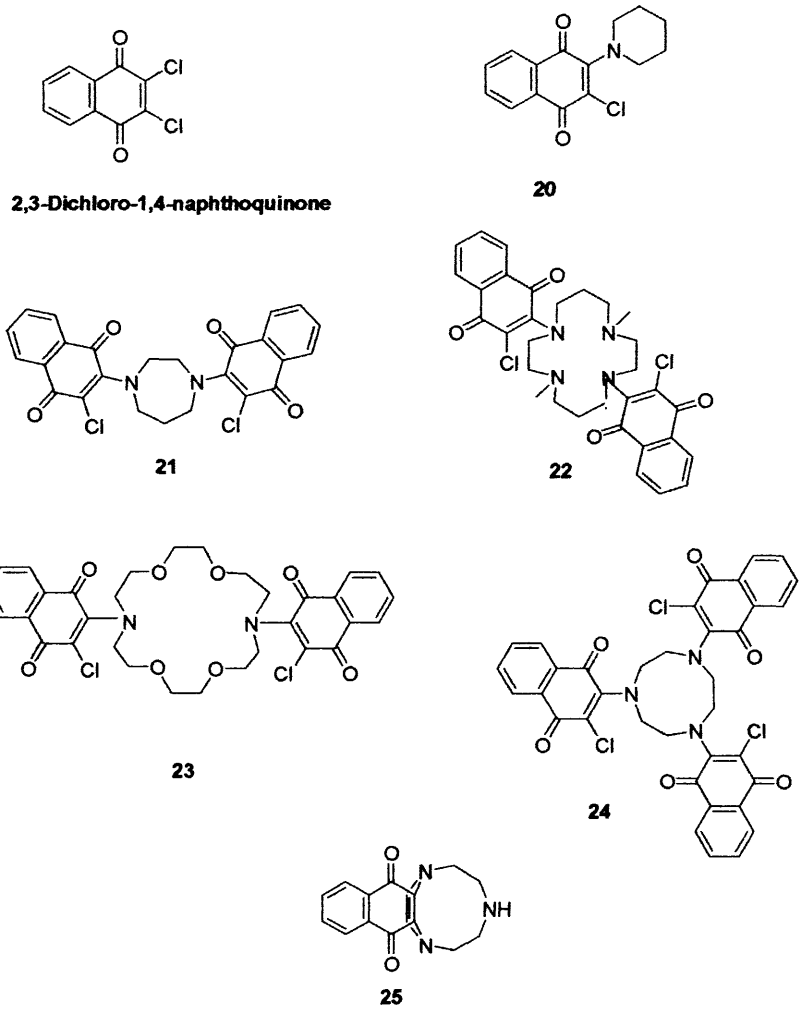

Figure 2.14: Compounds 20-25

Compounds **21-25** are novel. **20-23** were prepared by an adaptation of the method used by Beer and co-workers.[38] Compounds **24** and **25** however required slightly different conditions. Whilst **20-23** were formed in very good yields from the specific amines and 2,3-dichloro-1,4-naphthoquinone using acetonitrile as the solvent

and potassium carbonate as the base, in order to form **24** and **25** in reasonable yield, ethanol and triethylamine were employed as solvent and base respectively as by the method of Kuo and co-workers.[9] The suspensions were heated under an atmosphere of nitrogen for 6-18 hrs followed by filtration of the potassium carbonate (where appropriate) and purification via silica gel column chromatography or recrystallisation when required to afford the products as bright red solids (aside from **25** which is a blue solid).

The IR spectrum of compound **20** reveals characteristic C=O stretches with peaks at 1670 cm^{-1} and 1638 cm^{-1} and C-Cl stretches at 801 cm^{-1} and 714 cm^{-1}. The UV spectrum is consistent with previously reported quinone data[7,8,9] displaying absorptions at 507 (log ε 3.60), 286 (log ε 4.14), 248 (log ε 4.04) and 229nm (log ε 3.99). The ^{1}H-NMR demonstrates that the symmetry of the molecule has changed from the parent DCNQ however the two aromatic protons H5 and H8 experience this change more than H6 and H7. The aromatic protons H5 and H8 adjacent to the quinone have split into two multiplets compared with one for the parent quinone. This is in line with the presence of one chloride and one piperidine attached to the quinone instead of two chlorides. The high yield (91%) and ease of synthesis of compound **20** prompted further investigations into various other amine ligands of higher mass (**21-25**).

Table 2.2 demonstrates how the piperidine, homopiperazine, dimethyl cyclam, 4,13-diaza-18-crown-6;1,4,10,13 tetraoxa-7,16-diazacyclooctadecane and tacn affects the shifts in the ^{1}H-NMR spectra of the H5, H6, H7 and H8 protons of the naphthoquinone.

Quinone derivative	H5 (ppm)	H6 (ppm)	H7 (ppm)	H8 (ppm)
(DCNQ)	8.15	7.75	7.75	8.15
20	7.95	7.65	7.65	8.05
21	7.95	7.65	7.65	8.05
22	7.97	7.65	7.65	8.06
23	7.90	7.65	7.65	8.03
24	7.81	7.57	7.57	7.95
25	7.99	7.60	7.60	7.99

Table 2.2: Chemical shifts for proton resonances of 20-25 in ppm ($CDCl_3$)

Compounds **21, 22** and **23** were synthesised in the same manner to compound **20** and were afforded in 88%, 75% and 88% yields respectively. Characterisation was carried out and similar data was obtained to that of compound **20**.

Preparation of compound **24** (64% yield) was carried out following the method Kuo and co-workers had previously used to synthesise 2-chloro-3-methyamino-5,8-dimethoxy-1,4-naphthoquinone.[9] Characterisation was consistent with the proposed structure. The synthesis of compound **25** (68%) was analogous to that for **24** aside from the ratios of starting materials used. The ^{1}H-NMR of compound **25** confirms the symmetry about the quinone since a total of 2 aromatic peaks appear for protons H5, H6, H7 and H8 instead of 3 or 4 peaks as for **20-24**. The absence of a strong peak at approx 800cm^{-1} in the IR spectrum confirms the absence of the C-Cl bond in compound **25**.

2.7.2 Attempted synthesis of 2,3-dichloro-1,4-napthoquinone derivatives of 1,4,7,10-tetraazacyclododecane

With the reaction procedure proven to work for compounds **20** to **25** it was applied to the synthesis of the compounds **31, 33, 35, 37** and **41** which are illustrated in figure 2.15.

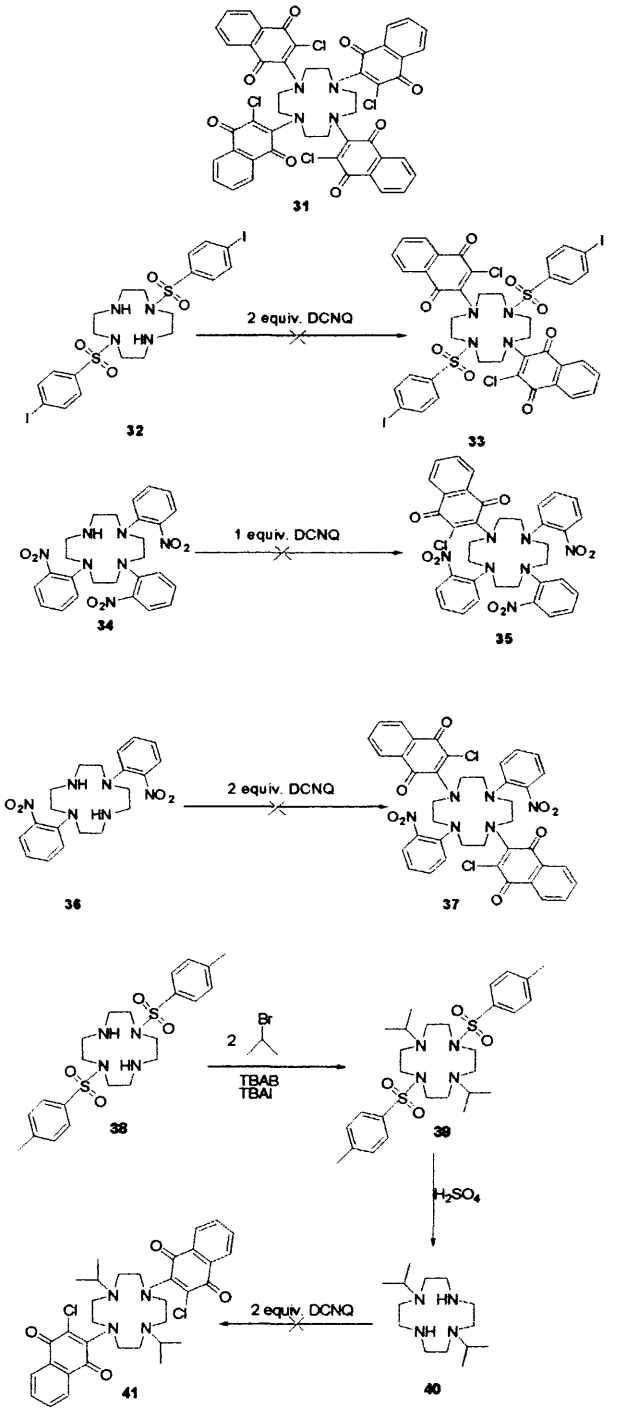

Figure 2.15:Compounds **31-41**.

In order to prepare compound **31**, the reflux of cyclen with 4.4 equivalents of 2,3-dichloro-1,4-naphthoquinone in acetonitrile with potassium carbonate for 24hr was carried out. TLC and ^{1}H-NMR analysis revealed the majority of the compound to be starting material hence reflux of the red suspension was continued for a further 48hr. Separation of starting material quinone from the product was achieved by flash column chromatography on silica gel (chloroform). ^{1}H-NMR suggested the desired reaction had occurred however mass spectrum analysis (ES+) demonstrated that the main peak occurrs at 223.0 m/z, possibly indicating the presence of the starting material quinone, despite purification. Numerous peaks were also observed in the range 530-910 m/z. The peaks accounted for are those appearing at 833.3 and 908.3 m/z representing fragments of **31** however, both signals are extremely small in comparison to the peak at 223 m/z. The MALDI (matrix assisted laser desorption ionisation) mass spectrum showed peaks in the 840-900 m/z region again owing to likely mono, di and tri substitution of cyclen with the DCNQ. The attempted synthesis of compound **31** was repeated using the alternative route used by Kuo and co-workers.[9] Results suggested the mono-substituted compound was formed.

To investigate the result obtained for compound **31**, ligand **32** was prepared by slight alteration of a standard procedure.[36] To **32**, 2.2 equivalents of the parent naphthoquinone (DCNQ) was added and heated at 80°C under nitrogen with K_2CO_3 in dimethylformamide in order to attempt to obtain **33**. After an 18hr reflux, separation by column chromatography on silica gel (chloroform) of the two products obtained was carried out. The occurrence of only one cyclen peak in the ^{1}H-NMR spectra for both compounds suggested the target compound was not present since two peaks

should be seen for the cyclen protons. Mass spectra (ES+ and MALDI) results established that the desired product **33** of molecular weight 1085 m/z was not present in either sample.

Further investigations were carried out on compounds **34** and **36** which were synthesised according to standard procedures.[37] Forcing one or two equivalents of 2,3-dichloro-1,4-naphthoquinone to react with the free nitrogen positions of **34** and **36** respectively under a variety of conditions in order to afford **35** and **37**, proved difficult. The ^{1}H-NMR spectra suggested that substitutions had taken place however characterisation by mass spectrometry revealed that compounds obtained from the reaction mixtures were in fact starting materials **34** and **36**.

A three step synthesis of ligand **40**[36] was carried out and two equivalents of DCNQ added to **40** in an attempt to produce compound **41** using both methods which have been discussed. Characterisation confirmed compound **41** had not been afforded since the majority of product was starting materials.

The results for compounds **31, 33, 35, 37** and **41** were unexpected since compounds **20-25** had been prepared without many complications. It is a general fact in cyclen chemistry that substitutions of all four positions on the nitrogens are rather difficult. Despite this, results show that compound **31** (tetra substitution) showed most promise of the cyclen compounds investigated. It is those onto which one and two equivalents of quinone were added that showed little or no reaction. Steric hindrance could be preventing the nucleophilic substitution from occurring to completion for 1,4,7-10-tetraazacyclotetradodecane and its derivatives.

2.7.3 Thiol and mixed Thiol/Amine derivatives of 2,3-dichloro-1,4-naphthoquinone

An adaptation of the method reported by Fukuyama and co-workers[39] was used to prepare compounds **26-30** shown in figure 2.16. For compound **26,** one equivalent of 2,3-dichloro-1,4-naphthoquinone and two equivalents of thiophenol were heated at 80°C under nitrogen for 2 hrs in dimethylformamide using caesium carbonate as base. This was followed by purification via column chromatography on silica gel (dichloromethane) to separate product from trace mono-substituted by-product, which had been produced. Compound **26** was isolated as an orange solid in 79% yield.

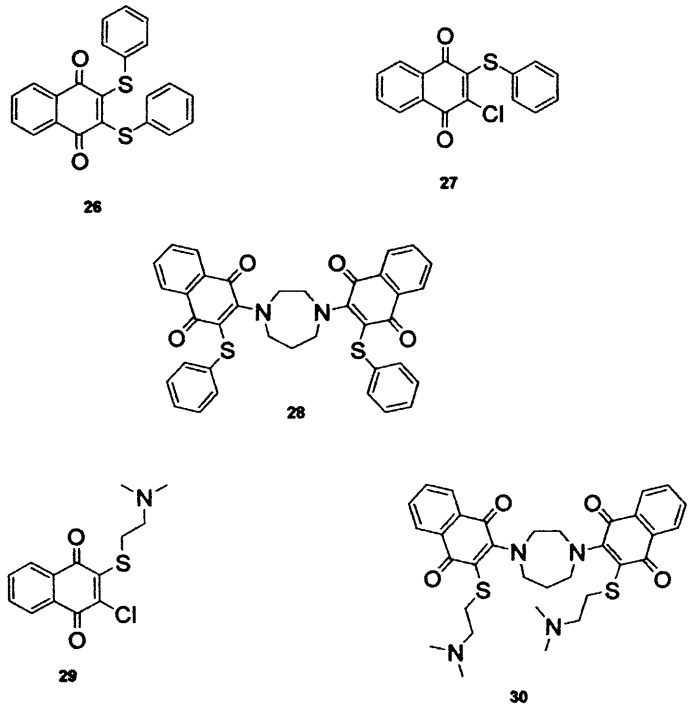

Figure 2.16: Thiol and mixed thiol/amine derivatives of 2,3-dichloro-1,4-naphthoquinone

The structure of **26** was confirmed by the presence of a peak at 1667cm^{-1} (C=O stretch), and the absence of a strong C-Cl stretch in the region 600-800cm^{-1} of the IR spectrum. The ^{1}H-NMR spectrum illustrates the symmetry of the compound by the occurrence of two peaks, one at 7.95 for H5 and H8 and one at 7.6ppm for H6

and H7 of the naphthoquinone. This is accompanied by multiplets at 7.2 and 7.3 ppm representing the thiophenol protons. Additional support of the proposed structure is provided by the APCI mass spectrum which displays the parent ion at 375 m/z. The mono-substituted analogue (**27**) was prepared using the same route to **26** and the compound has also been fully characterised. Protons H6 and H7 do not feel the affect of the broken symmetry of the quinone to the extent of H5 and H8 since the former pair is further away. The IR spectrum for compound **27** differs from that of compound **26** by the occurrence of a C-Cl stretch at 799cm^{-1}.

Compound **28** was prepared from **21** in the same manner to **26** and **27**. Recrystallisation from dichloromethane/ethanol afforded **28** as a purple solid in 73% yield. The ^{1}H-NMR spectrum demonstrates significant upfield shifting with respect to compound **21,** in line with replacement of Cl by a less electronegative moiety (sulphur). Characterisation by IR spectroscopy and mass spectrometry are also in line with the proposed structure.

Utilising the same procedure, compound **29** was prepared. From a co-ordination point of view, quinone compounds derived from this particular thiol should be more interesting to study. The soft nature of the thiol allows efficient binding of soft acids such as Cu^{+}, Ag^{+}, Au^{+}, Hg^{+}, Hg^{2+}, Pd^{2+}, Pt^{2+}. Again, the IR spectrum of compound **29** shows characteristic absorptions for C=O and C-Cl. Additionally, ^{1}H-NMR and mass spectra demonstrate that the proposed structure is correct. Attempted synthesis of the di-substituted analogue of **29** was unsuccessful due to the steric hindrance of 2 dimethylamino ethanethiol chains.

2.7.4 Metal complexes of amine derivatives of 2,3-dichloro-1,4-naphthoquinone

Complexation of **22** was achieved with both copper (II) and nickel (II) utilising the nitrate salts in both cases. The two nitrogen atoms of the macrocycle which are not attached to quinone moieties appear to be aiding complex formation since difficulties were encountered with complexation of **21**, **23** and **24** which only possess nitrogen atoms that are quinone bound.

The IR spectrum of the copper complex of **22** displays shifts in C-Cl and C-N absorptions. The shift in C-N stretch from 1234 and 1035cm^{-1} in **22** to 1227 and 1021cm^{-1} in the complex implies a weakening of the bond in line with complex formation. Shifts in the UV spectrum and an additional absorption for the d-d transition occurs at 525 nm (log ε 2.10) confirming the presence of the Cu^{2+} complex. Similar results were obtained for the nickel (II) complex. The C=O stretch appears to have weakened for the nickel complex, implying that the Ni is coordinated to the quinone. The UV spectrum demonstrates the quinone absorptions have shifted slightly and a weak absorption at 685 nm (log ε 2.33) suggests the nickel complex has been formed (d-d transition).

2.7.5 Hydrogenation reactions

Hydrogenation reactions of quinones have been studied since the 1930s by Neunhoeffer and Pelz, Bonney and Huff and Rosenblatt[4O] to name but a few. Palladium or platinum are required as the catalyst for the system.

The co-ordination capabilities for metal cations of the nitrogens bearing quinone moieties in ligands **21, 23** and **24** appear to be hindered. The most reasonable

explanation for this is the "deactivated vinylogous amide nature of aminoquinones as seen in the resonance forms."[5] Kulpe has previously suggested that compound **42** is analogous to a coupled polymethine **43** (figure 2.17).[16] Support for this argument lies in our IR spectra which indicate that the C=O stretch for all compounds synthesised in this chapter is weakened compared with DCNQ.

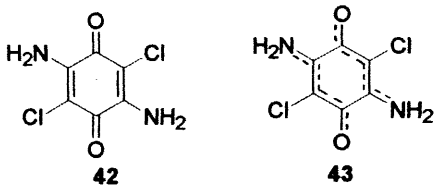

Figure 2.17: Analogy by Kulpe

Resulting from numerous unsuccessful attempts by us to complex compounds **21** and **24** with metal salts, it was decided to convert these compounds to the hydroquinone/quinol forms (figure 2.18) in an attempt to improve the ligand donating abilities.

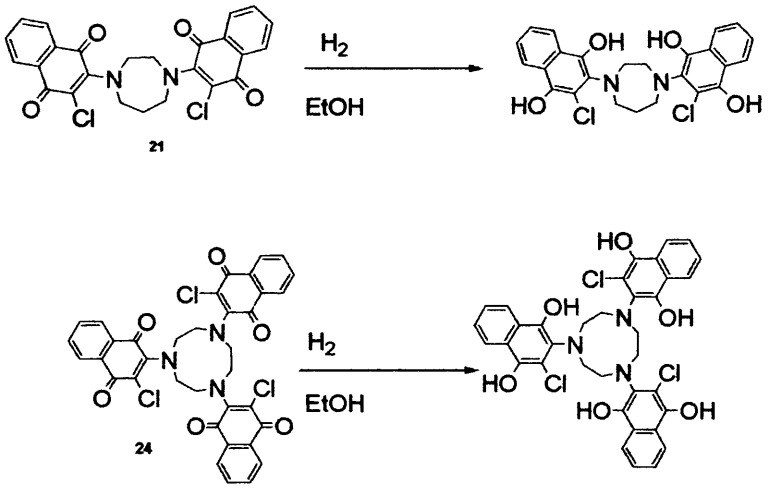

Figure 2.18: Hydrogenations of ligands **21** and **24**

Hydrogenation of ligands **21** and **24** followed by complexation using transition metals was carried out to isolate the complexes of these novel hydroquinone ligands. The solvent used was ethanol containing a trace of acetic acid and palladium on

carbon as the hydrogenation catalyst. Our quinone ligands were not overly soluble in ethanol however with vigourous stirring under a hydrogen atmosphere the hydrogenations were complete in less than 30 minutes. Once the reactions had begun, the hydroquinones were "dragged" into solution as they are more soluble in ethanol whereas the quinones have a preference for dichloromethane.

Once complete hydrogenation had taken place, the palladium catalyst was removed prior to addition of nickel. The hydrogenations alone are characterised by a colour change from red (quinone) to colourless (quinol) followed by a colour change from white to pale green upon complexation of hydrogenated **24** and white to pale yellow for complexation with hydrogenated **21**. It is implied that the quinol groups participate in co-ordination with the metal since weakening of the O-H absorption is evident in both complexes compared with the quinol free ligands. The quinol complexes are quite unstable in air and tend to slowly re-oxidise to the quinones. Disappearance of the intense ketone peak at $1668cm^{-1}$ in the infrared spectrum for hydrogenated **21,** in addition to a new strong and broad peak at $3390cm^{-1}$ (O-H) supports the formation of the hydrogenation of **21**. Shifts in the UV spectrum support the proposed transformation. Analogous trends were seen for the tacn ligand.

Comparison of the quinones and hydroquinones via ^{1}H-NMR spectroscopy was complicated due to their differing solubilities, and instability of the hydroquinones in air. The solubility problem was avoided by using deuterated acetone in which both quinone and hydroquinones are soluble. The occurrence of two new aromatic multiplets post-hydrogenation which gradually reduced in integration to be replaced by the original quinone peaks upon exposure of the sample to air (re-

oxidised), confirms the presence of the quinol species. Mass spectra support the formation of the quinol complexes.

2.7.6 Metal complexes of thiol and thiol/ amine derivatives of 2,3-dichloro-1,4-naphthoquinol

Complexation of compound **26** with palladium (II) chloride was achieved by refluxing for 4 days in acetonitrile. The yellow solid complex displayed shifts in the IR and UV spectra. The copper and Ni complexes of compound **28** obtained by reflux in ethanol for several hours also showed shifts compared with **28** in both the IR and UV spectra. The mass spectra for all three complexes display the corresponding parent ions as the main mass.

2.8 Electrochemistry discussion

Cyclic voltammetry and differential pulse voltammetry were used to study the redox chemistry of all the ligands synthesised in this chapter and the results are summarised in table 2.3. All measurements were carried out in dichloromethane.

Comp. no	Potential of couple 1 (mV) W.R.T. ferrocene	Pk-Pk Sep mV	Potential of couple 2 (mV) W.R.T. ferrocene	Pk-Pk Sep mV	Potential of couple 3 (mV) W.R.T. ferrocene	Pk-Pk Sep mV	Potential of couple 4 (mV) W.R.T. ferrocene	Pk-Pk Sep mV
DCNQ	-797 (1 e^-)	85	-1496 (1e^-)	246	_	_	_	_
20	-1234 (1e^-)	118	-1677 (1e^-)	224	_	_	_	_
21	-1141 (1e^-)	27	-1255 (1e^-)	119	-1682 (2e^-)	121	_	_
24	-1047 (1e^-)	57	-1164 (1e^-)	31	-1321 (1e^-)	119	-1718 (3e^-)	192
25	-1460 (1e^-)	90	-1969 (1e^-)	146	_	_	_	_
22	-1198 (2e^-)	121	-1752 (2e^-)	251	_	_	_	_
23	-1198 (4e^-)	191	_	_	_	_	_	_
27	-1283 (2e^-)	81	_	_	_	_	_	_
26	-967 (1e^-)	56	-1506 (1e^-)	121	_	_	_	_
28	-1196 (2e^-)	73	-1323 (2e^-)	75	_	_	_	_
29	-1345 (1e^-)	120	-1837 (1e^-)	131	_	_	_	_
30	-1270 (4e^-)	111	_	_	_	_	_	_

Table 2.3: Summary of electrochemical results for ligands **20-30**.

Clearly certain peaks are reversible whilst others are quasi-reversible or irreversible in some cases. As discussed in the background to electrochemistry, reversible behaviour is characterised by specific parameters. In order for a compound to display reversible electrochemical behaviour, the peak width must be equal to 28.5/n mV for all scan rates (where n is the number of electron equivalents transferred during the redox process), the peak current ratio must be equal to 1 for all scan rates, the peak current should increase linearly as a function of the square root of the scan rate and finally the peak potential separation should equal 57/n mV for all scan rates. To illustrate the general reversibility of the first quinone reductions, plots of peak height against the square root of the scan rate are shown for a few of the compounds which will been discussed.

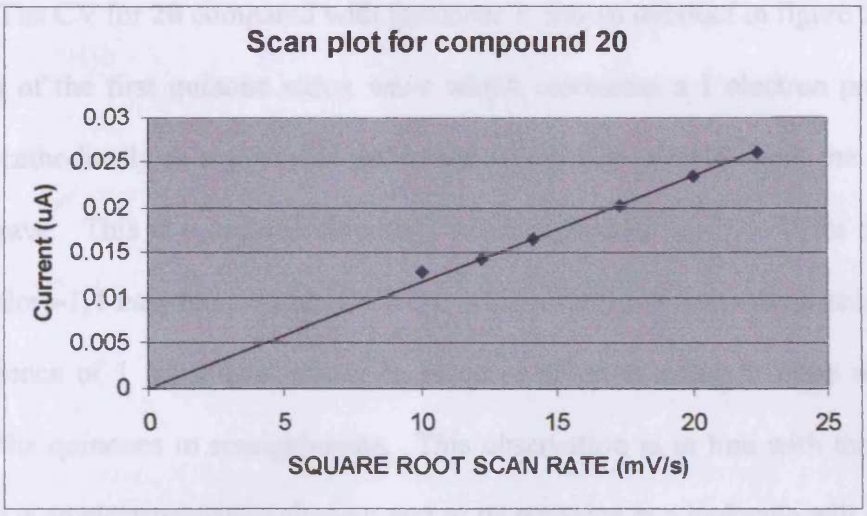

Figure 2.19: Scan plot for compound **20**

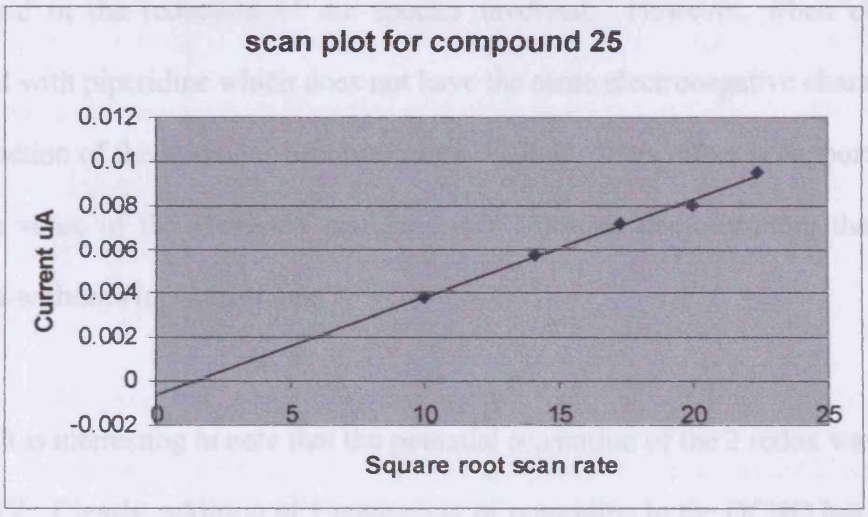

Figure 2.20: Scan plot for compound **25**

Electrochemical measurements for 2,3-dichloro-1,4-naphthoquinone show that the potential difference between the first quinone redox wave and the ferrocene redox wave is -0.797V. The first redox wave demonstrates conversion from the quinone to the radical anion. In addition the results show a potential difference of 0.699V between the 2 reversible redox waves for the compound under discussion.

The CV for **20** compared with ferrocene is shown overleaf in figure 2.21. The position of the first quinone redox wave which represents a 1 electron process has shifted cathodically to a potential difference which lies -1.234V from the ferrocene redox wave. This is a considerable shift when compared to -0.797V for the parent 2,3-dichloro-1,4-naphthoquinone (DCNQ). This result leads us to the conclusion that the presence of 1 piperidine moiety in place of chlorine makes it more difficult to reduce the quinones to semiquinones. This observation is in line with the fact that chlorine is an electronegative element and so its presence in a molecule will inevitably stabilise the radical anion ($Q^{\cdot-}$) and hydroquinone dianion (Q^{2-}) reaction products, hence aid in the reduction of the species involved. However, when chlorine is replaced with piperidine which does not have the same electronegative character, then the reduction of the quinones becomes more difficult. This effect is supported by the positive value of the Hammett parameter for chlorine, demonstrating that it is an electron-withdrawing substituent.

It is interesting to note that the potential separation of the 2 redox waves for **20** is 0.443V. Clearly, addition of 1 equivalent of piperidine to the DCNQ has the effect of reducing the potential separations between the 2 reduction processes. It is therefore evident that although upon addition of piperidine the reduction of quinone to semiquinone becomes more difficult, once the semiquinone is formed it is easier to reach the hydroquinol (second reduction) than it is in the parent compound (DCNQ). The mechanism of reduction is regarded as EE (Electrochemical followed by electrochemical).

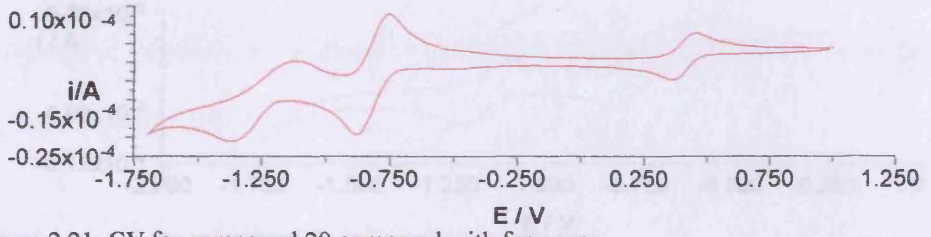

Figure 2.21: CV for compound 20 compared with ferrocene

The position of the first reduction for **21** with respect to ferrocene is –1.141V. It is therefore evident that the first reduction for this ligand occurs with more ease than the same reduction for **20** (-1.234V). Compound **21** can in theory accept a total of 4 electrons to become a tetraanion. Figure 2.22 shows the cyclic voltammogram (CV) of compound **21**. Clearly three redox waves are present for this species. This is reinforced as shown by the differential pulse measurement in figure 2.22**A** which also displays the ferrocene couple at 0.5V. The wave couples at -1.141V and -1.255V in the CV are attributed to one-electron transfers to each of the quinone moieties present in the molecule.[32] Both of these one electron transfers occur on each of the quinone moieties to produce two quinone anion radicals. This accounts for the fact that the two redox couples are separated by such a small potential. It is assumed that the third and fourth electron transfers form the third wave which appears at a potential of -1.682V. This resembles the results obtained by Beer and co-workers using calix[4]arenediquinones[32] since the third and fourth electron transfers are thought to form a single wave here also. The non-Nernstian broadness of the third wave is an indication that it is representative of the merging of two waves. Combining the above discussions, the reduction of **21** may be thought of as an EEE mechanism. The separation of the first and last reduction is greater in this case than for **20**.

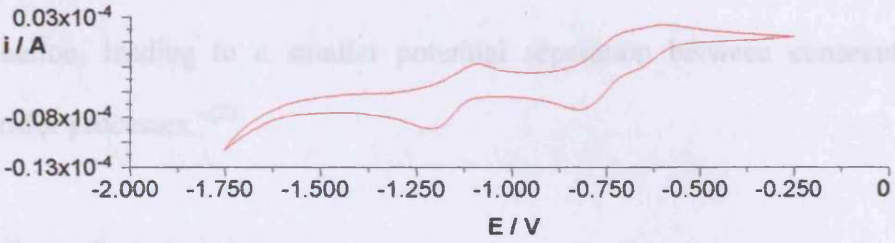

Figure 2.22: CV of compound **21**.

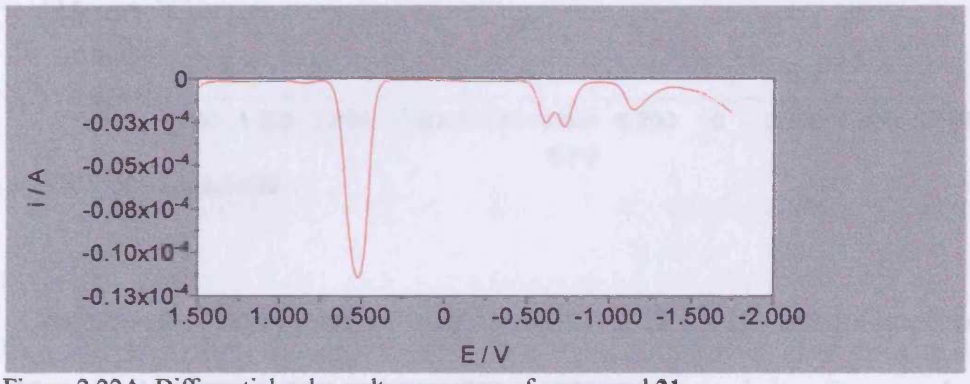

Figure 2.22A: Differential pulse voltammogram of compound **21.**

In the same way, the first reduction observed for **24** occurs at -1.047V with respect to ferrocene hence is reduced at a lower potential than the two ligands discussed so far. Compound **24** is capable of accepting a total of 6 electrons to become a hexaanion. It is noteworthy that there are four redox waves observed for this ligand (figure 2.23) the first and last being separated by 0.671V. Clearly the reduction potential is decreasing as the ligand increases in size and the number of quinone groups attached increases. Wave couples at -1.047V, -1.164V and -1.321V are a result of the initial one-electron transfers to each of the quinone moieties present in order to form 3 $Q^{\cdot-}$. Similar to compound **21**, the final wave arising at -1.718V for **24** is believed to be due to the fourth, fifth and sixth electron transfers. Confirmation of the six electron transfer is given by CPC (bulk electrolysis) studies. The mechanism for reduction of **24** is therefore regarded as an EEEE mechanism. Beer and co-workers suggested that this one-wave feature of the final redox couple may be

attributed to "minimised repulsive interaction between the reduced quinone groups upon protonation, leading to a smaller potential separation between consecutive electron-transfer processes."[32]

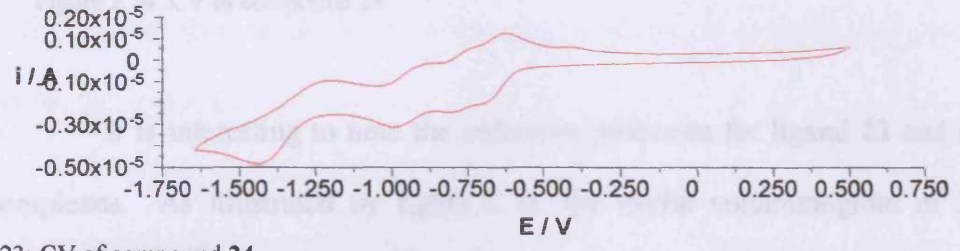

Figure 2.23: CV of compound **24**

Comparison of compound **24** with figure 2.13**A** (2.4.3 Di- and tri-aza Crown Ether Macrocycles containing quinone/ferrocene) synthesised by Beer and co-workers[35] is possible since both compounds are composed of three quinone moieties. Electrochemical data for 2.13**A** reveals only two wave couples generated from formation of 3 Q^{-} followed by 3 Q^{2-}. Measurements were however recorded by Beer and co-workers in acetonitrile whereas ours were obtained using dichloromethane.

As predicted, a greater potential (more negative) is required to reduce **25** than the other quinones synthesised in this chapter. Such behaviour is not surprising when the electronegativity of the chloride is considered. The CV of **25** is illustrated in figure 2.24. The mechanism appears to be EE.

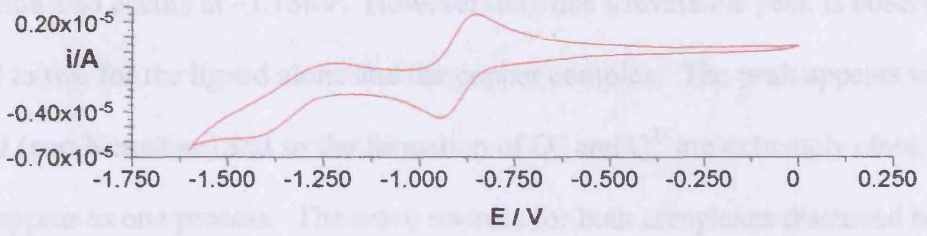

Figure 2.24: CV of compound **25**

It is interesting to note the reduction processes for ligand **22** and its metal complexes. As illustrated by figure 2.25, the cyclic voltammogram of **22** reveals two redox processes separated by 0.554V. Each reduction wave corresponds to a two-electron process hence a total of four electrons are therefore transferred for the entire process (EE mechanism). This information is supported by results from CPC (bulk electrolysis) studies.

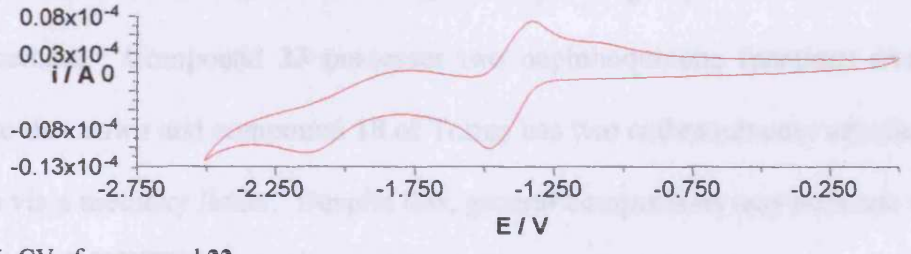

Figure 2.25: CV of compound **22**

The copper complex of **22** also has two redox waves. These are irreversible bearing a separation of 0.331V and the shift of the first reduction compared to ferrocene is –1.188V. The presence of the copper (II) has given rise to a decrease in reduction potential as anticipated. Addition of metal cations to the quinone will allow reduction to occur more readily since the positive charge will attract the electron(s) permiting reduction to proceed more efficiently than it would without the cation. This is also the case for the analogous nickel (II) complex since

the reduction also occurs at –1.188V. However only one irreversible peak is observed compared to two for the ligand alone and the copper complex. The peak appears very broadened (non-Nernstian) and so the formation of $Q^{\cdot-}$ and Q^{2-} are extremely close, so that they appear as one process. The wave couples for both complexes discussed here are irreversible since total re-oxidation to the quinone does not seem to occur once reduction has taken place.

Unexpectedly, only one reduction is obvious for **23**. This process appears to be the result of two reductions occurring almost simultaneously since it appears very broad and non-Nernstian. This was confirmed by differential pulse as shown in figure 2.26. Comparison of electrochemical results for compound **23** with **18** (*2.4.1 Quinone-substituted Lariat Ethers and Podands*) prepared by Torres and co-workers[31] can be made since they are identical crown ether macrocycles bearing two quinone moieties. Electrochemical investigations by both groups were carried out in dichloromethane. Compound **23** possesses two naphthoquinone functions directly attached to the crown and compound **18** of Torres has two anthraquinones attached to the crown via a methoxy linker. Despite this, general comparisons may be made with regards to redox behaviour. Two quasireversible wave couples are observed in the case of **18** each corresponding to a two-electron process ie. 2 $Q^{\cdot-}$ followed by 2 Q^{2-}.

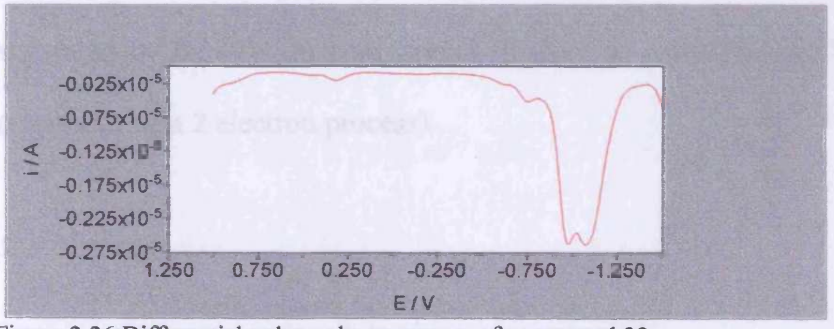

Figure 2.26:Differential pulse voltammogram of compound **23**

The cyclic voltammogram for **23** when treated with a source of sodium is characterised by an anodic shift in reduction potential of 40mV to –1.158V, typical of cation addition.[32-35] Again the presence of one broadened reduction peak implies the two reduction processes are occurring very closely. Similar to the copper and nickel complexes of **22,** the irreversible nature of the wave implies that once reduction has occurred, the complex will not re-oxidise fully. Addition of 1 equivalent of Na^+ to compound **18** resulted in the observation of two additional redox couples.

The cyclic voltammograms for **26** (figure 2.27) and **27** (figure 2.28) portray how the reduction of DCNQ is affected by substitution of one and both of the chlorides with thiophenol. Clearly, there is a cathodic shift for both **26** and **27** when compared to the parent quinone. Unexpectedly, it was found that **26** was in fact reduced at a more anodic potential than **27** (-0.967V cf. –1.283V). After investigation of this anomalous result, it was determined that during cyclic voltammetry analysis, the chlorine atom of **27** was dissociating due to sensitivity to light which has been reported previously by Rapoport and co-workers.[5] This results in the redox peak being substantially shifted cathodically. Hence this cyclic voltammogram actually represents 3-thiophenol-1,4-napthoquinone. Additionally, the CVs illustrate two reversible reductions for compound **26** (each representing a 1 electron process) separated by 0.539V, in comparison to the one reversible peak for compound **27** (representing a 2 electron process).

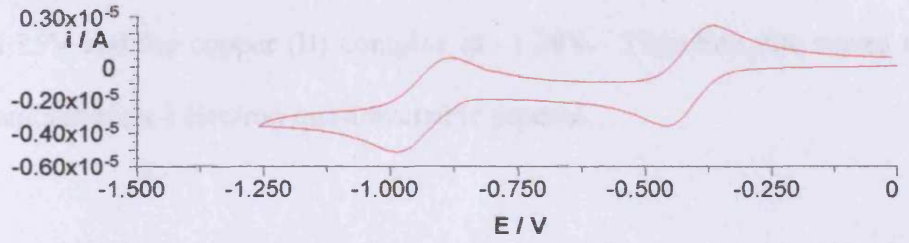

Figure 2.27: CV of compound **26**

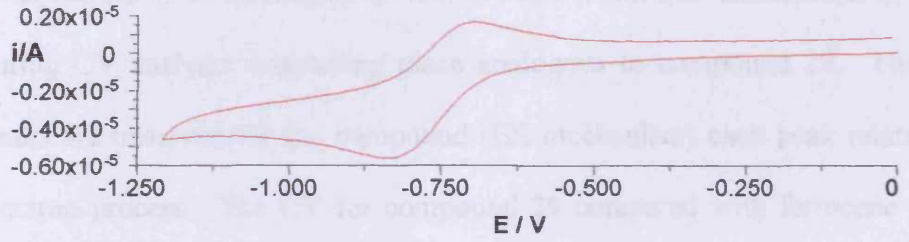

Figure 2.28: CV of compound **27**

The effect of replacing both chlorides in ligand **21** with thiophenol to form **28** is illustrated clearly in figure 2.29 by a shift to a more negative potential. This cathodic shift is consistent with the displacement of chloride as the stabilisation of negative charge upon reduction is decreased. The two reversible redox processes that take place are separated by 0.127V and each wave represents a two electron process. The suggested mechanism for reduction is EE.

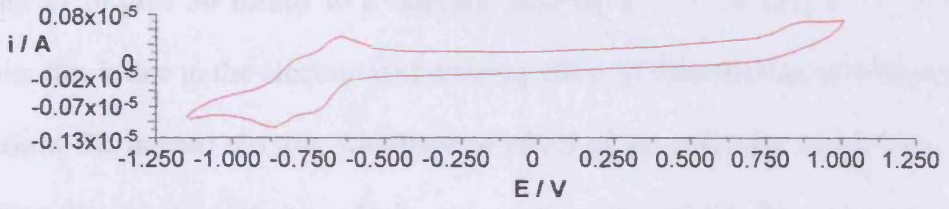

Figure 2.29:CV of compound **28**

Of particular interest are the reduction potentials of the copper (II) and nickel (II) complexes of **28** compared to the free ligand. For both complexes, the reductions seem to have merged into one broad peak which is shifted slightly

cathodically compared to the first reduction for **28.** The nickel (II) complex occurs at –1.25V and the copper (II) complex at –1.24V. Therefore, the waves in each case demonstrate a 4 electron quasireversible process.

Substitution of one chloride of DCNQ with dimethylamino ethanethiol resulted in a shift of -1.345 V from ferrocene for the first reduction. This considerable potential led us to investigate **29** and it was evident that dissociation of the chloride during CV analysis was taking place analogous to compound **27.** Two reversible peaks are observed for the compound (EE mechanism) each peak relating to a one electron process. The CV for compound **29** compared with ferrocene is shown in figure 2.30.

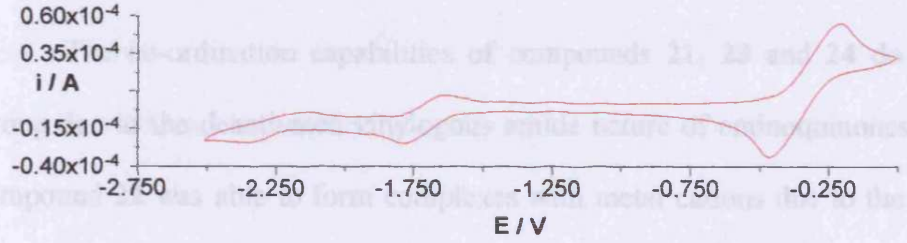

Figure 2.30: CV of compound **29** compared with ferrocene.

Using dimethylamino ethanethiol to displace the chlorides in ligand **21** to give **30** results in a cathodic shift from -1.141V (**21**) to -1.270V (**30**). Again, this is due to the electron withdrawing effect of dimethylamino ethanethiol not matching the intense electron withdrawing effect of the chlorides which have a more positive Hammett parameter. Only one peak is present for this compound and is irreversible. Since total reduction would result in the formation of a tetraanion, it is thought that this peak represents a 4 electron process.

2.9 Conclusions and future work

The synthesis of the amine derivatives of 2,3-dichloro-1,4-naphthoquinone (**20-25**) can be accomplished in good yield (64-91%) to generate a series of novel compounds with varied reduction potentials. The electrochemical results demonstrate that compound **24** was reduced with the greatest of ease followed by **21**, then **22** and **23.** The compounds reduced at more negative potentials were **20** and finally **25** as expected. Predictable 2 wave reductions were observed for compounds **20**, **22**, **25** and the presence of 1, 3 and 4 waves for compounds **23**, **21** and **24** respectively allowed us to establish information on the mechanism of the reductions in each case. CPC studies confirmed the number of electrons being transferred during reductions although results were not as accurate as we would have liked due to the differing solubilities of the quinones and their subsequent hydroquinones.

The co-ordination capabilities of compounds **21**, **23** and **24** do not appear strong due to the deactivated vinylogous amide nature of aminoquinones. However compound **22** was able to form complexes with metal cations due to the donicity of the two nitrogens not associated with the naphthoquinone moieties. Hydrogenation of the quinones **21** and **24** was found to be successful and complexation of the hydroquinols was achieved but their stability in the quinone form requires investigation.

It is evident that the chlorine (compound **21**) is more efficient in stabilising the quinone radical anion and the dianion than is the thiophenol moiety (compound **28**) as expected. Electrochemical results also establish that reduction of the quinones bearing the thiophenol is more efficient than that which occurs for the analogous

diethyl amino ethanethiol quinone. Replacement of the chlorine(s) with sulphur aided the ability of the compounds to act as ligands and complex successfully with metal cations as exemplified by the reactions of compound **28** with copper and nickel.

With regards to previous studies carried out by Beer[35] and Gokel[24], we have shown that by utilising naphthoquinone as a replacement for anthraquinone, and by direct attachment of the quinone to a crown ether instead of via a methyl group,[18] electrochemical recognition of a cation is improved since the crown ether binding site and quinone moieties are in closer proximity. Further electrochemical investigation of the ligands synthesised here with a variety of cations must be carried out.

Since our interests lie in photosynthetic models, future work by our group could concentrate on designing and synthesising 2,3-dichloro-1,4-naphthoquinone-porphyrin systems and analysing the charge separated states electrochemically. The research of Thomas Moore and co-workers (Chapter1) lies in this area.

2.10 References

1) J. E. Heffner, J. C. Raber, O. A. Moe, C. T. Wigal, *Journal of Chemical Education*, Vol. **75**, No. 3, March 1998, 365-367.

2) A. A. Kutyrev, *Tetrahedron*, **47**, No. 38, (1991), 8043-8065.

3) J.S Driscoll, G.F Hazard, H.B Wood, A. Goldin, *Cancer Chemother. Rep.* **4** (Part 2), (1974), 1-363.

4) G. Powis, *Free Radical Biology and Medicine*, **6,** (1989), 63-101.

5) H. Rapoport, S.N. Falling, *J. Org. Chem.*, **45**, (1980), 1260-1270.

6) H. Rapoport, J.R. Luly, *J. Org. Chem*, **46**, (1981), 2745-2752.

7) H. Rapoport, J.R. Luly, *J. Org. Chem*, **47**, (1982), 2404-2413.

8) S. Kuo, J. Lien, J. Wang, C. Teng, K. Lee, *Bioorg. Med. Chem.*, **5**, No. 12, (1997), 2111-2120.

9) S. Kuo, C. Teng, J. Wang, K. Lee, F. Chang, L. Huang, *Bioorg. Med. Chem.*, **6**, (1998), 2261-2269.

10) B. Prescott, *Notes*, **12,** (1969), 181-182.

11) V. Tandon, R. Chhor, R. Singh, S. Rai, D. Yadav, *Bioorg. Med. Chem. Lett.*, **14,** (2004), 1079-1083.

12) T. Iyanagi, I. Yamazaki, *Biochim. Biophys. Acta*, **216,** (1970), 282-294.

13) H. Zimmer, D.C Lankin, S.W. Horgan, *Chem. Rev.*, **71**, (1971), 229.

14) R.G. Bacon, A.R Izzat, *J. Chem. Soc. (C)*, (1966), 791.

15) R. Ceicil, J.S. Littler, *J. Chem. Soc. (B)*, (1968), 1420.

16) G.J. Gleicher, *The Chemistry of the quinonoid compounds*, **Part 1**, Edited by Saul Patai, (1974), 1-37.

17) O.C. Musgrave, *Chem. Rev.*, **69**, (1969), 499.

18) J.Q. Chambers, *The Chemistry of the quinonoid compounds*, **Part 2**, Edited by S. Patai, (1974), 737-791.

19) P.H. Given, M.E. Peover, *J. Chem. Soc.*, **385,** (1960).

20) S. Wawzonek, R. Berkey, E.W. Blaha, M.E. Runner, *J. Electrochem. Soc*, **103,** (1956), 456.

21) D.E.G Austen, P.H Given, D.J.E. Ingram, M.E. Peover, *Nature,* **182,** (1958), 1784.

22) L. Echegoyen, D.A. Gustowski, V.J. Gatto, G.W. Gokel, *J. Chem. Soc., Chem. Commun.*, (1986), 220-223.

23) D.A. Gustowski, M. Delgado, V.J Gatto, L. Echegoyen, G.W. Gokel, *J. Am. Chem. Soc.*, **108,** (1986), 7553-7560.

24) D.A. Gustowski, M. Delgado, V.J. Gatto, L. Echegoyen, G.W. Gokel, *Tet. Lett.*, **27**, (1986), 3487-3490.

25) L. Echeverria, M. Delgado, V.J. Gatto, L. Echegoyen, G.W. Gokel, *J. Am. Chem. Soc.*,**108**, (1986), 6825-6826.

26) H.K. Yoo, D.A. Gustoski, M. Delgado, V.J. Gatto, L. Echegoyen, G.W. Gokel, *J. Am. Chem. Soc.*, **110**, (1988), 119-124.

27) L.E. Echegoyen, V.J. Gatto, L. Echegoyen, G.W. Gokel, *J. Am. Chem. Soc.*, **111,** (1989), 2440-2443.

28) H.K. Yoo, D.M. Davis, Z. Chen, L. Echegoyen, G.W. Gokel, *Tet. Lett.*, **31,** (1990), 55-58.

29) Z. Chen, L. Echegoyen, G.W. Gokel, *J. Org. Chem.*, **56**, (1991), 3369-3372.

30) T. Nagaska, S. Okazaki, T. Fuginaga, *J. Electroanal. Chem.*, **133**, (1982), 89.

31) L. Echegoyen, Y. Hafez, R. Lawson, J. de Mendoza, T. Torres, *J. Org. Chem.*, **58**, (1993), 2009.

32) S. R. Cooper, M. Delgado, R. Wolf, J. Hartman, G. McCafferty, R. Yagbassan, S. Rawle, D. Watkin, *J. Am. Chem. Soc.*, **114**, (1992), 8983-8991.

33) Z. Cheng, P.A. Gale, J. Heath, P.D. Beer, *J. Chem. Soc. Faraday Trans.*, **90**(19), (1994), 2931-2938

34) P.D. Beer, Z. Cheng, P.A. Gale, *Tetrahedron*, **50**, (1994), 931-940.

35) P.D. Beer, P.A. Gale, Z. Cheng, M. Drew, J. Heath, M. Ogden, H. Powell, *Inorg. Chem.* **36**, (1997), 5880-5893.

36) Jason A. Halfen, William B. Tolman, Karl Weighardt, *Inorg. Synth.*, **32,** (1998), 75-81.

37) D. Gurden, Formation and Complexation of functionalised and tethered aza-macrocycles-Towards a model system for the active site of the oxygen evolving centre in Photosystem II, PhD thesis, UWC, 2003.

38) P.D. Beer, P.B. Crowe, M. Ogden, G. Drew, B. Main, *J. Chem. Soc., Dalton Trans.*, (1993), 2107-2116.
39) T. Fukuyama, K. Toshiyuki, W. Kurosawa, *Org. Synth. Coll. Vol.* **10**, 482.

40) E.F. Rosenblatt, *J. Am. Chem. Soc.*, **62**, (1940), 1092-1094.

Chapter 3

Porphyrin and Polypyridine Coupling

3.1 Background to Porphyrins

There is currently a great deal of research surrounding porphyrins.[1] This planar macrocycle containing 18 π electrons consists of four pyrrole rings joined via methine bridges. The basic framework of the porphyrin macrocycle is shown in figure 3.1.

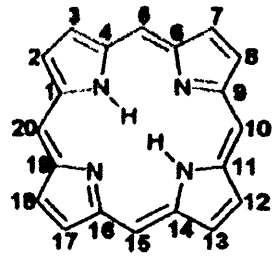

Figure 3.1: Basic framework of the porphyrin macrocycle

The bright purple or red colours of porphyrin compounds are one of their distinguishing features. In fact, the red colour of blood is due to iron (II) porphyrin.[2] Many coloured compounds found in nature are the result of porphyrin and its derivatives. In addition to its occurrence in nature, synthetic porphyrins have been prepared which can be used for a variety of applications. As well as being used for the purpose of mimicking naturally occurring porphyrins and in the field of biomedical research,[3] synthetic porphyrins have found a range of applications in materials science,[4] catalysts, redox switches, gas sensors and many others.

Porphyrins possess a strong absorption at approximately 420 nm known as the Soret band, along with several weaker absorptions between 450 and 700 nm. Altering the porphyrin framework often results in slight changes in the intensity and wavelength of these absorptions. Hence the UV spectrum is used to acquire structural information about a porphyrin-containing compound.

These highly conjugated macrocycles are well known for their robust nature as well as their photochemical and thermal stability. Of particular interest is the fact that the extensive π system of both porphyrins and metalloporphyrins gives rise to a HOMO and LUMO that are separated by only 2eV.[5] Further conjugation or polymerisation leads to a decrease in this gap, thus providing porphyrins with interesting conductivity and photophysical properties to investigate.

Lindsey has studied porphyrins in great depth and has succeeded in synthesising some very impressive light-harvesting porphyrin arrays.[6,7,8] The function of light-harvesting arrays is to absorb intensely and transfer the resulting electronic excited-state energy to one site with high efficiency. Multiporphyrin arrays can also function as nanoscale hole/electron storage reservoirs because porphyrins form relatively stable π-cation radicals.[8]

Two distinct types of porphyrins exist: *β*-substituted porphyrins and *meso*-substituted porphyrins (Figure 3.2). *β*-substituted porphyrins closely resemble naturally occurring porphyrins whereas *meso*-substituted porphyrins are purely synthetic. Despite this, *meso*-substituted porphyrins have found wide application as biomimetic models[6,7,8] and useful components in materials chemistry.[9] *Meso*-substituted porphyrins are used more frequently due to their ease of synthesis and amenability towards synthetic elaboration. The list of *meso*-substituents that have been prepared by various groups is vast and includes alkyl, aryl, organometallic, heterocyclic, other porphyrins and many more.[1]

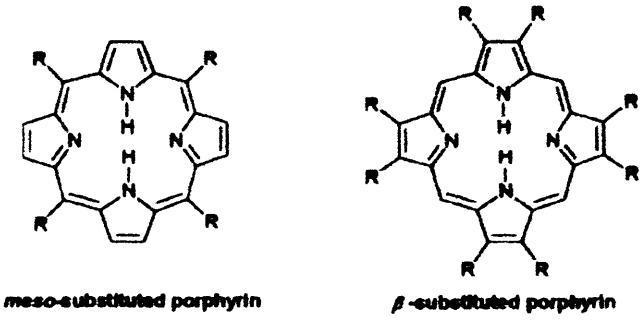

Figure 3.2: The two patterns of substitution for porphyrins

The importance of metal complexes of porphyrins in nature is vast. Many enzymes and vitamins contain metal porphyrins as do molecules which assist in oxygen transport and energy conversion.[2] For example, haemoglobin contains an iron-porphyrin complex and chlorophyll is composed of magnesium-porphyrin. A wide variety of metals are able to form complexes with the porphyrin macrocycle in a 1:1 ratio, bound via the two free pyrrole nitrogens which have been deprotonated. Most metals form equatorial porphyrin complexes and many are able to bind axial ligands which relates to the catalytic and biological activity of many such structures.

3.2 Metal Derivatives

The size of the porphyrin cavity with a covalent radius in the range 1.1-1.35Å is too small for early transition metals hence they tend to lie above or below the plane of the porphyrin with axial ligands in a cis position and metals at the bottom left of the periodic table give rise to unstable complexes. The most stable porphyrin complexes are known to be formed from first row transition metals and the axial ligands under these circumstances are in the trans position.

Metalloporphyrins can be demetallated using various agents depending upon the initial stability of the complex. Those less stable metalloporphyrins, for example

those that contain larger metal ions can be demetallated using neutral water while acetic, hydrochloric or concentrated sulphuric acid is required to remove the metal from porphyrins with greater stabilty.

3.3 Routes to Porphyrins

There are three main synthetic routes for preparing *meso*-substituted porphyrins from non-porphyrin materials.

1. The Rothermund method which was developed in 1936[10] achieves reaction between an aldehyde and pyrrole at high concentration and high temperature in a sealed vessel in the absence of added oxidant. Rothermund reported that the addition of zinc acetate, to the reaction mixture doubled the yield of tetraphenyl porphyrin from 5% to 10%. The metal salt does not increase the yields for all porphyrins which is why further studies were required.

2. The Adler-Longo method developed in the 1960s[11, 12] also involves the use of high temperature in conjunction with high concentration, however it takes place in the presence of air during a 30-minute reflux in propionic acid to afford the porphyrin in approximately 20% yield. No metal salt is used and this method affords all varieties of porphyrins in reasonable yields. This method is favourable for the preparation of porphyrins on a relatively large scale. The drawback of this method is the high percentage of polymerised pyrrole formed during the reaction and the reduced porphyrin, known as chlorin which often contaminates the sample. The latter can be removed by treatment with DDQ (2,3-dichloro-5,6-dicyano-1,4-benzoquinone), by refluxing in toluene.[13] Alternatively, the chlorin will be removed by column chromatography. It was later discovered by Dolphin[14] that a porphyrinogen

intermediate was present in the mechanism of the reaction and this lead to the development of the Lindsey method.

3. The Lindsey method[15] which is the most recent of the three methods is a two step one-flask reaction, which permits the formation of *meso*-substituted porphyrins under milder conditions. It is useful for the synthesis of porphyrins from sensitive aldehydes which is difficult to achieve utilising the Adler-Longo synthesis. Equimolar concentrations of pyrrole, benzaldehyde, and triethylorthoacetate (water scavenger), are stirred at room temperature with boron trifluoride in DCM. After 30-60 minutes, the porphyrinogen is formed hence the DDQ is added to oxidise the porphyrinogen to the porphyrin which is generally formed in yield of 30-40%. The dilute concentrations, which are required for this route, limit it to small scale synthesis.

All porphyrins which will be dealt with here shall be prepared via the Adler-Longo method. High concentrations of aldehyde and pyrrole are refluxed together in propionic acid in an open flask, and porphyrin crystals are isolated upon cooling, filtration and washing. The drawback of this method is that a great deal of post-synthetic purification is required to afford workable materials.

3.4 Previous Work

3.4.1 Lanthanide Double Decker Porphyrin sandwich complexes

Closely spaced porphyrin type π systems are found in photosynthetic proteins and some organic conductors.[16] Multichromophoric chemical species, including the bacteriochlorophyll dimer of the reaction centre in photosynthesis contains porphyrin macrocycles in close proximity. Such systems have been shown to display extraordinary optical, redox, electron transfer and conductivity properties due to the strength of the electronic interactions between molecules.[17-25] These strong interactions arise due to the extent of π-π interactions in such assemblies as a direct result of the overlap of the porphyrin HOMO orbitals. One outcome of this is the raising of the HOMO energy level which gives rise to a complex which is easier to oxidise than the monoporphyrins from which it is constructed. In this regard, lanthanide porphyrin sandwich complexes serve as excellent models for multichromophoric chemical species and many investigations of these interactions have been carried out in order to further knowledge of the functions of porphyrin complexes in these biological systems. Porphyrin-phthalocyanine lanthanide complexes are also used for such purposes and an example is illustrated in figure 3.3.

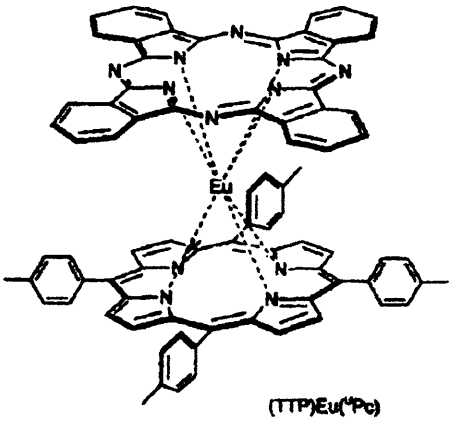

Figure 3.3: Porphyrin-phthalocyanine europium double decker complex synthesised by Lindsey and co-workers[22]

Bocian and co-workers have undertaken many studies on the $\pi\pi$ interactions in various double decker lanthanide porphyrin sandwich complexes and their corresponding π cation radicals.[17, 18, 19] Preparation of the complexes and their cations was achieved using the method of Buchler[26] and involves refluxing the free base porphyrins with the appropriate Ln(acac) in 1,2,4-trichlorobenzene under an atmosphere of nitrogen. Oxidation to the cations was carried out with phenoxathiinylium hexachloroantimonate in 1,2-dichloroethane again under a nitrogen atmosphere.[27] The neutral bis-porphyrin Ln(III) sandwiches contain a single hole in the porphyrin π system and spectroscopic investigation of these complexes revealed delocalisation of the hole over both porphyrin rings. The lanthanide is capable of holding the porphyrin macrocycles in closer proximity than their van der Waals distance of 3.4 angstroms. The ionic radius of Ce^{IV} is among the smallest of the lanthanides hence $\pi\pi$ interaction is expected to be greatest of the lanthanides for such complexes. Earlier work by Buchler and co-workers[27] demonstrated the decrease in oxidation potential of the sandwich complex as the radius of the metal ion decreases.[28] Bocian and co-workers carried out one study comparing a series of Ln(III) $(OEP)_2$ (OEP=octaetylporphyrin) complexes with the sandwich cationic species $Ce^{IV}(OEP)_2^{+}$.[17] Whilst the size of the lanthanide ion influences the magnitude of overlap, in no instance was the separation between the porphyrins large enough to result in a measurable barrier to hole transfer. Removal of a second electron to form a double-hole complex was shown to further increase the extent of $\pi\pi$ interaction. The studies also suggested that the extent of π-π overlap could be adjusted by altering the steric interactions arising from the various conformations of the ethyl substituents.

In order to further investigate their results, Bocian and his group examined the properties of a series of *meso*-substituted double decker porphyrin sandwich complexes. Tetraphenylporphyrin and tetrapentylporphyrin were used for the investigation in order to compare the effects of varying electrostatic and steric effects.[18] Spectroscopic data showed that the extent of overlap can be altered by varying the substituent on the porphyrin macrocyle. Use of tetraphenylporphyrin demonstrated that the overlap can be influenced by the steric interactions between the macrocyles. The bulky phenyl substituents are thought to cause a decrease in the $\pi\pi$ overlap in terms of steric effects whereas the tetrapentylporphyrin complexes were expected to demonstrate enhanced overlap as a result of the efficient electron-donating capabilities of the pentyl groups. Electrochemical and near-IR data indicates a larger overlap in the case of the tetrapentylporphyrin. However various conformers of both groups were shown to be evident at room and low temperatures. In certain cases, specific conformers of the tetraphenylporphyrin (TPP) complexes were shown to exhibit equal or greater overlap than conformers of the tetrapentylporphyrin (TPnP) complexes.

Following the suggestion that increased overlap is observed for double hole complexes of the type Ce^{IV} $(porphyrin)_2$ $^+$, Bocian and co-workers set out to investigate these double decker complexes containing two holes within the structure.[19] The complexes $Eu^{III}(OEP)_2^+$, $Eu^{III}(TPnP)_2^+$ and $Eu^{III}(TPP)_2^+$ were prepared and investigated. The significant energies and blue-shift of the near-IR absorption bands for these complexes, compared to the single hole species, is consistent with enhanced overlap. Further overlap is thought to occur when the temperature is lowered which may be explained by the system acquiring a more

favourable conformation upon cooling. Overall there was found to be a significant difference in the size of $\pi\pi$ overlap in the ground states of the single and double hole species investigated. Relating these results to the special pair in bacterial photosynthetic reaction centres, Bocian concluded that the $\pi\pi$ interaction in the $\pi\pi^*$ excited state is much larger than that which occurs in the ground state, therefore this could allow the bacteriochlorophylls to move closer together upon excitation, enhancing the interaction.

Further research based on double-decker porphyrin sandwich complexes has been carried out by Collman and co-workers.[20] Their interest lies in bis(porphyrin) sandwich complexes as candidates for charge-transfer materials. In such complexes, the porphyrin acts as the electron donor and acceptor. Studies showed that OETAP (octaethyltetraazaporphyrin) complexes are more easily reduced than the corresponding OEP complexes. Neutral species of this type exist in two different forms. Firstly the $Ln(Por)_2$ type which has been discussed up to this point and secondly the $Ln(Por)_2H$, in which a proton is bound to the pyrrole nitrogens. Collman reported the synthesis of $Gd(OETAP)_2$ and $Lu(OETAP)_2$ along with their reduced proton forms in addition to the conductivity of the charge-transfer complexes formed with these and zirconium(IV) porphyrin sandwich complexes. Cyclic voltammetry demonstrated the ease with which these complexes are reduced. Further electrochemical data showed that the zirconium(IV) complexes were partially oxidised by the lanthanide(III)complexes and conductivity measurements established that the charge-transfer materials prepared were semiconductors despite the acceptor (lanthanide bis-porphyrin sandwich) and donor (zirconium bis-porphyrin sandwich) both being insulators. Arising from the low conductivity values observed for the

charge-transfer materials, it was concluded that strong interactions which would give rise to greater conductivity values were prevented due to the presence of the ethyl substituents.

3.4.2 Lanthanide Triple Decker Porphyrin sandwich complexes

More recently, studies have begun on lanthanide triple decker porphyrin sandwich complexes and triple decker porphyrin-phthalocyanine complexes[21-25] as shown in figure 3.4. They are the next stage towards extended assemblies with extended $\pi\pi$ interaction.

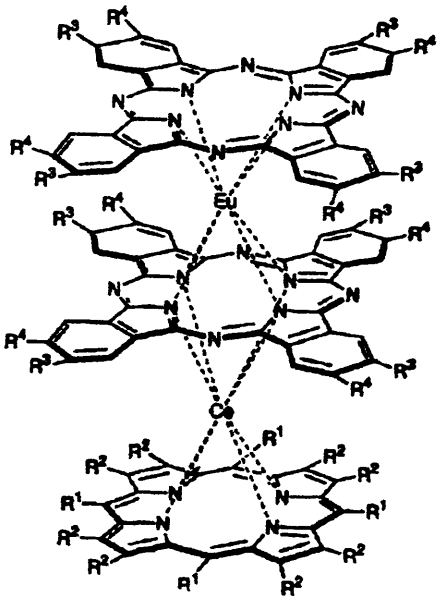

Figure 3.4: Triple decker complex synthesised by Lindsey and co-workers[22]

Holten and co-workers have studied the photophysical behaviour of $La_2(OEP)_3$, $Eu_2(OEP)_3$ and $Ce_2(OEP)_3$.[21] Many of the properties displayed by the triple-decker complexes were analogous to those observed in double-decker complexes. Surprisingly, a lack of luminescence was observed for the europium complex owing to deactivation of the triplet excited state through low energy ligand-

field states of the europium ion. Similarly, the cerium triple decker was non-luminescent due to deactivation of the singlet excited state by low lying (f,f) states. Holtens' results highlighted the role of the metal-centred excited states in shaping the relaxation rates and pathways subsequent to photoexcitation of such complexes.

As mentioned, a series of lanthanide double and triple decker tetraphenylporphyrin-phthalocyanine complexes have been reported by various groups including, Weiss,[29] Lindsey,[22, 23, 24] and Jiang.[30] Investigations by Weiss and co-workers[29] demonstrated that for complexes containing Gd^{III} and Ce^{IV} (which can not be oxidised), the phthalocyanine is oxidised as opposed to porphyrin, indicated by the presence of new bands in the near-IR. It was also observed that in the instance when the metal could be oxidised, for example Ce^{III}, it occurs with greater ease in the symmetric triple decker containing two phthalocyanines and one porphyrin.

Current research surrounding lanthanide triple decker sandwich complexes is aimed at designing systems for molecular-information storage. This relies on the capability of attaching the triple decker complexes and arrays of triple deckers to electroactive surfaces. The desire for a system with a number of available oxidation states for greater information storage density makes these systems appealing as a result of the number of redox states in addition to the low oxidation potentials and reversible electrochemistry they are known to display. Four oxidation potentials are generally observed for triple deckers owing to successive formation of monocation, dication, trication and finally the tetracation making these assemblies attractive in the area under discussion.

Lindsey and co-workers have recently carried out extensive research on these compounds for their use in molecular-based information storage.[22-24] Previous methods for preparing triple deckers firstly reported by Buchler[26] were inadequate for these purposes since direct attachment to an electroactive surface via a tether attached to one of the macrocyclic rings is required. Attachment is usually via a thiol group as shown in figure 3.5 which binds to the gold surface. Hence an approach was called for to synthesise triple deckers of a given type with distinct metals in each layer.

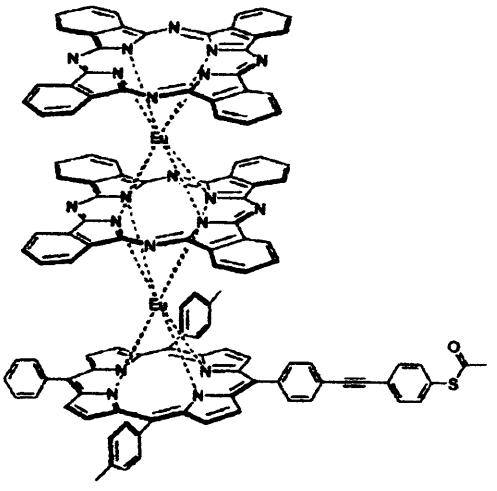

Figure 3.5: Triple decker (phenylethynylphenyl linker) prepared by Bocian, Lindsey and co-workers[23]

Lindsey and co-workers investigated the directed "monomer + dimer" route to preparing triple decker compounds as described by Weiss.[31] The route for overall preparation of a triple decker porphyrin-phthalocyanine system is shown in scheme 3.6.

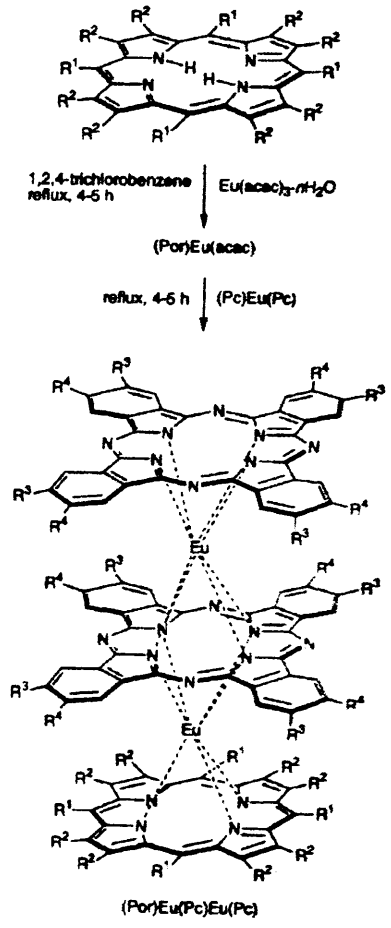

Figure 3.6: Weiss "monomer + dimar" method for preparation of triple deckers[31]

After obtaining mixtures of triple deckers in some cases, Lindsey was prompted to develop a new method for their preparation.[22] This method involved utilising a reactive, non-acac lanthanide reagent formed in situ and reacting with a porphyrin in bis(2-methoxyethyl)ether to afford the half sandwich. This is followed by reaction with a double decker to afford the triple decker. Various substituted porphyrins were incorporated into the triple deckers and those tetraarylporphyrins with ethynyl or iodo substituents provide ideal building blocks for applications in information storage and are shown in figure 3.7.

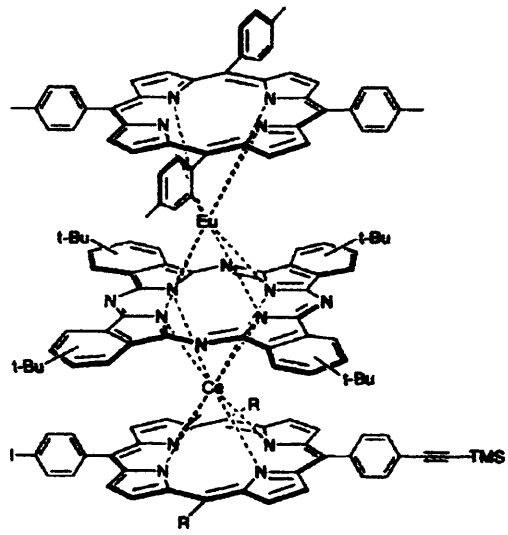

Figure 3.7:Triple deckers prepared by Lindsey and co-workers bearing iodo and ethynyl groups[22]

Further studies by Lindsey and co-workers regarding information storage have been examined and it was recently found that the use of a tripodal tether as illustrated in figure 3.8 results in surface coverage of the electroactive surface which is 4-fold higher than that obtained for monopodal functionalised triple deckers.[24] Work surrounding triple deckers for molecular-based information storage is on-going.

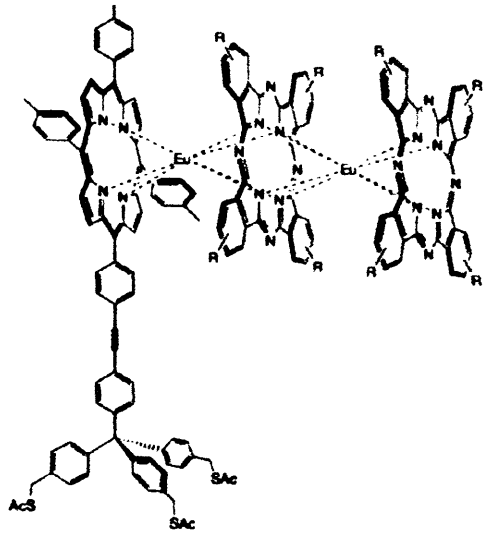

Figure 3.8: Triple decker prepared by Bocian, Lindsey and co-workers bearing tripodal tethers for surface attachment[24]

3.5 Sonogashira Coupling

The Sonogashira palladium-catalysed cross-coupling reaction[32] involves the coupling of terminal alkynes with aryl/vinyl halides. The Sonogashira coupling reaction is similar to the Stille[33] and Suzuki[34] couplings but involves the displacement of a proton instead of tin or boron respectively. The reaction occurs in the presence of base and requires a Pd (0) complex as the main catalyst and Cu (I) as a co-catalyst. The mechanism for the reaction is shown in figure 3.9. It is essential that the reaction is carried out in the absence of light since the co-catalyst, copper (I) iodide is known to be light sensitive. As shown, oxidative addition of an organic halide forms a Pd (II) intermediate which undergoes transmetallation with an alkynyl copper, followed by reductive elimination. The coupling reaction takes place and the Pd (0) catalyst is regenerated in the process.

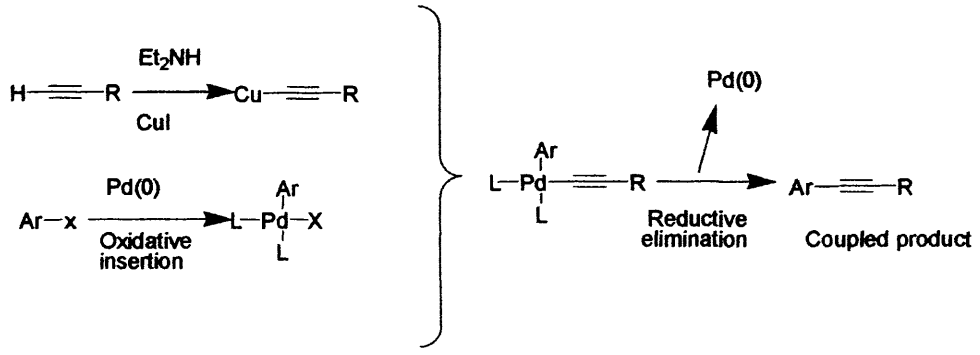

Figure 3.9: Mechanism for Sonogashira coupling reaction

It is far more convenient to use stable and soluble Pd (II) derivatives for example bis(triphenylphoshine) palladium (II) acetate which can be generated in situ. During the course of the reaction, the Pd (II) will be reduced to Pd (0) which is catalytically active since it is coordinatively unsaturated.

The Sonogashira reaction has proven to be high-yielding and capable of tolerating a variety of functional groups, however it does have one limitation. This is

the bi-product which often results from the reaction in reasonable yields. This bi-product known as the Hay[27] or Glaser[28] coupling product is formed from the homocoupling of the terminal acetylenes. Formation of the homocoupled bi-product is a major drawback in crosscoupling reactions since the terminal acetylene is usually an expensive starting material or it may have been difficult to synthesise.

The process of synthesising model photosynthetic systems relies on methods for joining together large numbers of components into light harvesting arrays. The Sonogashira reaction has been used extensively[6, 37, 38, 39, 40] in light-harvesting systems since it has been demonstrated to act as an efficient linker in energy transfer in addition to providing architectural rigidity which is essential for such systems. Furthermore it has been used for the coupling of pyridine, bipyridine and terpyridine[41-45] and products have been isolated in excellent yields. For these reasons, we shall use the Sonogashira coupling reaction as the key for joining all components in this chapter.

3.6 Aims and objectives

Transfer of an excited electron from a donor molecule covalently linked to an acceptor to afford charge separated states is termed Photoinduced electron transfer (PeT). Such reactions are of great interest due to the fact that photosynthesis is the main example where a system of electron donors and acceptors can be arranged to harvest and store photon energy. We set out to design a system which would further our knowledge of PeT in a system where two porphyrins which are connected via a terpyridine moiety, sandwich a lanthanide ion. Furthermore terpyridine which is known to be an excellent ligand for a wide variety of metals will also be metallated in order to investigate the effect on the porphyrin emission. The porphyrin-terpyridine array which is our target molecule is shown in figure 3.10.

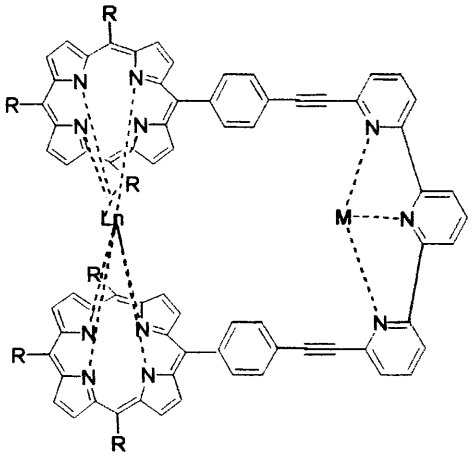

Figure 3.10: Target Porphyrin-terpyridine system.
M represents a transition metal and Ln a lanthanide.

As presented earlier in the work of Lindsey,[22-24] Buchler,[27, 28] Bocian,[17-19] and many others[20, 21, 29, 30] the photophysics of lanthanide double and triple decker porphyrin sandwich complexes has become widely studied. The strong π-π interactions between the porphyrins results in compounds with extremely interesting redox, electron transfer and conductivity properties. Such studies are vital towards

the development of understanding the mechanisms occurring in multichromophoric species.

If our target molecular array is successfully prepared, then metallation of the terpyridine with various transition metals and the porphyrins with a single lanthanide ion will be carried out and the photophysics studied. Terpyridine is known to act as a chromophore as is the porphyrin macrocycle. Terpyridine possesses three lone pairs of electrons and upon excitation, these lone pairs would be available to quench the emission of an excited state porphyrin, hence lowering the luminescence of the lanthanide porphyrin complex to which it is attached. Preventing the availability of the lone pairs for quenching by chelating terpyridine with a metal[40] should result in an increase in the luminescence. Various metals will give rise to various degrees of emission depending on the degree of binding to the lone pairs. Metals that bind more strongly with the terpyridine are likely to give rise to stronger lanthanide emission as opposed to those, which bind weakly.

Further variation of the lanthanide ion sandwiched between the porphyrin macrocycles will affect the degree of π-π overlap of the porphyrins hence the degree of electron delocalisation and stability within the structure. The smaller lanthanide ions such as Ce^{IV} and Eu^{III} have been shown to allow the porphyrins to come into close proximity hence the magnitude of the $\pi\pi$ interaction is large and electron and hole delocalisation is large.[17, 18] Our aim therefore is to synthesise and investigate the photophysics of the porphyrin-terpyridine molecular array by altering the lanthanide and transiton metals within the structure. Although one would envisage the stability of such a bisporphyrin-terpyridine species to increase when $\pi\pi$ overlap is

greatest, it is likely that an optimum separation exists due to the angles at which the porphyrins are held by the terpyridine.

Various synthetic organic transformations are required for the preparation of this compound. The coupling method, which will be employed in these systems, is the Sonogashira reaction.[32] In addition to providing rigid centre to centre distances, the alkyne spacer group appears to be an appropriate length to take part in efficient energy transport (inter-pigment couplings). The 6,6"-dibromo-2,2':6'2"-terpyridine which is required for the array will be prepared by a known method.[46] Furthermore, we shall be preparing a variety of porphyrin macrocycles using the Adler-Longo[11, 12] synthesis which is convenient for large scale synthesis. Since 4-iodobenzaldehyde is the ideal compound for the preparation of a porphyrin to participate in the Sonogashira reaction but is very expensive to purchase, it is our aim to investigate and find a more efficient method for its preparation.[47-50]

We therefore set out to investigate different routes to the preparation of the desired porphyrin-terpyridine array shown in figure 3.10, linked using the Sonogashira coupling method. Preliminary studies were carried out with several simpler and less costly pyridine analogues to establish the feasibility of applying the Sonogashira reaction.

3.7 Experimental

3.7.1 Sonogashira reactions on Bromo-pyridine

2,6-Bis(2-methyl-3-butyn-2-ol) pyridine (42).[39]

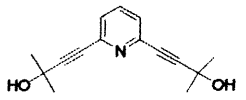

Copper (I) iodide (0.019g, 0.1mmol), palladium (II) acetate (0.022g, 0.1mmol), and triphenyl phosphine (0.052g, 0.2mmol) were added to a solution of 2,6-dibromopyridine (2.36g, 10mmol) and 2-methyl-3-butyn-2-ol (2.13mls, 22mmol) in acetonitrile (20mls) and triethylamine (20mls) and the mixture refluxed under nitrogen for 3 hrs at 80°C. After cooling, aqueous sodium hydrogen carbonate (100mls) was added, and the brown solution extracted with dichloromethane (3 x 50 mls), dried over magnesium sulphate and evaporated under reduced pressure to yield a brown/red oily product. Purification by flash chromatography on silica gel (chloroform/methanol 98:2) afforded the title compound as a brown oil (77%). δ_H (400MHz, $CDCl_3$): 7.6 (1H, t, J=7.62, C4-*H*), 7.3 (2H, d, J=7.74, C3-*H*, C5-*H*), 3.9 (2H, s, O*H*), 1.6 (12H, s, CH_3). MS m/z EI: 243 [M] (41%), 228.2 [M-O] (72%), 210.2 [M-2O] (97%). m/z CI: 244.1 [M+H] (100%).

2,6-Bis-ethynyl pyridine (43).[39]

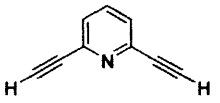

2,6-Bis(2-methyl-3-butyn-2-ol) pyridine (**42**) (1.089g, 4.48mmol) was dissolved in toluene (50mls) and after the addition of finely powdered dry sodium hydroxide (0.36g, 9.0mmol), the mixture was refluxed for 3 hrs under nitrogen. The cooled brown suspension was filtered and the filtrate concentrated on a rotary evaporator followed by drying to yield the title compound as a brown solid product (75%). δ_H (400MHz, $CDCl_3$): 7.6 (1H, t, J=8.02, C4-*H*), 7.4 (2H, d, J=7.39, C3-*H*, C5-*H*), 3.1 (2H, s, CC*H*). MS m/z EI: 128.0 [M] (100%).

2-Bromo,6(2-methyl-3-butyn-2-ol) pyridine (44). [39]

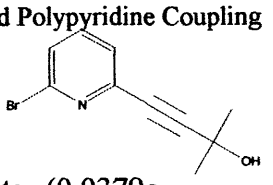

Copper(I) iodide (0.0322g, 0.169mmol), palladium(II) acetate (0.0379g, 0.169mmol) and triphenyl phosphine (0.0887g, 0.338mmol) were added to a solution of 2,6-dibromopyridine (4g, 16.9mmol) and 2-methyl-3-butyn-2-ol (2.45mls, 25.3mmol) in acetonitrile (40mls) and triethylamine (40mls) and the mixture refluxed under nitrogen at 100°C for 3 hrs. After cooling, aqueous sodium hydrogen carbonate solution (150mls) was added and the solution extracted in dichloromethane (3 x 50mls). The solvent was evaporated under reduced pressure to afford the crude product. Purification by column chromatography (dichloromethane/methanol 98:2) yielded the title compound as a brown oil (22%). δ_H (400MHz, $CDCl_3$): 7.45 (1H, t, J=7.60, C4-*H*), 7.35 (1H, d, J=7.74, C5-*H*), 7.3 (1H, d, J=7.50, C3-*H*), 1.6 (6H, s, CH_3). MS m/z EI+: 241.0 $[M+H]^+$ (96%), 239.0 [M-2H] (100%).

2,(2-Methyl-3-butyn-2-ol) pyridine (45). [39]

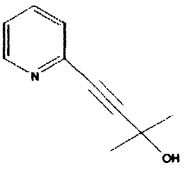

Copper (I) iodide (0.06g, 0.316mmol), palladium(II) acetate (0.07g, 0.316mmol), and triphenyl phosphine (0.17g, 0.632mmol) were added to a solution of 2-bromopyridine (3.018mls, 31.6mmol) and 2-methyl-3-butyn-2-ol (3.058mls, 31.6mmol) in acetonitrile (20mls) and triethylamine (20mls) . The mixture was refluxed under nitrogen for 4 hrs. After cooling, aqueous sodium hydrogen carbonate was added and the mixture extracted in dichloromethane (3 x 50mls), dried over magnesium sulphate, filtered and evaporated under reduced pressure to yield a brown solid (3.859g, 77%). δ_H (400MHz, $CDCl_3$): 8.6 (1H, d, J=4.32, C6-*H*), 7.6 (1H, t, J=7.85, C4-*H*), 7.4 (1H, d, J=7.88, C3-*H*), 7.15 (1H, t, J=4.70, C5-*H*), 3.9 (2H, s, O*H*), 1.6 (6H, s, CH_3). MS m/z EI+: 161.0 $[M+H]^+$ (98%).

Bis-2,6-(ethynyl pyridyl) pyridine (46).

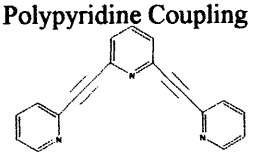

A solution of 2,(2-methyl-3-butyn-2-ol) pyridine (2g, 12.4mmol) **(45)**, and dibromopyridine (1.47g, 6.21mmol) in toluene (100mls) was added to tetrabutylammonium bromide (0.1256g, 0.39mmol), copper (I) iodide (0.1066g, 0.56mmol), palladium (II) acetate (0.126g, 0.56mmol) and triphenyl phosphine (0.146g, 0.56mmol). A 5.5 mol aqueous solution of sodium hydroxide was added under nitrogen and the resulting brown solution stirred under an atmosphere of nitrogen for 50hrs at 85°C. Once cooled the brown solution was stirred with saturated ammonium chloride solution for 1hr at room temperature, followed by extraction in dichloromethane (3 x 100mls). After the solution was dried ($MgSO_4$) and filtered, evaporation under reduced pressure afforded a brown oily solid as the crude product which was filtered through silica gel using dichloromethane (96%)/methanol (4%). Further purification via column chromatography on silica gel using chloroform (96%) and methanol (4%) was carried out followed by recrystallisation from hexane to yield the pure compound (51%). δ_H (400MHz, $CDCl_3$): 8.61 (2H, d, J=4.64, terminal pyridine *H's*), 7.75 (3H, m, centre pyridine *H's)*, 7.62 (2H, m, terminal pyridine *H's*), 7.51 (2H, m, terminal pyridine *H's*), 7.23 (2H, m, terminal pyridine *H's*). IR KBr/cm^{-1}: 3080 (m), 2262 (s), 1699 (s), 1594 (s), 1573 (m), 1473 (w), 1307 (s), 1261 (s), 1137 9s), 1096 (s), 1074 (s), 1021 (m), 911 (m), 897 (s), 840 (m), 807 (s), 749 (s), 719 (s). MS m/z APCI: 282.5 $[M+H]^+$ (100%).

3.7.2 Synthesis and Sonogashira reaction of Bis(2-(6-bromopyridyl) ketone

Bis(2-(6-bromopyridyl) ketone (47).[49]

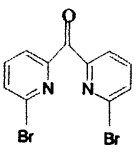

A solution of 2, 6-dibromopyridine (5g, 21mmol) in diethyl ether (150mls) was cooled to -78°C and n-BuLi in hexane (14.4 mls) was added drop wise

to form a yellow solution. A solution of diethyl carbonate (9.5mmol, 1.15mls in 20mls diethyl ether) was added to the solution of the lithiate and the resulting solution stirred overnight at -78°C. Due to warming overnight, the reaction mixture was cooled to 0°C and the resulting creamy/yellow solution quenched with 10% HCl until acidic, then with 10% K_2CO_3 until basic. The crude product was extracted in $CHCl_3$ twice and the organic layers dried over Mg_2SO_4, filtered and evaporated under reduced pressure to yield a cream solid (2.855g, 79%). Recrystallisation from methanol afforded bis(2-(6-bromopyridyl) ketone as a white solid (1.331g, 39%). δ_H (400MHz, $CDCl_3$): 8.0 (2H, d, J=7.43, C3-*H*), 7.7 (2H, t, J=7.83, C4-*H*), 7.62 (2H, d, J=7.99, C5-*H*). IR KBr/cm^{-1}: 3360 (w), 3078 (m), 2628 (w), 2501 (w), 1981 (w), 1901 (w), 1824 (w), 1738 (w), 1690 (s), 1573 (s), 1559 (s), 1436 (s), 1423 (s), 1393 (s), 1323 (s), 1261 (w), 1236 (m), 1189 (m), 1155 (s), 1115 (s), 1076 (s), 984 (s), 963 (s), 913 (m), 823 (s), 806 (s), 754 (s), 726 (s), 695 (s), 649 (m), 631 (s), 505 (m).

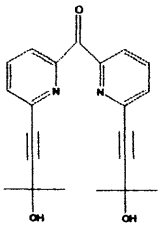

Bis(2-(6-(2-methyl-3-butyn-2-ol pyridyl) ketone (48).

Copper (I) iodide (0.0028g, 0.0146mmol), palladium (II) acetate (0.0033g, 0.0146mmol) and triphenyl phosphine (0.0077g, 0.0292mmol) were added to a solution of bis (2-6-bromopyridyl) ketone (0.5g, 1.46mmol) and 2-methyl-3-butyn-2-ol (0.31mls, 3.218mmol) in acetonitrile (10mls) and triethylamine (10mls). The mixture was refluxed under nitrogen for 3 hrs at 90°C. After cooling, aqueous sodium hydrogen carbonate (100mls) was added and the brown solution extracted in dichloromethane (3 x 40mls), dried over magnesium sulphate, filtered and evaporated under reduced pressure to yield the product as a brown oily compound (0.339g, 67%). δ_H (400MHz, $CDCl_3$): 7.95 (2H, d, J=7.95, C3-*H*), 7.8 (2H, t, J=7.90, C4-*H*), 7.55

(2H, d, J=7.97, C5-*H*), 5.25 (2H, s, O*H*), 1.6 (12H, s, CH_3). IR KBr/cm^{-1}: 3450 (s), 3072 (m), 2628 (w), 2215 (w), 1981 (w), 1825 (w), 1746 (w), 1687 (s), 1573 (s), 1559 (s), 1436 (s), 1423 (s), 1393 (s), 1323 (s), 1265 (w), 1238 (m), 1189 (m), 1156 (s), 1120 (s), 1076 (s), 990 (s), 971 (s), 920 (m), 825 (s), 810 (s). MS m/z ES+: 349.2 $[M+H]^+$ (70%), 279.2 $[M-C_4H_7O]^+$ (98%), 380.3 $[M+Na]^+$ (80%).

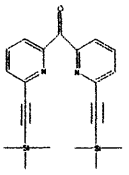

Bis(2-(6(trimethylsilyl acetylene) pyridyl ketone (49).

Palladium (II) acetate (0.00225g, 0.01mmol), copper iodide (0.00525g, 0.02mmol) and triphenyl phosphine (0.0019g, 0.01mmol) were added to a solution of bis(2-6-bromopyridyl) ketone (0.341g, 1mmol) and TMS acetylene (0.57mls, 4mmol) in acetonitrile (5mls) and triethylamine (5mls). The solution was heated for 12 hrs at 80°C and after cooling, water (90mls) was added and the brown solution extracted in dichloromethane (3 x 50mls). The organic layer was dried over magnesium sulphate, filtered, and the solvent removed to yield a light brown coloured solid (0.321g, 85%). δ_H (400MHz, $CDCl_3$): 7.85 (2H, d, J=7.60, C3-*H*), 7.75 (2H, t, J=7.17, C4-*H*), 7.54 (2H, d, J=7.89, C5-*H*), 0.2 (18H, s, CH_3). IR KBr/cm^{-1}: 3360 (m), 3070 (m), 2700 (m), 2630 (w), 2200 (m), 1978 (w), 1750 (w), 1691 (s), 1574 (s), 1560 (s), 1441 (s), 1423 (s), 1393 (s), 1323 (s), 1265 (w), 1239 (m), 1189 (m), 1159 (s), 1121 (s), 1075 (s), 992 (s), 975 (s), 911 (m), 820 (s), 798 (s). MS m/z EI+: 376.2 $[M+H]^+$ (100%).

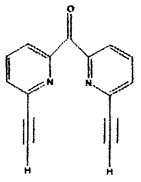

Bis(2-(6-ethynyl pyridyl) ketone (50).

Bis(2-(6(trimethylsilyl acetylene) pyridyl ketone , (0.05g, 0.133mmol) was stirred under nitrogen with tetrabutylammonium fluoride (0.069g, 0.266mmol) in

dichloromethane (10mls) for 100 hrs and filtered through silica to yield the title compound (0.029g, 94%). δ_H (400MHz, $CDCl_3$): 8.0 (2H, d, J=7.85, C3-*H*), 7.8 (2H, t, J=7.73 C4-*H*), 7.6 (2H, d, J=7.64, C5-*H*), 3.1 (2H, s, *H*). IR KBr/cm^{-1}: 3412 (m), 3310 (s), 3070 (m), 2651 (w), 2203 (m), 1969 (w), 1699 (s), 1578 (s), 1561 (s), 1441 (s), 1423 (s), 1391 (s), 13222 (s), 1267 (w), 1189 (m), 1159 (s), 1121 (s), 1075 (s), 990 (m), 951 (m), 819 (m), 800 (w). MS mz ES+: 233.2 $[M+H]^+$ (100%).

3.7.3 Synthesis and Sonogashira reaction of 6,6"-Dibromo-2,2':6'2"-terpyridine

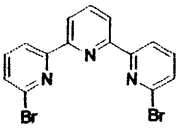

6,6"-Dibromo-2,2':6'2"-terpyridine (51)[46]

To a solution of 2,6-dibromopyridine (11.85g, 50mmol) in diethyl ether (50ml) cooled to -60°C, was added a solution of butyllithium in hexane (1.6M, 31.25ml, 50mmol) while stirring. After stirring for 2 hours at -40°C, a solution of phosphorous trichloride (1.72g, 12.5mmol) in diethyl ether (50ml) was added drop wise over 2 hours and the mixture placed in a -50°C freezer for 4 days with occasional stirring. The mixture was allowed to warm to room temperature and water (100ml) was added. The product was filtered, washed with water and dried. The crystals were dissolved in hot toluene (400ml), filtered and the hot toluene solution was then passed through a short silica gel column. Toluene was removed under reduced pressure and the residue washed with ether to give 6,6"-dibromo-2,2':-terpyridine as a white solid (2.35g, 36%). δ_H (400MHz, $CDCl_3$): 8.57 (2H, d, J=7.48, H_5 ,$H"_5$); 8.49 (2H, d, J= 7.74, H'_3, H'_5); 7.91 (1H, t, J=7.71, H'_4); 7.68 (2H, t, J=7.45, H_4 ,$H"_4$); 7.45 (2H, d, J=4.9, H_3, $H"_3$). IR KBr/cm^{-1}: 3086 (w), 3046 (w), 2963 (m), 1700 (w), 1653 (w), 1569 (s), 1553 (s), 1425 (s), 1261 (s), 1090 (s), 1020 (s), 986 (m), 862 (w), 798 (s),

786 (s), 696 (m), 632 (w). MS: m/z EI+: 391.0 $[M]^+$ (100%), 312.1 $[M-Br]^+$ m/z CI+: 392.0 $[M+H]^+$ (100%)

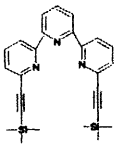

6,6"Bis-trimethylsilyl acetylene-2,2':6'2"-terpyridine (52).

To 6,6"-Dibromo-2,2':6'2"-terpyridine (0.25g, 0.64mmol) and TMS-acetylene (0.36mls, 2.56mmol) in acetonitrile (5mls) and triethylamine (5mls) was added copper (I) iodide (1.22mg, 0.0064mmol), palladium (II) acetate (1.44mg, 0.0064mmol) and triphenyl phosphine (3.35mg, 0.0128mmol). The mixture was then degassed and refluxed for 12 hours. After cooling, water was added (50mls) and the brown solution extracted in dichloromethane (3 x 40mls). The organic layers were combined and dried ($MgSO_4$). After filtering, the solvent was removed under reduced pressure to give 6,6" bis trimethylsilyl acetylene-2,2':6'2"-terpyridine as a brown oil (0.21g, 77%). δ_H (400MHz, $CDCl_3$): 8.50 (4H, t, J=8.25, *H5 ,H"5, H'3, H'5)*, 7.89 (1H, t, J=7.94, *H'4)*, 7.74 (2H, t, J=7.85, *H4 , H"4)*, 7.45 (2H, d, J=5.38, *H3, H"3)*, 0.2 (18H, s, *CH3)*. MS m/z ES+: 426.0 $[M+H]^+$ (78%), 411 $[M-CH_3]^+$ (99%).

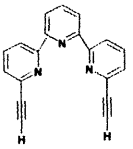

6,6"Diacetylene-2,2':6'2"-terpyridine (53).

To a solution of 6,6" bis-trimethylsilyl acetylene-2,2':6'2"-terpyridine (0.122g, 0.29mmol) in dichloromethane (30mls) was added tetrabutyl ammonium fluoride (0.165g, 0.63mmol) and the solution stirred for 96 hrs. The resulting brown solution was filtered through a plug of silica and the solvent removed to give a cream coloured solid (0.079g, 98%). δ_H (400MHz, $CDCl_3$): 8.5 (2H, d, J=7.18, *H5, H"5)*, 8.4 (2H, d, J=7.83, *H'3, H'5)*, 7.9 (1H, t, J=7.72, *H'4)*, 7.77 (2H, t, J=7.72, *H4 ,H"4*), 7.45 (2H, d, J=7.46, *H3 ,H"3)*, 3.13 (1H, s, CC*H*). IR KBr/cm^{-1}: 3274 (m), 3061 (w), 2962 (m),

2109 (w), 1997 (w), 1674 (w), 1573 (s), 1475 (w), 1433 (s), 1361 (w), 1261 (s), 1205 (w), 1159 (w), 1073 (s), 1025 (m), 990 (s), 846 (w), 795 (s), 740 (m), 698 (m), 668 (s), 636 (m), 625 (m). MS m/z EI+: 281.2 $[M]^+$ (60%), 49.2 $[C_4H]^+$(100%).

3.7.4 Synthesis and Sonogashira reaction of 4-Iodobenzaldehyde

4-Iodo(bromomethyl)benzene (54).

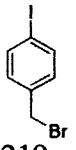

A mixture of 4-iodotoluene (6.721g, 30.8mmol), N-bromosuccinimide (8.219g, 46mmol) and benzoyl peroxide (0.0678g, 0.28mmol) in CCl_4 (61ml) was refluxed for 3 hrs. The solution was cooled, filtered and concentrated under reduced pressure to yield a peach coloured solid. The crude product (6.5g, 71%) was used without purification in the next step. δ_H (400MHz, $CDCl_3$): 7.65 (2H, d, J=8.88, C3-*H*, C5-*H*), 7.15 (2H, d, J=9.16, C2-*H*, C6-*H*), 4.38 (2H, s, CH_2Br). IR KBr/cm^{-1}: 3061 (w), 2967 (w), 1904 (m), 1788 (m), 1701 (m), 1581 (s), 1480 (s), 1435 (m), 1398 (s), 1305 (w), 1279 (m), 1218 (s), 1202 (s), 1175 (m), 1142 (m), 1089 (s), 1055 (s), 1006 (s), 952 (m), 872 (m), 826 (s), 712 (s), 588 (s), 472 (s), 418 (m). MS m/z EI+: 298.1 $[M+H]^+$(30%), 217.0 $[M-Br]^+$(50%), 126.9 $[I]^+$(100%).

4-Iodobenzaldehyde (55).

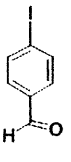

A mixture of 4-iodo(bromomethyl)benzene (crude weight 6.5g, 22mmol) and hexamethylenetetraamine (12.76g, 91mmol) in methanol/water (25mL, 1:1) was refluxed for 4hrs. Concentrated aqueous HCl (7.43ml) was added drop wise to the cooled solution and the mixture refluxed for a further 0.5 h. The solution was cooled and extracted into CH_2Cl_2 (3 x 30 ml), the solvent removed under reduced pressure and the residue recrystallised from $EtOH/H_2O$ to give the title compound (4.127g, 82%) as a white crystalline solid. δ_H (400MHz, $CDCl_3$): 10.0 (1H, s, C*H*O), 8.1 (2H, d, J=6.83, C2-*H*, C6-*H*), 7.75 (2H, d, J=6.82, C3-*H*, C5-*H*). IR KBr/cm^{-1}: 2828 (m),

2735 (w), 2029 (w), 1908 (w), 1686 (s), 1651 (w), 1582 (s), 1565 (s), 1478 (m), 1402 (w), 1379 (s), 1291 (m), 1272 (w), 1204 (s), 1162 (s), 1095 (m), 1051 (s), 1007 (s), 939 (w), 832 (s), 804 (s), 675 (s), 623 (m), 468 (s). MS: m/z EI+: 233.1 [M+H] (76%), 126.9 $[I]^+$ (97%).

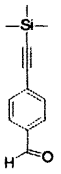

4-TMS-ethynyl benzaldehyde (56).

4-Iodobenzaldehyde (0.51g, 2.2mmol) in acetonitrile (5ml) and triethylamine (5ml) was degassed for 10 minutes. Copper iodide (0.004g, 0.02mmol), palladium (11) acetate (0.002g, 0.02mmol), triphenyl phosphine (0.01g, 0.04mmol) and TMS-acetylene (0.47g, 4.7mmol) were added under nitrogen and the reaction mixture refluxed for 12 hours. After cooling, water (10ml) was added and the mixture extracted with dichloromethane (3 x 10ml), dried over magnesium sulphate, filtered and evaporated under reduced pressure to yield the crude product as a brown oil. Column chromatography using CH_2Cl_2/hexane (6:4) afforded the title compound as a pale yellow crystalline solid (0.28g, 64%). δ_H (400MHz, $CDCl_3$): 9.5 (1H, s, C*H*O), 7.75 (2H, d, J=8.29, C2-*H*, C6-*H*), 7.51 (2H, d, J= 8.24, C3-*H*, C5-*H*), 0.2 (9H, s, CH_3). IR KBr/cm^{-1}: 2966 (m), 2834 (w), 2734 (m), 2157 (s), 1956 (w), 1927 (w), 1897 (w), 1824 (w), 1700 (s), 1601 (s), 1563 (s), 1499 (w), 1453 (w), 1379 (m), 1300 (s), 1289 (m), 1249 (s), 1217 (s), 1205 (s), 1162 (s), 1100 (s), 1015 (w), 953 (w), 842 (s), 760 (s), 704 (m), 669 (s), 638 (s), 536 (s). MS m/z EI+: 202.0 $[M]^+$ (20%), 187.0 $[M-CH_3]^+$ (100%).

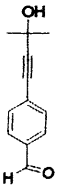

4-(2-Methyl-3-butyn2-ol) benzaldehyde (57).

4-Iodobenzaldehyde (0.51g, 2.2mmol) in acetonitrile (5ml) and triethylamine (5ml) was degassed for 10 minutes. Copper iodide (0.004g, 0.02mmol), palladium (11)

acetate (0.002g, 0.02mmol), triphenyl phosphine (0.01g, 0.04mmol) and 2-methyl-3-butyn-2-ol (0.40g, 4.7mmol) were added under nitrogen and the reaction mixture refluxed for 12 hours. After cooling, water (10ml) was added and the mixture extracted with dichloromethane (3 x 10ml), dried over magnesium sulphate, filtered and evaporated under reduced pressure to yield the crude product as a brown oil. Yield 79%. δ_H (400MHZ, $CDCl_3$): 9.91 (1H, s, C*H*O), 7.72 (2H, d, J=8.14, C2-*H*, C6-*H*), 7.43 (2H, d, J=8.12, C3-*H*, C5-*H*), 2.89 (1H, s, O*H*), 1.59 (6H, s, CH_3). δ_C: 191.91, 135.15, 132.10, 129.50, 98.43, 84.21, 80.97, 66.08, 65.30, 46.27, 31.27, 8.81.

4-Ethynyl benzaldehyde (58).[37]

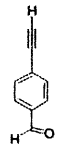

4-TMS-ethynyl benzaldehyde (0.15g, 0.743mmol) was dissolved in absolute methanol (5mls) and potassium carbonate (0.011g, 0.0785mmol) was added and the reaction mixture stirred under an atmosphere of nitrogen for 3hrs. The solvent was removed and dichloromethane (7mls) added. The potassium carbonate was extracted into water (2 x 7mls) and the organic phase washed with 5% potassium hydrogen carbonate (2 x 7mls) followed by brine (2 x 7mls) and then dried over sodium sulphate and filtered. Removal of the dichloromethane afforded a cream solid which was purified by column chromatography on silica gel (CH_2Cl_2/hexane 1:1) to yield the title compound (0.052g, 53%). δ_H (400MHz, $CDCl_3$): 9.95 (1H, s, C*H*O), 7.79 (2H, d, J=6.68, C2-*H*, C6-*H*), 7.57 (2H, d, J=8.25, C3-*H*, C5-*H*), 3.25 (1H, s, CC*H*). IR KBr/cm^{-1}: 3219 (m), 2955 (w), 2825 (w), 2734 (w), 2363 (w), 2102 (m), 1686 (s), 1605 (s), 1561 (m), 1389 (w), 1304 (m), 1288 (m), 1261 (m), 1207 (s), 1166 (s), 1100 (s), 1016 (s), 828 (s), 740 (m).

3.7.5 Synthesis of compounds for the preparation of the Terpyridine-Porphyrin system

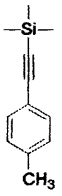

4-TMS ethynyl toluene (59).

4-Iodotoluene (0.51g, 2.3mmol) in acetonitrile (5ml) and triethylamine (5ml) was degassed for 10 minutes. Copper iodide (0.004g, 0.02mmol), palladium (11) acetate (0.002g, 0.02mmol), triphenyl phosphine (0.01g, 0.04mmol) and TMS-acetylene (0.46g, 4.7mmol) were added under nitrogen and the reaction mixture refluxed for 12 hours. After cooling, water (10ml) was added and the mixture extracted with dichloromethane (3 X 10ml), dried over magnesium sulphate, filtered and evaporated under reduced pressure to yield the crude product as a brown solid (84%). δ_H (400MHz, $CDCl_3$): 7.30 (2H, d, J=8.12, C3-*H*, C5-*H*), 7.13 (2H, d, J=7.85, C2-*H*, C6-*H*), 2.28 (3H, s, CH_3), 0.1-0.2 (9H, s, TMS CH_3). MS m/z ES+: 189.0 $[M+H]^+$ (65%), 174.0 $[M-CH_3]^+$ (100%).

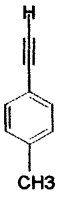

4-Ethynyl toluene (60).

4-TMS-ethynyl toluene (0.13g, 0.743mmol) was dissolved in absolute methanol (5mls) and tetrabutyl ammonium fluoride (0.19g, 0.743mmol) was added and the reaction mixture stirred under an atmosphere of nitrogen for 24hrs. The resulting solution was filtered through a plug of silica and the solvent removed to afford a cream solid (89%). δ_H (400MHz, $CDCl_3$): 7.30 (2H, d, J=8.10, C3-*H*, C5-*H*), 7.13 (2H, d, J=8.08, C2-*H*, C6-*H*), 2.98 (1H, s, CC*H*), 2.27 (3H, s, CH_3). MS m/z ES+: 117.0 $[M+H]^+$ (100%).

2,6-Bis(4-ethynyl toluene) pyridine (61).

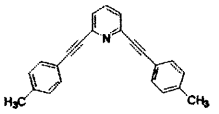

To 2,6,-dibromopyridine (1g, 4.23mmol), in acetonitrile (10mls) and triethylamine (3mls) was added compound **60** (0.9g, 8.5 mmol) and the Sonogashira catalysts (same as above) were added and the solution refluxed under nitrogen for 4 hrs. After cooling, aqueous sodium hydrogen carbonate solution (15mls) was added and the solution extracted in dichloromethane (3 x 15mls). Removal of the solvent was followed by recrystallisation from hexane to afford the title compound as a cream solid (61%). δ_H (400MHz, $CDCl_3$): 7.61 (1H, t, J=7.82, pyridine H_4), 7.45 (4H, d, J=8.85, toluene H_3, H_5), 7.38 (2H, d, 7.75, pyridine H_3, H_5), 7.10 (4H, d, J=8.00, toluene H_2, H_6), 2.31 (6H, s, CH_3). δ_C: 142.90, 138.35, 135.35, 131.00, 128.15, 124.96, 86.20, 88.94, 20.59. IR KBr/cm^{-1}: 3437 (m), 2955 (m), 2363 (s), 2202 (m), 1553 (s), 1506 (s), 1444 (s), 1257 (s), 1162 (m), 1096 (s), 1021 (s), 860 (w), 810 (s). MS m/z APCI: 308.0 $[M+H]^+$ (100%).

6,6"-(Bis p-ethynyl toluene)-2,2':6',2"-terpyridine (62).

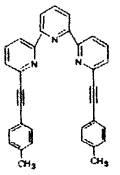

A solution of 6,6"-dibromo-2,2':6'2"-terpyridine (0.122g, 0.312mmol) in acetonitrile (15ml) and triethylamine (15ml) was degassed for 10 minutes. Copper (I) iodide (0.0006g, 0.00312mmol), triphenyl phosphine (0.0016g, 0.00624mmol), palladium (II) acetate (0.00033g, 0.00312mmol) and p-ethynyl toluene (0.08g, 0.686mmol) were added under nitrogen and the mixture refluxed for 4 hours. After cooling, sodium hydrogen carbonate solution was added (10ml) and the mixture extracted with dichloromethane (3 x 20ml), dried over magnesium sulphate, filtered and evaporated under reduced pressure to yield the crude product as a brown solid. Column chromatography on alumina (CH_2Cl_2 and hexane 1:1) afforded the title compound as

a white solid (0.106g, 74%). δ_H (400MHz, $CDCl_3$): 8.51 (2H, d, J=7.32, *H*$_{5terp}$, *H''*$_{5terp}$), 8.50 (2H, d, J=7.77, *H'*$_{3terp}$, *H'*$_{5terp}$), 7.90 (1H, t, J=7.83, *H'*$_{4terp}$), 7.8 (2H, t, J=7.83, *H*$_{4terp}$, *H''*$_{4terp}$), 7.51 (4H, d, J=7.63, *H*$_{2tol}$, *H'*$_{2tol}$, *H*$_{6tol}$, *H'*$_{6tol}$), 7.49 (2H, d, J=7.12, *H*$_3$, *H''*$_3$), 7.1 (4H, d, J=7.98, *H*$_{3tol}$, *H'*$_{3tol}$, *H*$_{5tol}$, *H'*$_{5tol}$), 2.32 (6H, s, *CH*$_3$). IR KBr/cm^{-1}: 2982 (m), 2210 (w), 1569 (m), 1435 (m), 1250 (s), 1096 (s), 1020 (s), 797 (s). MS m/z APCI: 462 $[M+H]^+$ (100%)

3.7.6 Synthesis, metallation and coupling reactions of symmetrical and unsymmetrical Porphyrins

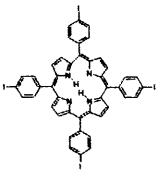

***Meso*-5,10,15,20-tetra (4-iodophenyl) porphyrin (63).**

A mixture of 4-iodobenzaldehyde, (0.5g, 2.16mmol) and pyrrole (0.14g, 2.09mmol) in propionic acid (15ml) was refluxed for 30 minutes. After cooling, the reaction mixture was filtered (glass fibre filter paper) and washed with ice cold propionic acid followed by ice cold methanol to afford a black solid which was purified by flash column chromatography (CH_2Cl_2). A purple coloured solid was afforded as the title compound (0.193g, 33%). δ_H (400MHz, $CDCl_3$): 8.8 (8H, s, pyrrole *H*), 8.15 (8H, d, J=8.09, C3-*H*, C5-*H*), 7.88 (8H, d, J=9.13, C2-*H*, C6-*H*), -2.86 (2H, s, N*H*). IR KBr/cm^{-1}: 3322 (m), 2969 (w), 2922 (w), 1651 (s), 1562 (s), 1472 (s), 1399 (m), 1348 (m), 1259 (m), 1173 (w), 1091 (s), 1016 (s), 966 (s), 846 (w), 801 (s), 504 (s). UV (CH_2Cl_2)/nm: 589.5 (log ε 3.06), 549.5 (log ε 3.26), 515.5 (log ε 3.52), 420 (log ε 4.77). MS m/z (FAB) 1118.0 $[M+H]^+$ (100%), 991.8 $[M-I]^+$ (25%).

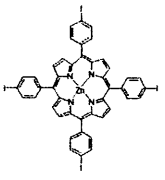

Zinc (II) *meso*-5,10,15,20-tetra(4-iodophenyl) porphyrin (64).[52]

To a solution of meso-5,10,15,20-(4-tetraiodophenyl) porphyrin (**63**) (0,1021g, 0.0913mmol) in dimethylformamide (5mls) was added zinc (II) acetate dihydrate

(0.2g, 0.913mmol) and the mixture refluxed for 3hrs. After cooling at room temperature, water (7mls) was added and the precipitate filtered and washed with water, methanol and acetone. The purple residue was dissolved in the minimum amount of chloroform, filtered and a little methanol was added to the purple solution. After reducing the volume of the solvent, the solution was cooled at 4°C to crash out the product as a purple solid. The solid was filtered and dried under vacuum to give the title compound as a bright purple/pink coloured solid (0.105g, 97%). δ_H (400MHz, $CDCl_3$): 8.8 (8H, s, pyrrole *H*), 8.15 (8H, d, J=8.15, C3-*H*, C5-*H*), 7.88 (8H, d, J=9.21, C2-*H*, C6-*H*). IR/KBr cm^{-1}: 1741 (w), 1653 (s), 1581 (w), 1489 (s), 1387 (s), 1258 (s), 1094 (w), 1072 (w), 1009 (m), 797 (s), 502 (s), 464 (s). UV (CH_2Cl_2)/nm: 548 (log ε 3.83), 422 (log ε 5.21). MS m/z FAB: 1181.2 $[M+H]^+$ (95%), 1054.0 $[M-I]^+$ (70%).

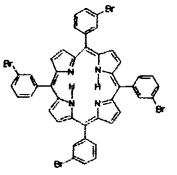

***Meso*-5,10,15,20-tetra(3-bromophenyl) porphyrin (65).**

Using 3-bromobenzaldehyde and pyrrole, compound **65** was prepared in the same manner as that for compound **63**. Purification via flash column chromatography on silica gel (chloroform) afforded compound **65** as a purple solid (35%). δ_H (400MHz, $CDCl_3$): 8.82 (8H, s, pyrrole *H*), 8.31 (4H, s, C2-*H*), 8.09 (4H, d, J=7.53, C6-*H*), 7.91 (4H, d, J=8.94, C4-*H*), 7.55 (4H, t, J=7.82, C5-*H*), -2.88 (2H, s, N*H*). δ_C ($CDCl_3$): 180.50, 145.63, 140.81, 135.85, 134.61, 131.58, 130.01, 122.66, 119.00. IR KBr/cm^{-1}: 3323 (m), 2986 (m), 1905 (m), 1700 (s), 1648 (m), 1575 (m), 1536 (m), 1489 (m), 1472 (m), 1393 (m), 1344(m), 1282 (w), 1252 (w), 1205 (w), 1173 (w), 1070 (s), 1013 (s), 967 (s), 881 (m), 835 (m), 795 (s), 779 (s), 723 (s), 693 (m). UV (CH_2Cl_2)/nm: 680, 644, 588, 548, 514, 420. MS m/z FAB: 930.4 $[M+H]^+$ (55%), 850.0 $[M-Br]^+$ (100%).

Zinc (II) *meso*-5,10,15,20-tetra(3-bromophenyl) porphyrin (66).

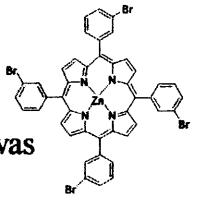

Using compound **65** and zinc(II) acetate dihydrate, compound **66** was prepared in the same manner as previously described for metallation of porphyrins (compound **64**). Compound **66** was afforded as a bright purple/pink coloured solid (94%). δ_H (400MHz, $CDCl_3$): 8.83 (8H, s, pyrrole *H*), 8.30 (4H,s, C2-*H*); 8.09 (4H, d, J=6.5, C6-*H*), 7.85 (4H, d, J=8.08, C4-*H*), 7.54 (4H, t, J=7.27, C5-*H*). δ_C ($CDCl_3$):161.46, 148.86, 145.21, 140.77, 139.65, 134.76, 130.85, 128.68, 121.16, 118.61. IR KBr/cm^{-1}: 1908 (w), 1741 (w), 1653 (s), 1581 (m), 1489 (s), 1386 (m), 1258 (s), 1094 (s), 1072 (s), 1008 (s), 797 (s), 662 (m). UV (CH_2Cl_2)/nm: 549.5 (log ε 4.55), 421.5 (log ε 5.85). MS m/z FAB: 993.0 $[M+H]^+$ (60%), 913.0 $[M-Br]^+$ (100%).

Zinc (II) *meso*-5,10,15,20-tetra(3-butyl acrylate phenyl) porphyrin (67).

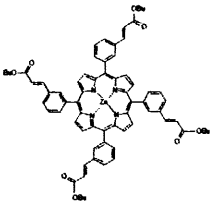

A solution of zinc (II) meso-5,10,15,20-tetra(3-bromophenyl) porphyrin (**66**) (1.315g, 1mmol), butyl acrylate (1.282g, 10mmol), tributyl amine (1g, 10mmol), triphenyl phosphine (0.01g, 0.026mmol) and palladium acetate (0.005g, 0.012mmol) in dimethyl acetamide (6mls) was heated at 140°C in a pressure tube for 18hrs. After cooling, water (50mls) was added and the mixture was extracted with dichloromethane (3x50mls). The organic phases were washed with 5% HCl (10mls), 10% $NaHCO_3$ (aq) solution (10mls) and dried over magnesium sulphate. The solvent was removed under vacuo and column followed by preparative plate chromatography (dichloromethane) afforded the title compound as a purple solid (0.76g, 51%). δ_H(400MHz, $CDCl_3$): 8.9 (8H, s, pyrrole *H*); 8.31 (4H, s, porph C2-*H*); 8.19 (4H, d, J=5.84, porph C6-*H*); 7.85 (4H, d, J=8.00, porph C4-*H*); 7.84 (4H, d, J=17.00,

C*H*=CHCO$_2$); 7.71 (4H, t, J=7.56, porph C5-*H*); 6.53 (4H, d, J=15.83, CH=C*H*CO$_2$); 4.06 (8H, t, J=6.59, CO$_2$C*H*$_2$); 1.58 (8H, quintet, J=6.72, CO$_2$CH$_2$C*H*$_2$); 1.32 (8H, septet, J=7.34, CO$_2$CH$_2$CH$_2$C*H*$_2$); 0.85 (12H, t, J=6.12, C*H*$_3$). IR KBr/cm^{-1}: 2954 (s), 2383 (w), 2203 (w), 1699 (s), 1675 (w), 1638 (m), 1576 (m), 1453 (w), 1426 (m), 1341 (m), 1260 (s), 1107 (m), 1097 (s), 1023 (s). UV (CH_2Cl_2)/nm: 549.5 (log ε 3.47), 423 (log ε 4.85). MS m/z FAB: 1117.0 $[M+H]^+$

Zinc (II) *meso*-5,10,15,20-tetra(3 *t*-butyl styrene phenyl) porphyrin (68).

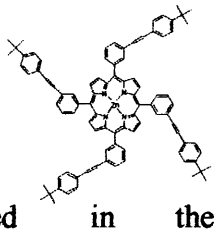

Using compound **66** and t-butyl styrene, compound **68** was prepared in the same way as compound **67**. Purification via flash column chromatography on silica gel (dichloromethane) afforded the title compound as a purple solid (78%). δ_H (400MHz, $CDCl_3$): 8.87 (8H, s, pyrrole *H*), 8.29 (4H,s, porph C2-*H*), 8.18 (4H, m , porph C6-*H*), 7.82 (4H, d, J=7.65, porph C4-*H*), 7.50 (4H, t, J=8.01, porph C5-*H*), 7.25 (16H, s, C_6H_4), 5.60 (4H, d, J=17.60, C*H*), 5.11 (4H, d, J=10.89, C*H*), 1.23 (36H, s, t-butyl). IR KBr/cm^{-1}: 2966 (s), 2383 (w), 2188 (w), 1694 (w), 1674 (w), 1629 (m), 1576 (m), 1453 (w), 1419 (m), 1327 (m), 1260 (s), 1096 (s), 1021 (s). UV (CH_2Cl_2)/nm: 548.5 (log ε 3.73), 421.5 (log ε 4.97). MS m/z FAB: 1309.4 $[M+H]^+$.

***Meso* 5,10,15-tri-*p*-methoxyphenyl-**

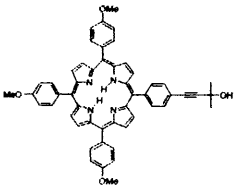

***Meso* 5,10,15-tri-*p*-methoxyphenyl-**

20-(*p*-(2-methyl-3-butyn-2-ol-phenyl)porphyrin (69).

A mixture of *p*-anisaldehyde (4.200g, 31mmol) and *p*-butynol-benzaldehyde (**57**) (0.306g, 1.63mmol) was added to hot propionic acid (40mls), followed by addition of pyrrole (2.070g, 31mmol). The solution was heated to reflux for a further 30 minutes and then allowed to cool. After filtering through glass fibre filter paper, the purple

solid was washed with a few drops of cool propionic acid then a small quantity of cool methanol. The purple solid was dried and column chromatography on silica gel (CH_2Cl_2) followed by further preparative plate chromatography on silica plates yielded the title compound as a purple solid (2% yield). δ_H (400MHz, $CDCl_3$): 8.50-8.81 (8H, m, pyrrole *H*), 8.05-8.10 (6H, m, OMe Ar C3-*H*, C5-*H*), 7.91 (2H, d, J=8.69, butynol Ar C3-*H*, C5-*H*), 7.78 (2H, d, J=7.97, butynol Ar C2-*H*, C6-*H*), 7.18 (6H, d, J=5.31, OMe Ar C2-*H*, C6-*H*), 4.0-4.05 (9H, s, OCH_3), 1.7 (6H, s, CH_3), -2.91 (2H, s, N-*H*). δ_C: 163.71, 162.46, 158.00, 152.52, 141.32, 139.89, 139.83, 134.93, 134.52, 133.89, 132.78, 132.12, 131.99, 131.13, 130.41, 128.94, 127.20, 121.05, 120.89, 119.12, 112.78, 111.86, 111.14, 93.86, 81.10, 64.76, 54.52, 54.46, 30.57, 29.92. IR KBr/cm^{-1}: 3443 (s,b), 2966 (s), 2926 (w), 1734 (w), 1718 (w), 1651 (m), 1609 (m), 1559 (m), 1507 (s), 1456 (w), 1439 (w), 1383 (w), 1350 (w), 1260 (s), 1241 (s), 1175 (s), 1105 (s), 1028 (s), 936 (m), 802 (s), 668 (s). UV (CH_2Cl_2)/nm: 422 (log ε 4.32), 522 (log ε 2.50), 554 (log ε 2.41). MS m/z ES+: 787.6$[M+H]^+$.

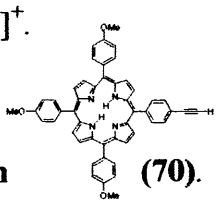

Meso 5,10,15-tri-*p*-methoxyphenyl-20-(*p*-ethynylphenyl)porphyrin (70).

A solution of *meso* 5,10,15-tri-*p*-methoxyphenyl-20-(*p*-butynolphenyl)porphyrin (**69**) (0.008g, 0.01mmol) and powdered sodium hydroxide (0.6g, 15mmol) in toluene (50mls) were heated to reflux under nitrogen for 12 hrs. After cooling, the solution was filtered and the filtrate evaporated to yield the title compound as a purple solid (84% yield). δ_H (400MHz, $CDCl_3$): 8.75-8.92 (8H, m, pyrrole *H*), 8.08-8.12 (6H, m, OMe Ar C3-*H*, C5-*H*), 7.91 (2H, d, J=8.72, ethynyl Ar C3-*H*, C5-*H*), 7.82 (2H, d, J=8.00, ethynyl Ar C2-*H*, C6-*H*), 7.22 (6H, d, J=8.63, OMe Ar C2-*H*, C6-*H*), 4.05-4.1 (9H, s, OCH_3) 3.22 (1H, s, C*H*), -2.90 (2H, s, N-*H*). IR KBr/cm^{-1}: 3401 (m, b), 2963 (s), 2352 (m), 2293 (w), 1624 (w), 1598 (w), 1499 (w), 1457 (m), 1262 (s), 1096

(s), 1020 (s), 801 (s). UV/nm (CH_2Cl_2): 594 (log ε 2.30), 556 (log ε 3.30), 520 (log ε 3.40), 422 (log ε 5.04). MS m/z ES+: 735.4 $[M+H]^+$.

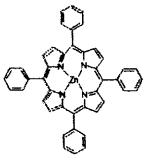

Zinc (II) *meso*-5,10,15,20-tetraphenyl porphyrin.(71)

Using 5,10,15,20-tetraphenyl porphyrin and zinc (II) acetate dihydrate, compound **71** was prepared in the same way as compound **64** (98%). δ_H (400MHz, $CDCl_3$) δ_H 8.85 (8H, s, pyrrole *H*); 8.12 (8H, d, J=6.72, C-2H, C-6H); 7.63 (12H, m, J=18.64, C-3*H*, C-4*H*, C-5*H*). δ_C 149.09, 141.93, 133.42, 130.84, 126.35, 125.44, 119.93. IR KBr/cm^{-1}: 2973 (m), 1900 (w), 1690 (s), 1594 (s), 1522 (m), 1486 (m), 1440 (m), 1338 (m), 1260 (s), 1205 (w), 1178 (w), 1095 (s), 1016 (s), 863 (w), 801 (s), 752 (s), 702 (s), 675 (m). UV(CH_2Cl_2)/nm: 686, 640, 584, 548, 422.

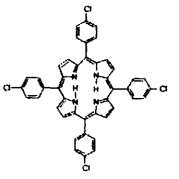

***Meso*-5,10,15,20-tetra(4-chlorophenyl) porphyrin.(72)**

Using 4-chlorobenzaldehyde and pyrrole, compound **72** was prepared in the same way as compound **63** (30%). δ_H 8.76 (8H, s, pyrrole *H*); 8.05 (8H, d, J=8.406, C-2*H*, C-6*H*); 7.66 (8H, d, J=8.18, C-3*H*, C-5*H*); -2.88 (2H, s, N*H*). δ_C 139.17, 134.33, 133.21, 125.88, 117.82. IR KBr/cm^{-1}: 3322 (m), 2969 (w), 2922 (w), 1651 (s), 1562 (s), 1472 (s), 1399 (m), 1348 (m), 1259 (m), 1173 (w), 1091 (s), 1016 (s), 966 (s), 846 (w), 801 (s), 668 (s). UV(CH_2Cl_2)/nm: 686, 590, 548, 516, 422.

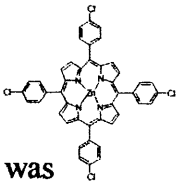

Zinc (II) *meso*-5,10,15,20-tetra(4-chlorophenyl) porphyrin.(73)

Using compound **72** and zinc (II) acetate dihydrate, compound **73** was prepared in the same way as compound **64** (95%). δ_H 8.84 (8H, s, pyrrole *H*); 8.06 (8H, d, J=8.56, C-2*H*, C-6*H*); 7.66 (8H, d, J=7.21, C-3*H*, C-5*H*). δ_C 150.10, 140.99, 135.37, 134.13, 132.08, 126.91, 119.97. IR KBr/cm^{-1}: 1807 (w), 1698 (w), 1589 (w),

1480 (s), 1433 (w), 1397 (m), 1337 (s), 1254 (w), 1206 (m), 1174 (m), 1089 (s), 997 (s), 851 (m), 796 (s), 723 (s), 704 (m), 567 (m), 497 (s). UV(CH_2Cl_2)/nm: 686, 548, 512, 422.

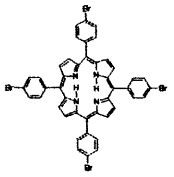

Meso-5,10,15,20-tetra(4-bromophenyl) porphyrin.(74)

Using 4-bromobenzaldehyde and pyrrole, compound **74** was prepared in the same way as compound **63** (29%). δ_H 8.77 (8H, s, pyrrole *H*); 7.99 (8H, d, J=7.19, C-2*H*, C-6*H*); 7.82 (8H, d, J=8.607, C-3*H*, C-5*H*); -2.88 (2H, s, N*H*). δ_C 180.50, 140.81, 135.85, 131.58, 130.01, 122.66, 119.00. IR KBr/cm^{-1}: 3323 (m), 2986 (m), 1905 (m), 1700 (s), 1648 (m), 1575 (m), 1536 (m), 1489 (m), 1472 (m), 1393 (m), 1344(m), 1282 (w), 1252 (w), 1205 (w), 1173 (w), 1070 (s), 1013 (s), 967 (s), 881 (m), 835 (m), 795 (s), 779 (s), 723 (s), 693 (m). UV(CH_2Cl_2)/nm: 680, 644, 588, 548, 514, 420.

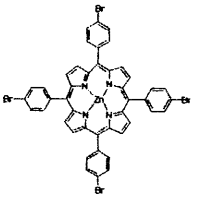

Zinc (II) _meso_-5,10,15,20-tetra(4-bromophenyl) porphyrin.(75)

Using compound **74** and zinc (II) acetate dihydrate, compound **75** was prepared in the same way as compound **64** (97%). δ_H 8.84 (8H, s, pyrrole *H*); 8.0 (8H, d, J=8.304, C-2*H*, C-6*H*); 7.83 (8H, d, J=9.133, C-3*H*, C-5*H*). δ_C 161.46, 148.86, 140.77, 134.76, 130.85, 128.68, 121.16, 118.61. IR KBr/cm^{-1}: 1908 (w), 1741 (w), 1653 (s), 1581 (m), 1489 (s), 1386 (m), 1258 (s), 1094 (s), 1072 (s), 1008 (s), 797 (s), 662 (m). UV(CH_2Cl_2)/nm: 684, 582, 546, 508, 500, 420.

3.8 Results and discussion

3.8.1 Preliminary Sonogashira reactions

Prior to carrying out Sonogashira reactions using 6,6"-dibromo-2,2':6'2"-terpyridine, it was considered necessary to carry out a series of trial reactions on a number of simpler and less costly compounds. Hence the Sonogashira reaction was used to synthesise compound **42** from 2,6-dibromopyridine and 2-methyl-3-butyn-2-ol. The target compound **42** was obtained after purification via column chromatography on silica gel (chloroform/methanol 98:2) in 77% yield. The compound was fully characterised and conversion to **43** was achieved as shown in scheme 3.11.[39] Compound **43** was afforded from the reaction in 75% yield. The ^{1}H-NMR spectrum proved the reaction had proceeded as desired since the peaks representing the 2-methyl-3-butyn-2-ol at 3.9 ppm (OH) and 1.6 ppm (CH_3) present in the spectrum of **42** had been replaced by a singlet at 3.1 ppm integrating to 2, representing the alkyne protons. Mass spectrometry (ES+) displayed the peak at 128.0 m/z for the parent ion.

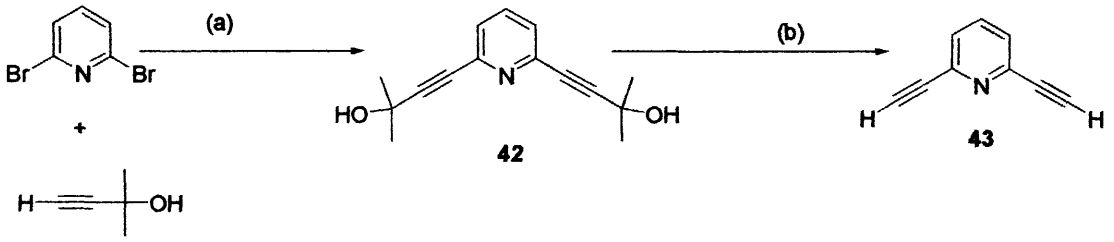

Reagents and conditions: (a) Sonogashira reaction. Copper (I) iodide, palladium (II) acetate, triphenyl phoshine, as catalysts in acetonitrile and triethylamine. Reflux carried out in absence of light for 3hrs under N_2. (b) Reflux with sodium hydroxide in toluene for 3hrs.

Scheme 3.11: Reaction scheme for the synthesis of compound **43**

To further examine the utility of this reaction, compound **45** was prepared in the same manner as **42** followed by a one-pot synthesis of **46** as shown in scheme 3.12. Compound **45** and 2,6-dibromopyridine were used to prepare **46** using a modification of the method developed by Rossi and co-workers.[42] Again de-protection is carried out using NaOH as the base to afford the terminal alkyne which will then undergo Sonogashira reaction with the bromides. Tetrabutyl ammonium bromide is used as a phase transfer reagent in the process to accomplish transfer of the OH^- from the aqueous phase to the organic phase. Purification via column chromatography on silica gel (96% chloroform, 4% methanol) followed by recrystallisation from hexane afforded the target compound **46** in 51% yield.

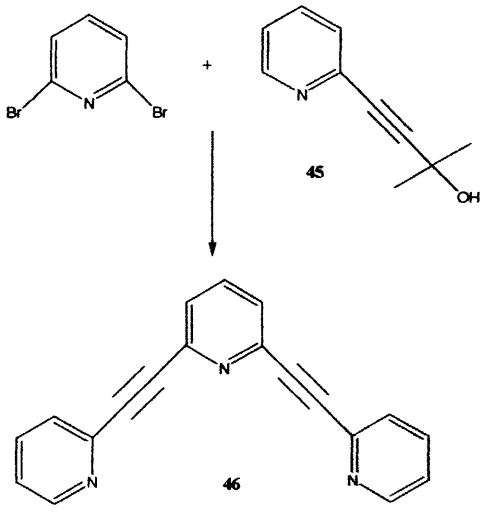

Reagents and conditions: CuI, Pd (II) acetate, triphenyl phosphine in toluene under N_2 and addition of tetrabutyl ammonium bromide and aq. NaOH. Reflux at 85°C for 50hrs in the dark.

Scheme 3.12: Synthesis of compound **46**

Characterisation of compound **46** was in line with the proposed structure. The one-pot synthesis of the novel compound **46** in reasonable yield (51%) allows us to further such reactions to the development of new macrocyclic systems based on

acetylene type terpyridine[55] and sexipyridine[56, 57] systems. As time did not permit these further investigations, it is a possibility for future work by the research group. Such synthesis would require high dilution or template synthesis to assist in the formation of the macrocyclic rings.

As another preliminary reaction it was decided to synthesise **47** and carry out a Sonogashira reaction on the compound, as it slightly more complicated in addition to being a larger molecule than 2,6-dibromopyridine. In addition, compound **47** is a cheaper and more accessible alternative than 6,6"-dibromo-2,2':6'2"-terpyridine (**51**) which is discussed further on. The ketone **47** was prepared by the method of Li and co-workers[49] and was obtained in a 39% yield.

Once characterised, compound **47** was reacted with 2-methyl-3-butyn-2-ol in the usual Sonogashira manner and the product **48** was afforded in a 67% yield as a brown coloured oil. The reaction scheme is shown in 3.13. The mass spectrum obtained (ES+) confirmed compound **48** had been synthesised due to the presence of a peak in the spectrum arising at 349.2 m/z which is correct for the parent ion of the target compound **48.** The spectrum demonstrates a fragment of the parent ion equal to 279.2 m/z which relates to the parent compound minus one of the 2-methyl-3-butyn-2-ol groups (69 m/z). It also seems to be the case that homocoupling of the butyn-ol has occurred since an intense peak shown at 102 m/z may correspond to a fragment of the homocoupled product of 2-methyl-3-butyn-2-ol. This is very often the case in Sonogashira reactions.[43]

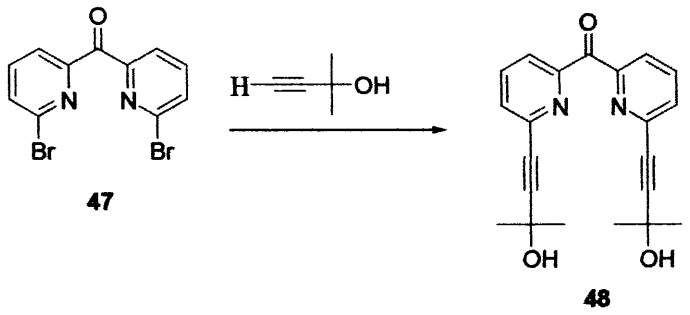

Scheme 3.13: Sonogashira reaction of **47** with 2-methyl 3-butyn-ol

Prior to de-protection of the 2-methyl-3-butyn-2-ol, it was considered that another acetylene containing moiety may give better yields and prove easier to de-protect. Thus the Sonogashira reaction was carried out with bis(2-(6-bromopyridyl) ketone and trimethyl silyl acetylene[6, 7] using the same catalysts and reaction conditions as before. Compound **49** shown in scheme 3.14 was afforded as a light brown coloured solid in 85% yield. The fact that the compound is a solid is an improvement on the 2-methyl-3-butyn-2-ol equivalent which is an oily product since solids are far easier to utilise and the increase in yield is also an added benefit for using this protecting group. De-protection following the method of Lindsey[6] also shown in scheme 3.14 (b) was carried out to afford compound **50** in excellent yield (94%). The ease of conversion of the TMS acetylene to the ethynyl product in addition to the high yield made this strategy the more efficient and useful for further reactions.

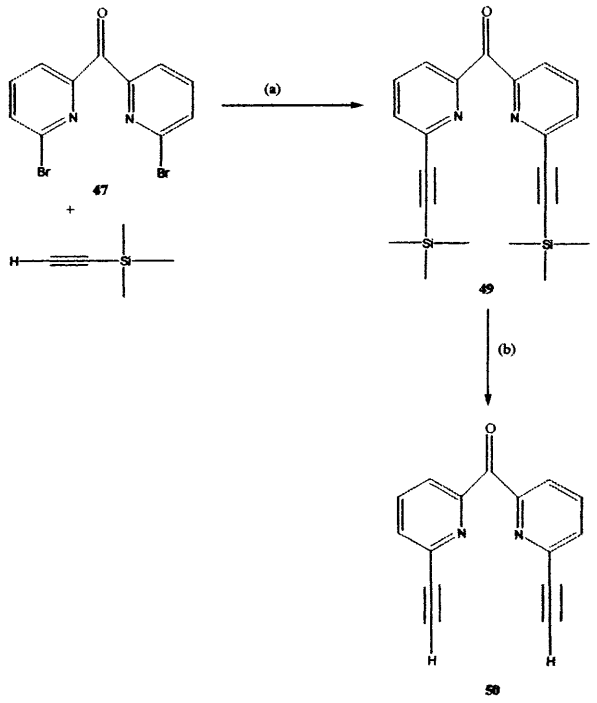

Reagents and conditions: (a) Sonogashira conditions. 12 hour reflux. (b) Stirring with tetrabutyl ammonium fluoride in CH_2Cl_2 under N_2 followed by filtering through silica gel.

Scheme 3.14: Reaction scheme for synthesis of compound 50.

3.8.2 Sonogashira reaction to prepare 6,6"diacetylene-2,2':6'2"-terpyridine(53)

6,6"-Dibromo-2,2':6'2"-terpyridine **51** was prepared using the low temperature method of Uchida, Oae and co-workers[46] using 2,6-dibromopyridine, BuLi in hexane and phosphorous trichloride. A slight modification of the synthesis was utilised since it was difficult to maintain a temperature of -40°C for 20 hours whilst stirring. Thus the reaction mixture was kept in a fridge at a temperature of -50°C for 100 hours with occasional stirring. The white coloured product was isolated in 36% yield and the ^{1}H-NMR, IR and mass spectra fully support the proposed structure.

6,6"-Bis trimethylsilyl acetylene-2,2':6'2"-terpyridine **52** was prepared from 6,6"-dibromo-2,2':6'2"-terpyridine since the use of TMS acetylene had proven more

efficient than 2-methyl-3-butyn-2-ol. The product **52** was afforded in 77% yield and de-protection was carried out as previously described and the acetylene **53** was obtained in 98% yield. The spectra obtained are all in accord with the proposed structure. Compound **53** is essential in the preparation of the target molecule **78** proposed and this shall be discussed in the final section of this chapter.

3.8.3 Novel synthetic route to 4-Iodobenzaldehyde

In order to carry out porphyrin synthesis incorporating the Sonogashira reaction, it was decided to firstly produce 4-iodobenzaldehyde. The overall synthesis is illustrated in scheme 3.15. This was achieved using the route reported by Plater and co-workers to produce 3,5-di-tert-butylbenzaldehyde from 3,5-di-tert-butyltoluene.[50] In the first stage of the reaction 4-iodo(bromomethyl)benzene **54** was obtained in 71% yield. The structure was confirmed by ^{1}H-NMR and IR spectroscopy as well as mass spectrometry.

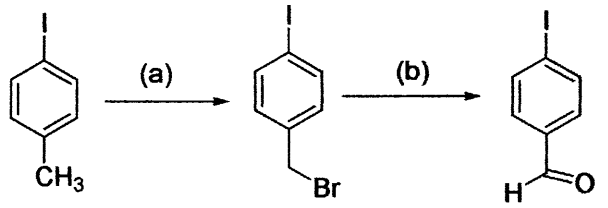

54 **55**

Reagents and conditions: a) N-Bromosuccimide and benzoyl peroxide in CCl_4, 3h reflux at 80°C:
b) hexamethylenetetramine in methanol/water (1:1) 4h reflux, add concentrated aqueous HCl dropwise and reflux for a further 0.5 h.

Scheme3.15: Novel two stage synthesis of 4-iodobenzaldehyde **55** from 4-iodotoluene.

Compound **54** was then used to produce 4-iodobenzaldehyde **55**. The ^{1}H-NMR of this compound displayed a singlet at 10 ppm owing to the aldehyde proton in addition to the 2 aromatic doublets at 8.1 and 7.75 ppm. Information gathered from the IR spectrum indicated the presence of C=O (1686cm^{-1}), aldehyde C-H (2828,

2735cm^{-1}) and C-I (468cm^{-1}) vibrations, all of which are in support of the target compound **55**. The mass spectra confirmed the structure of the compound due to the presence of a peak at 233 m/z representative of the parent ion **55**.

4-Iodobenzaldehyde is a relatively sensitive compound with regard to air and is extremely sensitive to light therefore must be stored and used appropriately. It is an expensive compound to purchase and preparations of this compound have been previously reported by various groups.[7, 47, 48] Zhongwu and co-workers have reported the preparation of 4-iodobenzaldehyde from 4-aminotoluene.[48] Diazolization and iodination of this compound gave 4-iodotoluene in 86% yield. Oxidation of the latter compound with CrO_3 in AcOH and Ac_2O afforded the corresponding ester in 41% yield. Reduction to the benzaldehyde with H_2SO_4 occurred with 96% yield. Additionally Lindsey and co-workers have converted 4-iodoaniline to the benzonitrile intermediate in 11% yield using CuCN, HCl and $NaNO_2$. 4-Iodobenzaldehyde was achieved following addition of DIBAL-H in 81%.[7] The novel approach to synthesising 4-iodobenzaldehyde reported here affords the compound in excellent yield and is a more convenient route than those previously reported. Therefore this strategy will provide an ideal alternative to existing methods.

3.8.4 Porphyrin Synthesis

To begin our porphyrin studies, it was decided to synthesise *meso*-5,10,15,20-tetra(4-iodophenyl) porphyrin (**63**) using the Adler-Longo method. The 4-iodobenzaldehyde was used for this purpose. Purification by flash column chromatography on silica gel (CH_2Cl_2) afforded **63** as a purple solid in 33% yield which is good for Adler-Longo porphyrin synthesis. The ^{1}H-NMR and IR spectra are

in line with the proposed structure. The structure is also confirmed by the UV spectrum displaying a strong peak at 420 nm (Soret band) and several smaller absorptions at 590, 550 and 515 nm (Q bands), all typical for porphyrins. Electronic transitions from the ground state to the second excited state(S_0-S_2) correspond to the Soret band and those transitions from the ground state to the lowest excited state (S_0-S_1) are represented by the Q-bands.

Complexation of compound **63** with zinc (II) following the metallation procedure of Clegg[51] was carried out to yield **64** as a bright purple compound in 97% yield. The ^{1}H-NMR was identical to that of compound **63**, with the exception of the disappearance of the broadened singlet at -2.86 ppm due to the loss of the two internal pyrrole protons in place of the Zn. The IR spectrum was also very similar to compound **63** without the N-H stretch at 3322cm^{-1} and there was a slight shift in the UV spectrum as expected for complex formation. The presence of two peaks at 422 nm (Soret band) and 548 nm confirmed a change in the structure of **63** had occurred. The extinction coefficients for the metallated porphyrin appeared to be greater than those for the free base porphyrin and there appear to be fewer absorptions which coincides with complex formation. This trend is also seen for the other metallated porphyrins synthesised in this chapter. Confirmation of the mass of **64** was obtained from the FAB mass spectrum which showed a peak at 1181.2 m/z corresponding to **64**.

3.8.5 Luminescence of Porphyrins

The excited state emission of porphyrins resulting from π-π^* electron transfer is quenched by heavy atoms, an effect known as the heavy atom effect. This was first

identified by F.Perrin as a physical quenching process[52] and has been the subject of many studies. The heavy atom may form part of the chromophore under study and this is referred to as internal heavy atom effect. Alternatively the heavy atom may be external to the chromophore and this process is termed the external heavy atom effect.

A number of important processes come under the heading of "quenching". Factors such as temperature and concentration can produce fluorescence quenching. When the sample is too concentrated, very little light can pass through to cause excitation and therefore the sample shows very low fluorescence and temperature increase also results in lowering of the fluorescence. However both variables have been eliminated for the samples herein discussed since identical concentrations of 0.25 μmol L^{-1} were used and measurements have been taken under a temperature control (room temperature).

Comparison of the luminescence of compound **63** (*Meso*-5,10,15,20-tetrakis (4-iodophenyl) porphyrin with its chloro and bromo analogoues in addition to *meso* 5,10,15,20-tetraphenyl porphyrin has been carried out as have the zinc porphyrins(compounds **64**, **71**, **73** and **75**). The emission spectra for these are shown in figures 3.16 and 3.17 below. Following preparation and characterisation of the corresponding porphyrins and their zinc derivatives, solutions of 0.25 μmol L^{-1} in dichloromethane were prepared. The spectrum for each was obtained to attempt to investigate the variation on the fluorescence emission upon modification of the halide at the *para*-position of the aryl group of the porphyrin.

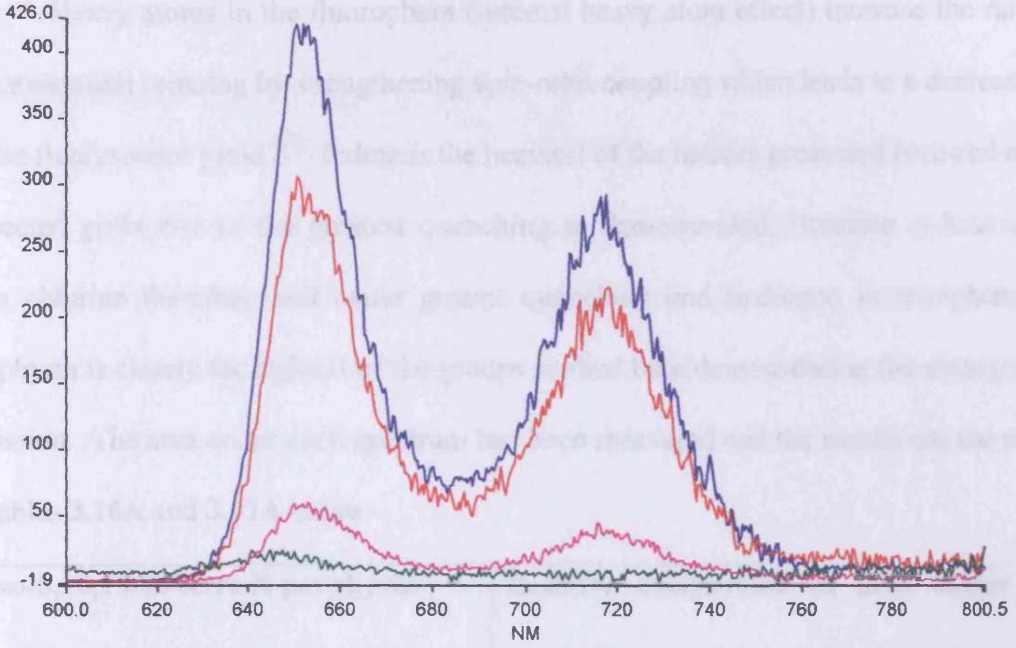

Figure 3.16: Emission spectra for free-base porphyrins. Green=iodo, pink=bromo, red=chloro, blue=no halogen(tetraphenylporphyrin)

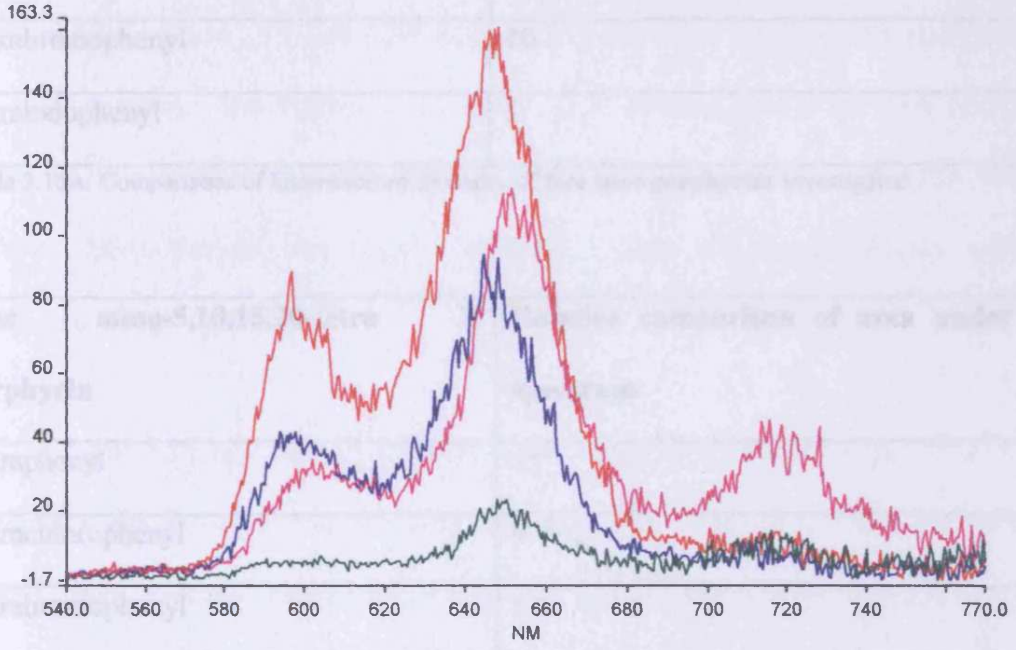

Figure 3.17: Emission spectra for zinc porphyrins. Green spectrum represents Iodo, blue=bromo, pink=chloro and red is for tetraphenylporphyrin

Heavy atoms in the fluorophore (internal heavy atom effect) increase the rate of intersystem crossing by strengthening spin-orbit coupling which leads to a decrease in the fluorescence yield.[53] Iodine is the heaviest of the halides presented here and as expected gives rise to the greatest quenching as demonstrated. Bromine is heavier than chlorine therefore will cause greater quenching and hydrogen in tetraphenyl porphyrin is clearly the lightest of the groups studied here demonstrating the strongest emission. The area under each spectrum has been measured and the results are shown in tables **3.16A** and **3.17A** below.

Meso-5,10,15,20-tetra X porphyrin	**Relative comparison of area under spectrum**
Tetraphenyl	80
Tetrachlorophenyl	59
Tetrabromophenyl	10
Tetraiodophenyl	1

Table 3.16A: Comparisons of luminescence intensity of **free base porphyrins** investigated

Zinc meso-5,10,15,20-tetra X porphyrin	**Relative comparison of area under spectrum**
Tetraphenyl	11
Tetrachlorophenyl	6
Tetrabromophenyl	5
Tetraiodophenyl	1

Table 3.17A: Comparisons of luminescence intensity of **zinc porphyrins**

Following the same decreasing trend, the zinc tetraphenylporphyrin is the most fluorescent, chased by the chloro substitution and bromo substitution, again

displaying a big gap from its predecessor the tetrakis(iodophenyl)porphyrin. The latter compound as expected is almost non fluorescent. Clearly zinc which is a heavy atom also, further increases the quenching of all four porphyrins hence resulting in lower emissions than seen for the free-base porphyrins. Considering the values obtained for the free base and metallated porphyrins, it appears as though the effect of changing the 4-substituent of the porphyrin phenyl ring from H to Cl to Br to I has less of an effect when the porphyrin is metallated with zinc(II) than in the free base.

3.8.6 Heck Reaction and Luminescence investigation

Another coupling reaction which has not been discussed so far is the Heck reaction.[54] This reaction is very similar to the Sonogashira[32] but is carried out using, palladium acetate, triphenyl phosphine and tributyl amine in dimethylacetamide to achieve coupling of an alkene. To date little work linking the Heck reaction with porphyrins has been covered. The synthesis of *meso*-5,10,15,20-tetra(3-butyl acrylate phenyl) porphyrin is reported here out using *meso*-5,10,15,20-tetra(3-bromophenyl) porphyrin. 3-Bromo benzaldehyde was readily available unlike 4-iodobenzaldehyde which involved a 2 stage synthesis.

Meso-5,10,15,20-tetra(3-bromophenyl) porphyrin **(65)** was isolated in a 35% yield as a purple solid. After characterisation of compound **65** was complete, complexation with zinc was again carried out. The Zn complex **66** was afforded in 94% yield as a bright pink solid which followed the same trend as **63/64** with respect to ^{1}H-NMR and IR and UV characterisation.

The Heck reaction was carried out with compound **66** and butyl acrylate to afford compound **67** in a 51% yield. The purpose of this reaction was to obtain a fluorescent tetraphenylporphyrin from a porphyrin which displayed low fluorescence by substitution of a covalently bound heavy atom. As discussed, the heavy atom effect quenches the fluorescence of the porphyrin, however, it has been confirmed that if the fluorophore containing the heavy atom is consumed during the coupling reaction regeneration of the porphyrin fluorescence is achieved. The chemistry involved in the Heck reaction is outlined in Scheme 3.18.

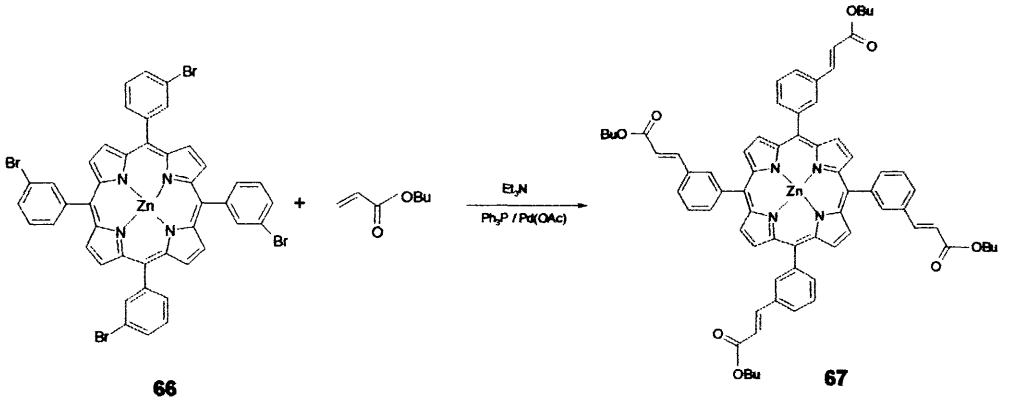

Scheme 3.18: Heck reaction to obtain compound **67**

There is a considerable change in the IR spectrum of compound **67** compared with **66**, with the most significant differences being removal of the C-Br stretch at 662 cm^{-1} from compound **66** to **67** and the onset of a strong C=O absorption at 1699cm^{-1}. There appears little shift in the UV spectra of **66** and **67** since the shift for each of the peaks is merely plus 1nm.

As described for *meso*-5,10,15,20-tetraphenyl porphyrin and its halide derivatives, luminescence studies were carried out on compound **67** and compound **65** in order to clarify the increase in the emission spectra when the bromine groups are replaced (Figure 3.19). Despite the fact that *meso*-5,10,15,20-tetra(3-bromophenyl)

porphyrin (**65**) is a free base porphyrin and compound **67** is metallated with zinc, a significant increase is observed in the spectra in going to compound **67** due to replacement of the bromides via the Heck reaction. In fact a three fold increase is observed demonstrating that changing the substituent on the phenyl ring has a greater effect than metallation of the porphyrin in this case.

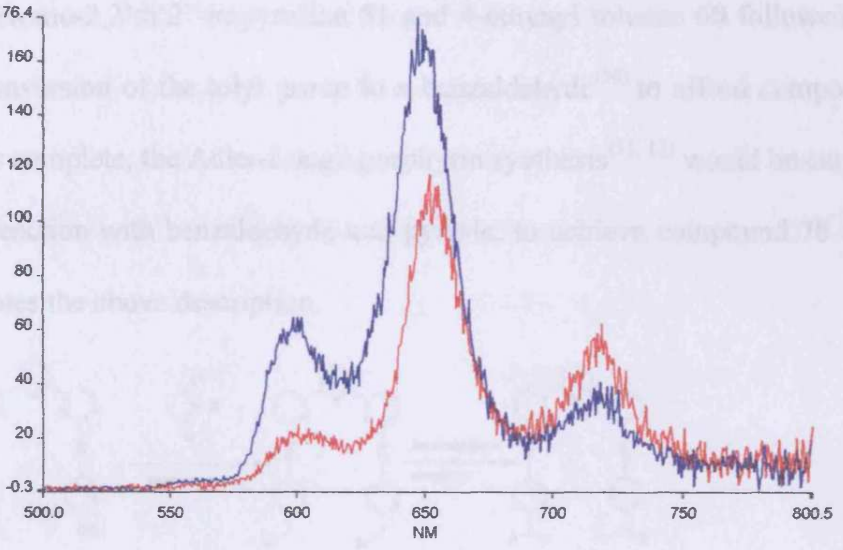

Figure 3.19: Emission spectra of compound 67 (blue) and meso-5,10,15,20-tetra(3-bromophenyl) porphyrin (red).

To the best of our knowledge, little work has been reported on porphyrin Heck reactions therefore a further synthesis was carried out with compound **66** and *t*-butyl styrene. Following the same procedure as that for compound **67,** the novel product zinc (II) *meso*-5,10,15,20-tetra(3 *t*-butyl styrene phenyl) porphyrin (**68**) was isolated in 78% yield after purification by column chromatography on silica gel (CH_2Cl_2). With regards to the UV spectrum, minor shift of the Q band absorption has occurred going from compound **66** to **68,** however the Soret band remains in the same position at 422nm. Confirmation of compound **68** was achieved from FAB mass spectrometry.

3.9 Porphyrin-Terpyridine system design

To attempt the preparation of the bisporphyrin-terpyridine system **78** shown in figure 3.20, three different routes were carried out and are described as follows:

3.9.1 *Building the porphyrin rings onto the terpyridine*

The intention of this method was to carry out a Sonogashira reaction[32] between the 6,6"-dibromo-2,2':6'2"-terpyridine **51** and 4-ethynyl toluene **60** followed by the two step conversion of the tolyl group to a benzaldehyde[50] to afford compound **77**. Once this is complete, the Adler-Longo porphyrin synthesis[11, 12] would be carried out on **77** via reaction with benzaldehyde and pyrrole, to achieve compound **78**. Figure 3.20 illustrates the above description.

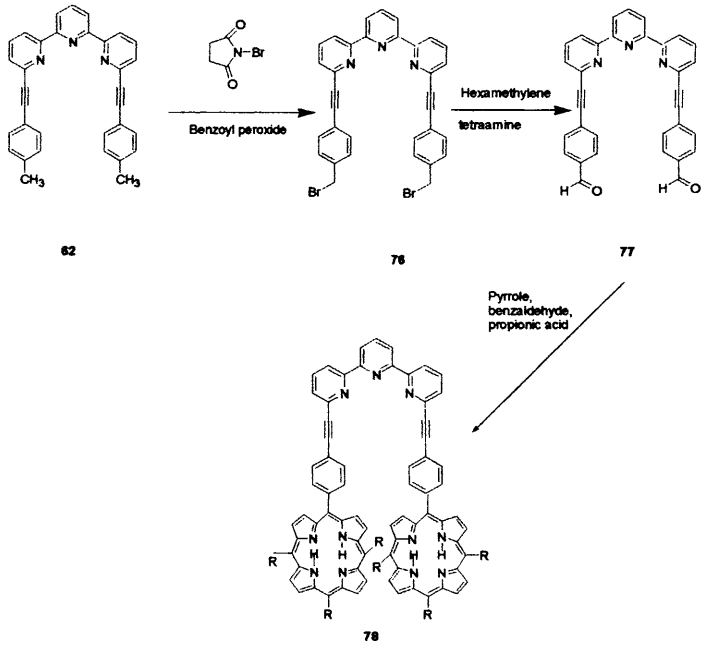

Figure 3.20: Attempted synthesis of bisporphyrin-terpyridine system

As a preliminary reaction, Sonogashira coupling for the production of 2,6-bis(4-ethynyl toluene) pyridine **61** from 2,6-dibromopyridine and 4-ethynyl toluene **60** was carried out with success (61% yield).

Reaction of 6,6"-dibromo-2,2':6'2"-terpyridine **51** and 4-ethynyl toluene **60** under Sonogashira conditions proceeded as desired to give the product **62** in 74% yield. The next stage involved conversion of the CH_3 groups to CH_2Br using N-bromo-succinimide followed by oxidation to CHO via reaction with hexamethylene tetraamine. Following a 4 hour reflux with N-bromosuccinimide the ^{1}H-NMR spectrum displayed more peaks than expected in the aromatic region. It appears that there is a mixture of starting material **62** and product **76**. The reaction was repeated for a longer period of 6 hours and also carried out with the test reactant 2,6-bis(4-ethynyl toluene) pyridine. The results for both showed no change to the initial reaction, which indicated a mixture of CH_3 and CH_2Br groups. TLC on alumina ($CHCl_3$:hexane 1:1) showed a mixture of 4 products in addition to the starting material.

Without further purification of the CH_2Br, the oxidation of CH_2Br to CHO was attempted. The ^{1}H-NMR of the product was almost identical to that for the starting material with bromomethyl groups present. There was no trace of benzaldehyde product **77** present in the spectrum. A peak at approximately 10ppm is expected for the proton of this functional group. It was therefore evident that another route was required in order to prepare the desired porphyrin-terpyridine system **78**.

3.9.2 *Coupling of terpyridine with 4-iodobenzaldehyde*

The Sonogashira reaction between 6,6"diacetylene-2,2':6'2"-terpyridine **53** and 4-iodobenzaldehyde **55** was attempted in order to form the target compound **77** illustrated in figure 3.20. After the formation of this compound, the next step in the procedure would involve building on the benzaldehyde groups by reaction with

further equivalents of a simple benzaldehyde and pyrrole (Adler-Longo) to form compound **78**.

Sonogashira coupling of **53** and **55** as shown in scheme 3.21 over a period of 4 hours followed by ^{1}H-NMR analysis revealed a large amount of 4-iodobenzaldehyde in the reaction mixture. Therefore the reaction was continued for a further 12 hours. The ^{1}H-NMR displayed 7 multiplets in the aromatic region as expected for the desired compound **77**. However the peaks appeared to be in the same positions as both starting materials and there also appeared to be 3 peaks representative of the benzaldehyde protons, which implies the presence of a mixture.

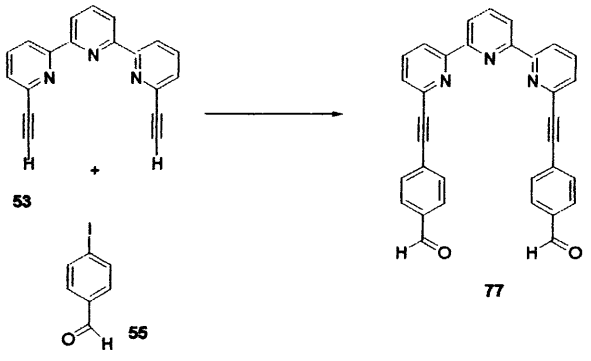

Reagents and conditions: Copper (I) iodide, palladium (II) acetate, triphenylphosphine, reflux in triethylamine/acetonitrile under N_2 in absence of light.

Scheme 3.21: Attempted synthesis of compound **77.**

The reaction was repeated for 48 hours (adding further catalysts after 24 hours to ensure reaction) and the yellow/brown coloured solid purified by filtering through alumina using dichloromethane. Characterisation via ^{1}H-NMR spectroscopy showed identical results to those obtained after 12 hours with 7 multiplets in the aromatic region and 3 benzaldehyde peaks occurring just below 10 ppm. A small peak was present at 3.2ppm which would indicate the presence of alkyne C-H ie. trace

6,6"diacetylene-2,2':6'2"-terpyridine, however this peak had no integration so was considered an insignificant quantity.

The IR spectrum of the product suggested the desired compound **77** was formed since the following vibrations were observed: 1685 (s) C=O, 1435, 1261 (s) C-N, 2361 cm^{-1} (s) alkyne CC. The alkyne C-H stretch (3273 cm^{-1}) present in 6,6"-diacetylene-2,2':6'2"-terpyridine had disappeared which is also sign that the reaction had proceeded as anticipated.

To confirm the structure as **77,** a mass spectrum (ES+) was carried out on the compound. The expected mass for the desired compound **77** is 490 m/z however there was no evidence of this in the spectrum. It is interesting to note the peak which arises at 550.4 m/z. Clearly this is larger than that which is expected for our structure. In fact this peak is due to the Cu complex of the target compound **77** (490+59=549). Copper insertion seems to have taken place during the reaction, which utilises Cu (I) as a catalyst. There is no trace of the target compound itself and Cu has unfavourable quenching properties, therefore another route must be undertaken to reach the target porphyrin-terpyridine system **78.** Removal of the copper ion from the terpyridine is a route which could have been investigated if time had allowed.

3.9.3 *Direct coupling of terpyridine with porphyrin*

Clearly a copper-free Sonogashira method is required for the direct coupling of porphyrin with terpyridine since the aim is to design a system to mimic light-harvesting and energy transfer which requires no interference from quenching effects. A procedure developed by Lindsey and co-workers[38] makes use of

tris(dibenzylideneacetone)dipalladium(0) in conjunction with triphenylarsine under anaerobic conditions in toluene/triethylamine (5:1) to afford the Sonogashira coupled product in good yield with minimal higher molecular weight byproduct. This appeared an ideal method to synthesise the desired system **78**.

The ideal porphyrin macrocycle in these circumstances is an unsymmetrical A_3B-substituted since it is then more likely that the reaction will occur in a 2:1 porphyrin:terpyridine ratio. Again the Adler-Longo synthesis was utilised and the procedure for the preparation of unsymmetrical-substituted porphyrins is the same as symmetrical A_4 substituted except the amounts of each reactant will differ. In fact a 1:19 minor:major benzaldehyde ratio generally applies. The amount of pyrrole used is eqimolar to the benzaldehyde in excess, hence a 1:19:19 ratio exists for the reactants. This ensures that only two porphyrin products are obtained, making purification more straightforward than if a mixture of 5 or 6 porphyrin products were obtained. Flash column chromatography (pre-columning) is essential in each case to remove the black coloured pyrrole biproducts obtained in porphyrin preparations.

The first unsymmetrical A_3B-substituted porphyrin to be synthesised was *meso* 5,10,15-tri-phenyl-20-(*p*-iodophenyl)porphyrin. The symmetrical A_4 tetraphenyl porphyrin proved difficult to separate from the unsymmetrical A_3B porphyrin and after purification by column chromatography on silica gel (CH_2Cl_2/hexane 7:3), some A_4-substituted porphyrin was still present.

In order to increase the polar separation between the A_4 and A_3B substituted porphyrins, it was decided to repeat the above reaction using anisaldehyde instead of

benzaldehyde. After working up the reaction, purification by column chromatography on silica gel (CH_2Cl_2) followed by further separation using preparative plate chromatography was carried out. The iodine containing porphyrin had an R_f of 0.7 in contrast to the A_4-substituted methoxy porphyrin with an R_f of 0.35. Despite this substantial separation, a trace of A_4-substituted was still apparent along with the A_3B-substituted following purification. Further separation would have resulted in an extremely low yield of porphyrin therefore it was decided to use an alternative benzaldehyde.

Further attempts at preparing a pure A_3B substituted porphyrin were carried out. *Meso* 5,10,15-tri-phenyl-20-(*p*-TMS-ethynylphenyl)porphyrin was prepared together with tetraphenyl porphyrin however separation by preparative plate chromatography (CH_2Cl_2/hexane 7:3) was unsuccessful since the polarity of both compounds was so similar (0.05 difference). Extensive preparative plate chromatography was not successful in isolating pure A_3B substituted porphyrin.

Again using 4-TMS-ethynyl benzaldehyde, preparation and purification of *meso* 5,10,15-tri-*p*-methoxyphenyl-20-(*p*-TMS ethynyl phenyl)porphyrin was attempted. The *meso*-5,10,15,20-tetra(methoxyphenyl) porphyrin has an R_f of 0.5 whilst the target A_3B porphyrin has an R_f of 0.7 (CH_2Cl_2). Despite the obvious difference in polarity between the two products, complete purification proved difficult and the yield rapidly decreased to almost zero.

Alternatively, the synthesis of *meso* 5,10,15-tri-*p*-methoxyphenyl-20-(*p*-ethynylphenyl)porphyrin was carried out using 4-ethynyl benzaldehyde as the minor

benzaldehyde and 4-anisaldehyde as the major. The R_f of the target A_3B-substituted ethynyl substituted porphyrin in CH_2Cl_2 was found to be 0.67 in comparison to 0.45 for tetra methoxyphenyl porphyrin. This resulted in a difficult separation once more. Hence a final route was attempted in order to obtain a useable yield of porphyrin for the target reaction.

It was decided that this final attempt would involve the production and purification of *meso*-5,10,15-tri-*p*-methoxyphenyl-20-(*p*-2-methyl-3-butyn-2-olphenyl)porphyrin **69**. If successful, this product would be converted to *meso* 5,10,15-tri-*p*-methoxyphenyl-20-(*p*-ethynylphenyl)porphyrin **70** by reaction with sodium hydroxide. Therefore the Adler-Longo synthesis was carried out and **69** was afforded as the minor (A_3B) porphyrin and *meso*-5,10,15,20-tetra(4-methoxyphenyl) porphyrin as the major (A_4) product. The R_f of the target compound **69** was 0.15 whereas the R_f of the unwanted A_4 substituent was 0.76 (CH_2Cl_2). As this separation was considerably larger than those presented earlier purification proved to be much simpler. After carrying out a pre-column, eluting with chloroform 97% and methanol 3%, further separation via preparative plate chromatography was required. The target compound **69** was isolated in 2% yield, which is greater than the previous efforts made.

The structure was assigned by ^{1}H-NMR and it is noteworthy that the occurrence of a few peaks for the pyrrole protons at 8.5-8.8ppm shows the unsymmetrical nature of the A_3B *meso*-tetraaryl porphyrin since a symmetrical A_4 tetraaryl porphyrin would only display one singlet for the external pyrrole protons. The IR demonstrates the N-H stretch (3443 cm^{-1}), and the C-O (1000-1300 cm^{-1}). The UV absorptions for the

compound are all characteristic of a porphyrin occurring at 422 (4.32), 522 (2.50) and 554 (2.41) nm and final confirmation of the product was achieved via mass spectrometry (ES+) revealing a peak corresponding to the parent ion of **69** at 787.6 m/z.

Conversion of *meso*-5,10,15-tri-*p*-methoxyphenyl-20-(*p*-2-methyl-3-butyn-2-olphenyl)porphyrin **69** into *meso*-5,10,15-tri-*p*-methoxyphenyl-20-(*p*-ethynylphenyl)porphyrin **70** was achieved as shown in scheme 3.22. The porphyrin compound **70** was afforded in excellent yield (84%). The ^{1}H-NMR spectrum confirmed the reaction had taken place as the peak previously present at 1.7 ppm for the CH_3 groups of the 2-methyl -3- butyn-2-ol have been replaced by a singlet at 3.22 ppm signifying the alkyne proton. It was also apparent that most of the peaks had shifted very slightly downfield compared with the parent compound **69**.

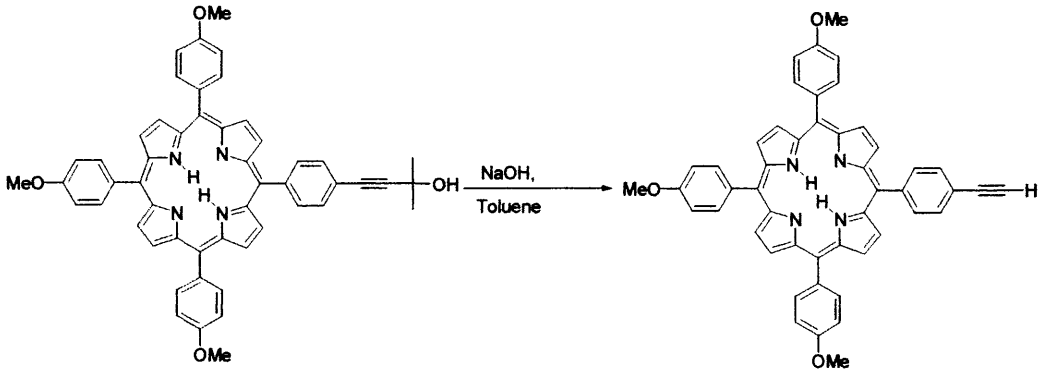

69 70

Scheme 3.22: Deprotection of compound **69**

The UV spectrum of compound **70** demonstrated the increase of the extinction coefficients compared with compound **69**. Mass spectrometry (ES+) of the sample showed a peak at m/z of 735.4 which is equal to the mass of the target compound confirming conversion to compound **70** had been achieved.

The copper free coupling reaction between two equivalents of the porphyrin and one equivalent of 6,6"-dibromo-2,2':6'2"-terpyridine was attempted.[38] The reaction is shown in scheme 3.23. Despite the suggestion from the ^{1}H-NMR that the reaction had not occurred, the UV spectrum of the mixture showed a slight increase in the wavelength the absorptions. The Q band absorption had undergone an increase of 14 nm whist the Soret band increased by 7 nm from porphyrin to bisporphyrin/terpyridine system. This increase is generally an indication of increase in size of the porphyrin array.[8] Mass spectrum results indicated the desired array was not present within the mixture.

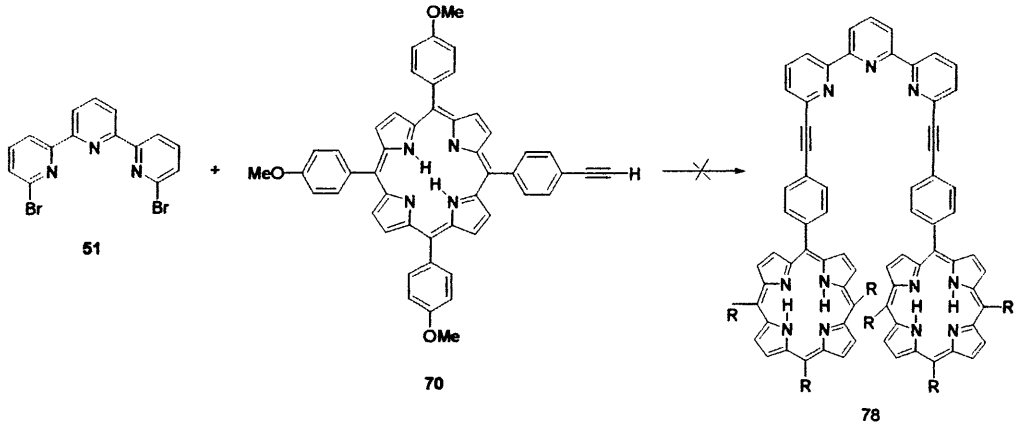

Reagents and conditions: Reflux with tris(dibenzylideneacetone)dipalladium(0) and triphenylarsine under anaerobic conditions in toluene/triethylamine (5:1).

Scheme 3.23: Attempted synthesis of compound 78 using the copper-free Sonogashira method of Lindsey [38]

3.10 Conclusions

In conclusion, the work outlined in this chapter has produced a number of novel A_4-substituted and A_3B substituted porphyrins using the Sonogashira[32] and Heck[54] methods of coupling, both achieving good yields of products.

A novel synthetic strategy for the convenient high yield preparation of 4-iodobenzaldehyde is reported and this compound was used in the Sonogashira coupling reaction since iodide is the most reactive of the halogens for the purpose of this reaction.

The luminescence studies undertaken demonstrate the effectiveness of the halogens in quenching the luminescence. Altering the 4-substituent of the symmetrical A_4 porphyrin has less of an effect on the luminescence when the porphyrin is metalated with zinc(II) than in the free base.

The final method for the synthesis of compound **78** showed the most promise since it involves direct coupling of the terpyridine with two A_3B substituted porphyrins using a copper free Sonogashira reaction.[38] Further investigations are required in order to successfully isolate compound **78**. The synthetic strategy to obtain this structure does require some more attention and more extensive chromatography methods would prove useful. Once the compound has been obtained further studies involving metallating the terpyridine chelate with various metals and the porphyrins sites with a single lanthanide ion can then proceed.

3.11 References

1) Johnathan S. Lindsey, *The Porphyrin handbook*, 2000.

2) Edwin C. Constable, *Co-ordination Chemistry, Oxford Chemistry Primers*, 1998.

3) W. Hausmann, Biochem. Z., 1911, **30**, 276.

4) B. A. Gregg, M. A . Fox, A.J. Bard, J. Am. Chem. Soc., 1989,**111**, 3024.

5) K.S. Suslick, N.A. Rakow, M.E. Kosal, J.H. Chou, *J. Porphyrins and Phthalocyanines*, 2000, **4**, 407.

6) S. Prathapan, T.E Johnson, J.S Lindsey, *J. Am. Chem. Soc.*, 1993, **115**, 7519.

7) J.S Lindsey, S. Prathapan, T.E. Johnson, R.W Wagner, *Tetrahedron*, **50**, 1994, 8941.

8) M. del Rosario Benites, T.E. Johnson, S. Weghorn, L. Yu, P.D Rao, J.R. Diers, S.I. Yang, C. Kirmaier, D. F. Bocian, D. Holten, J.S. Lindsey, *J. Materials Chem.*, 2002, **12,** 65.

9) E. Tsuchida, Macromolecular Symposia, 1998, 131(7th International Symposium on Macromolecule-Metal Complexes, 1997), 155.

10) P.J Rothermund, *J. Am. Chem. Soc.*, 1936, 625.

11) A.D Adler, F.R. Longo, W. Shergalis, *J. Am. Chem. Soc.*, 1964, **86,** 3145.

12) A.D Adler, F.R. Longo, J.D Finarelli, J. Goldmacher, J. Assour, L. Korsakoff, *J. Org. Chem.* 1967, **32**, 476.

13) G. Barnett, M. Hudson, K. Smith, *Tetrahedron Lett.*, 1973, 2887.

14) D. Dolphin, *Heterocycl. Chem.*, 1970, **7**, 275.

15) J.S. Lindsey, I.C. Schreiman, H.C. Hsu, P.C. Kearney, A.M. Marguerettaz, *J. Org. Chem.*, 1987, **52**, 827.

16) J. Diesenhofer, O. Epp, K. Miki, R. Huber, H. Michel, *Nature*, 1985, **318**, 618-624.

17) J. Duchowski, D. Bocian, *J. Am. Chem. Soc.* 1990, **112**, 3312.

18) J. Perng, J. Duchowski, D. Bocian, *J. Phys. Chem.* 1990, **94**, 6684-6691.

19) J. Perng, J. Duchowski, D. Bocian, *J. Phys. Chem.* 1991, **95**, 1319-1323.

20) J. Collman, J. Kendall, J. Chen, *Inorg. Chem.*, 2000, **39**, 1661-1667.

21) L. Wittmer, D. Holten, *J. Phys. Chem.*, 1996, **100**, 860-868.

22) T. Gross, F. Chevalier, J. Lindsey, *Inorg. Chem.*, 2001, **40,** 4762-4774.

23) K. Roth, D. Gryko, C. Clausen, J. Li, J. Lindsey, W. Kuhr, D. Bocian, *J. Phys. Chem.*, 2002, **106**, 8639.

24) K. Padmaja, W. Youngblood, L. Wei, D. Bocian, J. Lindsey, *Inorg. Chem.*, 2006, **45,** 5479.

25) J. Duchowski, D. Bocian, *J. Am. Chem. Soc.*, 1990, **112**, 8807.

26) J. Buchler, A. DeCian, J. Fisher, M. Kiln-Botulinski, H. Paulus, R. Weiss, *J. Am. Chem. Soc.*, 1986, **108,** 3652.

27) J. Buchler, K. Elsasser, M. Kiln-Botulinski, B. Scharbert, *Angew. Chem., Int. Ed. Engl.*, 1986, **25**, 286.

28) J. Buchler, B. Scharbert, *J. Am. Chem. Soc.*, 1988, **110**, 4272.

29) D. Chabach, A. DeCian, R. Weiss, *J. Phys. Chem.*, 1994, **98**, 8279.

30) J. Jiang, Y. Bian, F. Furuya, W. Liu, M. Choi, N. Kobayashi, H. Li, Q. Yang, T. Mak, D. Ng, *Chem. Eur. J.*, 2001, **7, No. 23,** 5059.

31) D. Chabach, A. DeCian, J. Fishcer, R. Weiss, M. Bibout. *Angew. Chem., Int. Ed. Engl.*, 1996, **35,** 898.

32) K. Sonogashira, Y. Tohda, N. Hagihara, *Tet. Lett.* 1975, 4467.

33) J.K Stille, D. Milstein, *J. Am. Chem. Soc.*, 1979, **101 (17),** 4992.

34) A. Suzuki, *J. Organometalic Chem.*, 1999, **576 (1-2),** 147.

35) A.S. Hay, *J. Org. Chem.*, 1962, **27, 7,** 3320.

36) C. Glaser, *Am. Chem. Pharm.*, 1870, **154**, 137.

37) F. Li, I.K. Yang, Y. Ciringh, J. Seth, C.H. Martin, III, D.L. Singh, D. Kim, R.R. Birge, D.F. Bocian, D. Holten, J.S. Lindsey, *J. Am. Chem. Soc.*, 1998, **120,** 10001

38) R.W. Wagner, T.E. Johnson, F. Li, J.S. Lindsey, *J. Org. Chem.*, 1995, **60,** 5266.

39) L. Yu, J.S. Lindsey, *J. Org. Chem.*, **66, No. 22,** 2001, 7403.

40) A. Harriman, M. Hissler, O. Trompette, R. Ziessel, *J. Am. Chem. Soc.*, 1999, **121,** 2516.

41) R. Ziessel, J. Suffert, M. Youinou, J. Org. Chem., 1996, 61, 6535.

42) A. Carpita, A. Lessi, R. Rossi, *Synth. Commun.*, 1983, 571.

43) A. Elangovan, Y. H. Wang, T.I. Ho, *Org. Lett.*, 2003, **5, No. 11,** 1841.

44) A. Harriman, R. Ziessel, *Chem. Comm.*, 1996, 1707.

45) J. Suffert, R. Ziessel, *Tet. Letts.*, **32, No. 6**, 757.

46) Y. Uchida, M. Okabe, H. Kobayshi, S. Oae, *Synthesis*, 1995, 939

47) A. McKillop, M. Ford, *Synthetic Comm.*, 1974, **4, (1)**, 45.

48) G. Zhongwu, *Huaxue Shiji*, 1990, **12(6),** 381, 363.

49) X. Li, C.L.D. Gibb, M.E Kuebel, B.C. Gibb, *Tetrahedron*, 2001, **57**, 1175.

50) M. J. Plater, S. Aiken, G. Bourhill, *Tetrahedron*, 2002, **58**, 2405.

51) I. Blake, H. Anderson, D. Beljonne, J. Luc Bredas, W. Clegg, *J. Am. Chem. Soc.*, 1998, **120**, 10764.

52) F. Perrin, *J. Chim. Phys.*, 1928, **25**, 531.

53) M. Berberan-Santos, *Phys. Chem. Comm.*, 2000, 5.

54) H. Dieck, F.R Heck, *J. Organomet. Chem.*, 1975, **93**, 259.

55) E.C. Constable, J.M. Holmes, *Polyhedron*, **Vol. 7,** 1988, 2531.

56) J.L. Toner, *Tet. Lett.*, **Vol. 24, No. 27,** 1983, 2707.

57) S. Howard, I.A. Fallis, *J. Chem. Soc., Perkin Trans. 2*, 1999, 2501.

Chapter 4

Synthesis and Complexation of Tetraaza macrocycles functionalised with phenol side arms

4.1. Phenoxyl Radical complexes in PSII

During the transfer of electrons from PS II to PS I by a number of quinones, an electron hole is generated at P680 (primary donor) which oxidises a tyrosine residue to a neutral, deprotonated phenoxyl radical. Furthermore, the phenoxyl radical then acts as a one-electron oxidant of a tetranuclear manganese cluster and once the oxidation process has taken place a total of four times, two water molecules are produced. Upon oxidation to a dioxygen molecule, electrons and protons are generated. It is the transfer of the electrons generated in PS II during this process that drives the photosynthetic process and gives rise to the reduction of carbon dioxide to energy rich organic compounds.

Wieghardt and co-workers are amongst those who carry out research in this area.[1-9] The research group are interested in developing the coordination chemistry of phenoxyl radicals bound to transition metal ions. Their research is not only focused on the development of systems to mimic PS II. The occurrence of phenoxyl radicals in the active sites of some copper containing enzymes such as galactose oxidase[11] and glyoxal oxidase[12] has drawn attention to the development of phenol containing ligands.

4.1.1 Complexes of 1,4,7-tris(3,5-di-tert-butyl-2-hydroxylbenzyl)-1,4,7-triazacyclononane and its derivatives

Wieghardt and co-workers have carried out a great deal of work on the N-functionalisation of tacn with phenol-type pendant arms[1-3, 5-7] using the Mannich reaction.[13] Such hexadentate ligands are known to bind strongly to di and tri-valent transition metal ions. Analogous amino and mercaptobenzyl ligands have also been

prepared as shown in figure 4.1 which also offer strong binding to di and tri-valent transition metal ions.[1,6]

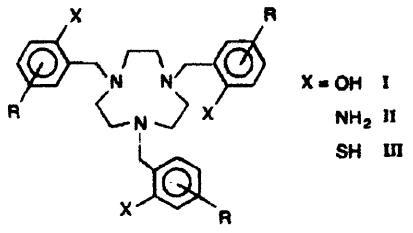

Figure 4.1: Tris(o-hydroxylbenzyl) I, tris(o-aminobenzyl) II, and tris(o-mercaptobenzyl) III -1,4,7-triazacyclononane ligands studided by Wieghardt[1]

Complexes of the ligands exist in a variety of oxidation states affording the possibility of interesting metal versus ligand-centred redox chemistry. One electron oxidation of such a complex will give rise to one of the paths shown in scheme 4.2(metal or ligand centred oxidation).

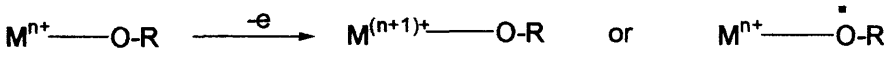

Scheme 4.2: One electron oxidation of a transition metal phenalto complex

Wieghardt was interested in deducing whether the above are resonance structures of the same ground state or if they are two different chemical species. In order to do this he has synthesised a variety of hexadentate trianionic tacn ligands and complexed them with a variety of metals in +II and +III oxidation states. Electrochemical measurements indicated the +III oxidation states of the transition metals are stabilised to a greater extent by the phenolato ligands as oppose to their thiophenolato analogues. It was shown that bulky non-oxidisable substituents at the ortho and para positions of the pendant o-hydroxybenzyl groups further increase the stability of the of the phenoxyl radical.[2] The *tert*-butyl group is most commonly

used for this purpose. Additionally, metal-phenoxyl bonds are less stable than metal-phenolate bonds hence without the stability provided by the *tert*-butyl groups, the monodentate ligands will rapidly dissociate.

The first phenoxyl radical complex the group were able to characterise by X-ray crystallography was the chromium monocation complex.[4] The structure shows that the two coordinated phenolato groups have an average Cr-O bond distance of 1.920 angstroms and the Cr-O distance for the phenoxyl is longer at 1.943 angstroms. The crystal structure (a) and the inequivalent phenolate (b) and phenoxyl (c) radical ligands are shown in figure 4.3. It seems to be the case that the unpaired electron of the radical is in fact delocalised over the organic ring for each pendant arm.

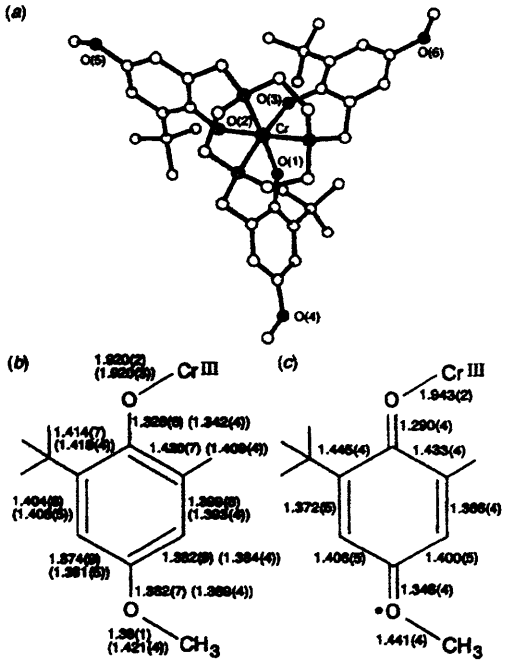

Figure 4.3: a) Crystal structure for Chromium ^{III} 1,4,7,-tris(3-tert-butyl-5-methoxy-2-hydroxylbenzyl)-1,4,7-triazacyclononane[4] b) Phenolate arms present in a. c) phenoxyl radical present in a.

For most metal complexes only ligand-centred oxidation was observed, however the manganese complex also displayed metal-centred oxidation.[2] Manganese (IV) is detected in the monocation complex but investigation of the dication suggests the process is ligand centred as no Mn (V) is observed. However, Koikawa, Okawa, Kida and co-workers have shown that high oxidation states do exist for coordinated phenolates since they have described octahedral complexes for manganese (V) and iron (IV).[12,14-16]

Wieghardt and co-workers have also synthesised and investigated complexes with zinc (II)[3] since it is redox inactive for a wide potential which allowed them to focus on ligand centred processes without the involvement of metal centred redox processes. Of particular interest are complexes **2** and **2a** shown in figure 4.4. A coordinated phenol was achieved with the zinc (II) unlike those for gallium(III) and scandium(III) by protonation of coordinated phenolate groups leading to weakening of the Zn-O bond. Compound **2** contains two coordinated phenols and one phenolate pendant arm whilst **2a** contains two coordinated phenolate and one coordinated phenol. Electrochemistry carried out on the neutral species **2a** in acetonitrile showed two reversible one electron waves owing to oxidation of the two coordinated phenolate pendant arms. Complex **2** shows only one reversible one-electron wave in acetonitrile which, owing to oxidation of the phenolate to form a coordinated phenoxy radical. Above potentials of +0.80 V irreversible oxidation of coordinated phenols generally occurs. Potentials are referenced versus the ferrocenium/ferrocene (Fc^+/Fc) couple. EPR spectroscopy undertaken on these compounds demonstrated that not only is the unpaired electron delocalised over the aromatic ring as earlier observed but over the metal ion and the coordinated phenolates in close proximity. The electron

however was not delocalised over the bound phenol ligands. Resonance Raman spectroscopy was used to distinguish between coordinated and uncoordinated phenoxyls and as a comparison for this, the group used the data obtained by Lippard and co-workers[17] for their complex [Zn-(BIDPhE)Cl_2] which possesses an uncoordinated phenoxyl arm. (BIDPhE =1,1-bis[2-(1-methylimidazolyl]-1-(3,5-di-tert-butyl-4-oxylphenyl)ethane).

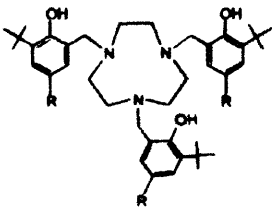

$[Zn(L^2H_2)]BF_4 \cdot H_2O$ **2**

$[Zn(L^2H)]$ **2a**

Figure 4.4: Ligands and zinc (II) complexes prepared by Wieghardt[3] where R is methoxy.

Further investigations by Wieghardt have involved studying the nature of the metal ion and phenoxyl radical as a function of the d^n electron configuration.[5] In order to do this Wieghardt generated a series of octahedral complexes using Tolmans' ligand[18] (1,4-di-iso-propyl-7-(3,5-di-tert-butyl-2-hydroxy-benzyl)-1,4,7-triazacyclononane) and an analogous ligand where one *tert*-butyl group is replaced by a methoxy group. Bidentate acetylacetonate derivatives or oxalates were used to complete the octahedral coordination as shown in figure 4.5. Chromium(III), manganese(III), cobalt(III) and nickel(II) were used for the investigation.

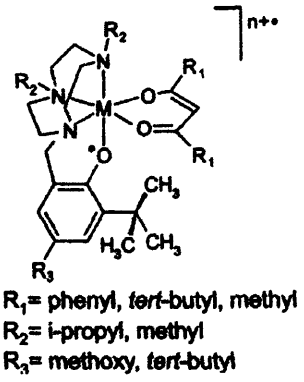

Figure 4.5: Complexes prepared by Wieghardt[5] based on Tolmans ligand[18]

Again potentials are referenced to the Fc^{+}/Fc couple. A one electron ligand centred oxidation corresponding to formation of the phenoxyl species is observed for all the complexes apart from the nickel (II) species in the range +0.24 to 0.51V. For the nickel, this oxidation is displayed below -0.3V owing to the fact that this oxidation takes place from the neutral species to the monocation whereas all the others are monocation to dicationic oxidations. The manganese species were shown to possess an extra reversible redox wave below -0.5 V due to the Mn^{III} /Mn^{II} couple and an irreversible wave above +0.8 V due to either metal or ligand centred oxidation. The metal centred reduction waves of all the complexes investigated will occur at very low potential providing the metal is redox active. The UV data obtained shows that the neutral species tend to display 2 absorptions at 200-400 nm for the phenolate and acac species and further d-d transitions in the visible region. Once the phenoxyl radical is formed, another two peaks in the range 400-500 nm were observed.

4.1 2 Manganese clusters with phenoxy radicals

Coordinated phenolates are now classed together with porphyrins and quinones all of which are redox active organic compounds. More recently, Wieghardt

and co-workers have begun to look at manganese clusters with phenol containing ligands.[7-9] Their interest evolves from evidence of a tetranuclear manganese cluster located at PS II. As mentioned earlier, in PS II generation of an electron hole oxidises a tyrosine residue to a radical and the phenoxyl radical itself acts as a one-electron oxidant of the tetramanganese cluster which results in the production of dioxygen.

A dimer of di(μ-oxo)dimanganese dimers is thought to form the cluster found in PS II and the manganese ions cycle between the +II, +III and +IV oxidation states. However the exact mechanism of interaction of the manganese cluster with the phenoxyl radical is ambiguous. This has led to Wieghardt and his group designing systems to model the initial charge separation and the electron-transfer chain from the manganese cluster through to the reaction centre. Tris(bipyridyl)-ruthenium (II) complexes were used to mimic the reaction centre because they endure light-energy induced charge separation hence behaving as a model for the reaction centre. These complexes were covalently bound to the dinuclear manganese centre bridged by a redox active phenolate. This was the first example of its kind and the structures for mono, di and tri-manganese complexes are shown in figure 4.6.[7]

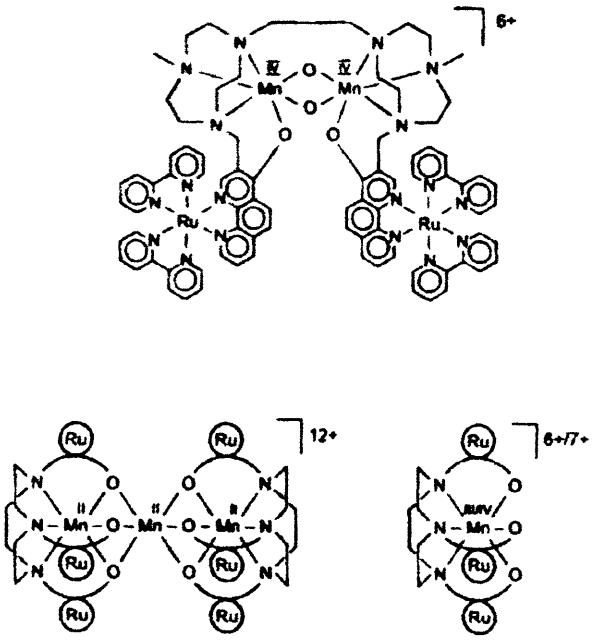

Figure 4.6: Manganese complexes **A** (dimanganease species), **B** (trimanganease species) and **C** (monomanganease species) synthesised by Wieghardt[7]

The bismacrocyle based on tacn was utilised since it stabilises the $Mn_2(\mu O)_2$ moiety. The phenolato oxygen donor was attached to the $Ru(bpy)_3$ unit to decrease the overall charge on this unit and also to increase the affinity of the ligand system towards the manganese ions as earlier experiments had shown the CH_2 linkers to decrease the likelihood of manganese complexation taking place. Coordination of only one pendant arm is possible since nitrogens from the tacn and oxo bridges occupy all other sites. Electrochemical measurements showed that the manganese centres exist in the +II, +III and +IV oxidation states and are capable of undergoing metal-centred reversible one-electron transfer. Compounds **A** and **B** and **C** in figure 4.6 were found to undergo similar processes to those in the reaction centre and PS II when the ruthenium part of the molecule was photochemically excited.

Further investigations by Wieghardt involved preparation of a system to mimic the strong manganese-manganese exchange and the weak manganese-radical coupling present in PS II. Synthesis of the compounds **1-6** shown in figure 4.7[9] was undertaken.

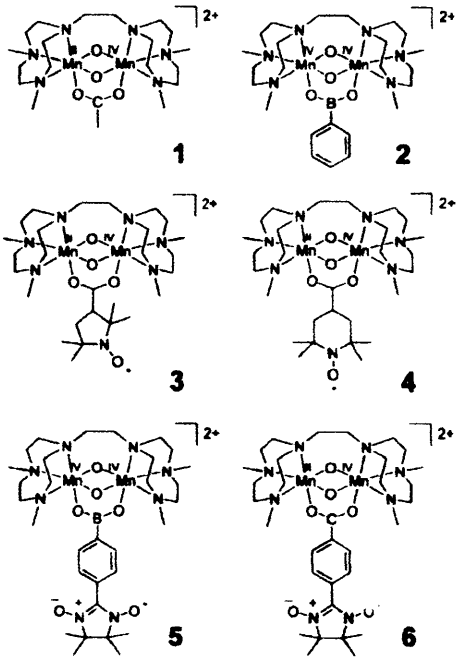

Figure 4.7: $Mn^{III}Mn^{IV}$ complexes prepared and investigated by Wieghardt[9]

By varying the organic residues attached to the dimanganese core as shown, the distance between the manganese core and the residue is varied. The π and σ pathways for through bond exchange are also varied as the residue attached to the organic core via carboxylate or boronate bridges is varied. The boronate and carboxylate bridges were shown to not affect the exchange mechanism however the weakest manganese-radical coupling was observed for compound **4** in the solid state. It was concluded that compounds **3** and **4** of figure 4.7 were thought to be good models for PS II. However compound **6**, which demonstrates a short separation (hence strong coupling) between the manganese core and the radical due to

delocalisation of the radical spin density towards the manganese core, is not an accurate model of PS II.

Considerable work based on the phenoxyl and phenolate triazacyclononane complexes have been reported, however little work surrounding tetrazacyclododecane has been carried out to date.

4.2 Lanthanide complexes with tetrazacyclododecane bearing pendant arms

Our interests lie in extending Wieghardts' studies on phenolate/phenoxyl species to cyclen-lanthanide complexes. Much work has been undertaken in the past 20 years on the functionalisation of ligands based on the 1,4,7,10-tetraazacyclododecane (cyclen) framework. The macrocyclic framework itself is relatively rigid however the functional groups attached to the macrocycle via the nitrogen atoms are more flexible making them capable of adapting themselves geometrically according to the metal to which they are coordinating. All four pendant arms of the macrocycle can act as donor groups for larger metals such as the lanthanides as the possibility of 8 donor atoms meets the coordination requirements of lanthanide (III), in addition to the added stability due to the macrocyclic effect. As lanthanide ions are hard and polarising, it is essential to use donor atoms such as amine nitrogens or hard anionic donors in to achieve stable complexes in aqueous solutions.

Many cyclen derivatives bearing pendant arms functionalised by carboxylate,[19, 20] amide[21, 22] and phosphinate[23, 24] groups have been prepared. Some complexes of this kind have been achieved which have high thermodynamic stability and kinetic inertness hence resulting in their use for medicinal purposes. One particular compound that has attracted a great deal of attention is DOTA shown in figure 4.8.

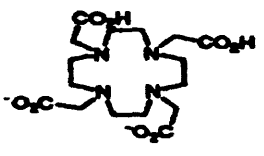

Figure 4.8:Structure of DOTA

DOTA is able to form incredibly stable complexes especially with trivalent metal ions. Such complexes are used as NMR shift agents (Tb^{3+} complexes)[25] and MRI contrast agents (Gd^{3+} dota complex)[26] and as probes in biochemical processes (Eu and Tb^{3+} complexes).[27] A great deal of work surrounding this area of chemistry has been carried out by Parker and co-workers.[28, 29] They have synthesised and examined the luminescence of many compounds based on and similar to the DOTA framework.

Bunzli has investigated the orientation of the chromophore to the ligand-to-metal energy transfer in lanthanide complexes based on cyclen bearing 4 pendant arms derivatives.[30] Synthesis of the ligands shown in figure 4.9 and their subsequent complexes was carried out in order to gain a better insight into the energy transfer process between the ligand and the lanthanide core. By varying the nature and the length of the chromophoric group as shown, Bunzli and co-workers demonstrated the importance of the geometric and energy parameters in the energy transfer process.

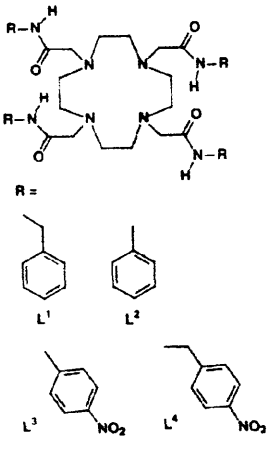

Figure 4.9: Ligands prepared by Bunzli and co-workers[30]

The europium (III) complexes were shown to display a low luminescence due to the high energy of the triplet state. The results are shown in the table in figure 4.1. The quantum yield for EuL^1 is three times greater than that for EuL^2 and this is thought to be a result of preferred orientation of the pendant arms for L^1 arising from the flexibility of the methylene group. The data shown for TbL^1 and TbL^2 are analogous to the europium complexes again due to the preferable energy and geometrical advantages of L^1.

LnL	$Ø_{abs}$ (%)	LnL	$Ø_{abs}$ (%)
EuL^1	0.06	**TbL^1**	6.4
EuL^2	0.02	**TbL^2**	0.22
EuL^3	0.003	**TbL^3**	5×10^{-3}
EuL^4	Too low to be measured	**TbL^4**	5.6×10^{-2}

Table 4.1: Table of quantum yields measured in dry degassed acetonitrile at 293K.

The very low luminescence of the EuL^3 complex in solution is quite astonishing since the solid state luminescence carried out showed the compound to possess a strong luminescence. The high values for the luminescence of EuL^3 in the solid state were explained by a short distance between the triplet state on the NO_2 of one molecule which acts as the sensitiser and the europium centre of a neighbouring molecule. This distance is only 4.79 angstroms in comparison to 9.82 angstroms which is the intramolecular distance between the centre of the NO_2 group and the europium ion. TbL^3 demonstrates the same features as the europium complex. In addition, the luminescence of the europium complex of L^4 was low for both solid and solution measurements. The presence of only one triplet state bearing a large energy

gap of 5070 cm^{-1} from the metal ion excited state is an unfavourable situation for efficient energy transfer hence resulted in very low values for the luminescence. An increase was observed on going from TbL^3 to TbL^4 owing to preferred energy and geometrical aspects.

4.2.1 Cu^{2+} complexes of tetraazacyclododecane functionalised with benzyl side chains bearing phenolic groups

Further research around this area is carried out by Kaden and co-workers.[31] Of more relevance to our work, Kaden and co-workers have synthesised the ligands shown in figure 4.10 which consist of a cyclen macrocycle bearing four benzyl groups which in turn possess four phenolic groups. However, unlike the work of Parker and Bunzli, Kaden has obtained the corresponding Cu (II) complexes. Although our interests lie in lanthanide complexes, it is interesting to look at these complexes to further understand the link between ligand structure and complex geometry.

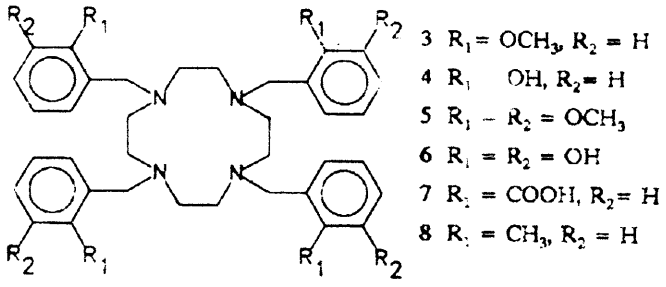

Figure 4.10: Ligands prepared and investigated by Kaden and co-workers[31]

Results showed that in all cases, tetra substitution did not hinder the co-ordination of the copper ion. Absorption spectra carried out on all complexes demonstrated the spectra of complexes of ligands **4**, **6** and **7** which possess carboxylic and phenolic groups were affected upon altering the pH of the solution owing to their

donor properties. Stability constants calculated for Cu (II) complexes with ligand **7** were compared with those for DOTA and it was revealed that DOTA which contains more flexible pendant arms is the more stable ligand.

Kaden and co-workers obtained crystal structures of copper (II) complexes with ligands **4** and **7**, both of which had a square pyramidal geometry. With respect to complex **4** the phenolic oxygens had no involvement in co-ordination of the Cu(II) and the metal ion was penta co-ordinated by four nitrogens and a chloride ion. Co-ordination of a sixth atom appears to be prevented since the macrocycle is folded. Again with **7** the Cu (II) is penta co-ordinated however unlike the previous case, the fifth donor is one of the carboxylate pendant arms. The group used the crystal structure of the Cu(II) complex of DOTA as a comparison and the geometry of the latter is cis-octahedral, the six donors being the four nitrogens in addition to the two carboxylate pendant arms. The extra co-ordination site for the Cu (II) complex of DOTA suggests that in complexes **4** and **7**, there is a limitation of the number of available co-ordination sites owing to the aromatic moieties.

4.3 Reported cyclen-porphyrin system

We are interested in synthesising an array composed of four phenol containing porphyrins linked to a cyclen centre via the nitrogen atoms of the cyclen. Setsune and Takeda[32] have reported the synthesis of the porphyrin-cyclen composite shown in figure 4.11.

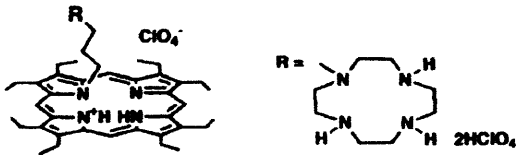

Figure 4.11: N,N'-(Trimethylene)-linked porphyrin-cyclen composite prepared by Setsune and co-workers[32]

Setsune and co-workers are interested in producing ligand assemblies containing bimetallic sites, prompted by the detection of such sites in various metalloenzymes. Porphyrin and cyclen macrocycles both possess four nitrogens however they have completely different stereochemical and electronic properties and combining the two of them in one system affords two sites for metal ions having different redox and ligand donor properties.

Preparation took place via N-alkylation of octaethyl-porphyrin with 3-iodopropyldiphenylsulfonium tetrafluoroborate and the iodine was then substituted with 1,4,7,10-tetraazacyclododecane. Characterisation of this compound by ^{1}H-NMR spectroscopy suggested the lack of flexibility of the trimethylene linker since three broad singlets were observed instead of the three multiplets as seen in the starting material. Communication between the porphyrin and cyclen was therefore considered to be limited. It is noteworthy that the porphyrin-cyclen composite was found to be relatively stable against dealkylation in typical organic amides despite the fact that N-alkylporphyrins generally suffer dealkylation under such conditions.

4.4 Aims and objectives

To further the investigations undertaken by Kaden[31] and Wieghardt[1-9], it was decided to use the Mannich[18] reaction to synthesise some novel 1,4,7,10-tetraazacyclododecane and other tetraaza macrocyclic ligands bearing phenolic pendant arms. Although our interest lies in Photosystem II, in this instance we were mainly interested in looking at the interaction of lanthanides with these phenol compounds.

We aim to prepare compound **89** shown in figure 4.12, consisting of 1 cyclen macrocycle surrounded by 4 porphyrin units. Such a system could assist in furthering knowledge and understanding of light harvesting and energy transfer.

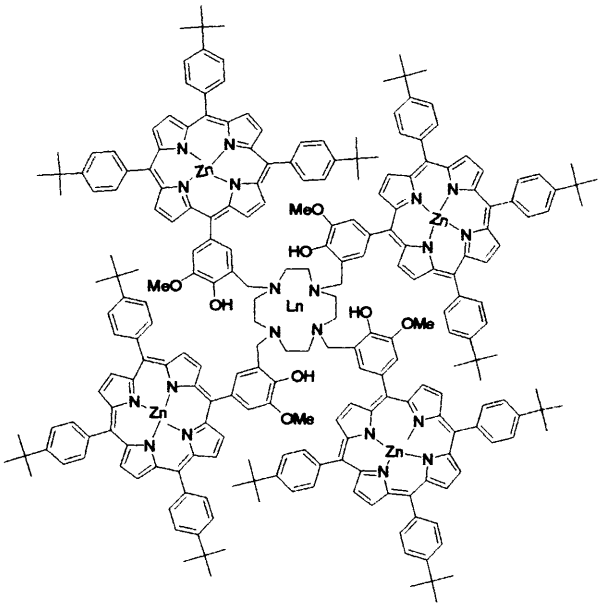

Figure 4.12: Target cyclen-porphyrin system **89**

The light harvesting ability of the porphyrins followed by transfer of energy to the lanthanide will result in luminescence to varying extents depending on the identity of the lanthanide centre. By varying the nature of the lanthanide centre and varying the metallation states of the porphyrins, we may develop our knowledge of light harvesting and energy transfer.

4.5 Experimental

4.5.1 Synthesis and Complexation of tetraaza macrocycles bearing 2,4-di-tert-butyl phenol as a pendant arms

1,4,7,10-Tetrakis(3,5-di-*tert*-butyl-2-hydroxybenzyl)-1,4,7,10-tetraazacyclododecane (74).

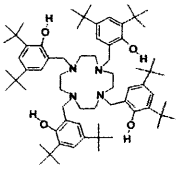

A solution of 1,4,7,10-tetraazacyclododecane (1g, 5.8mmol) and paraformaldehyde (0.7g, 23.2mmol) in methanol (50mls) was refluxed for 2hrs. After cooling, 2,4-di-*tert*-butylphenol (4.79g, 23.2mmol) and a few drops of concentrated hydrochloric acid were added and the solution refluxed for a further 3 hrs. After cooling, the white solid was collected by filtration and recrystallised from acetonitrile. The product was isolated by column chromatography (dichloromethane/hexane 1:1) R_f: 0.5. Yield: 1.09g, 19%. δ_H (400MHz, $CDCl_3$): 9.85 (4H, bs, O-*H*), 7.12 (4H, d, J=2.24, *H*4-aromatic), 6.65 (4H, d, J=2.15, *H2*-aromatic), 3.57 (8H, s, ArCH_2N), 2.77 (16H, s, CH_2N), 1.3 (36H, s, C(CH_3)$_3$), 1.18 (36H, s, C(CH_3)$_3$). δc 152.38, 139.87, 134.60, 122.64, 122.20, 119.74, 59.51, 49.36, 33.78, 33.07, 30.63, 28.56. IR KBr/cm^{-1}: 3507 (m), 2962 (s), 2907 (m), 2873 (w), 2827 (w), 1771 (w), 1651 (w), 1609 (s), 1482 (s), 1456 (m), 1386 (m), 1362 (s), 1304 (w), 1260 (s), 1242 (m), 1201 (m), 1164 (w), 1095 (s), 1023 (s), 878 (s), 798 (s), 760 (w), 721 (w), 668 (w). UV (Dichloromethane/nm): 282 (log ε 3.67), 234 (log ε 3.94). MS m/z ES+: 1045.8 $[M+H]^+$ (90%), 827.8 $[M-CH_2C_6H_2OH(C_4H_9)_2]$ (100%), 609.4 $[M-2CH_2C_6H_2OH(C_4H_9)_2]^+$ (20%).

[Dy(III) 1,4,7,10-Tetrakis(3,5-di-tert-butyl-2-hydroxybenzyl)-1,4,7,10-tetraazacyclododecane] $[Cl]_3$ (75). To a solution of compound **74** (0.05g, 0.0478mmol) in acetonitrile (8ml) was added dysprosium (III) chloride (0.018g,

0.0478mmol). Triethylamine (0.08g, 0.14 mmol) was added and the resulting solution was refluxed for 4 hrs followed by cooling at 4°C for 12hrs. The cream coloured precipitate was filtered and dried under vacuum. IR KBr/cm^{-1}: 3504 (m), 2961 (s), 2911 (w), 2861 (w), 2838 (w), 1776 (w), 1652 (w), 1608 (s), 1558 (m), 1481 (s), 1460 (w), 1443 (w), 1422 (w), 1390 (m), 1362 (s), 1324 (w), 1301 (m), 1260 (s), 1240 (s), 1168 (m), 1145 (m), 1120 (m), 1084 (w), 1026 (w), 980 (w), 953 (w), 762 (m), 724 (m). UV (Dichloromethane/nm): 421 (log ε 3.38), 278 (4.15), 234 (4.58). MS m/z FAB: 1206.7 $[M]^+$ (10%), 1045.8 $[M-Dy]^+$ (5%), 986.4 $[M-CH_2C_6H_4(C_4H_9)_2]^+$ (10%), 218.9 $[CH_2C_6H_2OH(C_4H_9)_2]^+$ (100%).

[Tb(III) 1,4,7,10-Tetrakis(3,5-di-tert-butyl-2-hydroxybenzyl)-1,4,7,10-tetraazacyclododecane] $[Cl]_3$ (76). To a solution of **74**(0.06g, 0.0574mmol) in acetonitrile (9mls) was added terbium (III) chloride (0.0215g, 0.0574mmol). Triethylamine (0.010g, 0.17mmol) was added and the resulting solution refluxed for 4hrs followed by cooling at 4°C for 12hrs. The white coloured precipitate was filtered and dried under vacuum. IR KBr/cm^{-1}: 3500 (m), 2960 (s), 2909 (w), 2861 (w), 2838 (w), 1776 (w), 1652 (w), 1608 (s), 1558 (m), 1481 (s), 1460 (w), 1443 (w), 1422 (w), 1390 (m), 1362 (s), 1324 (w), 1301 (m), 1260 (s), 1240 (s), 1204 (m), 1168 (m), 1148 (m), 1118 (m), 1086 (w), 1068 (m), 1042 (w), 1024 (w), 983 (w), 953 (w), 881 (s), 799 (s), 764 (m), 724 (m). UV (Dichloromethane/nm): 421 (log ε 2.72), 282 (3.75), 234 (3.98). MS m/z MALDI: 1201.7 $[M-2H]^+$ (100%).

[La(III) 1,4,7,10-Tetrakis(3,5-di-tert-butyl-2-hydroxybenzyl)-1,4,7,10-tetraazacyclododecane] $[ClO_4]_3$ (77). To a solution of **74** (0.05g, 0.0479mmol) in acetonitrile (6mls) was added lanthanum (III) perchlorate (0.026g, 0.0479mmol).

Triethylamine (0.14mmol, 0.008g) was added and the resulting solution refluxed for 5 hrs. After cooling, the volume of acetonitrile was reduced and water added to precipitate out a cream coloured solid. The title compound was collected by filtration and dried under vacuum. δ_H (400MHz, $CDCl_3$): 9.8 (4H, bs, O-*H*), 7.08 (4H, d, *H*4-aromatic), 6.61 (4H, d, *H*2-aromatic), 3.55 (8H, s, ArCH_2N), 2.75 (16H, s, CH_2N), 1.35 (36H, s, C(CH_3)$_3$), 1.2 (36H, s, C(CH_3)$_3$). IR KBr/cm^{-1}: 3499 (m), 2957 (s), 2911 (w), 2856 (w), 2838 (w), 1660 (w), 1608 (s), 1560 (m), 1481 (s), 1460 (w), 1443 (w), 1422 (w), 1390 (m), 1362 (s), 1324 (w), 1301 (m), 1260 (s), 1239 (s), 1203 (m), 1150 (m), 1119 (m), 1086 (w), 1068 (m), 1042 (w), 1024 (w), 983 (w), 953 (w), 880 (s), 766 (m). UV (Dichloromethane/nm):418 (log ε 2.98), 341 (3.25), 272 (4.02), 233 (4.20). MS m/z FAB: 1181.7 $[M-2H]^+$ (10%), 1045.7 $[M-La]^+$ (10%), 963.4 $[M-CH_2C_6H_2OH(C_4H_9)_2]^+$ (5%), 743.3 $[M-2CH_2C_6H_2OH(C_4H_9)_2]^+$ (5%), 218.9 $[CH_2C_6H_2OH(C_4H_9)_2]^+$ (100%).

[Zn(II) 1,4,7,10-Tetrakis(3,5-di-tert-butyl-2-hydroxybenzyl)-1,4,7,10-tetraazacyclododecane] $[C_2O_2H_3]_2$ (78). To a solution of **74** (0.046g, 0.044mmol) in acetone (5mls) was added zinc (II) acetate dihydrate (0.0097g, 0.044mmol). Triethylamine (0.009g, 0.088mmol) was added and the resulting solution refluxed for 24hrs. After cooling the solution was evaporated under vacuum to give a cream coloured solid. δ_H (400MHz, $CDCl_3$): 7.3 (4H, d, J=2.48, *H*4 aromatic), 6.88 (4H, d, *H*2-aromatic), 3.55 (8H, s, ArCH_2N), 2.85 (16H, s, CH_2N), 1.35 (36H, s, C(CH_3)$_3$), 1.20 (36H, s, C(CH_3)$_3$). IR KBr/cm^{-1}: 3504 (m), 2960 (s), 2909 (w), 2861 (w), 2838 (w), 1776 (w), 1652 (w), 1608 (s), 1558 (m), 1443 (w), 1425 (w), 1390 (m), 1334 (w), 1261 (s), 1235 (s), 1200 (m), 1168 (m), 1148 (m), 1116 (m), 1086 (w), 1068 (m), 1042 (w), 1024 (w), 880 (s), 760 (m). UV(Dichloromethane/nm): 421 (log ε 3.01),

283 (3.85), 234 (4.06). MS m/z FAB: 1109.7 $[M+H]^+$ (10%), 889.4 $[M-CH_2C_6H_2OH(C_4H_9)_2]^+$ (5%), 220.8 $[CH_2C_6H_2OH(C_4H_9)_2]^+$ (100%).

1,8-Dimethyl-4,11-(3,5-di-*tert*-butyl-2-hydroxybenzyl)-1,4,8,11-tetraazacyclotetradecane (79).

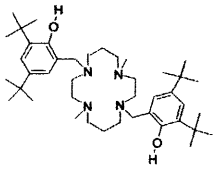

A solution of 1,8-dimethyl-1,4,8,11-tetraazacyclotetradecane (1g, 5.8mmol) and paraformaldehyde (0.35g, 11.6mmol) in methanol (50mls) was refluxed for 2hrs. After cooling, 2,4-di-*tert*-butylphenol (2.40g, 11.6mmol) and a few drops of concentrated hydrochloric acid were added and the solution refluxed for a further 3 hrs. After cooling, the white solid was collected by filtration and recrystallised from acetonitrile (58%). δ_H (400MHz, $CDCl_3$) 9.9 (2H, bs, O-*H*), 7.10 (2H, d, J=1.90, *H4*-aromatic), 6.77 (2H, d, J=1.83, *H2*-aromatic), 3.97 (4H, s, ArCH_2N), 2.4-3.2 (20H, m, macrocycle), 2.05 (6H, s, CH_3), 1.4 (18H, s, C(CH_3)$_3$), 1.15 (18H, s, C(CH_3)$_3$). IR KBr/cm^{-1}: 3427 (m,b), 3156 (m,b), 2960 (s), 2789 (s), 1593 (w), 1480 (m), 1458 (m), 1420 (w), 1388 (w), 1365 (m), 1281 (m), 1232 (m), 1199 (m), 1148 (w), 1120.1(m), 1078.7(w), 1047 (w), 954 (w), 913 (w), 877 (m), 821 (m), 795 (m),668 (m). UV (Dichloromethane): 282 (log ε 3.40), 234 (3.48). MS m/z ES+: 665.66$[M+H]^+$ (100%), 447.54 $[M-CH_2C_6H_2OH(C_4H_9)_2]^+$ (10%).

Nickel 1,8-dimethyl-4,11-(3,5-di-*tert*-butyl-2-oxybenzyl)-1,4,8,11-tetraazacyclotetradecane (80). A solution of nickel (II) nitrate (0.013g, 0.0452mmol) in the minimum amount of ethanol was added to a solution of ligand **79** (0.03g, 0.0452mmol) in the minimum amount of ethanol. After addition of triethylamine (0.09mmol, 0.009g), the suspension was refluxed for 12 hours and the yellow coloured solution was cooled at -4°C and the suspension filtered. The solution

was evaporated under reduced pressure to afford the complex as a yellow/green oil (57%). IR KBr/cm^{-1}: 3413 (m), 2961 (s), 2865 (m), 2664 (w), 1659 (m), 1469 (m), 1383 (s), 1307 (m), 1260 (s), 1232 (s), 1197 (w), 1162 (w), 1077 (s), 1031 (s), 877 (s), 803 (s). UV(Dichloromethane/nm): 424 (log ε 3.38), 309 (3.94), 277 (4.13), 251 (4.44), 202 (5.33). MS m/z APCI: 721.7 $[M+H]^+$(15%), 503.5 $[M-CH_2C_6H_2OH(C_4H_9)_2]^+$(40%),

4.5.2 Synthesis of Cyclen bearing four 2-methoxybenzyl arms and conversion to 2-hydroxybenzyl

1,4,7,10-Tetrakis(2-methoxybenzyl)-1,4,7,10-tetraazacyclododecane dihydrochloride (81)[31].

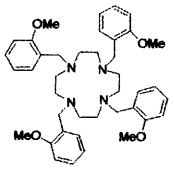

To 1,4,7,10-tetraazacyclododecane (0.3g, 1.74 mmol) and potassium hydroxide (0.42g, 7.49 mmol) dissolved in absolute ethanol (4mls), a solution of 2-methoxybenzylchloride (1.62g, 10.34 mmol) in absolute ethanol (1.25 ml) was added over 2 hrs at 65°C. After complete addition the reaction mixture was kept at 65°C for a further 3hrs, then cooled to room temperature, filtered and the solvent evaporated. The oily residue was dissolved in acetone (20mls), heated to 65°C and the hydrochloride was precipitated by addition of concentrated HCl (0.25mls). The precipitate was filtered, washed with acetone (4mls) and recrystallised from acetone/water/HCl. The pure compound was filtered, washed with acetone, and dried thoroughly to give the compound in 41% yield (0.46g). Free base characterised by NMR: δ_H (400MHz, dimethylsulfoxide): 7.55 (4H, d, *H6*-aromatic, J=7.9), 7.50 (4H, t, *H4*-aromatic, J=6.85), 7.19 (4H, d, *H3*-aromatic, J=7.96), 7.05 (4H, t, *H5*-aromatic, J= 6.98), 4.60 (12H, s, O-C*H*$_3$), 4.25 (8H, s, C*H*$_2$-aromatic), 3.88 (16H, s, C*H*$_2$-N).

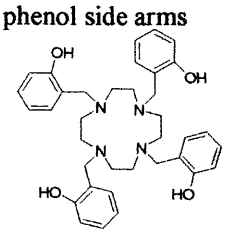

1,4,7,10-Tetrakis(2-hydroxybenzyl)-1,4,7,10-tetraazacyclododecane dihydrochloride (82).[31]

To absolute dichloromethane (10ml), cooled to 0°C and purged with dry nitrogen for 30 minutes, compound **81** (0.416g, 0.638mmol) and BBr_3 (1.18 mls, 14.1 mmol) were added. The reaction mixture was left for 12 hours to reach room temperature, then treated with water (20 mls), concentrated HCl (2mls) and stirred for 1 hr at 50°C. The precipitate was filtered, washed with cold water (4mls) and recrystallised twice from acetone/water/HCl. The pure product was dried at 50°C under high vacuum to afford the title compound as a white solid in 40% yield. IR KBr/cm^{-1}: 3374 (s), 3217 (s), 3003 (w), 2967 (w), 2850 (m), 2714 (w), 2590 (m), 1699 (w), 1652 (w), 1606 (s), 1506 (s), 1458 (s), 1393 (m), 1351 (m), 1259 (s), 1184 (m), 1159 (m), 1109 (s), 1065 (w), 1022 (m), 983 (w), 942 (w), 909 (m), 864 (w), 756 (s), 718 (w). MS m/z ES+: 597.4 $[M+H]^+$ (30%), 491.3 $[M-CH_2C_6H_4OH]^+$ (20%), 385.3 $[M-2CH_2C_6H_4OH]^+$ (35%), 107.1 $[CH_2C_6H_4OH]^+$ (100%).

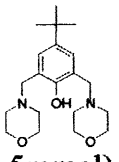

4.5.3 Mannich reaction of 4-tert-butyl phenol with morpholine

2,6-(Bis morpholine)-4-tert-butyl-1-hydroxy xylene (83).

A solution of morpholine (2.55g, 29.3mmol) and paraformaldehyde (0.7g, 13.5mmol) in methanol (50mls) was refluxed for 2hrs. After cooling, 4-*tert*-butylphenol (2g, 13.5mmol) and a few drops of concentrated hyrochloric acid were added and the solution refluxed for a further 3 hrs. After cooling, the solvent was removed to afford the compound as clear oil. δ_H (400MHz, $CDCl_3$): 6.9 (2H, d, J=2.1, *H3*-aromatic, *H5*-aromatic), 3.7 (4H, m, OC*H*), 3.6 (4H, s, Ar-CH_2-N), 2.65 (4H, m, NC*H*), 1.2 (9H, s, CH_3). MS m/z EI+: 348.3 $[M+H]^+$ (10%), 261.2 $[M-C_4H_8NO]^+$ (30%), 86.1

$[C_4H_8NO]^+$ (100%). m/z CI: 349.3 $[M+H]^+$ (60%), 250.2 $[M-CH_2C_4H_8NO]^+$ (100%), 88.1 $[C_4H_8NO]^+$ (30%).

4.5.4 Synthesis and Complexation of an Unsymmetrical Porphyrin bearing a phenol group

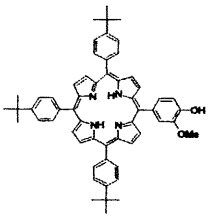

5,10,15-Tris(4-*tert*-butylphenyl)-20-(4-hydroxy-5-methoxy phenyl)porphyrin (84).

A mixture of 4-*tert*-butylbenzaldehyde (21.32g, 0.13mol), vanillin (1g, 6.57mmol) and pyrrole (8.38g, 0.12mol) were refluxed in propionic acid (167mls) for 30 mins. After cooling, the purple solid was filtered (glass fibre filter paper) and pre-columned on silica (chloroform to elute tetra substituted and then chloroform/methanol to elute mono substituted) followed by preparative plate chromatography on a silica (dichloromethane/hexane 3:1) to yield the title compound as a purple solid (0.75g, 3%). δ_H ($CDCl_3$): 8.70-8.78 (8H, m, *pyrrole H*); 8.10 (6H, d, J=7.33, Ar *H2* + *H6*); 7.75 (6H, d, J=9.58, Ar *H3* + *H5*); 7.74 (2H, m, vanillin *H*); 7.26 (1H, d, J=8.54, vanillin *H*); 5.91 (1H, s, O*H*); 3.94 (3H, s, OCH_3); 1.55 (27H, s, C(CH_3)$_3$); -2.86 (2H, s, NH_{int}). δc 149.41, 144.40, 143.78, 138.13, 133.46, 133.42, 133.35, 127.11, 122.56, 119.15, 118.66, 116.66, 111.67, 55.14, 35.46, 33.86, 30.66, 30.39. IR KBr/cm^{-1}: 3436 (s), 3336 (w), 3028 (w), 2960 (s), 2907 (w), 2873 (w), 1651 (m), 1559 (m), 1503 (s), 1473 (m), 1416 (w), 1400 (w), 1386 (w), 1363 (w), 1347 (w), 1416 (s), 1231 (w), 1198 (w), 1099 (s), 1023 (s), 972 (s), 668 (s). UV(dichloromethane)/nm: 686 (log ε 2.9), 650 (log ε 3.02), 594 (log ε 3.07), 556 (log ε 3.32), 522 (log ε 3.52), 424 (log ε 4.86). MS m/z (FAB): 829.4 $[M+H]^+$ (50%).

Zinc (II) 5,10,15-tris(4-*tert*-butylphenyl)-20-(4-hydroxy 5-methoxy phenyl)porphyrin (85).

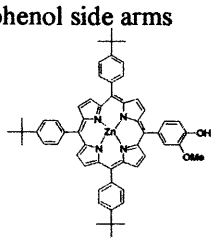

A solution of **84** (0.075g, 9.05mmol) and zinc (II) acetate dihydrate (0.02g, 9.05mmol) in dimethylformamide (10mls) was refluxed for 3 hrs. Water (12mls) was added and the precipitate filtered and washed with water, methanol and acetone. The residue was dissolved in chloroform and filtered. Methanol was added and the volume reduced to precipitate the product. Filtration gave the title compound (0.072g, 90%) as a bright purple coloured solid. δ_H ($CDCl_3$): 8.9-8.95 (8H, m, *pyrrole H*); 8.10 (6H, d, J=7.33, Ar *H2* + *H6*); 7.75 (6H, d, J=9.58, Ar *H3* + *H5*); 7.74 (2H, m, vanillin *H*); 7.26 (1H, d, J=7.88, vanillin *H*); 5.91 (1H, s, O*H*); 3.90 (3H, s, OCH_3); 1.55 (27H, s, C(CH_3)$_3$). IR KBr/cm^{-1}: 3440 (s), 3035 (w), 2963 (s), 2903 (w), 2359 (s), 2353 (m), 1648 (w), 1448 (w), 1409 (w), 1361 (w), 1338 (w), 1260 (s), 1093 (s), 1018 (s), 864 (s), 797 (s), 702 (m), 664 (w). UV(dichloromethane)/nm: 686 (log ε 2.55), 588 (log ε 3.44), 550 (log ε 2.91), 424 (log ε 4.80). MS m/z ES+: 891.4 $[M+H]^+$ (10%), 63.1 $[C_4HN]^+$ (100%).

4.5.5 Synthesis of 5-Iodovanillin and its symmetrical Porphyrin

5-Iodovanillin (86).[33]

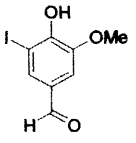

To a solution of vanillin (1g, 6.57mmol) and sodium iodide (1.18g, 7.89mmol) in dimethylformamide (30mls) at 25°C was added chloramine T trihydrate (2.22g, 7.89mmol). The mixture was stirred for 1 hr. The product was diluted with water, acidified with 5% hydrochloric acid solution and extracted with ethyl acetate. The organic solution was washed successively with 5% sodium thiosulphate solution and brine and was dried over anhydrous magnesium sulphate. The crude product was crystallised from ethyl acetate to afford 5-iodovanillin as a cream solid (1.81g, 98%).

δ_H (400MHz, $CDCl_3$): 9.7 (1H, s, C*H*O) ; 7.80 (1H, s, C-6 *H*); 7.3 (1H, s, C-2 *H*); 6.65 (1H, s, O*H*); 3.91 (3H, s, OCH_3). δc 188.60, 150.38, 145.46, 135.19, 130.00, 128.70, 125.43, 107.56, 55.50. IR KBr/cm^{-1}: 3171 (s,b), 3003 (m), 2850 (m), 1719 (s), 1668 (s), 1587 (s), 1570 (m), 1489 (s), 1461 (s), 1417 (s), 1352 (s), 1295 (s), 1260 (s), 1161 (s), 1140 (s), 1098 (w), 1039 (s), 854 (s), 784 (s) and 668 (s).

Meso-5,10,15,20-tetra(5-iodo-4-hydroxy-3-methoxy phenyl) porphyrin (87).

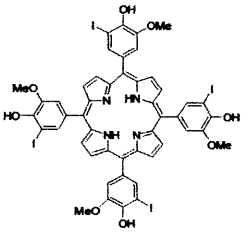

A mixture of 5-iodovanillin (**86**) (4g, 14.30mmol) and pyrrole (0.897g, 13.37mmol) were refluxed for 30 minutes in propionic acid (18mls) followed by cooling for 12hrs at 4°C. The purple solid was filtered (glass fibre filter paper), pre-columned on silica ($CHCl_3$ 99%, MeOH 1%) and dried under vacuum to yield the title compound as a purple solid. δ_H (400MHz, $CDCl_3$): 8.86 (8H, s, pyrrole *H*); 8.12 (4H, s, C-6 *H*); 7.65 (4H, s, C-2 *H*); 6.35 (4H, s, O*H*); 3.94 (12H, s, OCH_3); -2.88 (2H, s, N*H*). δ_C 144.76, 143.16, 135.46, 134.56, 117.66, 116.48, 55.54. UV/nm: 659 (log ε 2.96), 594 (log ε 3.04), 556 (log ε 3.21), 520 (log ε 3.48), 426 (log ε 4.80). MS m/z FAB: 1300.4 $[M]^+$ (40%).

Zinc (II) meso-5,10,15,20-tetra(5-iodo-4-hydroxy-3-methoxy phenyl) porphyrin (88).

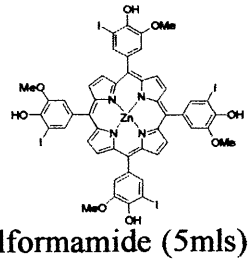

To a solution of compound **87** (0,1021g, 0.0913mmol) in dimethylformamide (5mls) was added zinc (II) acetate dihydrate (0.2g, 0.913mmol) and the mixture refluxed for 3hrs. After cooling at room temperature, water (7mls) was added and the precipitate filtered and washed with water, methanol and acetone. The purple residue was dissolved in the minimum amount of chloroform, filtered and a little methanol was

added to the purple solution. After reducing the volume of the solvent, the solution was cooled at 4°C to crash out the product as a purple solid. The solid was filtered and dried under vacuum to give the title compound (0.105g, 97%). δ_H (400MHz, $CDCl_3$) 8.9 (8H, s, pyrrole *H*); 8.1 (4H, s, C-6 *H*); 7.6 (4H, s, C-2 *H*); 6.4 (4H, s, O*H*); 3.9 (12H, s, OCH_3). δ_C 161.36, 149.26, 144.49, 142.99, 135.39, 130.95, 116.42, 55.50, 35.44, 30.32, 28.68. UV(dichloromethane)/nm: 550, 426. MS m/z MALDI: 1363.8 $[M]^+$ (100%), 1237.9 $[M\text{-}C6H_3OHOCH_3]^+$ (90%), 1114.0 $[M\text{-}4C_4H_9\text{-}OH]^+$.

4.6 Results and discussion

4.6.1 Synthesis and attempted synthesis of novel phenol ligands and their complexes

The first Mannich reaction carried out was between 1 equivalent of cyclen and 4 equivalents of 2,4-di-*tert*-butylphenol to form compound **74** as illustrated in figure 4.13**A**. Analogous reactions have been carried out by Wieghardt and co-workers[1-6] using tacn as the macrocycle.

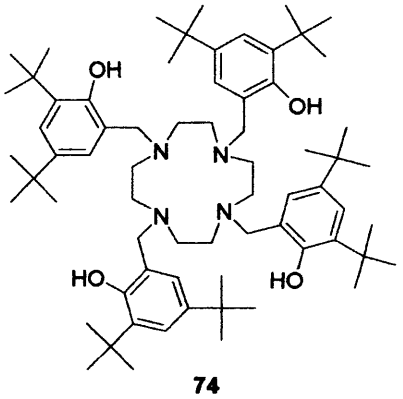

74

Reagents and conditions: Cyclen and paraformaldehyde refluxed for 2 hr in MeOH. 2,4-Di-tert butyl phenol and HCl added and further 3 hr reflux. Recrystallisation in MeCN.

Figure 4.13**A**: 1,4,7,10-Tetrakis(3,5-di-tert-butyl-2-hydroxybenzyl)-1,4,7,10-tetraazacyclododecane (**74**).

The structure of **74** was assigned by ^{1}H-NMR and IR spectroscopy in addition to mass spectrometry. Two doublets at 7.12 and 6.65 ppm in the proton NMR spectrum confirmed that one of the three original aromatic protons of the phenol had been substituted and the proton removed. The singlet appearing at 3.57 ppm (8 protons) represents the CH_2 groups linking the phenol pendant arms with cyclen. The protons of the cyclen macrocycle are represented by a singlet since it is substituted in all four positions by identical groups. This singlet occurs in the spectrum at 2.77 ppm and the remaining *tert*-butyl groups at 1.3 and 1.18 ppm. It is noteworthy that the phenol protons appear as a broad singlet at 9.8 ppm in the spectrum.

Infrared absorptions at 3507(m,b), 2962(s) and 2907(m) cm^{-1} relate to the O-H and C-H groups respectively. Confirmation of the structure was given by the mass spectrum (ES+) which shows the parent ion at 1045 m/z (90%) along with a further peak arsing at 827.6 m/z (100%) owing to a fragment of the parent ion which has only 3 of the pendant arms.

Single crystals of compound **74** were obtained by slow evaporation of an acetonitrile solution of the compound. The crystal structure is shown in figure 4.13**B.**

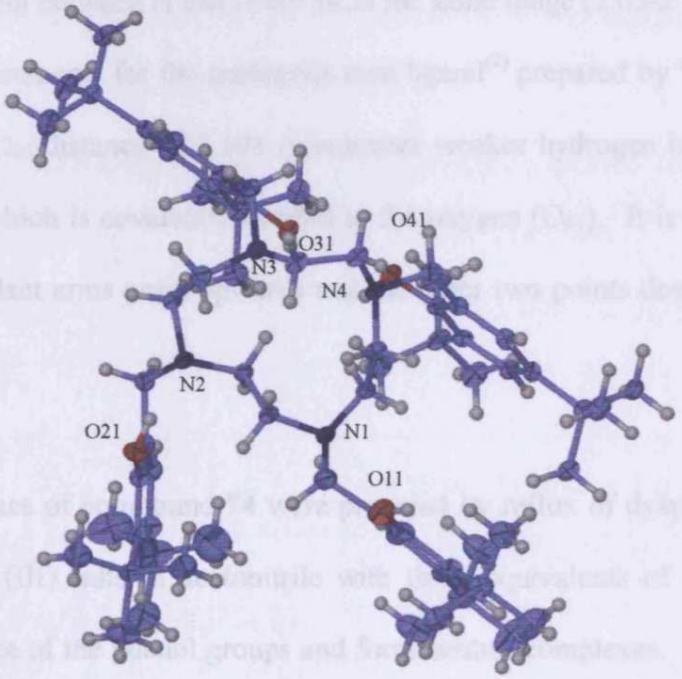

Figure 4.13**B**: Crystal structure of 1,4,7,10-Tetrakis(3,5-di-tert-butyl-2-hydroxybenzyl)-1,4,7,10-tetraazacyclododecane (**74**).

The structure unequivocally proves that compound **74** is 1,4,7,10-tetrakis(3,5-di-tert-butyl-2-hydroxybenzyl)-1,4,7,10-tetraazacyclododecane and it is evident from the data that intramolecular hydrogen bonding exists in the structure between N and H-O. The contact length for each N-H-O bond is shown in table 4.2.

Nn-On	Contact length (Å)
N_3-O_{31}	2.724 (5)
N_2-O_{21}	2.742 (4)
N_1-O_{11}	2.659 (5)
N_4-O_{41}	3.108 (5)

Table 4.2: Contact length of N-O in structure of compound **74**

The contact lengths for the N_1, N_2 and N_3 to oxygen distances arising from hydrogen bonding between N and H are all in the same range (2.65-2.75 Å) and are in line with measurements for the analogous tacn ligand[2] prepared by Wieghardt. The anomalous N_4-O_{41} distance of 3.108 Å indicates weaker hydrogen bonding between the N_4 and H which is covalently bonded to the oxygen (O_{41}). It is noteworthy that two of the pendant arms point upwards and the other two points downwards in a cis arrangement.

Complexes of compound **74** were prepared by reflux of dysprosium, terbium and lanthanum (III) salts in acetonitrile with three equivalents of triethylamine to deprotonate three of the phenol groups and form neutral complexes. The dysprosium complex (**75**) was characterised by IR spectroscopy. No sharp absorptions were observed for the O-H which would imply that deprotonation has in fact taken place to give the phenolate. However, the IR spectrum of ligand **74** does not actually show a sharp absorption for the O-H. It is rather broad and it is therefore difficult to use this absorption to tell us whether deprotonation of the phenol has occurred. Results obtained from the mass spectrum confirmed the presence of the parent ion of **75** at 1206.7 m/z and a smaller peak also occurs at 1045.8 m/z owing to the free ligand **74**. The isotope pattern is in line with the proposed complex.

The mass spectrum of the terbium complex **76** confirmed that complexation with terbium had occurred since the main peak arises at 1201.7 m/z which represents the parent ion of **76**. The isotope pattern observed is again in line with the complex. Attempts at preparing the europium complex of **74** using europium chloride and europium perchlorate showed the products of the reactions to be free ligand. Production of the lanthanum complex **77** was confirmed via FAB mass spectrometry, showing the presence of a peak at 1181.7 m/z corresponding to the parent ion. The ^{1}H-NMR of **77** displayed a slight shift compared with the free ligand. The zinc (II) complex **78** was also prepared, the characterisation following similar trends to **75-77** and the UV data for **74-78** is shown in table 4.3.

Compound/complex	λ_{max}[nm] (Log ε[Lmol^{-1}cm^{-1}])
74	282(3.67), 234 (3.94)
75	421 (3.38), 278 (4.15), 234 (4.58)
76	421 (2.72), 282 (3.75), 234 (3.98)
77	418 (2.98), 341 (3.25), 272 (4.02), 233 (4.20)
78	421 (3.01), 283 (3.85), 234 (4.06)

Table 4.3:UV data of **74-78** in dichloromethane

Clearly, complexes **75-78** display enhanced extinction coefficients compared with ligand **74.** The transitions shown at approximately 230 and 280 nm correspond to two π-π^* transitions of the phenol pendant arms as seen for the free ligand **74**, implying that at least one of the O-H bonds remains upon complexation with the metals. Wieghardt's analogous tacn ligand and its complexes show a shift from 230 and 280nm to 250 and 300nm upon coordination with Ga, Sc, Fe (III) and Mn (IV) due to formation of the phenolate. In contrast, the absorptions for complexes **75-78**

do not undergo a similar shift upon complexation suggesting that deprotonation of the phenol groups has not occurred. Coordination of one, two, three or four of the phenol groups to the metal centre is therefore likely to be the case for the above complexes since there is no indication of phenolate species. It may be the case that the phenolate species has indeed formed but has later been protonated as was the case for the analogous zinc tacn complex prepared by Wieghardt.[3] For complexes **75-78**, there appears to be an extra absorption present at 420 nm (and at 341 nm for **77**). Wieghardt has reported the presence of two intense transitions between 390 and 430 nm and a further one of lower intensity at 600-800 nm owing to phenoxyl radicals. [2] As we only observe one (or two) band for each complex in this region of the UV, instead of three as reported by Wieghardt, it is a possibility in this instance that the transition is a result of ligand to metal charge transfer from the oxygen lone pair to the metal centre as we did not generate the oxidised forms of the complexes as Wieghardt did.

To this end, as far as the UV absorption properties are concerned, complexation of ligand **74** to Dy(III), Tb(III), La(III) and Zn(II) produces increases in the extinction coefficients of the ligand making it a more efficient antennae. The dysprosium complex **75** appears to display the greatest degree of absorption, followed by lanthanum, zinc and finally terbium. Numerous attempts at growing crystals of **75-78** were unsuccessful.

The Mannich reaction described for the synthesis of compound **74** was also used to prepare 1,8-dimethyl-4,11-(3,5-di-tert-butyl-2-hydroxybenzyl)-1,4,8,11-tetraazacyclotetradecane (**79**). The product was afforded from the reaction in 58%

yield which is much improved compared with compound **74** (19%), since chromatography was not required in this instance. Compound **79** was characterised by ^{1}H-NMR, IR spectroscopy and mass spectrometry as follows. Again, two doublets in the aromatic region at 7.1 and 6.7 ppm indicated that the carbon adjacent to the hydroxy group had undergone substitution as anticipated. The singlet at 3.97 ppm representing 4 protons refers to the CH_2 groups linking the macrocycle and phenols. The protons of the tetraazacyclotetradecane (cyclam) macrocycle are shown by a series of multiplets in the region 2.4-3.2 ppm and represent a total of 20 protons. Finally, the presence of a singlet at 2.05 ppm representing 6 protons corresponds to the methyl groups attached to two of the nitrogens, and the t-butyl groups are shown at 1.4 and 1.15 ppm. Again, the phenol protons (2H) appear as a broad singlet at 9.9 ppm.

The IR spectrum closely resembles that of compound **74** with the characteristic O-H and C-H absorptions appearing at 3427 cm^{-1}, 2960 and 2789 cm^{-1} respectively. Confirmation that the compound had been formed was obtained from the mass spectrum (ES+) which shows the major peak at 665.66 m/z (100%) corresponding to the mass of the parent ion of **79.**

Since ligand **79** has 4 nitrogen donors and 2 potential oxygen donors, a metal requiring six coordination sites is preferable for complexation, typically a transition metal. Complexation was achieved by reflux of compound **79** with nickel (II) nitrate hexahydrate in ethanol with two equivalents of triethylamine to afford the green coloured complex **80**. The IR spectrum suggests that the phenolate species has been formed since there is no indication of the NO_3 absorption which would be present to

balance out the positive charge of the nickel if the phenolate was not present. Nickel, which prefers a coordination number of six has therefore formed 4 bonds with the nitrogens and 2 others with the oxygens. The UV displays a total of 5 absorptions ranging from 202 to 424 nm, compared with 2 absorptions for ligand **79.** Again, increased extinction coefficients demonstrate that complexation with Ni(II) makes ligand **79** a more efficient antennae. Compared with ligand **74** and its complexes, the π-π^* transitions for the phenol pendant arms for the nickel compex **80** appear to have shifted considerably compared with the free ligand **79**. The shift from 234 and 282 nm to 251 and 309 appears to have occurred. This suggests that deprotonation of the phenol groups using triethylamine has taken place in this instance to give the phenolate species. Presence of the phenolate gives rise to the absorptions at 251 and 309 nm, as is the case for the complexes of the tacn analogue prepared by Wieghardt.[2] Again the extra absorption at 420nm is likely to be a result of ligand to metal charge transfer. The mass spectrum carried out verifies that the nickel complex is formed since the peak at 721.7 m/z corresponds to the parent ion.

4.6.2 Preparation of 1,4,7,10-tetrakis(2-hydroxylbenzyl)-1,4,7,10-tetraazacyclododecane

In order to assess the yields of the Mannich reactions above and have a compound with which we could compare ligand **74,** it was decided to prepare 1,4,7,10-tetrakis(2-hydroxylbenzyl)-1,4,7,10-tetraazacyclododecane (**82**). Following the method of Kaden[31], 1,4,7,10-tetrakis (2-methoxybenzyl)-1,4,7,10-tetraazacyclododecane dihydrochloride (**81**) was prepared. The ^{1}H-NMR data of the free base is in line with the data reported by Kaden and co-workers. Conversion of the methoxybenzyl to hydroxybenzyl groups is shown in figure 4.14.[31] The product

1,4,7,10-tetrakis(2-hydroxylbenzyl)-1,4,7,10-tetraazacyclododecane dihydrochloride (**82**) was afforded in 40% yield and characterisation was again in line with existing data. The mass spectrum confirmed the identity of the compound as a result of the peak arising at 597.4 m/z which corresponds to the mass of the parent ion **82**.

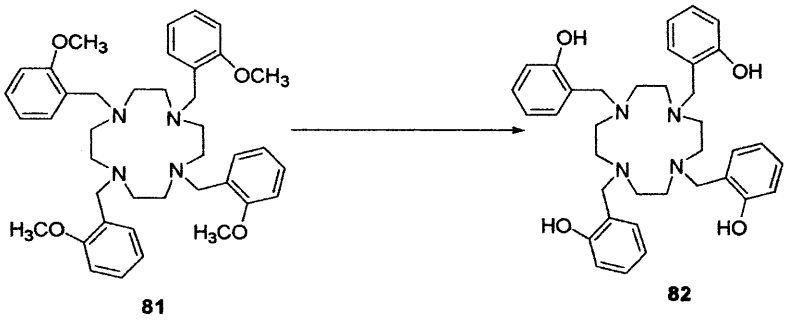

81 **82**

Reagents and conditions: Left at 0°C in CH_2Cl_2 purged with N_2 with BBr_3 for 12 hours to reach room temp. Treated with H_2O and HCl and stirred 2hrs at 50°C.

Figure 4.14: Conversion of methoxy to hydroxyl groups

The method for preparation of ligand **82** involves a 2 stage synthesis affording the product in 40% yield, whereas the Mannich reaction affords ligand **74** in 19% yield but is a quick 1 step reaction. An improved yield of 58% was observed for 1,8-dimethyl-4,11-(2,4-di-tert-butylphenol)-1,4,8,11-tetraazacyclotetradecane (**79**) since there are only 2 positions for the reaction to occur. An attempt to prepare the europium (III) complex of **82** was made, however results showed that the white precipitate afforded was ligand.

4.6.3 Attempted Mannich reaction with Cyclen and alternative phenol and naphthol derivatives

Due to the success encountered using 2,4-di-*tert*-butylphenol in the Mannich reaction, we were interested to see how other phenol and naphthol groups would react under the same conditions. Therefore, using cyclen and the appropriate phenol or

napthol groups, the synthesis of the functionalised cyclen macrocycles shown in figure 4.15 were attempted.

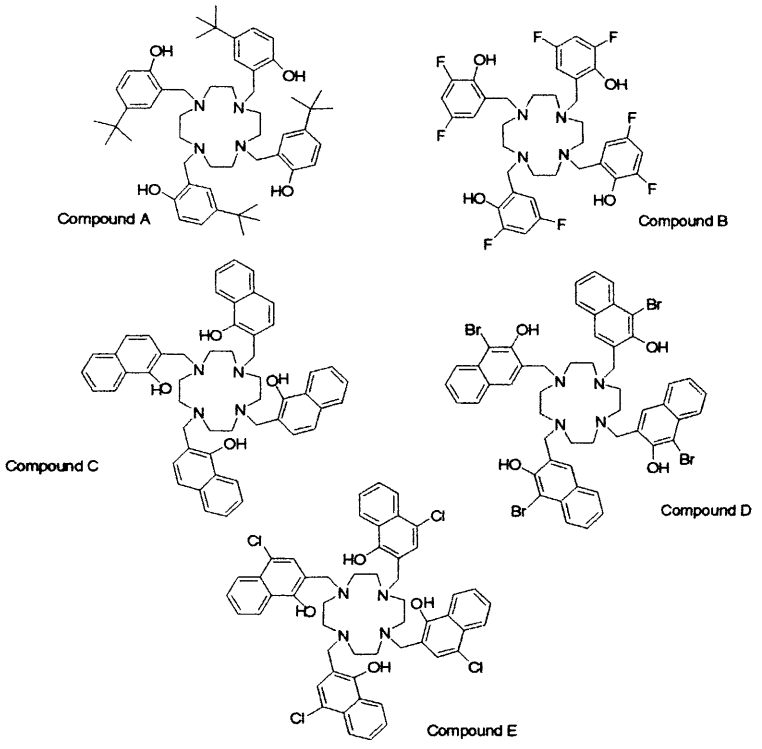

Figure 4.15: Ligands attempted via the Mannich reaction.

Analysis of the products by TLC and ^{1}H-NMR spectroscopy showed that in each case, the Mannich reaction did not occur to any detectable level as the isolated reaction mixtures were found to be starting materials. Steric effects of the t-butyl and fluorides in compounds **A** and **B** may be eliminated as possible causes for preventing reaction since we have shown that the reaction occurs using 2,4-di-tert-butyl phenol. Therefore, electronic effects must be the reason for no reaction taking place in these cases. In order to investigate the reasons for the lack of reaction in forming compound **A**, the same procedure was carried out using 4-*tert*-butylphenol and 2 equivalents of morpholine to form 2,6-(bis morpholine)-4-*tert*-butyl-1-hydroxyxylene **(83).** Formation of compound **83** would imply that the lack of reaction in the case of

the cyclen analogue is due to the lack of reactivity of the cyclen rather than the phenol. This reaction is shown in figure 4.16.

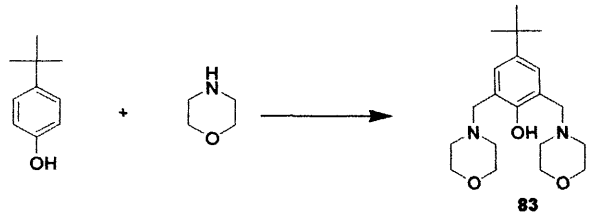

83

Figure 4.16: Mannich reaction to prepare compound **83**. Reagents and conditions: Morpholine and paraformaldehyde refluxed for 2hr in MeOH. 4-Tert butyl phenol and HCl added. Further 3hr reflux.

The ^{1}H-NMR spectrum of compound **83** showed the presence of some starting material 4-*tert*-butylphenol however there was strong indication that compound **83** had been formed. Once a mass spectrum of the compound (EI/CI) had been completed, the presence of the target compound 2,6-(bis morpholine)-4-*tert*-butyl-1-hydroxyxylene (**83**) was confirmed by the peak at 349.3 m/z (60%) in addition to another at 250.2 m/z which represents the mono-substituted by-product (100%). Since there are two possible positions at which the Mannich reaction can occur for the 4-tert-butylphenol as shown for compound **83**, reaction has taken place at both the 2 and 6 positions forming the di-morpholine compound linked by the phenol. Although this possibility also exists in forming the cyclen compound **A,** it clearly is not the case. The cyclen and phenol are in fact under reacting. The possible explanations for this is the stability of the cyclen intermediate (discussed further on) and lack of reactivity of the phenol due to the absence of a *tert*-butyl phenol group in the ortho position. This is also the case when attempting to form compounds **B-E**.

The presence of the electron withdrawing groups (F^-, Cl^- and Br^-) on the phenol make the position ortho to the hydroxyl group less electron rich, hence a weaker nucleophile and less inclined to attack the positively charged immonium ion

formed from reaction of the amine and paraformaldehyde as shown in figure 4.17. Therefore in terms of inductive effects, the presence of halogens in the ortho and para positions deactivate the reactivity of the phenol as they are strongly electron withdrawing and this is why the Mannich reaction is less likely to place for these substituents. It is noteworthy that in terms of resonance effects, halogens are weakly electron donating, however in this instance it seems as though the inductive effect has the greater influence. The analogous tacn ligands reported by Wieghardt bear *tert*-butyl or methoxy or methyl groups ortho and para to the hydroxyl group.[1-6] Based on inductive effects, the *tert*-butyl groups are electron donating hence increase the electron density and the nucleophilicity of the aromatic ring. This, together with our results for compounds **A-E**, shows that a *tert*-butyl group which is inductively more electron-releasing than a halogen is likely to increase the probability of the Mannich reaction taking place.

However, several reports are found where Mannich reactions do occur where the phenol compounds do not possess groups other than hydrogen adjacent to the hydroxy group.[36, 37] These reactions use alternative conditions to those we have used and they also use simpler amines such as morpholine, unlike cyclen which we are investigating. A bis tacn compound bearing two 4-hydroxy-1,10-phenanthrolin-3-yl methyl groups has been reported by Wieghardt.[7] Again, the groups adjacent to the hydroxyl are hydrogen, showing that tert-butyl groups at the ortho position are not essential. However the reaction conditions used differ to those utilised by us. Toluene is used as the solvent and no HCl catalyst was added in contrast to our preparations involving reflux in acetonitrile using HCl catalyst. It may therefore be

the case that using alternative conditions may aid nucleophilic attack of the immonium ion and yield the target compounds **A-E**.

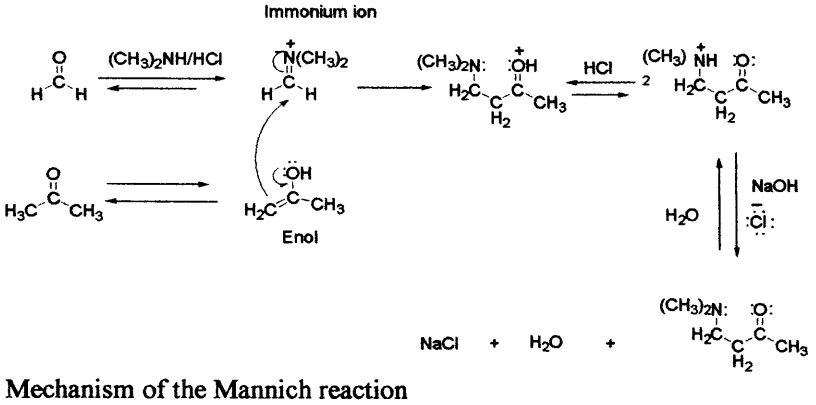

Figure 4.17: Mechanism of the Mannich reaction

Another factor determining the feasibility of the Mannich reaction is the stability of the positively charged cyclen intermediate of the Mannich reaction shown in figure 4.18. During the initial stage of the reaction, cyclen and paraformaldehyde react to form an immonium ion intermediate as shown in figure 4.17. Each of the nitrogen groups in turn should form an immonium ion and react with the corresponding phenol/naphthol group. It may be the case that the intermediate is relatively stable so that it requires a fairly reactive phenol species to form the Mannich product. If the nucleophilicity of the phenol is not sufficient, the reaction with the immonium ion will not occur. To this end, the success of the Mannich reaction is a compromise between the reactivity of the phenol/naphthol and the stability of the cyclen intermediate. If both are favourable, then the reaction is likely to occur. However, in the above cases it seems to be the case that the phenols were not reactive enough without the presence of the *tert*-butyl group in the ortho position.

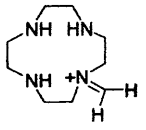

Figure 4.18: Possible stable intermediate of the Mannich reaction

4.6.4 Attempted Mannich reaction of cyclen and zinc (II) 5,10,15-tris(tert-butylphenyl)-20-(4-hydroxy 5-methoxy phenyl)porphyrin(85)

The synthesis of the cyclen-tetraporphyrin system **89** (Aims and objectives) was attempted by carrying out a Mannich reaction using 1 equivalent of cyclen and 4 equivalents of porphyrin. The first stage in this process was the synthesis of the porphyrin **84** shown in figure 4.19, accomplished using the Adler-Longo[34] method.

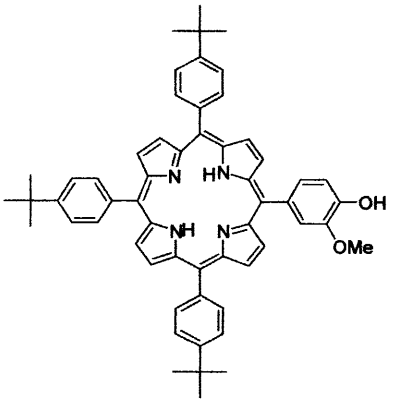

84

Figure 4.19: 5,10,15-Tris(tert-butylbenzaldehyde)-20-(vanillin)porphyrin **(84)**.

After the 30 minute reflux the purple solid was pre-columned on silica gel ($CHCl_3$:MeOH 95:5) to remove polymeric impurities. TLC analysis on silica (CH_2Cl_2/Hexane 75:25) showed the symmetric A_4 porphyrin which is the major product to have an R_f of 0.9, whilst the asymmetric A_3B porphyrin had an R_f of 0.4. The asymmetric porphyrin 5,10,15-tris(4-*tert*-butylphenyl)-20-(4-hydroxy 5-methoxy phenyl)porphyrin (**84**) was purified by column chromatography on silica gel (dichloromethane/hexane 75:25) followed by preparative plate chromatography. The target porphyrin **84** was afforded in 3% yield, which is reasonable for an A_3B substituted porphyrin. The ^{1}H-NMR spectrum of compound **84** demonstrates that it is A_3B substituted since there are 4 aromatic peaks apparent in the spectrum not including the set of peaks for the pyrrole external protons at 8.70-8.75 ppm. A total of

three peaks (including one for the pyrrole) would be observed in this region of the spectrum for the symmetrical porphyrin. The doublets at 8.10 and 7.75 ppm represent the aromatic protons of the *tert*-butyl phenyl whilst the multiplets at 7.74 and 7.26 ppm refer to the aromatic protons on the 4-hydroxy 5-methoxy phenyl group. Furthermore the singlet at 5.91 ppm corresponds to the OH group, the singlet at 3.94 ppm signifies the methoxy function and the large singlet at 1.55ppm represents the *tert*-butyl groups. Finally, the free base porphyrin **84** is confirmed by a singlet integrating to 2 protons occurring at -2.86 ppm.

The IR spectrum supports the results obtained from the ^{1}H-NMR. The broad absorption located at 3436 cm^{-1} demonstrates the presence of the O-H stretch in the compound. The weak absorptions at 3028 and 3336 cm^{-1} clarify the presence of the C-H (aromatic group) and the N-H bond respectively. A strong absorption which occurs at 2960 cm^{-1} in this spectrum demonstrates the presence of the alkyl groups within this structure. Peaks at 1559 and 1503 cm^{-1} correspond to the carbon-carbon bonds of an aromatic ring and finally the strong C-O absorption shown at 1099 cm^{-1} confirms the presence of the OMe fragment within the compound. It is also noteworthy that there is no indication of any aldehyde being present within the structure as there are no absorptions in the region 1680-1750 cm^{-1}. The UV spectrum of the compound under discussion is typical of a porphyrin, demonstrating the Soret absorption at 424nm and the others at 522, 556, 594, 650 and 686 nm. The structure was confirmed by after carrying out a FAB mass spectrum which showed the main peak occurred at 829.4 m/z which corresponds to the parent ion of **84**.

Conversion of compound **84** to metallated **85** was achieved by refluxing with an excess of zinc (II) acetate as described in chapter 3 to afford the bright pink/purple compound in 90% yield. The ^{1}H-NMR showed very little change compared to the free-base porphyrin with the exception of a slight downfield shift of the external pyrrole protons from 8.70-8.75 ppm to 8.9-8.95 ppm and the disappearance of the broadened singlet at -2.86 ppm representing the internal pyrrole protons. Clearly, the Zn has replaced both protons which gave rise to the latter peak so that it disappears from the spectrum of **85**. The N-H absorption does not appear in the IR spectrum of compound **85** clarifying the metallation of the porphyrin has occurred. The UV spectrum for the complex **85** is very similar to the free-base porphyrin. The Soret band again appears at 424 nm showing no change from **84**. There are fewer absorptions in the region 500-700 nm than there are for the free-base porphyrin. This is in line with results from chapter 3. ES+ mass spectrometry was carried out on the sample and this confirmed the proposed structure was correct since a peak arises at 891.4 m/z which is in line with the mass of the parent ion.

This led on to the attempted Mannich reaction utilising 4 equivalents of **85** and 1 equivalent of cyclen in order to prepare compound **89**. TLC investigation on a silica plate (dichloromethane/hexane 3:1) proved that a new compound had formed which had an R_f value 0.84, being different to that of compound **85** which was 0.68. When analysed it was found that there was a shift in the ^{1}H-NMR compared with compound **85** however the absence of cyclen was apparent. Low resolution MALDI mass spectrometry showed that the sample was not compound **89**. The mass shown was in fact 828.4 m/z (100%) which corresponds to 5,10,15-tris(*tert*-butylphenyl)-20-(4-hydroxy 5-methoxy phenyl)porphyrin (**84**). Hence not only did the Mannich

reaction not occur, but it appears as though the porphyrin has been de-metallated in the process probably due to the use of HCl in the reaction.

The reaction was repeated using dimethylformamide as the solvent in order to aid solubility of the reactants. After the initial 2 hour reflux between cyclen and paraforaldehyde, porphyrin and HCl were added and a further 6 hour reflux was undertaken to try to force the reaction to occur. The product was studied by TLC in the same way as the previous attempt and was found to possess the same R_f as **85**. The ^{1}H-NMR spectrum of the product showed similarities to compound **85** however there was also some indication of the presence of cyclen and the methyl linker. A UV spectrum for the compound was carried out which showed three absorptions at 588, 550 and 424 nm implying the compound was **85**. To clarify these results, a mass spectrum (MALDI) of the compound was carried out. It was considered that the 4-hydroxy-5-methoxy group of the porphyrin **85** may be reacting with the paraformaldehyde to form an analogue of compound **85** with a CH_2OH functional group adjacent to the hydroxyl group.[35] This of course is an undesirable reaction. Mass spectrometry results proved that the latter hypothesis was not the case since results showed the main mass at 753.3 m/z and this corresponds to a fragment of compound **84**. Additionally, a further peak observed at 890.4 m/z (27%) is in line with the structure of compound **85** (zinc porphyrin).

4.6.5 Mannich reaction of cyclen and vanillin

It therefore appears that the Mannich reaction between cyclen and porphyrin does not occur to form compound **89**. It may be the case that the steric hindrance of the porphyrin molecules prevents the reaction. Therefore it was decided to attempt to

prepare the porphyrin-cyclen system **89** via a 2 stage synthesis. Our aim was to carry out a Mannich reaction of cyclen with 4 equivalents of vanillin to form compound **90** shown in figure 4.20, followed by the Adler-Longo reaction of the benzaldehydes to build 4 porphyrin molecules onto the structure.

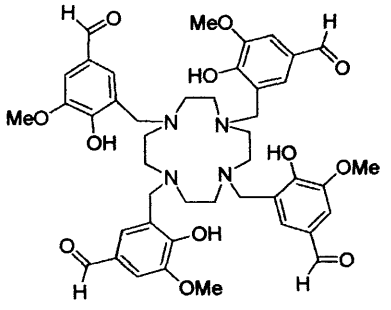

90

Figure 4.20: Target compound **90**

Prior to the Mannich reaction of cyclen with vanillin, a test reaction between 2 equivalents of vanillin and 1 equivalent of homopiperazine was attempted. As there appeared to be a substantial amount of vanillin present when analysed by TLC (chloroform/methanol 95:5), the compound was heated on the Kughelrohr distillation apparatus for a few hours to attempt to remove the starting material from the product. The ^{1}H-NMR spectrum of this compound indicated that a substantial amount of vanillin was still present however there also appeared to be multiple peaks in the region 2.8-4.0 ppm (homopiperazine) and it was thought that there may be a mixture of starting materials, mono-substituted and di-substituted product. Mass spectrometry (ES) confirmed there was a mixture of mono and di-substituted products due to the presence of peaks at 277.1 and 429.2 m/z respectively. Further fragments of vanillin were also apparent in the spectrum at 113 and 165 m/z owing to the presence of unreacted starting material.

Since the previous reaction had shown a certain degree of success arising from occurrence of the target compound in the mass spectrum, the synthesis of compound **90** was attempted. Following a three hour reflux, the TLC ($CHCl_3$) on a silica plate showed that a substantial amount of vanillin still remained in the reaction mixture therefore the reflux was continued for a further twelve hours. Further analysis by TLC showed that the majority of compound was vanillin, however a trace of product was apparent on the baseline of the plate. Following another 24 hr reflux period, the solution was cooled, followed by addition of large aliquots of diethyl ether. Upon cooling, a cream solid precipitate was formed and was then filtered. A series of small peaks in the ^{1}H-NMR of the precipitate suggested a mixture of vanillin containing compounds. However, the majority of the reaction mixture appeared to be vanillin. Mass spectrometry indicated extremely weak signals for mono, di and tri substituted analogues of compound **90** and more intense signals for vanillin and its fragments.

4.7 Preparation and use of 5-iodovanillin

It was considered that another method was necessary to prepare a cyclen tetraporphyrin array in which each porphyrin carries a phenol functional group. Use of the Mannich reaction is not essential as it is possible to link the cyclen and the porphyrin using a variety of reactions. We have considered the use of the Sonogashira[38] reaction as discussed in chapter 3.

The conversion of vanillin to 5-iodovanillin (**86**) in 98% yield has been achieved here following the method developed by Watt, Ji and Kometani[33] as demonstrated in figure 4.21. The ^{1}H-NMR spectrum was in accord with the reported data and the IR spectrum also suggested the vanillin had been converted to **86** since there was a shift in the overall spectrum and the presence of a strong absorption at 668 cm^{-1} demonstrates the presence of C-I bonds.

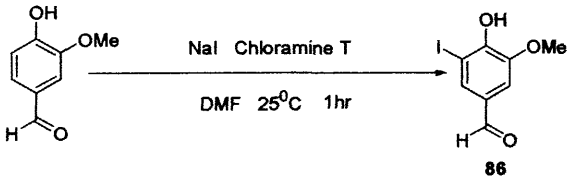

Figure 4.21: Conversion of vanillin to 5-iodovanillin (**86**)

The 5-iodovanillin was used to prepare *meso*-5,10,15,20-tetra(5-iodo 4-hydroxy 3-methoxy phenyl) porphyrin (**87**) shown in figure 4.22 following the Adler-Longo synthesis. The porphyrin was characterised by ^{1}H-NMR which demonstrated a downfield shift of the C6 and C2 aromatic protons to 8.12 and 7.65 ppm respectively in addition to the singlet at 8.86 ppm representing the pyrrole protons. The spectrum was fully in accord with the proposed structure and the singlet at -2.88 ppm confirmed the porphyrin was non-metallated. The UV spectrum was also in accord with

porphyrin data displaying characteristic absorptions at 426, 520, 556, 594 and 659 nm. Overall confirmation of the structure was afforded by the MALDI mass spectrum which shows the main mass at 1300.4 m/z corresponding to the parent ion.

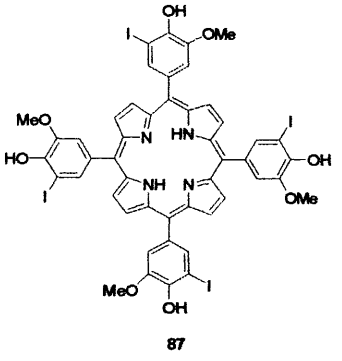

87

Figure 4.22: Porphyrin synthesised from Adler-Longo synthesis of pyrrole and compound **86**

Metallation of **87** was carried out to afford the zinc complex (**88**). Absence of the broadened singlet at -2.88 ppm in the ^{1}H-NMR spectrum confirmed the presence of a metal in the macrocyclic cavity. The other peaks in the spectrum did not undergo any change. The UV spectrum demonstrated that metallation of the porphyrin had occurred since there were only two absorptions apparent unlike five in compound **87**. The MALDI spectrum carried out showed two major peaks at 1363.8 and 1237.9 m/z, in addition to a smaller peak at 114.0 m/z. The main peak (100%) represents the parent ion, whilst those at 1237.9 and 1114.0 m/z denote the fragments of the parent ion having lost one and two iodide ions respectively.

Time limitations did not allow us to proceed any further with these investigations therefore future work by the group could involve using this porphyrin **87** or **86** as a starting point for a variety of reactions such as Sonogashira or simple nucleophilic substitution in order to form a cyclen-tetraporphyrin system such as the one which was intended.

4.8 Conclusions

The synthesis of the novel octadentate ligand 1,4,7,10-tetrakis(3,5-di-*tert*-butyl-2-hydroxybenzyl)-1,4,7,10-tetraazacyclododecane (**74**) and its lanthanide complexes in addition to the novel hexadentate ligand 1,8-dimethyl-4,11-(3,5-di-*tert*-butyl-2-hydroxybenzyl)-1,4,8,11-tetraazacyclotetradecane (**79**) and its transition metal complex are reported. Synthesis of the analogous octadentate cyclen ligands bearing four 2,4-di-fluorophenol, 4-*tert* butyl phenol, 1-napthol, 1-bromo-2-napthol, 4-chloro-1-napthol as pendant groups were attempted. We speculate that the cyclen intermediate formed in the Mannich reaction possesses high stability and the above phenols are not reactive enough to form the Mannich product. Formation of 2,6-(bis morpholine)-4-*tert*-butyl-1-hydroxybenzyl **(83)** demonstrates that the 4-*tert* butyl phenol will undergo reaction at both the 2 and 6 position simultaneously with morpholine as the amine.

An investigation into the synthesis of the cyclen- tetraporphyrin composite **(89)** was also undertaken and two different routes were investigated. The initial route was direct reaction of cyclen with porphyrin **84** however the reaction did not precede. After considering the sterics of the porphyrin, it was thought the best method of preparing **89** would be Mannich reaction of cyclen with vanillin followed by the Adler-Longo[34] synthesis of four porphyrins onto the vanillin pendant arms. Despite evidence that the trial reaction between two equivalents of vanillin and one equivalent of homopiperazine was successful, the synthesis of the cyclen tetra-vanillin compound **90** did not occur to completion and this is proposed to be due to the same reasons as discussed for the phenols and naphthols above.

4.9 References

1) T. Beissel, T. Glaser, F. Kesting, K. Wieghardt, B. Nuber, *Inorg. Chem*, **35**, (1996), 3936-3947.

2) B. Adam, E. Bill, E. Bothe, B. Goerdt, G. Haselhorst, K. Hildenbrand, A. Sokolowski, S. Steenken, T. Weyhermuller, K. Wieghardt, *Chem. Eur. J.*, **3**, No. 2, (1997), 308-319.

3) A. Sokolowski, J. Muller, T. Weyhermuller, R. Schnepf, P. Hildebrandt, K. Hildenbrand, E. Bothe, K. Wieghardt, *J. Am. Chem. Soc.*, **119**, (1997), 8889-8900.

4) A. Sokolowski, E. Bothe, E. Bill, T. Weyhermuller, K. Wieghardt, *Chem. Commun.*, (1996) 1671.

5) J. Muller, A. Kikuchi, E. Bill, T. Weyhermuller, P. Hildebrandt, L. Ould-Moussa, K. Wieghardt, *Inorg. Chim. Acta*, **297,** (2000), 265-277.

6) S. Kimura, E. Bill, E. Bothe, T. Weyhermuller, K. Wieghardt, *J. Am. Chem. Soc.*, **123** (2001), 6025-6039.

7) D. Burdinski, E. Bothe, K. Wieghardt, *Inorg. Chem.*, **39**, (2000), 105-116.

8) T. K. Paine, T. Weyhermuller, E. Bothe, K. Wieghardt, P. Chaudhuri, *Dalton Trans.*, (2003), 3136-3144.

9) D. S. Marlin, E. Bill, T. Weyhermuller, E. Bothe, K. Wieghardt, *J. Am. Chem. Soc.*, **127,** (2005), 6095-6108.

10) G. T. Babcock, M. K. El-Deeb, P. O. Sandusky, M. M. Whittaker, J. W. Whittaker, *J. Am. Chem. Soc.*, **114**, (1992), 3727.

11) M. M. Whittaker, P. J. Kersten, N. Nakamura, J. Sanders-Loehr, E. S. Schweizer, J. W. Whittaker, *J. Biol. Chem.*, **271**, (1996), 681.

12) M. Koikawa, H. Okawa, S. Kida, *J. Chem. Soc., Dalton Trans.*, (1988), 641.

13) F. F. Blicke, *Org. Reactions 1*, (1942), 303.

14) M. Koikawa, M. Gotoh, H. Okawa, S. Kida, T. Kohzuma, *J. Chem. Soc., Dalton Trans.*, (1989), 1613.

15) M. Koikawa, H. Okawa, Y. Maeda, S. Kida, *Inorg. Chim. Acta*, **194**, (1992), 75.

16) M. Koikawa, H. Okawa, N. Matsumoto, M. Gotoh, S. Kida, T. Kohzuma, *J. Chem. Soc. Dalton Trans.* (1989), 2089.

17) D. P. Goldberg, S. P. Watton, A. Maschelein, L. Wimmer, S. J. Lippard, *J. Am. Chem. Soc.*, **115**, (1993), 5346.

18) J. A. Hafen, B. A. Jazdzewski, S. Mahapatra, L. M. Berreau, E. C. Wilkinson, L. Que, W. B. Tolman, *J. Am. Chem. Soc.*, **119,** (1997), 8217.

19) J. A. K. Howard, A. M. Kenwright, J. M. Moloney, D. Parker, M. Port, M. Navet, O. Rousseau, M. Woods, *Chem. Commun.*, (1998), 1381.

20) S. Aime, A. S. Batsanev, M. Botta, J. A. K. Howard, D. Parker, M. P. Lowe, *New J. Chem.*, **23**, (1999), 669.

21) R. S. Dickins, J. A. K. Howard, C. W. Lehmann, J. Moloney, D. Parker, R. D. Peacock, *Angew. Chem., Int. Ed. Engl.*, **38**, (1997), 521.

22) S. Aime, A. Barge, J. Bruce, M. Botta, J. A. K. Howard, J. Moloney, D. Parker, A. S. de Sousa, M. Woods, *J. Am. Chem. Soc.*, **121**, (1999), 5762.

23) S. Aime, A. Batsanov, M. Botta, J. A. K. Howard, D. Parker, K. Senanayake, J. Williams, *Inorg. Chem.*, **33**, (1994), 4696.

24) S. Aime, A. Batsanov, M. Botta, R. Dickins, S. Faulkner, C. Foster, A. Harrison, J. A. K. Howard, J. Moloney, T. Norman, D. Parker, L. Royle, J. Williams, *J. Chem. Soc., Dalton Trans.*, (1997), 3623

25) J. Peters, J. Huskens, D. Raber, *J. Prog. Nucl. Magn. Reson. Spectrosc.*, **28**, (1996), 283.

26) P. Caravan, J. Ellison, T. McMurray, R. Lauffer, *Chem. Rev.*, **99**, (1999), 2293.

27) G. Mathis, *Clin. Chem*, **41**, (1995), 1391.

28) D. Parker, J.A.G. Williams, *J. Chem. Soc., Dalton. Trans.*, (1996), 3613-3628.

29) D. Parker, R. Dickins, H. Puschmann, C. Crossland, J. Howard, *Chem. Rev.*, **102**, (2002), 1977-2010.

30) G. Zucchi, R. Scopelliti, J. C. Bunzli, *J. Chem. Soc., Dalton Trans.*, (2001), 1975-1985.

31) U. Brunner, M. Neuburger, M. Zehnder, T. Kaden, *Supramolecular Chemistry.*, **Vol. 2,** 103-110.

32) J. Setsune, H. Takeda, *Tet. Letts.*, **36**, (33), (1995), 5903-5904.

33) T. Kometani, D. Watt, T. Ji, Tet. Letts., Vol. 26, No. 17, (1985), 2043-2046.

34) A.D Adler, F.R. Longo, W. Shergalis, *J. Am. Chem. Soc.*, 1964, **86,** 3145.

35) P. Rajakumar, V. Murali, *Tet. Letts.*, **43**, 2002, 7695.

36) A. Rivera, M. Maldonado, *Tet. Letts.*, **47**, 2006, 7467.

37) J. Tian, J. Zhang, X. Shen, H. Zou, *Journal Organomet. Chem.*, **584**, 1999, 240.

38) K. Sonogashira, Y. Tohda, N. Hagihara, *Tet. Lett.* 1975, 4467.

Crystal data and structure refinement for compound **74**.

Empirical formula	C68 H108 N4 O4	
Formula weight	1045.58	
Temperature	150(2) K	
Wavelength	0.71073 Å	
Crystal system	Monoclinic	
Space group	P 21/c	
Unit cell dimensions	a = 14.4031(2) Å	α= 90°.
	b = 15.6900(3) Å	β= 101.8790(10)°.
	c = 29.5104(5) Å	γ = 90°.
Volume	6526.08(19) $Å^3$	
Z	4	
Density (calculated)	1.064 Mg/m^3	
Absorption coefficient	0.065 mm^{-1}	
F(000)	2304	
Crystal size	0.25 x 0.20 x 0.20 mm^3	
Theta range for data collection	2.96 to 26.38°.	
Index ranges	-18<=h<=17, -19<=k<=19, -36<=l<=36	
Reflections collected	47970	
Independent reflections	13286 [R(int) = 0.1210]	
Completeness to theta = 27.47°	99.5 %	
Absorption correction	Semi-empirical from equivalents	
Max. and min. transmission	0.9871 and 0.9840	
Refinement method	Full-matrix least-squares on F^2	
Data / restraints / parameters	13286 / 6 / 713	
Goodness-of-fit on F^2	1.057	
Final R indices [I>2sigma(I)]	R1 = 0.0944, wR2 = 0.2209	
R indices (all data)	R1 = 0.1431, wR2 = 0.2468	
Largest diff. peak and hole	0.844 and -0.481 $e.Å^{-3}$